ANDCHRON

BGS/ODA Research and Development Project in the Andean Countries

1983–86

ANDCHRON

ANDEAN GEOCHRONOLOGY AND METALLOGENESIS

MAUREEN BROOK[1]
ROBERT J. PANKHURST[2]
THOMAS J. SHEPHERD[1]
BARUCH SPIRO[1]

with contributions from
NORMAN J. SNELLING[1]
IAN G. SWAINBANK[1]

Final Report for the OVERSEAS DEVELOPMENT ADMINISTRATION Research and Development Project on the Application of Geochronology, Isotope Geology and Fluid Inclusion Studies to Understanding the Geological Evolution of the Southern Andes and the Setting and Formation of Metallic Ore Deposits therein.

October 1983 - August 1986

1: British Geological Survey, (Natural Environment Research Council), Isotope Geology unit, 64 Gray's Inn Road, London WC1X 8NG, U.K.
2: British Antarctic Survey, (Natural Environment Research Council), High Cross, Madingley Road, Cambridge CB3 0ET, U.K.

ANDCHRON

ANDEAN GEOCHRONOLOGY AND METALLOGENESIS:
REPORT ON B.G.S./O.D.A. RESEARCH & DEVELOPMENT PROJECT 1983-86.

M. Brook, R.J. Pankhurst, T.J. Shepherd and B. Spiro

SCIENTIFIC ABSTRACT

A multidisciplinary project was carried out in an attempt to improve understanding of the evolution and inter-relationship of magmatism and metalliferous mineralization in the central and southern Andes. This has involved the co-ordinated application of geochronology, radiogenic and stable isotope geology, and fluid inclusion studies to both regional and specific magmatic and metallogenic occurrences throughout the area. A brief introduction to the principles and application of these techniques is given. Rb-Sr whole-rock geochronology (supplemented by K-Ar dating carried out in Chile) and Sr isotope methods have been used extensively, especially in Chile, where there was little previous data of this type, to elucidate the evolution of the Andean margin in space and time. Regional mineralization studies encompass sulphur and lead isotopes as well as geochronology. Finally, all techniques have been jointly applied in two case studies based on specific precious metal deposits.

More than 500 new Rb-Sr analyses are reported, from which about 60 new isochron ages have been determined. The igneous history extends throughout much of Phanerozoic time, in relation to long-lived eastward subduction of the Pacific Ocean floor beneath the South American continent. This has resulted in coast-parallel belts of intrusive rocks of various ages (generalized as late Palaeozoic-Triassic, Jurassic and Cretaceous-Tertiary), representing a migrating locus of calc-alkaline magmatism with changes in subduction geometry and kinematics. The relative distribution of these belts, as well as the time of the most intense magmatism within them, varies along the Andes and the results were therefore most instructively considered in terms of four main E-W transects across the continental margin:

(a) The Canal Region of the Chonos Archipelago of southern Chile (44-47°S). Only the Mesozoic belts were observed here, the basement consisting of metamorphosed fore-arc sedimentary assemblages, perhaps related to a Palaeozoic magmatic arc much further to the east, which were subsequently accreted onto the continent. New data suggest a maximum possible age for sedimentation of *c.* 370 Ma (Devonian), now largely overprinted by re-homogenization during deformational and thermal events associated with Mesozoic-Cenozoic subduction (170-130 Ma ago). The plutonic rocks are mostly of Cretaceous age (120-90 Ma) but with evidence of a Miocene (*c.* 25 Ma) or younger renewal of activity along a N-S axis associated with the Canal Moreleda. The initial $^{87}Sr/^{86}Sr$ ratios of all these plutons are low (mostly <0.7045), indicating melting within depleted (oceanic-type) mantle with very little interaction with pre-existing crustal rocks. (The lack of older crystalline crust is also reflected in the nature and Pb-isotope composition of metal ores in southern Chile).

(b) Central Chile (*c.* 30-38°S). This region is characterized by the western belt of the Southern Coastal Batholith, much of which formed during a short interval in late-Carboniferous to early Permian times (295 ± 5 Ma ago).

Triassic and Jurassic events within the batholith are recognized in renewed intrusive activity, and migmatization and isotopic resetting of the older rocks. Separate Cretaceous and Tertiary-Recent magmatic belts occur to the east, representing migrating activity, although these were not sampled during the project. There is a genetically significant distinction between Palaeozoic granitoids which have rather elevated initial $^{87}Sr/^{86}Sr$ ratios of >0.705, indicating contamination with crustal material, and the younger granitoids which are mantle-derived and largely uncontaminated as in the Canal Region.

(c) Chañaral - El Salvador, northern Chile (26-26°30'S). This transect is one where the geological record is most complete and where metallic mineraliztion is most significant. It has also been the mostly intensively studied, both in ANDCHRON and in previous work. The western Palaeozoic belt consists of Permo-Triassic granitoids north of Chañaral, emplaced into metasediments which are broadly equivalent to the basement of southern Chile but with an ancient (?shield-derived) detrital component. In addition, in the far east (Andean Altiplano) there is a second Palaeozoic belt which developed at the same time, as evidenced by several Rb-Sr isochrons of 270-210 Ma. As in the more southerly transects, the Palaeozoic plutons have elevated initial $^{87}Sr/^{86}Sr$ ratios of >0.705, in some cases up to 0.715, which demonstrate considerable contamination of the magmas, possibly even involving crustal melting at the time of magma generation. However, the late Triassic, Jurassic and Cretaceous magmatic belts, which represent subsequent activity migrating eastwards from the coast, exhibit progressively decreasing initial $^{87}Sr/^{86}Sr$ ratios in the range 0.7045-0.7035. These are thought to reflect magma generation at increasing depth within the underlying lithospheric mantle. The first reported Sm-Nd data from plutonic rocks in the Chilean Andes show a correlated increase in initial $^{143}Nd/^{144}Nd$ ratios which substantiate the Sr isotope data.

(d) Aguas Blancas - Imilac, northern Chile (24°30'-26°30'S). In the most northerly transect studied, which is also important for its precious metal mineralization, a detailed investigation of the Altiplano Palaeozoic outcrops is interpeted in the light of recent mapping which suggests that the plutonic and volcanic rocks of the area represent eroded collapsed caldera-like structures not unlike those of Miocene-Recent times. Two main episodes of magmatism at *c.* 270 Ma and *c.* 220 Ma are recognized. One intrusion close to the Argentine border gave an Ordovician age of 433 ± 22 Ma. Further west, in the Aguas Blancas district, reconnaissance dating defines magmatic events in mid-Jurassic and Cretaceous times. The igneous rocks of this transect show a pattern of decreasing initial $^{87}Sr/^{86}Sr$ ratios with time similar to those seen elsewhere.

Thus the overall evolutionary picture gained from these transects, despite local differences in timing and distribution, is a very consistent one, especially as regards the radiogenic isotope geochemistry. A model is proposed in which the Palaeozoic arc evolved under high stress, high heat-flow, shallow subduction, forming a continental margin which was then divided and separated by the Mesozoic-Cenozoic magmas under an increasingly extensional tectonic regime associated with steepening of the subduction angle. During late Cretaceous or Tertiary times this process was reversed, the present day situation resembling that of Permo-Triassic times. These variations in magma sources and pathways are likely to be of great significance in interpreting the

changing nature of mineralization once a proper regional time-frame is available for the latter.

Metallogenic processes during the Andean Mesozoic - Cenozoic orogeny are both extensive and varied, as manifested by the diverse types of mineral deposit. Their essentially episodic nature can be related on a regional scale to well defined magmatic and tectonic events and are consistent with metallogenesis at a destructive plate margin. However, ore emplacement takes place after the formation of the host rock and hence the temporal relationship is often uncertain.

Regional studies of polymetallic sulphide mineralization associated with the evolution of the Jurassic - Early Cretaceous magmatic arc in the sector 18°S - 46°S in Chile have been carried out using lead and sulphur isotopes. Lead in the ores displays a strikingly uniform isotopic composition, in contrast to the wider variation observed in other metallogenic belts of the Andean orogen. The isotopic ratios define a linear trend which is best explained by a model involving mixing of upper crust- and mantle-derived lead. Model ages are considerably older than the known or inferred ages of mineralization, implying that the source of metals was in pre-existing rocks, in some cases possibly the host rocks. Galena- bearing ores in Jurassic and pre-Jurassic host rocks show a higher contribution of components of upper crustal lead, while those associated with Cretaceous hosts contain a higher component of mantle-derived lead. The sulphur isotope composition, which records the source of sulphur and conditions during ore formation, reveals several important geological - geochemical controls on mineralization.. The deposits show differing proportions of magmatic and sea water-derived sulphur with respect to their morphotectonic setting (i.e. volcanic arc, back arc basin or landward margin). Also the host rocks influence the resultant sulphur isotope composition by their chemical composition and permeability characteristics. The understanding and elucidation of regional controls on metallogenesis provided a firm basis for detailed analysis of specific styles of mineralization.

In Chile, attention was focussed on the epithermal gold deposit at Silica del Hueso. This style of mineralization has only recently been appreciated as an important facet of Andean metallogenesis. The deposit is located in Late Triassic/Early Jurassic sediments and Early Tertiary volcanics and shows characteristics typical of sediment-hosted epithermal deposits in western USA. However, of special interest at Silica del Hueso is a possible link with porphyry copper mineralization at Portrerillos. Although the link with this deposit could not be established, the age of mineralization at Silica del Hueso as shown by the Rb-Sr data ($< 54\pm1$ Ma, $> 37\pm4$ Ma) corresponds to that of the intrusives of the nearby El Salvador porphyry copper deposit. The thermal regime and properties of the mineralizing fluids, as determined by fluid inclusions and oxygen isotope analyses, are similar to those of other epithermal deposits. Mineralization took place at 200°-280°C from low salinity fluids of predominantly meteoric origin which periodically boiled. High levels of dissolved CO_2 (up to 1 mole%) are typical for deposits with high gold/silver ratios, but the data for Silica del Hueso imply that this does necessarily result from near surface geothermal phenomena but could arise at deeper levels in older volcanic sequences. Sulphur and strontium isotope studies show that the fluids have interacted with sediments at high water/rock ratios; most

probably the underlying Triassic-Jurassic sedimentary sequences. The extent to which sedimentary rocks are an essential feature in the genesis of this deposit remains unanswered but their role is clearly apparent and should not be overlooked in formulating a conceptual model for exploration.

In the coastal copper-iron belt of central Peru, a study was made of manto-type magnetite deposits - tabular and conformable ore bodies hosted by Lower Palaeozoic and Mesozoic volcano-sedimentary sequences. K-Ar geochronology has confirmed an extended period of mineralization (160-113Ma), but the results for individual deposits generally indicate that burial metamorphism and mineralization are closely related and occurred soon after deposition. (Limited sulphur isotope data from one of the deposits (Raul-Condestable), to be reported separately, overall reflect a predominantly sea water origin with variable contribution from a magmatic source probably by leaching of the volcanic rocks). Similarities in mineral chemistry and paragenesis, together with associated country rock alteration, reflect the prolonged development of the extensional marginal basin of central Peru during Jurassic and early Cretaceous times.

The mineral deposit of Quiruvilca, La Libertad province, Peru, was studied in detail. Here, Ag-rich polymetallic sulphide veins are emplaced in Lower Tertiary andesites. Wall rock alteration, locally of advanced argillic grade, appears to have preceeded the deposition of ore minerals. Mineral zonation within the orefield suggests a geochemical/thermal control reflecting lateral variation in the source of metals or mode of transport. Conditions of deposition as indicated by sulphur isotope composition imply temperatures of 430°-500°C which are significantly higher than the range of fluid inclusion temperatures obtained for late stage quartz (150°-250°C). Sulphur isotope compositions further indicate a magmatic origin, and precipitation in a H_2S - dominated environment. The age of mineralization (15 ± 1 Ma) as estimated from Rb-Sr results for highly altered wallrock corresponds to that of early intrusives of the Cordillera Blanca batholith. Initial $^{87}Sr/^{86}Sr$ ratios for the mineralizing fluids demonstrate that the strontium was not derived solely from the enclosing volcanics by closed system rehomogenization but includes a more radiogenic component. The overall isotopic and geochemical characteristics of the Quiruvilca deposit suggest that it could be related to an igneous intrusion at depth. Since there is no other evidence for such intrusions in the proximity of the deposit, the proposed model of ore genesis offers a new approach to mineral exploration in the area.

Considerable further work of the type attempted here is desirable, particularly in order to advance our knowledge of the less well studied areas where even the basic geochronology is unclear, and on further mineral deposits in a greater variety of environments. The latter is especially necessary for the multidisciplinary approach since each technique has practical limitations and, even with careful modification to accomodate local conditions, any one may yield amibiguous or inconclusive results and will thus not always be available to support interpretation of the remainder. Nevertheless, we believe that the results of ANDCHRON have fully justified the attempt and will be of great value in future planning for geological and mining enterprises alike.

ACKNOWLEDGEMENTS

The final version of this report was compiled by the four senior authors, who take responsibility for its conclusions as well as any errors or omissions.

Project ANDCHRON was a truly multidisciplinary and international collaboration. It owes its inception to the foresight and enthusiasm of many contributors, amongst whom we especially acknowledge:

Dr. Norman J. Snelling, British Geological Survey
Dr. Jorge Skarmeta, SNGM, Chile
Prof. Francisco Hervé, Universidad de Chile, Santiago

The success of the extensive fieldwork component of ANDCHRON was due to the official assistance of South American geological and mining organisations, which are here gratefully acknowledged. Nevertheless, we also wish to record our personal debt to the enthusiastic support and friendship of individual members of these organisations, as follows:

Servicio Nacional de Geología y Mineria, Santiago de Chile:
Ricardo Boric, John Davidson, Tuco Diaz, Felipe Diaz, Carmen Espejo, Miguel Hervé, Ramon Moscoso, Constantino Mpodozis, Carlo Nasi, Orlando Peres, Alvaro Puig, Sergio Rivano, Sonia Vogel.

Departamento de Geología y Geofisica, Universidad de Chile:
Carlos Garcia, Ivan Garrido, Estanislao Godoy, Francisco Munizaga, Miguel Angel Parada, Armando Siña.

British Geological Survey
Charles Branch, Peter Greenwood, Linda Thrift (for stable isotope analyses), Mike Allsop.

Corporación Chilena del Cobre:
Santiago: Enrique Tidy; El Salvador: Pedro Carrasco, Jose Luis Fuenzalida, Luis Olcay, Marcial Vergara.

Instituto Geologico Minero y Metalurgico, Lima, Peru:
Jorge Injoque

Compania de Minas Buenaventura, S.A.:
A. Benavides.

Corporacion Minera Nor Peru, S.A.:
C. Jahncke.

Others:
Karsten Berg, Technische Universität, Berlin.
Alejandro Godoy, Coyhaique, Chile.
James Irwin, U.C. Berkeley, California.
All the drivers and assistants who made our fieldwork so profitable.
Captain Gumercindo and crew of R/V "Divina", Puerto Aysen.

R.J. Pankhurst contributed his time to ANDCHRON with the generous approval of Dr. R.M. Laws, Director of the British Antarctic Survey.

CONTENTS

SUMMARY

(a) Introduction.

The Andes comprise one of the major mountain chains of the world and, together with associated geomorphological features, form the western margin of the South American continent. They extend for over 4000 km, passing southwards from Colombia, through Ecuador, Bolivia, Peru and, for over half their length, Chile.

As well as their obvious geographical influence, they are also of great economic importance to these countries as a result of their metal ore reserves: Chile is the world's largest supplier of copper (Cu) and many have significant mining developments based on gold (Au), silver (Ag) and semi-precious metals. The efficient exploitation and management of these reserves is dependent on exploration techniques founded on a thorough understanding of the geological processes responsible for the derivation, concentration, transport and deposition of metallic elements. This, in turn, requires full background knowledge of the geological structure of the continental crust and its evolution.

The western margin of the Americas today is an expression of geological processes which have only recently been adequately described by the theory of *plate tectonics*. The floor of the Pacific Ocean is expanding towards the adjacent continent, where it is subducted (drawn beneath) the rigid plate of the continental crust (Fig. (i)). The chief consequences of subduction are frictional stress and disturbance of the thermal balance under the seaboard of the continent. The former is responsible for the well-known zone of earthquakes which ring the Pacific Ocean. Dehydration, degassing and melting associated with the latter are manifested in linear belts of active volcanoes and associated mineralization, parallel to the continental margin.

It is important to appreciate that the Pacific margin of South America results from the long-lived continuance of subduction processes. Processes essentially the same as those currently operative have existed, as confirmed by the results presented here, for at least the past 250 million years (Ma), if not 400 Ma. In geological terms this can be recognized from the following features: 1) coast-parallel volcanic belts (or arcs), 2) coast-parallel belts of plutonic

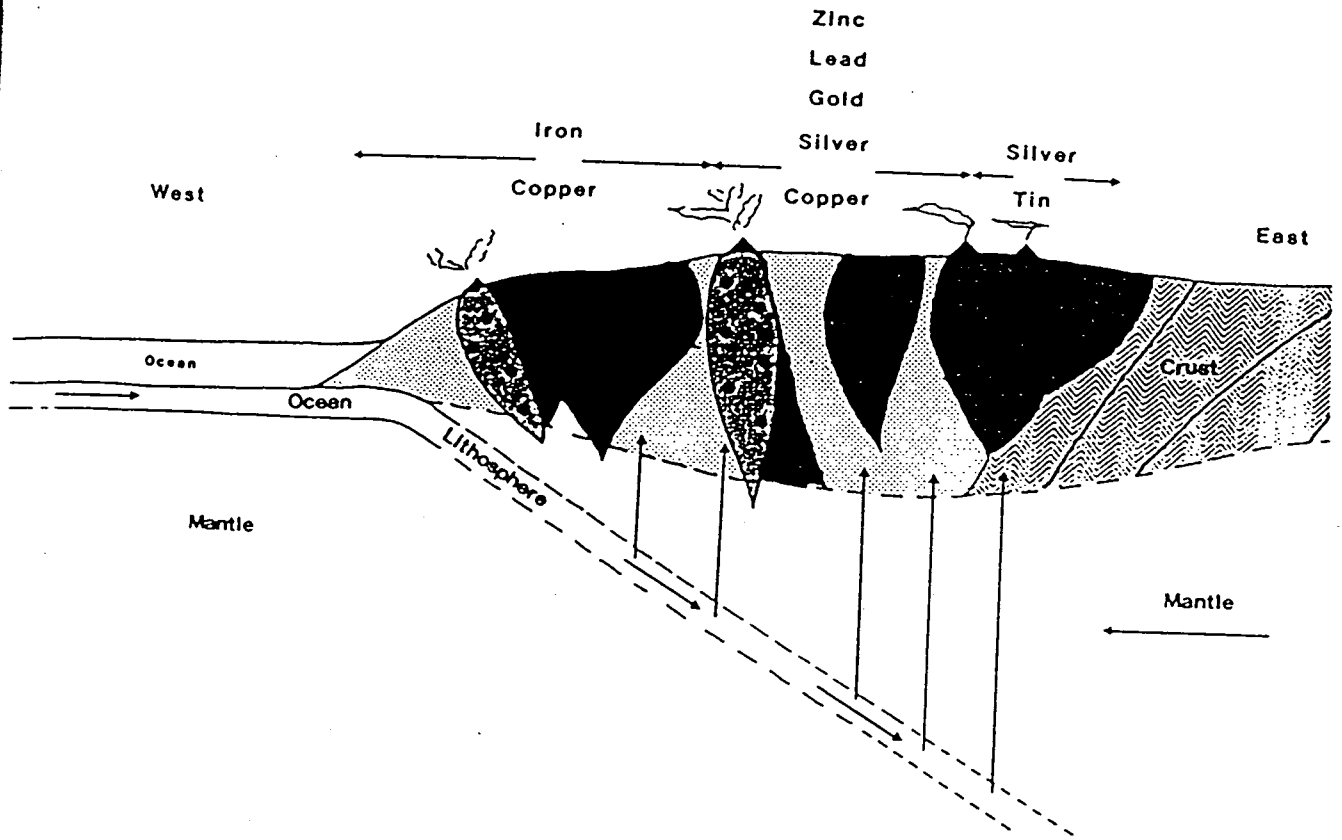

Fig. (i) Schematic section through a continental margin subduction zone, illustrating melting relationships and the zonation of magmatic and metalliferous products.

igneous rocks, e.g. granites, which represent the now uplifted and eroded roots of older volcanic arcs, 3) a broadly-consistent chemical composition of the igneous rocks (known as calc-alkaline), 4) superimposed trends in chemistry *transverse* to the continental margin, due to changing conditions as illustrated by the assymetry of Fig. (i), 5) coast-parallel zonation of the ore-mineral types, shown diagrammatically in Fig (i) and 6) offshore deposition of characteristic sediment types, which may be subsequently *accreted* onto the continent (although this feature is absent from the Andes at the present day and can only be seen in the older rocks). Finally, the relatively simple pattern at any one time is complicated in the geological record by episodic fluctuations and migration of the locus of the thermal disturbance due to changes in the mechanics of subduction. This has resulted, e.g. in northern Chile, in a rather complex repeated zonation of magmatic belts (Fig (ii)), and potentially a more complex distribution of ore types.

(b) Objectives.

The simple model outlined above provides a key to understanding the geological evolution and mineralization history of the Andes. The single objective of ANDCHRON was to elucidate this history as much as possible through a multi-disciplinary application of specialized research techniques, viz. geochronology, isotope geology and fluid inclusion studies, all of which are operated by the British Geological Survey but which had not previously been applied systematically to Andean problems on such a scale. As explained in Sections 1 and 2 of the report, geochronological methods are capable of dating rocks and geological events (thus providing an essential time-base for events), isotope geology can provide firm evidence for the origins of magmas (melts) and fluids as well as the conditions of emplacement of ores, and fluid inclusions contain much information on the nature of mineralizing fluids and metal transfer processes.

(c) Results and Benefits.

In the three years of the project, we were able to attempt a regional reconnaissance using these techniques throughout the more accessible parts of the southern Andes, as well as more detailed local studies on geological transects and specific ore-bodies. The work fell naturally into two phases.

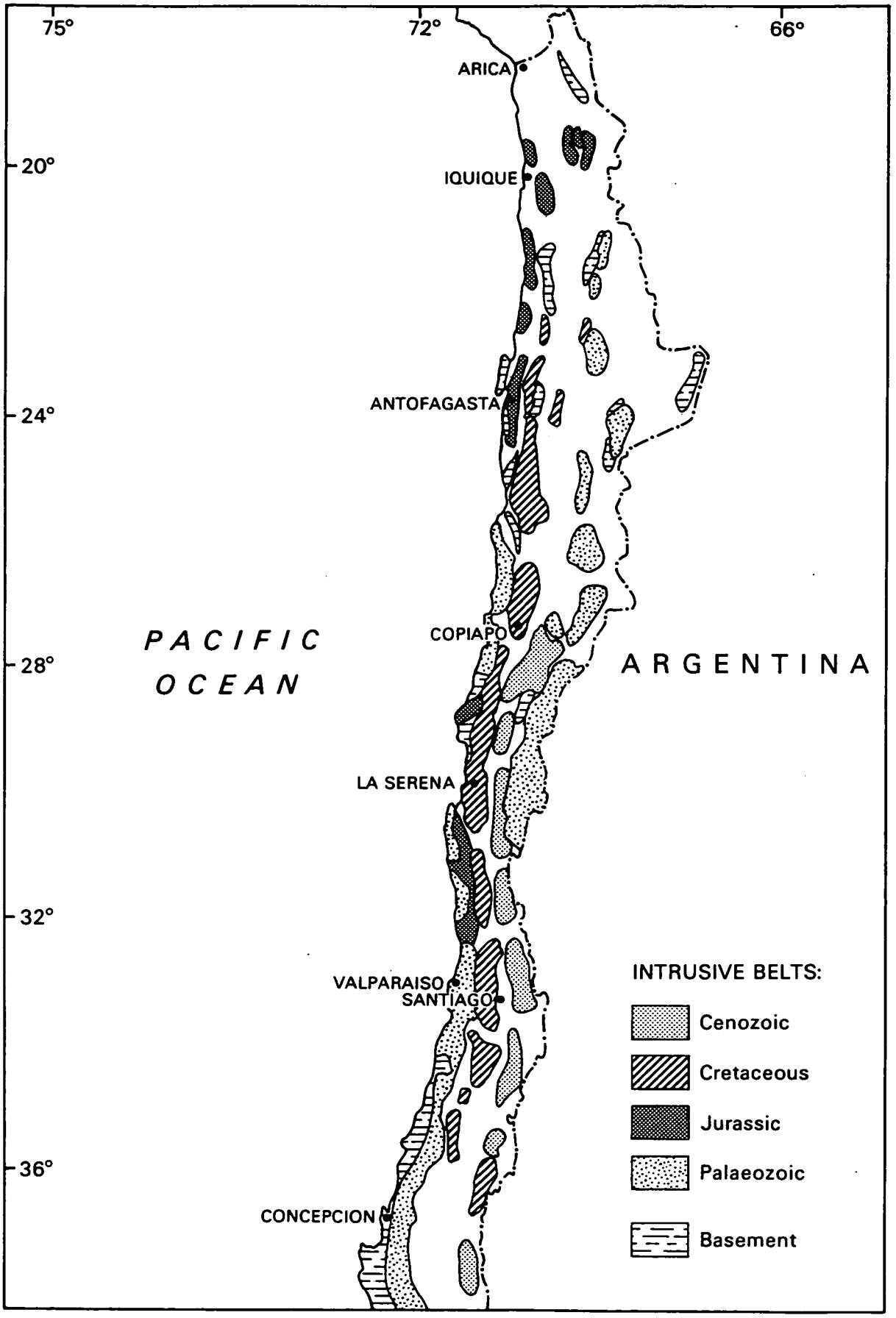
75°
72°
66°
20°
24°
28°
32°
36°
ARICA
IQUIQUE
ANTOFAGASTA
COPIAPO
LA SERENA
VALPARAISO
SANTIAGO
CONCEPCION
PACIFIC
OCEAN
ARGENTINA
INTRUSIVE BELTS:
Cenozoic
Cretaceous
Jurassic
Palaeozoic
Basement

Fig. (ii)

The first of these, which ran throughout the total period, involved geochronological and radiogenic isotope studies, providing the fundamental control on the geological evolution of the continental margin (Section 5). This required careful integration with field-geology and was accomplished only as a result of the excellent collaboration given by South American geological organizations and individuals. The approach was based on a number of contrasted transects through the Andes which have helped to refine knowledge of the distribution of igneous activity over the past 300 Ma, particularly in areas exhibiting complexities such as shown in Fig.(ii). The radiogenic isotopes have provided complementary evidence for the site of melting at different times and have resulted in a tectonic model for the development of the Andean continental crust (presented in Section 5.3c). Not only have these results given an essential framework for understanding the associated metalliferous belts, but they have also been of great benefit to geologists working on other aspects of Andean evolution, notably those from South American countries.

The second phase, a more specific approach to metalliferous deposits, commenced after the first year's work and involved all the techniques described above (Section 6). It concentrated on detailed study of two contrasting deposits, a silver vein type at Quiruvilca, Peru, and an epithermal gold prospect at Silica del Hueso, Chile. The results for each help to constrain the origin and properties of the ore-bearing fluids, the mechanisms of mobilization and deposition of the metals and the timing of ore emplacement in relation to magmatic and tectonic events in the country rocks. Genetic models are proposed which should be of value in determining exploration strategies. The importance of modern techniques in improving the quality of data for these models and in further refining this approach is emphasized.

It is hoped that the results of ANDCHRON will be of use to national government authorites in planning and legislating for resource management. Direct benefits to the mining organizations concerned are self-evident. In addition, the strongly collaborative mode of working has lead to open exchange of information. Indeed, the use of the techniques employed formed the basis of informal educational courses given during periods of fieldwork in Peru and Chile and a number of the South American counterparts have been able to visit the laboratories in London and gain direct experience in their application whilst at the same time contributing to the project.

(d) Dissemination and Future Work.

Some of the geological results of this work have already been published or presented for publication. Further papers, particularly developing the tectonic model, will be based on this report itself and prepared in the near future. The work on mineralization will be initially reported to the national geological surveys of Peru and Chile and to the mining companies which allowed access to the sites, with a view to subsequent publication in appropriate journals.

Much work in this area remains for the future. There is still a need for more precise or more intense time control on the geological history, and even some parts of the Andes where little geochronology has yet been carried out. The tectonic model based on the radiogenic isotopes should be further developed and tested in other locations. However, the most economically important work remains in the refinement of the models for ore genesis. This would depend on improving the intensity of sampling and data collection to resolve ambiguities, particularly in the ultimate source of the ore metals and the ore-bearing fluids and, in some cases, the timing of mineralizing event. It also requires an extension of this approach to other ore bodies in different geological situations for comparison. Much work along these lines would be necessary to substantiate the ideas presented here to the point where they could be applied routinely in exploration.

The first results of the geological collaboration represented in ANDCHRON were presented to the final meeting of Project 120 of the International Geological Correlation Programme (IUGC/UNESCO). It is hoped that the subsequent work, including that on some residual material not fully analysed in time for inclusion in this report, will form the basis of contributions to IGCP Project 249: Andean Magmatism and its Tectonic Setting (1986-1990).

1. PRINCIPLES OF ISOTOPE GEOLOGY

1.1 GEOCHRONOLOGY.

Radioactivity is the probability that in an attempt to form a more stable configuration, a nuclide will change, spontaneously and at a measureable rate, into another nuclide, with the emission of accompanying radiation. The type of radiation emitted with change of state varies. Alpha particles with a mass of 4 (two protons and two neutrons) can be viewed as positively charged He atoms which have well defined energies and are easy to quantify. They rapidly acquire the necessary neutralising electrons to become helium gas and in fact, the measurement of accumulated helium gas in uraniferous minerals gave the first geological age determinations. Emmission of an α-particle reduces the mass number of a radioactive nuclide by 4 and the atomic number by 2. β-particles are electrons resulting from the deterioration of a neutron within the atomic nucleus to become a proton so that, the atomic number (no. of protons) increases by one, but the mass number (protons and neutrons) remains unchanged. In comparison to the emission of α-particles, β-radiation is very low energy and until recently there have been problems in the counting of the radiation to determine the decay constant.

According to the theory of radioactivity, the rate of decay is proportional to the number of parent atoms present (P) and is unaffected by such factors as temperature, pressure and type of chemical combination. This law of radioactive decay can be expressed as a differential equation:

$$-dP/dt = \lambda P \qquad 1.$$

where t = time in years and λ is the decay constant (the proportion of atoms decaying per year, which must be experimentally determined for each radioactive nuclide). Integration of this equation yields:

$$P = P_o \times e^{-\lambda t} \qquad 2.$$

where P = number of parent atoms present now and P_o = number of parent atoms present at the formation of the system, t years ago. Since every parent atom which decays produces one daughter atom:

$$D = D_o + P_o - P$$

where D_o is the number initially present on formation of the system.

Since $P_o = P \times e^{\lambda t}$ from 2:

$$D = D_o + P(e^{\lambda t} - 1) \qquad 3.$$

Rearranging this we get the fundamental equation of geochronology:

$$t = 1/\lambda \log_e(1 + (D - D_o)/P) \qquad 4.$$

Thus the age of formation of a system is proportional to the amount of daughter accumulated in the system. When comparing different decay schemes it is convenient to describe the rate of decay by means of the "half-life", which is the time required for one half of the parent atoms to decay.

In order to date a rock or mineral accurately by this method it is necessary that there was a specific well defined point in time when the entire sample became a closed system to isotope migration. This criterion may be expected to be met by igneous rocks, which have formed from a homogeneous melt, but is less likely for sedimentary rocks or rocks with complex paragenesis. In addition, ideally, there should be no subsequent loss or gain of either parent or daughter isotope (except by <u>in situ</u> radioactive decay),e.g. during metamorphism, alteration or weathering.

There are numerous parent-daughter pairs of natural isotopes which could be used for isotope accumulation geochronometry, but there are certain definite requirements for a good geochronometer:

(i) The parent isotope should be present in the rock or mineral in sufficient quantity to be accurately measured

(ii) The rate of decay should be such that a measureable amount of daughter is produced over geological time and it must be possible to measure the decay constant accurately.

(iii) The amount of daughter present initially (i.e. not produced by in situ radioactive decay) must be sufficiently small to permit detection of the radiogenic component.

(iv) It must be possible to determine the amounts of daughter and parent isotopes accurately and on a routine basis.

Several decay schemes potentially meet these requirements and those used most frequently in routine geochronology are;

Parent	Daughter	Decay type	λ ($\times 10^{-10} a^{-1}$)	Half-life (Ma)
Rubidium-87	Strontium-87	Beta	0.142	48,813
Potassium-40	Argon-40	K-capture	5.543	1,250
Uranium-238	Lead-206	8 Alpha	1.551	4,468
Uranium-235	Lead-207	7 Alpha	9.849	704
Samarium-147	Neodymium-143	1 Alpha	0.0654	105,986

1.2 RADIOGENIC ISOTOPES AS PETROGENETIC TRACERS.

The previous section dealt with the determination of the time elapsed since the formation of a rock unit (e.g. since the crystallisation of an igneous rock.) to the present, by measuring the growth of the radiogenic isotopes over that interval. An important secondary aspect of the method depends on the significance of the relative amounts of radiogenic isotopes already present at the time of formation (D_o in equation 1(a).4), since these will be the result of many previous stages of radiogenic growth throughout Earth history and hence can relay information about the parent/daughter element ratios in the region from which the rock or magmas were derived. This is more easily explained graphically and for a particular case, e.g the Rb-Sr system (Fig. 1.1). A basic principle of radiogenic isotope geology is that when the Earth first formed about 4600 million years ago, the isotopic composition of heavy metallic trace elements was uniform. A value for the $^{87}Sr/^{86}Sr$ ratio at that time is deduced from isotopic studies of meteorites which give a precise estimate of 0.699 (point O in Fig. 1.1). The Earth's upper mantle (the region below the thin crust and extending down to about 700km.) is thought to be composed of ultramafic

rocks with a very low Rb/Sr ratio, so that their $^{87}Sr/^{86}Sr$ ratios increased only very slowly with time, to a mean value of about 0.704 today (line O-R in Fig. 1.1). On the other hand , crustal rocks contain significant proportions of Rb rich minerals and have very variable but higher Rb/Sr ratios. Since the crust has grown by differentiation of mantle material (e.g. by the repeated extraction of igneous melts with higher Rb/Sr ratios than their mantle sources), crustal growth lines will diverge from the mantle growth line and exhibit a much faster rate of increase in $^{87}Sr/^{86}Sr$. It is important to note that this has been a continuous process and that crustal rocks themselves are extremely variable. Nevertheless, the old Precambrian shield areas (such as the Brazilian shield) will probably approximate to a mean crustal growth line similar to Q-S in Fig. 1.1. The line P-T represents one of the oldest and Rb rich regions of such cratonic areas - the Amitsoq gneiss of West Greenland. These arguments set the pattern for interpreting the $^{87}Sr/^{86}Sr$ ratios of younger igneous rocks. Thus Phanerozoic rocks formed by melting within the 'typical' upper mantle will have <u>initial</u> $^{87}Sr/^{86}Sr$ in the same range as modern oceanic (uncontaminated) basalts, i.e. 0.7025 -0.7045, whereas those formed by anatexis of old crustal rocks will have a much higher values falling in the range 0.704 -0.710 and clearly contain a significant proportion of crustal Sr. It requires more detailed argument, involving a knowledge of local crustal structure, to decide whether such values are indicative of an intermediate crust/mantle source or whether they reflect partial contamination of a mantle derived magma with more radiogenic Sr acquired during their uprise through the crust. This is the essential problem tackled in the present work. Other decay schemes can provide complementary information, especially through Nd and Pb isotope compositions, although it is important to note that for these the parent/daughter ratio (i.e. Sm/Nd and U/Pb) is often <u>lower</u> in crustal rocks than in the upper mantle so that the relative rates of growth of $^{143}Nd/^{144}Nd$ and $^{206}Pb/^{204}Pb$ are in the opposite sense to those shown in Fig. 1.1 for $^{87}Sr/^{86}Sr$. These points will be treated in more detail when they arise in Section 5.

Reference:

Cox, K.G., Bell, J.D. & Pankhurst, R.J. 1977. *The Interpretation of Igneous Rocks.* George Allen & Unwin, London.

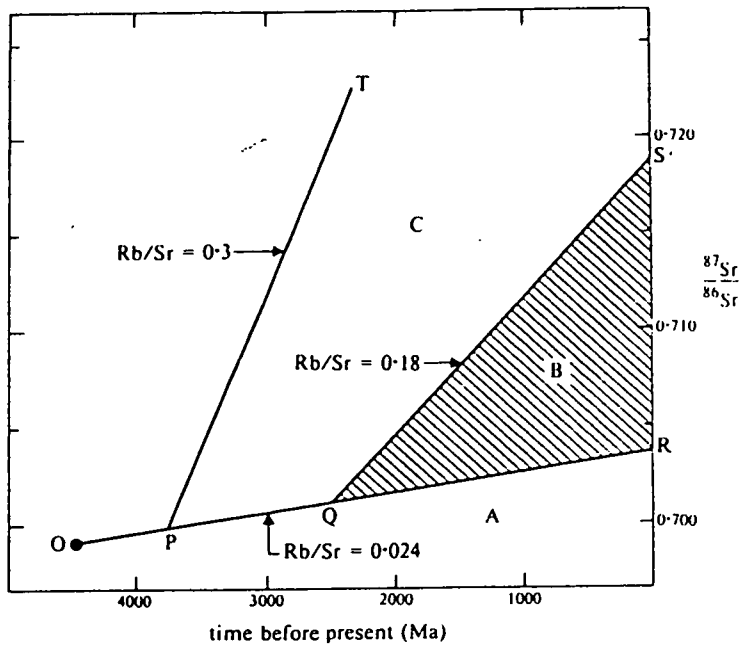

Fig. 1.1

Schematic illustration of the principle of Sr-isotope evolution in the Earth with time. Point O represents the primordial (homogeneous) $^{87}Sr/^{86}Sr$ of the mantle, which grows with time to its present day value (R) represented by the average composition of oceanic basalts. To all intents and purposes, the rate of growth is linearly dependent on Rb/Sr ratio. Thus Sr in continental crust with higher Rb/Sr ratios will evolve along much steeper paths diverging from OR at the time of its effective differentiation from the mantle. In practice, such crustal growth curves are merely notional – the Rb/Sr ratio and age of crustal rocks varying very widely indeed; but two are shown for illustrative purposes: PT represents some of the oldest known crustal rocks, the 3800 Ma-old Amitsoq gneisses of W. Greenland, with an average Rb/Sr of about 0.3. QS represents the 'average' composition of the North American shield areas (Faure & Powell 1972). The latter has been used, with the mantle growth curve OR to divide the diagram into fields A, B (shaded), and C in order to assess the relative contributions of crustal and mantle Sr to igneous magmas (see text).

from Cox et al., 1979

1.3 STABLE ISOTOPES.

Isotopes of an element are atoms whose nucleii contain the same number of protons but a different number of neutrons. The stability of a nuclide is characterised by structural features and the absence of measureable radioactive decay. Isotopes of an element differ slightly in their chemical and physical properties. The nature of the chemical bonds in a mineral greatly affects its isotopic composition. Bonds to ions with high ionic potential and low atomic mass are associated with high vibrational frquencies and tend to favour heavy isotopes. The crystal structure has only a secondary effect; heavy isotopes are concentrated in more closely packed or well ordered structures. The subtle but significant differences in the behaviour of stable isotopes cause isotopic fractionation during reactions or transformations in nature and forms the basis of stable isotope geochemistry. Since the magnitude of the isotope effect is proportional to the relative mass difference between isotopes, the most significant variations occur in the light elements, H, C, O, and S.Moreover, these elements are relatively abundant, participate in important geochemical reactions and are the most important elements in biological systems.

The relationship between the relative mass difference and the magnitude of the isotope effect makes it sufficient to determine the ratio of two isotopes of an element (D/H, $^{13}C/^{12}C$, $^{18}O/^{16}O$, $^{34}S/^{32}S$) in the investigation of terrestrial geochemical processes.

The isotope fractionation factor α is defined as the ratio R of the abundances of two isotopes in one chemical compound A divided by the corresponding ratio for another compound B such that:

$$\alpha_{A-B}=R_A/R_B$$

For analytical reasons, isotopic ratios of stable isotopes are not reported as absolute ratios but as deviations δ in per mil ($^{o}/_{oo}$) from the ratio of the same isotopes in a standard sample.

The main phenomena producing isotope fracionation can be divided into two types:

1) Isotope exchange reactions are a special case of chemical equilibrium. The dependence of the equilibrium constant of a chemical reaction and likewise the isotopic fractionation factor of an isotope exchange reaction on temperature may be used to calculate the temperature of formation of minerals. This is widely used in the study of ore deposits, hydrothermal systems and palaeoclimatology. Isotope geothermometry, which has the advantage of being virtually independant of pressure, is based primarily on oxygen and sulphur isotopes.

2) Kinetic fractionation occurs when chemical reactions such as sulphate reduction or physical processes such as evaporation have significantly different rate constants for the different isotopes.

From an isotopically homogeneous reservoir, minerals and fluids may be produced having different isotopic compositions depending on the chemical composition of the mineral, temperature, chemical and physical properties of the original reservoir as well as subsequent reactions and transformations. By constraining some of these variables using information derived from mineralogy, elemental and radiogenic geochemistry and fluid inclusion studies, the stable isotopes can be used as tracers for geochemical processes, providing information on the origin and geochemical and thermal histories of fluids and minerals.

1.4 FLUID INCLUSIONS.

Perfect crystals are unkown in nature and even under the most rigorous laboratory conditions it is virtually impossible to grow defect-free crystals. Crystal imperfections range from point defects on the atomic scale to gross defects on the macro scale. To the material scientist such imperfections are a constant nuisance but to the geologist gross imperfections in the form of occluded liquids, solids and vapour in minerals (i.e. fluid inclusions) provide a valuable key to the physical and chemical processes by which crystals grow in nature.

Fluid inclusion studies have proved particularly useful in the field of economic geology where the majority of mineral deposits are known to have formed via mineral depostion from metal-bearing, saline, aqueous fluids. In

this sense fluid inclusions represent real samples - with rare exception, the only samples - of mineralizing solutions which existed 10's or 100's of millions of years ago.

Because most inclusions are less than 10 micron in diameter and hence cannot be seen with the naked eye, their analysis poses a severe challenge. However, within recent years various techniques have been specifically developed for the task. Of these, thermometric analysis is the most widely used and provides data for the temperature and pressure of mineral formation, and overall chemical composition of the fluid phase.

Information of this nature is of paramount importance to the exploration geologist for the development of conceptual models of ore formation which can be used to predict the location of ore deposits not exposed at the surface. More sophisticated techniques pioneered by BGS involve the application of mass spectrometry to determine the isotopic and chemical composition of the dissolved gases. Relative or absolute variations of the more common constituents afford an important clue to the origin of the mineralizing solutions and their capacity to transport different metals. Indeed the chemical "fingerprinting" of mineralizing solution, albeit still in its infancy, is now recognised as a potential exploration guide for many types of mineral deposit (tungsten, copper, silver, gold, uranium).

Combined with the time framework of geological events provided by geochronology, applied fluid inclusion studies help to distinguish rock formations with a high probability of hosting mineral deposits. The above techniques formed an essential part of the ANDCHRON metallogenic research programme and their application is discussed more fully in sections 2 and 6.

2. METHODS EMPLOYED.

2.1 RUBIDIUM-STRONTIUM DATING.

The Rb-Sr method depends on the spontaneous decay of naturally occurring ^{87}Rb to ^{87}Sr by the emission of a β-particle. If the relative concentrations of parent (Rb) and daughter (Sr) isotopes, and the decay constant are known, then the accumulation time can be calculated according to the isochron age equation given in Section 1:

$$D = D_o + P\,(e^{\lambda t} - 1)$$

(where D is the amount of ^{87}Sr present now, D_o the amount present t years ago and P is the amount of ^{87}Rb present now). Strontium consists of four natural isotopes: masses 88, 87, 86 and 84, of which only 87 is radiogenic. If we express the amounts of ^{87}Rb and ^{87}Sr present in the rock as relative to the ^{86}Sr, we obtain the isochron equation:

$$(^{87}Sr/^{86}Sr) = (^{87}Sr/^{86}Sr)_o + (^{87}Rb/^{86}Sr).(e^{\lambda t} - 1)$$

This equation expresses the generalized isotope systematics in terms of quantities which can be obtained directly, or easily calculated, from mass-spectrometric measurements. In practice the equation is solved graphically using an isochron diagram (Fig. 2.1), by finding the best-fitting straight line to the data points (slope = $e^{\lambda t}-1$). It may be expected to yield the age of emplacement of the rock if:

1.) There has been no loss or gain of parent or daughter isotope since the formation of the system, except by the in situ radioactive decay of ^{87}Rb.

2.) The amount of daughter isotope incorporated in the system initially and not produced by in situ decay of parent is known.

3.) Cooling of the rock below the blocking temperature to isotope migration and ending of hydrothermal systems occurred relatively rapidly after emplacement.

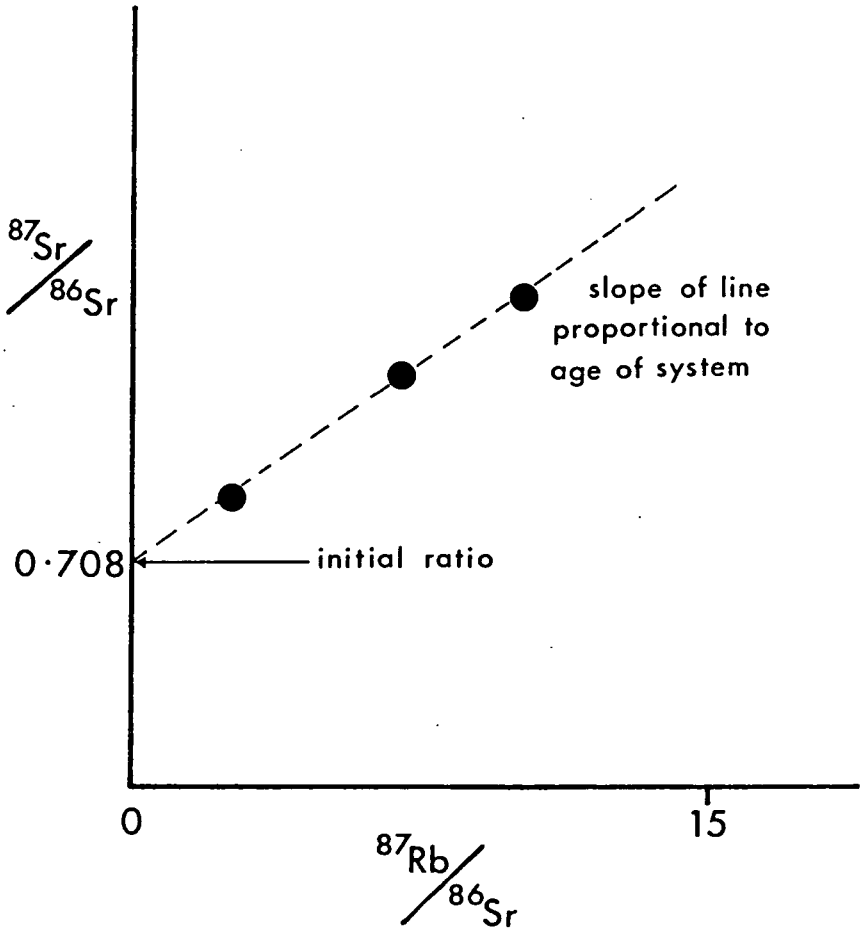

Fig. 2.1 Idealised Rb/Sr isochron diagram

For a suite of samples from the same rock body, having different Rb/Sr ratios, a plot of $^{87}Rb/^{86}Sr$ vs $^{87}Sr/^{86}Sr$ yields a straight line, or isochron, (provided assumption 1. above is met) with a slope equal to $(e^{\lambda t}-1)$ and an intercept which gives the initial $^{87}Sr/^{86}Sr$ ratio of the system. Rubidium-strontium whole-rock isochron dating is based on the assumption that, on cooling below the blocking temperature to Rb and Sr migration , all the samples subsequently collected from any particular igneous rock body contained Sr with the same isotopic composition (the initial ratio) and this was only modified subsequently by the addition of ^{87}Sr produced by the decay of ^{87}Rb in situ. During later thermal or hydrothermal disturbance, isotope migration may have taken place between adjacent minerals and over distances of a few centimetres, but it is assumed that this was a localised effect and that the whole-rock system remained closed.

2.2 POTASSIUM-ARGON DATING.

The method of K-Ar dating utilises the decay of ^{40}K to ^{40}Ar in natural systems. ^{40}K comprises 0.01167% of the total atomic abundance of potassium in present day rocks and minerals. It undergoes radioactive decay by various paths. 88.8% decays to ^{40}Ca, but unfortunately the *natural* abundance of non-radiogenic ^{40}Ca is very high, so that the amount produced by radioactive decay is swamped and this scheme is not generally of practical use. The remaining 11.2% of ^{40}K decays to ^{40}Ar by three routes;

(i) by electron capture direct to the ground state.

(ii) by emission of a β-particle.

(iii) decay by electron capture to an excited state of ^{40}Ar and the emission of a γ-ray dropping then to a ground state.

As with all other methods of geochronology, certain conditions must be met before the age obtained can be considered to be the true age of formation of a rock or mineral, i.e. the decay constant must be accurately known, there must be no loss or gain of either parent or daughter isotope other than by the process of radioactive decay, the analysis of the amount of daughter and parent must be accurate. The first assumption is long established and relatively well

validated (Table at end of Section 1.1). The second is in some respects the weak link in the K-Ar method since in certain circumstances argon is readily lost from the crystal lattice. This is due to its large atomic radius, chemical inertness combined with the fact that it is a gas. The effect of the above characteristics is that certain types of alteration products such as chlorite or minerals with expanded crystal lattices such as montmorillonite or glauconite, lose Ar by diffusion, even at room temperatures and the ages obtained can therefore only be a minimum estimate. Others such as the micas and amphiboles have a more predictable pattern of behaviour and hold the radiogenic Ar in their crystal lattices except under more extreme conditions of elevated temperatures, movement of fluids or tectonic stress. The critical temperatures at which radiogenic Ar will escape from the crystal lattices of muscovite and biotite are approximately 300°C and 380°C respectively. These are low temperatures relative to those reached in regional metamorphism. Hornblende retains Ar up to temperatures of about 400°C with massive outgassing at 500°C. One major benefit from this outgassing phenomena is that as individual minerals behave differently, a discordant age pattern for K-Ar ages in different minerals can be used as a very sensitive indicator of thermal disturbance. Accurate analysis of ^{40}Ar incorporated into the mineral at the time of formation is important. Present day atmosphere contains isotopes of mass 36, 38 and 40 of which only 40 is radiogenic. Because of initial degassing of the mantle in the Precambrian , the $^{40}Ar/^{36}Ar$ ratio in the atmosphere is thought to have changed little during the Phanerozoic. A correction for the amount of this atmospheric ^{40}Ar must always be applied, otherwise the age obtained would be erroneously old. As ^{36}Ar is non radiogenic and has remained in constant proportion to ^{40}Ar throughout time ($^{40}Ar/^{36}Ar$= 296), it is only necessary to quantify the amount of ^{36}Ar to obtain the true amount of ^{40}Ar produced in situ by the decay of ^{40}K. Another problem related to the method that should be considered is the incorporation into the crystal lattice at the time of formation of an "excess" amount of ^{40}Ar due to the mineral forming in an atmosphere of high argon partial pressure. This phenomena is relatively uncommon, but can be difficult to detect unless the results from other decay schemes are available.

2.3 URANIUM-LEAD METHOD.

All naturally occurring uranium contains radioactive ^{238}U and ^{235}U in the ratio 138:1. ^{238}U decays to ^{206}Pb and ^{235}U to ^{207}Pb. As this method was not

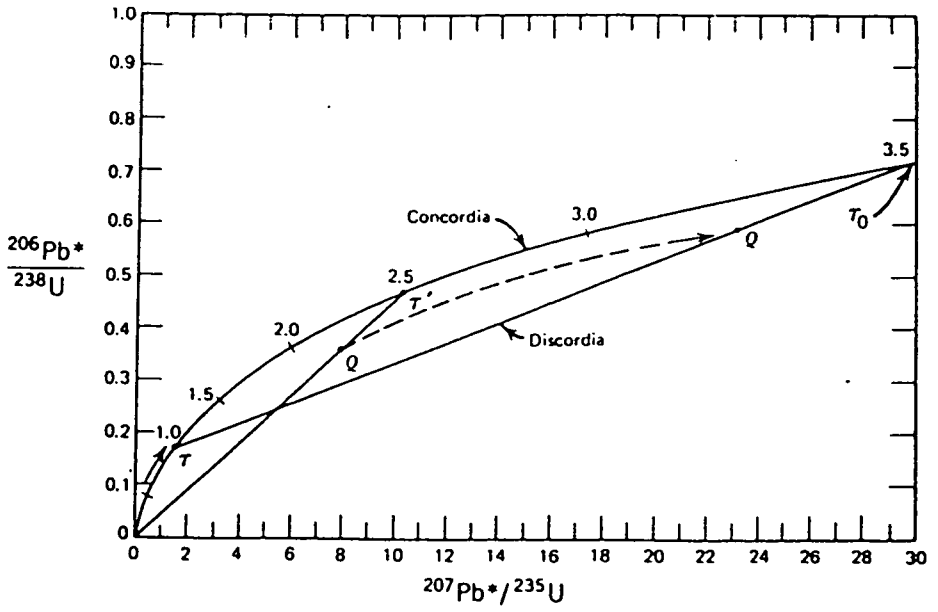

Fig. 2.2

Concordia diagram illustrating a history of episodic lead loss (or uranium gain). A U-bearing system on concordia lost lead when its age was τ'. As a result, the system moved along a straight line (discordia) directed toward the origin. Point Q represents a system that lost only a fraction of its radiogenic lead. A mineral that had lost all of its radiogenic lead would be represented by a point at the origin. Following the episode of lead loss (or uranium gain), the U-Pb systems reside on discordia that intersects concordia at τ and τ_0, where τ is the time elapsed since closure and τ_0 is the time elapsed since original crystallization of the minerals (or rocks).

from Faure 1977

used directly during the ANDCHRON project, only a brief resumé of the method will be given here, as background to the following section.

U nuclides decay through a series of intermediate daughter products which themselves are radioactive before they reach their stable Pb end-products. Minerals containing U as a major component are rare, but some accessory minerals, such as zircon, contain significant trace amounts. Original Pb in U-bearing minerals would cause the radiometric age to appear too old unless a correction is made. ^{204}Pb is not produced radiogenically and acts as a tracer to incorporated Pb and can be used to calculate the original quantities of ^{206}Pb and ^{207}Pb.

In a single mineral the ^{238}U-^{206}Pb and ^{235}U-^{207}Pb ages should agree with each other within error if the mineral has remained a closed system. This agreement is termed concordance. On a graph of $^{235}U/^{207}Pb$ vs. $^{238}U/^{206}Pb$, the locus of all the concordant ages is a curve called the concordia. If the U-Pb ages do not agree they do not fall on this curve and are said to be discordant (see Fig. 2.2). Discordant ages are usually caused by lead loss from minerals when the crystal is subject to heat or stress. If different quantities of Pb were lost from different sub-samples of a mineral concentrate during a single phase of heating, then samples from the body would not plot as a single point but as a straight line beneath the concordia. Ideally, the line produced will intercept the concordia at two points: (i) the initial time of crystallisation and (ii) time of later lead loss.

2.d) LEAD-LEAD METHOD.

Pb has four isotopes, three of which (206,207 & 208) are radiogenic products of natural U and Th isotopes. The fourth, ^{204}Pb, is non-radiogenic. Common Pb-bearing minerals such as galena contain no U or Th, so that their Pb-isotope compositions have remained unchanged since crystallization. Any radiogenic Pb component in the mineral must have been incorporated at the time of crystallisation and would reflect the isotopic composition of the source fluid at that time.

Taking a very simplistic view, the Earth's primaeval Pb was isotopically homogeneous, its composition being that deduced from the troilite phase of iron

meteorites. With time, the radioactive decay of U and Th would result in an increase in the amount of ^{206}Pb, ^{207}Pb and ^{208}Pb in the Earth's mantle. During the formation of the Pb-rich minerals, Pb is completely isolated from the U and Th so that its isotopic signature is a measure of the time elapsed between the formation of the Earth (t= 0) and the formation of the mineral. A model based on this theory was developed by Holmes and Houterman and is demonstrated in Fig 2.3. This simplistic model did not take into account the variation in different source regions throughout time and more sophisticated models have since been developed by various writers of which probably the most widely referred to is the 'plumbotectonics' model of Doe and Zartman (1979).

Reference:

Faure, G. 1977. *Principles of Isotope Geology*. Wiley & Sons, New York. 464pp.

2.5 NEODYMIUM-SAMARIUM METHOD.

In total there are eighteen rare earth elements (REE) of which both Nd and Sm are relatively abundant (igneous rocks frequently contain up to 30ppm Nd and 6ppm Sm). The radioactive isotope ^{147}Sm decays by emission of one α-particle to 143Nd and the isochron method of dating rocks is applicable to this system with certain limitations. The decay rate is very slow so that the accumulation of the daughter product is really only measureable in rock types which concentrate the heavy rare earths (i.e. Sm relative to Nd). This complements the Rb-Sr method in that heavy REE tend to be more highly concentrated in basic and, especially, ultrabasic rocks which are typically depleted in Rb. Because REE are not very mobile, especially at moderately low temperatures, the system often allows a "view" through a late event such as metamorphism which might otherwise have caused open system behaviour for Sr. The disadvantages to this method are that within most rocks there is very little spread in the Sm/Nd ratio, which together with the long half-life means that rocks younger than Precambrian are generally undateable. However, some minerals, such as garnet, concentrate heavy REE and may provide a good range of data points. As with Sr isotopes, Nd is used as a sensitive time tracer in petrogenesis and gives valuable information about magma source material.

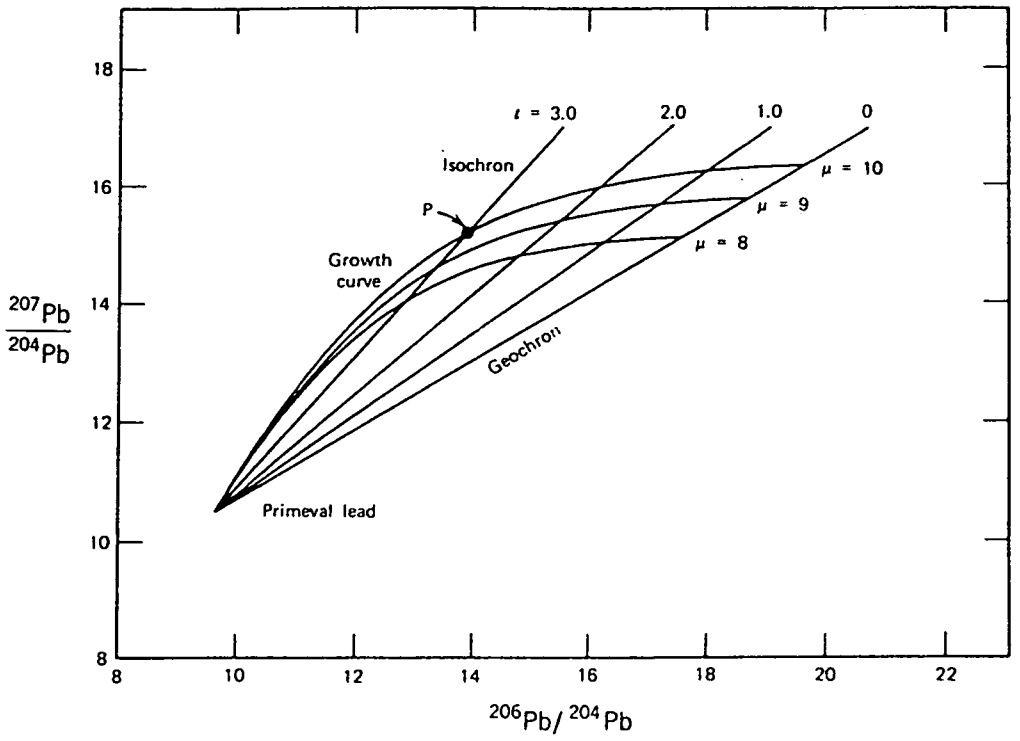

Fig. 2.3

Graphical representation of the Holmes-Houtermans model. The curved lines are lead growth curves for U-Pb systems having present-day μ values of 8, 9, and 10. The straight lines are isochrons for selected values of t. For example, the coordinates of point P are the $^{207}Pb/^{204}Pb$ and $^{206}Pb/^{204}Pb$ ratios of a galena lead that was withdrawn 3.0×10^9 years ago from a source region whose present $^{238}U/^{204}Pb$ ratio (μ) is 10.0. This diagram was constructed by solving Equations 13.4 and 13.5 assuming that the age of the Earth is $T = 4.55 \times 10^9$ y.

from Faure, 1977

2.6 SULPHUR AND OXYGEN STABLE ISOTOPES.

The sulphur isotope composition $\delta^{34}S$ of a mineral is determined by the isotopic composition of total sulphur in the fluid from which the mineral has formed $\delta^{34}\Sigma S_i$, the chemistry of the fluid in particular pH and fO_2, which determine the chemical speciation of sulphur, and the temperature of formation (Sakai 1968, Rye and Ohmoto 1979). Sulphur in terrestrial material originates primarily from two sources, sea water and magma. $\delta^{34}S$ of sea water sulphate is the same on a global scale, at present +20‰ and has undergone marked changes during the Phanerozoic (e.g. Ault and Kulp 1959, Claypool et al 1980). Where this secular variation is abrupt, $\delta^{34}S$ of oceanic derived evaporites can be used as stratigraphic markers or as indicators for mobilization of sulphate from certain strata. It is important to determine the age of the sulphur containing strata in question in order to assess the original possible $\delta^{34}S$ before using it as a geochemical tracer for subsequent processes. The fractionation between evaporites and sea water sulphate is small. Large fractionations occur in bacterially mediated sulphate reduction through kinetic fractionation. Sulphides of biogenic origin are normally associated with sedimentary strata rich in organic matter and have low $\delta^{34}S$ values; 25-65‰ lower than the original sulphate. Abiogenic sulphate reduction becomes important at temperatures higher than 25°C. Sulphur magmatic source has a composition of 0‰ but the chemistry of the fluid and temperature dependent fractionation give rise to sulphides of magmatic origin having a wide range of compositions. Sulphur minerals derived from mixed sources are also common,striking examples are the mid-oceanic ridge emanations.

The temperature dependent fractionation factor between dissolved species, oxidized and reduced forms and sulphide minerals can be used as geothermometers. Petrographic evidence is needed to ascertain that the mineral pairs were formed in contact with the same fluid. Extensive calculations and experimental work have been devoted to determine the temperature dependence of fractionation factors for sulphur species (see compilation by Friedman and O'Neil, 1977) but only a few have proven to be reliable, notably sphalerite-galena and chalcopyrite-galena.

The oxygen isotopic composition $\delta^{18}O$ in minerals is determined by the formation process, crystallization from a melt or from an aqueous solution. Water is an important constituent in ore forming fluids and is a major agent in

the process of rock and mineral alteration. Many of the questions relating to the genesis of ore deposits address the nature and origin of the fluid system which produced them. The stable isotope composition of water δD and $\delta^{18}O$)are affected by these reactions and so are the reacting minerals. As the hydrogen content of minerals is rather small relative to the reacting water as compared with oxygen, δD is less affected that $\delta^{18}O$ of the water during water rock interactions (e.g. Taylor and Forester 1971). Water for geochemical processes can be derived from three main sources; ocean, meteoric or magmatic. Ocean water has a world wide present value of $0‰_{SMOW}$. Possible changes in isotope composition during the Phanerozoic are still debated and probably small except for significant changes during periods of glaciation. The isotopic composition of meteoric water is a function of the evaporation-precipitation processes and depend on latitude, altitude and local climatological regime. Therefore interpretation of δD and $\delta^{18}O$ data relating to meteoric water has to take into account the of position of the recharge area at the given time. Magmatic water is referred to as water in equilibrium with magmatic rocks at magmatic temperatures.

The temperature dependent fractionation factor of oxygen between water and minerals can be used as geothermometer. This, however, requires the $\delta^{18}O$ value of the meter to be assumed. As in the case of sulphur this difficulty is overcome by using mineral pairs, the most sensitive of which is quartz-magnetite. It is usual to prove that the minerals under consideration are co-genetic. As the large oxygen reservoir of rocks may exchange with water during water-rock reaction assumptions on the isotopic composition of the fluid may be erroneous but it may be calculated from δD of hydrous minerals. Also, fluid inclusion thermometry can provide information on the temperature of formation of a mineral.Then by using $\delta^{18}O$ fractionation data (see compilation by Friedman and O'Neil) the isotopic composition of the water can be determined. By further using mineralogical and textural evidence the origin and history of the fluid can be traced (see Taylor 1979).

$\delta^{34}S$ and $\delta^{18}O$ provide information on source of sulphur and water which participate in geochemical processes. This information is particularly useful when studying mineral deposits as this information defines components, mechanism and the three dimensional extent of a mineralization process. The interpretation of stable isotope data is enhanced by integration with mineralogical fluid inclusion and geochronological information so as to provide

accurate parameters of geochemical processes which can form the basis for exploration concepts and strategies. Stable isotope geochemistry is applied in this study to different styles of mineralization each presenting different aspects of hydrothermal processes.

References:

Ault, W.V. and Kulp J.L. 1959: Isotopic geochemistry of sulphur. Geochim, Cosmochim Acta 16, 201-235.

Claypool, G.E., Holser, W.T., Kaplan, I.R.., Sakai, H, and Zak, I. 1980: The age curves of sulphur and oxygen in marine sulphate and their mutual interpretation.

Friedman, I. and O'Neil, J.R. 1977: Compilation of stable isotope fractionation factors of geochemical interest. U.S. Geological Survey Professional paper 440.KK.

Ohmoto, H. and Rye, R.O. 1979: Isotopes of sulphur and carbon in: Geochemistry of hydrothermal ore deposits (H.L. Barnes edit) 509-567, Wiley 798p

Rye, R.O. and Ohmoto, H. 1974: Sulphur and carbon isotopes and ore genesis: a review. Econ., Geol. 69. 826-842.

Sakai, H. 1968: Isotopic properties of sulphur compounds in hydrothermal processes: Geochem. Jour. 2, 29-49

Taylor, H.P. 1979: Oxygen and hydrogen isotope relationships in hydrothermal mineral deposits in: Geochemistry of hydrothermal ore deposits. (H.L. Barnes, editor) 236-277 Wiley 798p

Taylor, H.P. and Forester R.W. 1971: Low O^{18} igneous rocks from the intrusive complexes of Skye, Mull and Ardnamurchan, Western Scotland; J. Petrol 12, 465-497.

2.7 THERMOMETRIC ANALYSIS.

Thermometric analysis of fluid inclusions relies on the careful observation and recognition of the phase changes which take place in inclusions during controlled heating and freezing. By accurately measuring the temperature at which these changes take place it is possible, with reference to experimental data for simple systems (1, 2 or 3 components) to derive estimates of the pressure, temperature, density and composition of the fluids at the time of

mineral formation. Since most ore fluids are complex multi-component systems, compositional estimates are semi-quantitative; the data being reported as equivalent weight %. Meaningful interpretation of thermometric data requires that at the moment of trapping the fluid inclusion represents an homogeneous system (i.e. one phase). In general this is true but occasionally conditions prevail where the inclusion represents a heterogeneous sytem (e.g. fluid boiling during mineralization). After trapping and on cooling to ambient temperatures, differential contraction between the fluid and the host mineral results in the appearance of a vapour bubble. At the same time the fluid may unmix to yield two immiscible liquids or become saturated with respect to one or more solute components and precipitate out solid phases. Inclusions as seen at room temperature are therefore multi-phase. Secondly, it is assumed they have behaved as constant volume-constant composition systems (i.e. there has been no loss or addition of material). By reheating the sample the cooling history of the inclusion is thus reversed. This is one of the basic principles of thermometric analysis and the phase changes noted can be translated into temperature-composition data for the inclusion fluids at the time of trapping. At sub-ambient temperatures the inclusions are rapidly cooled to induce complete solidification. On warming, the melting temperatures recorded for the various solid phases provide additional data on fluid composition. Information obtained by thermometric analysis of ore minerals includes: depositional temperature, fluid pressure, fluid salinity/composition/density and the presence or absence of boiling during mineral formation. Unfortunately the need for visual observation restricts the technique to inclusions greater than 5 micron in transparent minerals. It is also necessary to distinguish between those inclusions formed during crystal growth and those formed in response to later, superimposed fluid processes. Hence petrographic examination of samples prior to analysis is a pre-requisite for such studies.

2.8 GAS MASS-SPECTROMETRIC ANALYSIS.

Gas mass spectrometry as applied to fluid inclusions concerns the analysis of the major volatile constituents H_2O, CO_2, CH_4, N_2, H_2, H_2S, Ar. The volatiles are released under vacuum either by crushing or heating the inclusion-bearing material and then passed into the source region of the mass spectrometer. Here the gas molecules are ionised and the resultant ion fragments analysed according to their mass/ion charge ratios. This facilitates precise

quantitative analysis of the inclusion volatiles. The composition and quantity of gas dissolved in ore solutions has a profound effect on their metal carrying capacity particularly for the epithermal precious metal deposits. Concentrations of Co_2 and H_2S fix for example the level of metal-sulphide complexing and determine the depth of boiling for near surface fluids. CO_2/CH_4 ratios reflect the oxidation state of the fluid and together with N_2 its probable origin. These and other geological parameters can be derived directly from volatile data as illustrated by the studies of Giggenbach (1980) for modern day geothermal fields.

Reference:

Giggenbach, W.F. 1980, Geothermal gas equilibria. Geochimica Cosmochimic Acta, v. 44, 2021-2032.

3. PREVIOUS BGS WORK IN SOUTH AMERICA.

The Isotope Geology unit of BGS (formerly Overseas Geological Surveys, then Institute of Geological Sciences) has had a long-standing involvement with South American countries in the field of geochronology in particular, through a variety of technical aid and co-operative research programmes funded by ODA and the former MOD. Indeed, systematic investigations began with work by the OGS in British Guiana (now Guyana) in the early 1960's and laid the foundation of an understanding of the evolution of the Precambrian Guyana Shield (Snelling, 1963; McConnell et al 1964). Subsequent mapping of Precambrian shield areas in Guyana and Bolivia by IGS/BGS teams also depended critically on geochronological support provided by the unit (Berrangé 1977, Litherland et al in press).

Geochronological work in the Andes was initiated in Chile (Clarke et al 1967), under the auspices of the Department of Technical Co-operation (until November 1964) and carried on for the Ministry of Overseas Development. Major contributions were subsequently made to determining the geochronological history of the Andes and their environment in Peru (see below), Ecuador (Kennerly 1980) and more recently in Colombia (for ODA), where successive accretion of westward-migrating igneous belts has been recognised (McCourt et al 1985). Work has also been undertaken in suppport of UN projects in Ecuador (Goosens & Rose 1973) and Argentina (Sillitoe 1976,1977).

Most of the above-mentioned work was in connection with broadly based reconnaissance programmes. In contrast to these, a large-scale programme of detailed study was carried out on the Coastal Batholith of Peru, where intensive mapping by BGS (Cobbing et al 1981) ran concurrently with in-depth research by workers from the University of Liverpool under the direction of Prof. W.S. Pitcher and with funding from MOD/ODA and the Natural Environment Research Council). An outline of the geochronology of the batholith was first given by Stewart et al (1974) and was extended by information acquired in the BGS laboratories by a succession of researchers who provided the detail necesary to a fuller understanding of its evolution (e.g. Wilson 1975, published in Snelling 1981; Sanchez-Fernandez 1982; Moore 1984; Beckinsale et al 1985). This culminated in one of the most comprehensive geological, geochemical and

geochronological memoirs ever produced on Andean magmatism (Pitcher et al 1985).

Other specific research projects involving only the Isotope Geology unit of BGS in collaboration with university groups are (i) an investigation of Bolivian mineral deposits, centred on the historic mining area of Potosi and (ii) a geochemical/geochronological study of Recent Andean volcanoes in northern Chile and Argentina. The first of these programmes is led by Dr C. Halls of Imperial College, London. One publication had already been completed before the initiation of Project ANDCHRON (Grant et al 1979), but further aspects of the work are included in this report. The second programme is in conjunction with Dr P.F. Francis of the Open University, with support from NERC and NASA (Baker 1977; Baker & Francis 1978), and follow-up work was again integrated with ANDCHRON.

Another relevant area where the unit has had a long-standing involvement is in West Antarctica, where Mesozoic-Cenozoic magmatic rocks correlative with the older parts of the Andes are developed throughout the Antarctic Peninsula. Within a wider geological context, they represent the once-continuous Pacific margin of the former supercontinent of Gondwana. Initial reconnaissance geochronology was carried out from 1964 under the auspices of the Overseas Geological Surveys, and since 1976 the British Antarctic Survey has had a resident staff member in the isotope geology unit working on this area (see Pankhurst 1982 and 1984).

As a result of this long association extending back over twenty years, the Isotope Geology unit of BGS has become a major contributor to the geological community's understanding of Andean problems and the main geochronological data bank for the Andes. With the recent work in Bolivia, Colombia, Ecuador and Peru, about half the length of the Andean chain had been covered, at least in outline, to modern standards of data collection and interpretation. The remaining half of the Andes which fell within Chile and Argentina and between the well-studied areas of southern Peru and the Antarctic Peninsula, represented a major gap in our knowledge and accordingly became the principal target of Project ANDCHRON. The main objectives of the project were thus:-

1. To undertake widespread geochronological data gathering within the relatively neglected regions of the Andes, particularly in Chile but to a lesser extent in Bolivia and Peru.

2. To incorporate new or previously untried techniques of investigation in order to constrain the petrogenetic controls on Andean magmatism (e.g. Sm-Nd isotope studies).

3. To consolidate the new data with existing knowledge and to produce an up-to-date interpretation of the geological evolution of these areas.

4. To compare the conclusions with current plate-tectonic theories for the evolution of the better-known parts of the Andes and West Antarctica.

5. To use stable isotope and fluid inclusion studies to investigate the evolution of typical metalliferous mineral deposits.

6. To direct attention to the impact of combined geochronological, radiogenic and stable isotope and fluid inclusion data on our understanding of metallogenic processes in the Andean environment.

7. To publicize this approach in South America and to foster relations with South American geologists so that such work could be continued in the future.

In practice, the project has served as a focus for interaction between several research groups in Britain and South America, especially in Chile where the main part of the work has been conducted as a three-way collaboration between BGS, the Servicio Nacional de Geologia y Mineria and the University of Chile in Santiago. Visits by Chilean counterparts to work and train in the BGS laboratories (in part with Royal Society funding) were coupled with the provision by the Chileans of invaluable organizational and logistic support for fieldwork by BGS staff. Renewed interest in the work on Bolivian metallogenesis (Imperial College) and Chilean volcanic studies (Open University) stimulated the recruitment of new research students. A Peruvian researcher based in Nottingham University was able to work in the BGS laboratories and in turn was able to facilitate the assistance of INGHEMET in fieldwork and an educational course in Peru.

The degree of international collaboration acheived has been a notable aspect of Project ANDCHRON. It has developed through the direct involvement of BGS (and BAS) staff in fieldwork which has carried over enormous benefits and understanding in the laboratory analysis, through the full involvement of Chilean and Peruvian geologists in the field collecting, through frequent consultation on the interpretation of new data and joint preparation of material for publication at conferences and in journals, through the visits of South American workers to Britain, through training (two research degrees have been awarded, including one to a visiting Chilean geologist from SNGM, and two further students are now completing their work) and through specialized training courses in the application of fluid inclusion and stable isotope techniques presentes by BGS staff in Santiago and Lima under the auspices of the local geological surveys. The interim results of the project have been advertized at the Sixth Gonwana Symposium in Ohio, August 1985 and at the final meeting of the IGCP Project 120 in Santiago, November 1985.

Project ANDCHRON began in October 1983 under the scientific management of Dr N.J.Snelling but since October 1984 has been directed and managed by Ms M. Brook. The other scientific staff who have been involved are Dr T.J. Shepherd, Dr B. Spiro and Dr R.J. Pankhurst (BAS).

References:

Baker, M.C.W. 1977. Geochronology of Upper Tertiary volcanic activity in the Andes of northern Chile. *Geol. Rundschau*, 66, 455-65.

Baker, M.C.W. & Francis, P.W. 1978. Upper Cenozoic volcanism in the central Andes: ages and volumes. *Earth Planet. Sci. Lett.*, 41, 175-87.

Beckinsale, R.D., Sanchez-Fernandez, A.W., Brook, M., Cobbing, E.J., Taylor, W.P. & Moore, N.D. 1985. Rb-Sr whole-rock isochron and K-Ar age determinations for the Coastal Batholith of Peru. In Pitcher et al 1985 (below).

Berrangé, J.P. 1977. The geology of southern Guyana, South America. *Overseas Memoir of the Institute of Geological Sciences, London*, No 4, 112pp.

Clarke, A.H., Mayer, A.E.S., Mortimer, C., Sillitoe, R.H. Cooke, R.U. & Snelling, N.J. 1967. Implications of isotopic ages of ignimbrite flows, southern Atacama Desert, Chile. *Nature*, 204, 115-8.

Cobbing, E.J., Pitcher, W.S., Wilson, J.J., Baldock, J.W., McCourt, W.J. & Snelling,

N.J. 1981. The geology of the Western Cordillera of northern Peru. *Overseas Memoir of the Institute of Geological Sciences, London*,No 5, 143pp.

Goosens, P.J. & Rose, W.I. 1973. Chemical composition and age determination of tholeiitic rocks in the Basic Igneous Complex, Ecuador. *Geol. Soc. Amer. Bull.*,84, 1043-52.

Kennerly, J.B. 1980. Outline of the geology of Ecuador. *Overseas Geol. Min Resources*, No. 55.

Litherland, M. & 15 others (in press). The geology and mineral resources of the Bolivian Precambrian shield. *Overseas Mem. Br. Geol. Surv.*, 9.

McConnell, R.B., Williams, E., Cannon, R.T. & Snelling, N.J. 1964. A new interpretation of the geology of British Guiana. *Nature*, 204, 115-118.

McCourt, W.J., Aspden, J.A. & Brook, M. 1984. New geological and geochronological data from the Colombian Andes: continental growth by multiple accretion. *J.geol. Soc. Lond.*, 141, 831-46.

Moore, N.D. 1984. Potassium-argon ages from the Arequipa segment of the Coastal Batholith of Peru and their correlation with regional tectonic events. *J. geol. Soc. Lond.*, 141, 511-19.

Pankhurst, R.J. 1982. Rb-Sr geochronology of Graham Land, Antarctica. *J. geol. Soc. Lond.*, 139, 701-12.

Pankhurst, R.J. 1984. Rb-Sr constraints of the ages of basement rocks of the Antarctic Peninsula. *In* R.L. Oliver, P.R. James & J.B. Jago (eds), *Antarctic Earth Science.* Australian Academy of Science, Canberra, 367-71.

Pitcher, W.S., Atherton, M.P., Cobbing, E.J. & Beckinsale, R.D. 1985. *Magmatism at a plate edge: the Peruvian Andes.* Blackie/Halstead Press, London.

Sanchez-Fernandez, A.W. 1982. Edades Rb-Sr en los segmentos Arequipa-Torquepala del batolito de la costa del Peru. *Quint. Congr. Lat.-Amer. Geol. Argentina, Actas*, III, 487-504.

Sillitoe, R.H. 1976. Andean mineralization: a model for the metallogeny of convergent plate margins. *Geol. Assoc. Canada, Spec. Paper*,14, 59-100.

Sillitoe, R.H. 1977. Permo-Carboniferous, Upper Cretaceous and Miocene porphyry copper-type mineralization in the Argentinian Andes. *Econ. Geol.*, 72, 99-103.

Snelling, N.J. 1963. Age of the Roraima Formation, British Guiana. *Nature*, 198, 1079.

Snelling, N.J. 1981. The radiometric ages. In Cobbing et al (1981) (above),90-102.

Stewart, J.W., Evernden, J.F. & Snelling, N.J. 1974. Age determinations from

Andean Peru: a reconnaissance survey. *Geol. Soc. Amer. Bull.*, 85, 1107-16.

Wilson, P.A. 1975. *Potassium-argon age studies in Peru, with special reference to the emplacement of the Coastal Batholith*. PhD thesis, Unive. of Liverpool.

4.AN INTRODUCTION TO ANDEAN GEOLOGY

The geomorphology of the South American continent is dominated by large-scale features which reflect fundamental geological sub-divisions: the Amazon Basin, the Brazilian Highlands, the Argentinian Pampas and the Andes. The Brazilian Highlands are based on one of the oldest geological features- Precambrian crystalline rocks first formed largely more than 2000 Ma ago. Other ancient shield areas or 'cratons' are the Guyana shield and the Arequipa massif in Peru (Fig. 4.1) and similar rocks may underlie the sedimentary cover of Amazonia and northern Argentina. These cratons acted as a framework of rigid kernels during the later geological evolution of the continent.

In contrast, the Andes, one of the major mountain chains of the world, contain some of the youngest rocks. Active volcanoes are distributed along the 7000km length of the Andes, several reaching heights of 6000m above sea level. The great elevation is partly due to the continuous construction of volcanic edifices over the past 50 Ma and partly due to the buoyancy of an exceptionally thick crust (up to 70km in the Central Andes). The next most obvious aspect is their continuous linear development close to the western margin of South America. The distribution and type of volcanic activity and associated earthquakes is related to the process of subduction of the eastern Pacific Ocean floor beneath the westward-moving landmass - an interpretation which combines the old idea of continental drift with the modern hypotheses of sea-floor spreading and plate tectonics. The production of distinctive calk-alkaline lavas such as *andesite* results both from frictional heating of the descending oceanic slab and from the release of volatiles into the overlying wedge of continental lithosphere. However, details such as the precise sites of melting and the relative contributions of mantle-derived and crustal materials (the latter either from the oceanic slab or from the base of the continent) are still contentious issues. Geochemical analysis, but especially isotope geology, is one of the most powerful tools available for resolving these problems, since it can be used to trace both magmatic source regions and interaction between magmas and the crust through which they pass before consolidation as granitoids or eruption as lavas.

Apart from the Arequipa massif, which is in an isolated position west of the Andes, most of the rocks exposed in the western seaboard region are of Palaeozoic age or younger. They are mostly of two types: deformed

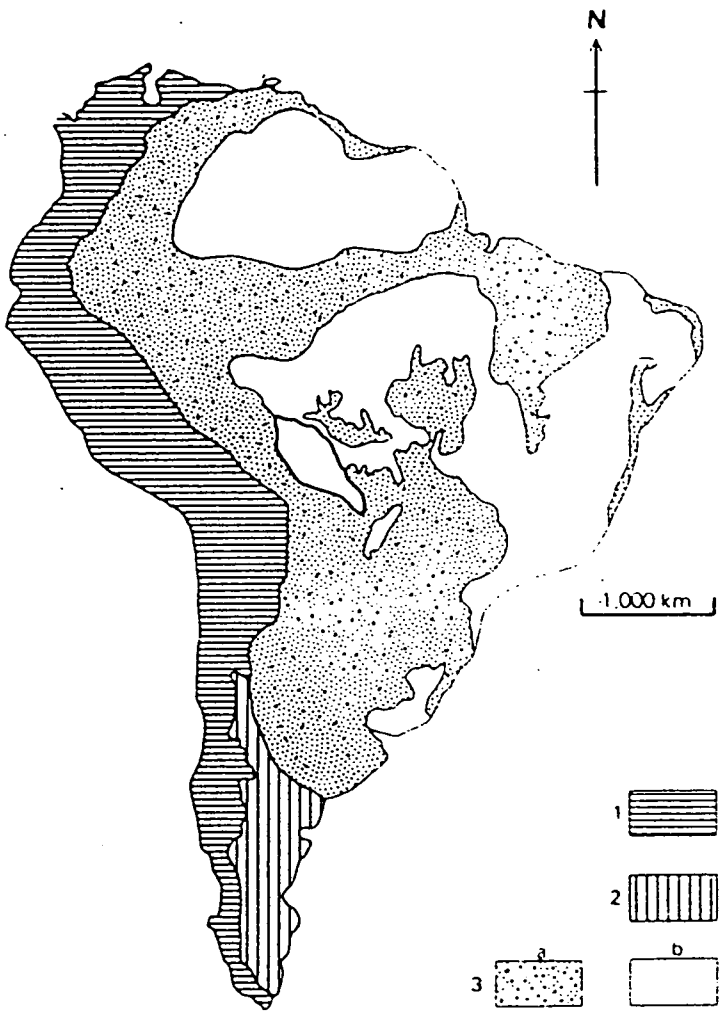

The major geotectonic regions of South America showing: (1) Andean Chain; (2) Patagonia Platform; (3) South America Platform—a, Phanerozoic cover; b, Brazilian Shield. The eastern Bolivia mapping area is in bold outline.

Fig. 4.1

metasedimentary sequences and long-lived belts of igneous rocks (again calc-alkaline granitoids and related volcanic rocks). The former are seen as largely of mixed oceanic and terrigenous provenance, having been deposited on the continental slope at an active margin. Together with the composition and coast-parallel distribution of the igneous belts, this argues for subduction-related tectonics and magmatism essentially similar to that currently taking place for at least the past 300 Ma. Since there is a significant mantle-derived input to the magmas of such arcs, subduction-related processes are considered to be a primary mechanism for continental growth, and South America has generally expanded westwards with time. Similar Mesozoic-Cenozoic magmatic arcs were concurrently active to the north in Central and North America and to the south in the Antarctic Peninsula. The longitudinal locus of magmatism clearly migrated episodically, mostly eastwards in the Central Andes, but westwards in Colombia, southernmost Chile and the Antarctic Peninula.

Two of the most outstanding questions on Andean geology concern the older rocks on which the mountain chain is constructed: (i) what is the full age range and nature of the Andean continental margin and to what extent is it floored by Precambrian or younger crystalline basement, and (ii) does it contain 'exotic terranes'? The latter are large areas of far-travelled crustal material carried along on the oceanic 'conveyor belt' but accreted onto the continental landmass rather than being dissipated by subduction. Many of these have now been recognized in North America.

Both questions are crucial to an understanding of metallogenic mineralization, since economic deposits are usually the end-product of re-distribution and concentration from pre-existing deeper crust. As with the igneous rocks, specific metalliferous occurrences in the Andes tend to form coast-parallel belts of considerable extent, implying a relationship to subduction processes. The way in which these belts vary, both transversely and along their length, partly depends upon their association with certain outcropping rock types, but much more importantly must be controlled by deep crustal stucture. Some metals are likely to be characteristically concentrated from old crystalline or metasedimentary basement, whereas others may be transported along with volatiles from sources in the underlying mantle.

A proper assessment of the observed metalliferous deposits and hence prediction of those not yet discovered will require a vast amount of background

investigation. Detailed isotopic study of individual mineral deposits and their surroundings are needed to identify the major ore processes involved and the extent to which local factors influence metal enrichment. However, the value of such data to metallogenic modelling can only be realised within the context of well understood regional crustal development. The Andes represent an excellent potential testing ground for this dual approach in that major north-south variations in geological evolution are apparent and clearly related to tectonic setting. Moreover, the vital significance of metal production to the economies of Andean countries makes this an especially worthwhile area. A disadvantage is that geological interpretation of the older history of the Andes is still rather undeveloped, especially as regards good geochronological data on the age relationships between important rock units. Thus a significant proportion of our contribution is in the field of geochronology. We have focussed our efforts on a number of traverses from the Pacific coast into the Andes from southern Peru to southern Chile. These were selected to display contrasting tectonic settings, from the north, where the continental crust is thick, old and complex, to southern Chile, where the situation is simpler.

Reference:

Litherland, M., Klinck, B.A., O'Connor, E.A. & Pitfield, P.E.J. 1985. Andean-trending mobile belts in the Brazilian Shield. *Nature*, 314, 345-8.

5. GEOCHRONOLOGY, ANDEAN MAGMA GENESIS AND REGIONAL TECTONICS.

In this section, our new geochronological results are presented and interpreted together with existing data in terms of the regional tectonic processes which have shaped the Andes. As explained above, the work has been concentrated in a number of transects from the coast to the main axis of the mountain chain, each of which exhibits significant differences in geological environments. This interpretation is then carried forward as a basis for the study of metallogenesis in the following Section.

5.1 CANAL REGION OF SOUTHERN CHILE.

The Andes of southern Chile are of rather subdued relief (<3000 m) and their geological environment is relatively simple. There are four main components, in order of increasing age:

I. A basement complex of low-grade metasedimentary rocks which crop out in the far west and appear to represent a mostly late Palaeozoic fore-arc accretionary prism.

II. A back-arc region of (? largely Jurassic) calk-alkaline or bimodal volcanic rocks which extend eastwards across the Magellanes continental platform of Argentina and Tierra del Fuego (e.g. the Tobifera formation).

III. A magmatic belt, mostly Mesozoic in age, to the west, comprising eroded plutons and volcanic rocks.

IV. Tertiary and Recent volcanic rocks, including some active volcanoes such as Cerro Hudson (45°50'S) which comprise the highest ground although they are not restricted to the main topographic axis.

These rocks are all related to long-lived subduction processes at the Pacific margin of South America. Within the Mesozoic magmatic belt south of 51°S, there is specific evidence of aborted marginal basins with oceanic floor which opened during the second half of the Jurassic period and closed during mid-Cretaceous times (e.g. the Sarmiento and Tortuga complexes). Unlike central and northern Chile, there are no outcrops of Palaeozoic plutonic rocks within the area and little evidence of any pre-existing continental crust. Some authors now regard this part of southern South America as comprising one or

several 'exotic terranes' of oceanic material accreted onto the continent during early Palaeozoic times.

In many respects these features may be seen as the northern continuation of the geological history of the Antarctic Peninsula region which is also composed of late Palaeozoic accretionary metasediments and a Mesozoic-Cenozoic magmatic arc and which would have been contiguous to southern Chile prior to the Miocene opening of the Scotia Sea.

For logistic reasons our work in this area was confined to the northern limits, in the Chonos Archipelago (by boat from Puerto Aysen) and the adjacent mainland, between latitudes 44°S and 47°S, following previous work by Chilean geologists (e.g. Hervé et al 1981) and the University of Leicester (Bartholomew & Tarney 1984). The results should be considered in relation to the above sub-divisions and Figure 5.1 and 5.2.

5.1a The Basement Complex

The metasedimentary rocks of the Chonos region have been divided into two N-S trending belts on the basis of lithological and structural variations (Godoy et al 1984). The eastern belt is composed of clastic rocks interpreted as submarine fan-turbidites with subordinate pelagic cherts, in which primary sedimentary structures are well preserved. It has itself been sub-divided into two units: the Potranca Unit, which is the more massive and represents a high-energy depositional environment close to the palaeo-shoreline, and the Teresa Unit, which is finer-grained amnd more thin-bedded, corresponding to more distal sedimentation. Both units exhibit NNW-trending subisoclinal-to-chevron folding, overturned to the SW and an axial plane cleavage (S_1) which is refolded to give a subhorizontal crenulation cleavage (S_2). The western belt is of more homogeneous mica-schists with minor greenschists representing deformed oceanic volcanic rocks. It is more intensely deformed by the second phase deformation, resulting in a pervasive NE-dipping S_2 foliation, and the metamorphic grade is higher than in the eastern belt. The nature and distribution of these structures is consistent with two successive stages of tectonism: the first associated with prograde construction of the prism, the second with intense shearing at the base during active subduction. It is not necessary that these separate events at specific times, since growth and

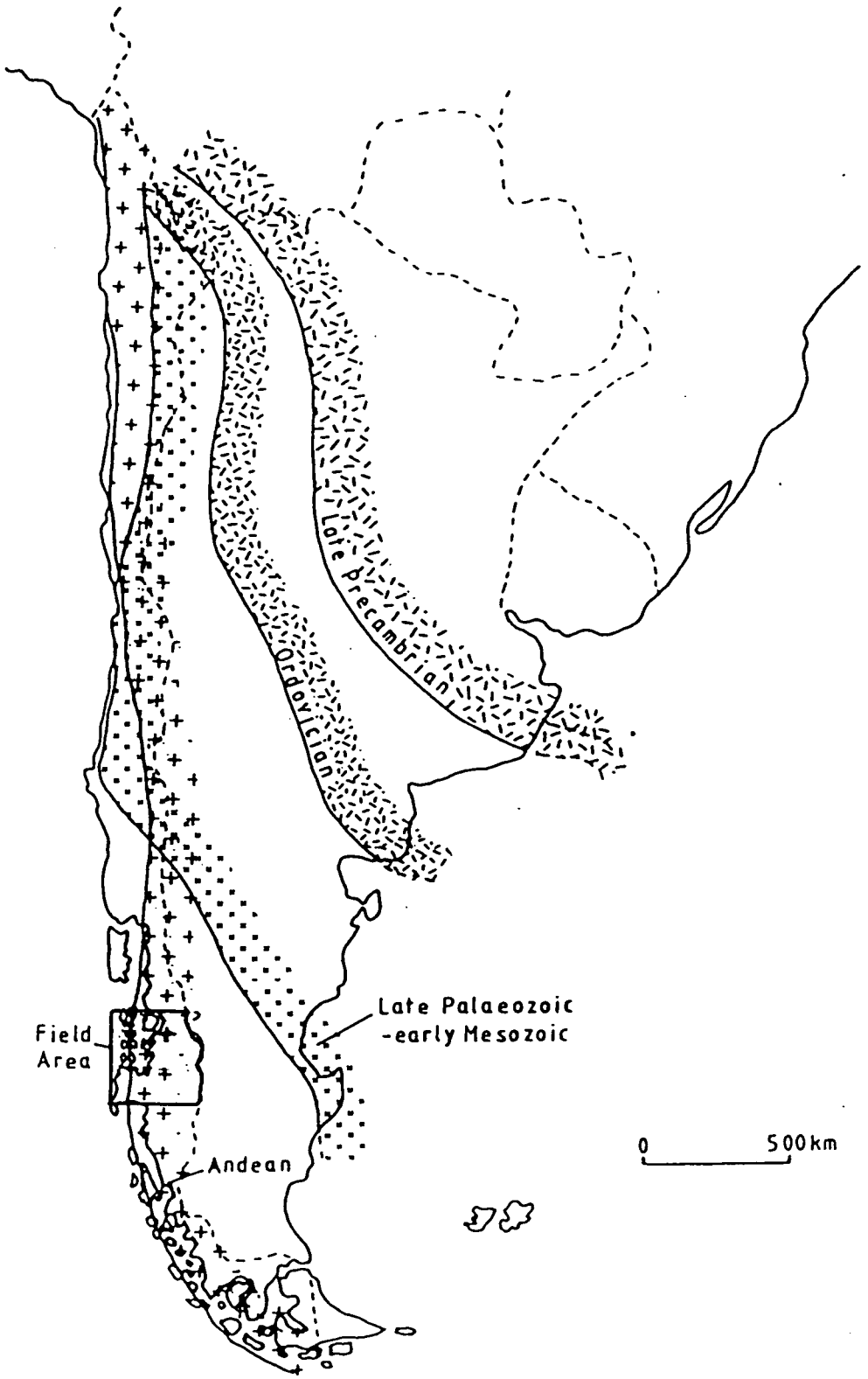

Fig. 5.1 Generalized sketch map of southern South America, showing the approximate positions of successive magmatic/metamorphic belts in late Precambrian, Early Palaeozoic, Late Palaeozoic and Mesozoic-Cenozoic (Andean) times. These could correspond to successive positions of the growing continental margin. The Canal Region field area is outlined. Adapted from Bartholomew (1984).

deformation of the accretionary wedge could be continuous throughout a long subduction history.

Only one fossil locality is known in the area, a fauna of deformed brachiopods from Isla Potranca having been assigned a Middle Devonian age by Miller & Sprechmann (1978). Elsewhere in southern Chile the majority of the sparse palaeontological evidence from discontinuous basement outcrops suggests a late Carboniferous to Permian age for deposition. Previous geochronological data from the study area consists of Rb-Sr and K-Ar dates from Islas Guaitecas (Godoy et al 1984), where Permian ages of close to 260 Ma were obtained from the less deformed eastern belt and Mesozoic ages of *c.* 140 Ma, interpreted as reset, from the western belt.

We have attempted Rb-Sr whole-rock isochron dating of fine-grained shales and schists from five new localities in an attempt to constrain the age range of depositon and deformation (Table 5.1). This method will tend to yield depositional (or rather, diagenetic) ages if the samples are (a) of very low metamorphic grade, (b) large (several kg) and (c) sampled over a moderately large area (e.g. 100 sq km). Conversely, small specimens of higher-grade rocks sampled over a few tens of metres are more likely to yield an age of local resetting. Intense deformation and cleavage formation can be as effective as metamorphism in this respect. Rocks with moderate Rb/Sr ratios which have accumulated appreciable amounts of radiogenic ^{87}Sr subsequent to diagenesis will, on complete resetting, generate a new isochron with an elevated $^{87}Sr/^{86}Sr$ ratio, provided that resetting occurs by closed system re-homogenisation, i.e. without loss of ^{87}Sr from the system or exchange with low $^{87}Sr/^{86}Sr$ fluids.

Isla Lemu.

Seven samples of coarse micaschists from a large sampling area (20x10 km) on islas Lemu, Kent and Dring (Figure 5.2.) were taken by Chilean collaborators early in the project and analysed in London. The data do not define an isochron, but scatter widely about a line corresponding to an age of 263 ± 52 Ma (Figure 5.3.). The slope of the line is to some extent justified by the intercept of 0.7079 ± 0.0011, which is reasonable for the mean initial $^{87}Sr/^{86}Sr$ ratio of such turbiditic sediments. Thus, despite the prevalence of a late cleavage in this area, the isochron systematics suggest that this is a close minimum age for either deposition or the pre-S_2 coarse metamorphic fabric. In essence this supports the late Palaeozoic sedimentation age inferred elsewhere.

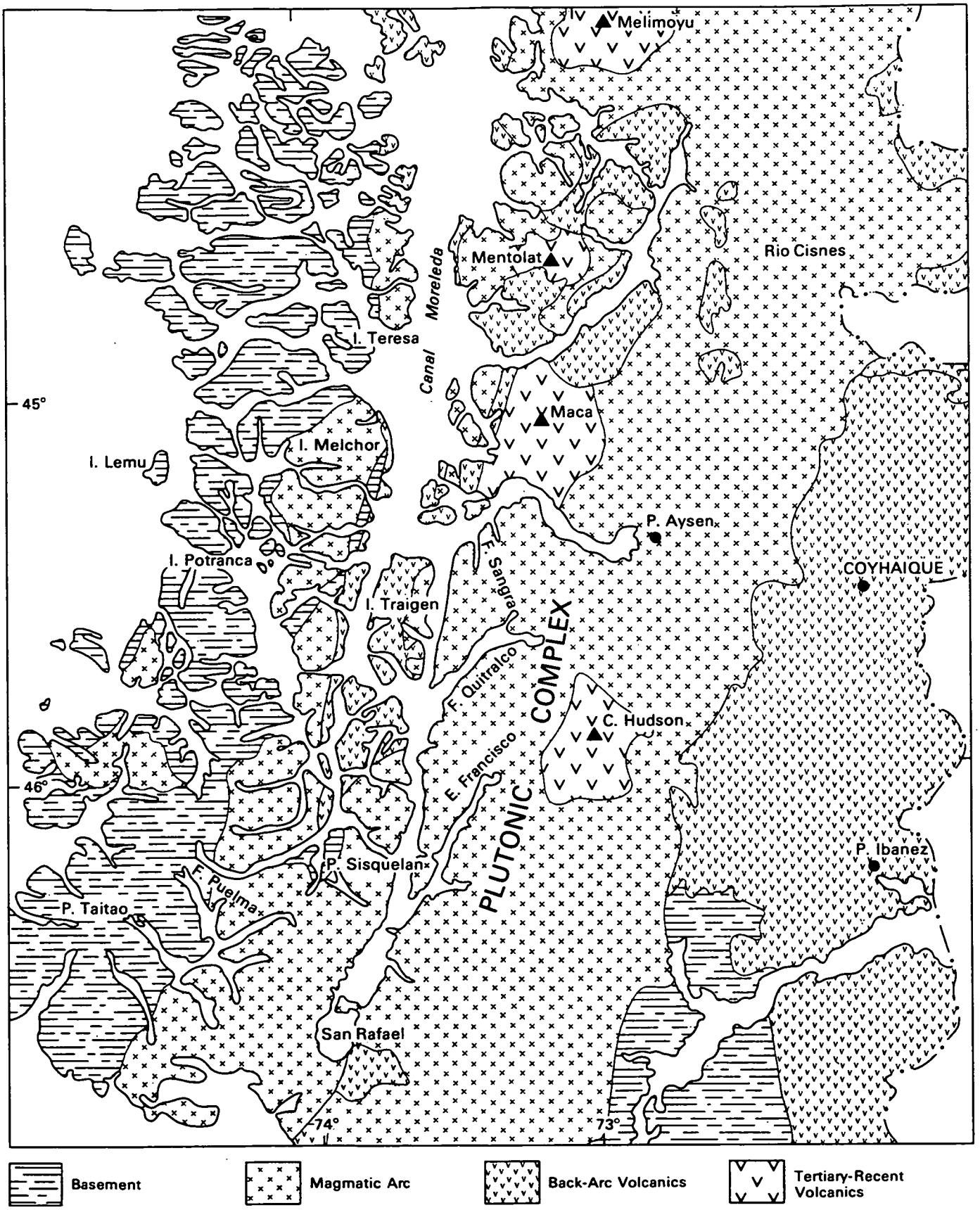

Fig. 5.2 Sketch map of the Canal Region of southern Chile, showing the major geological zones and place names referred to in the text.

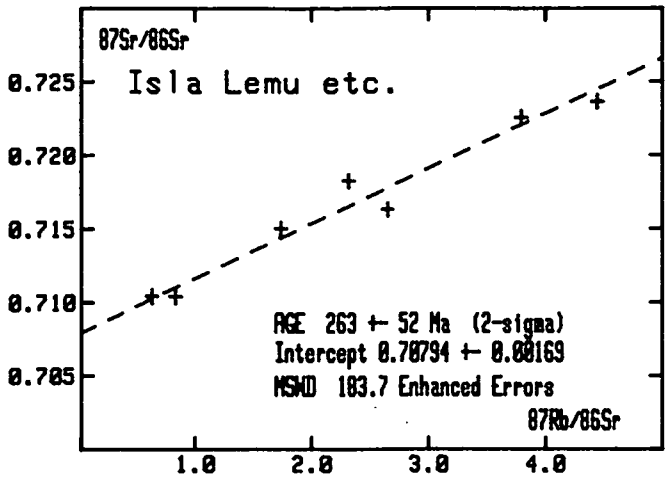

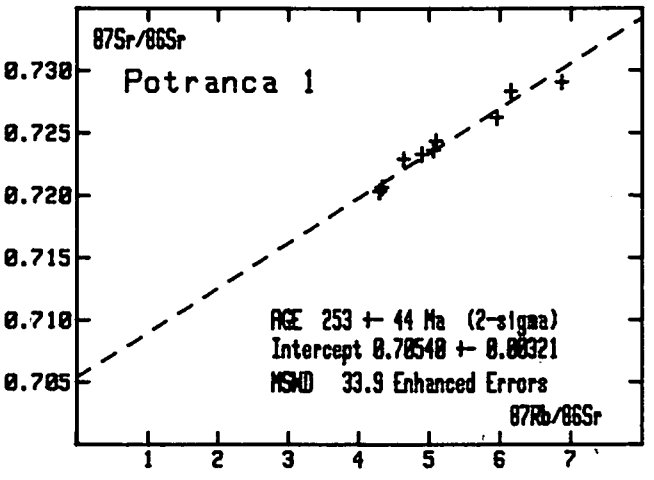

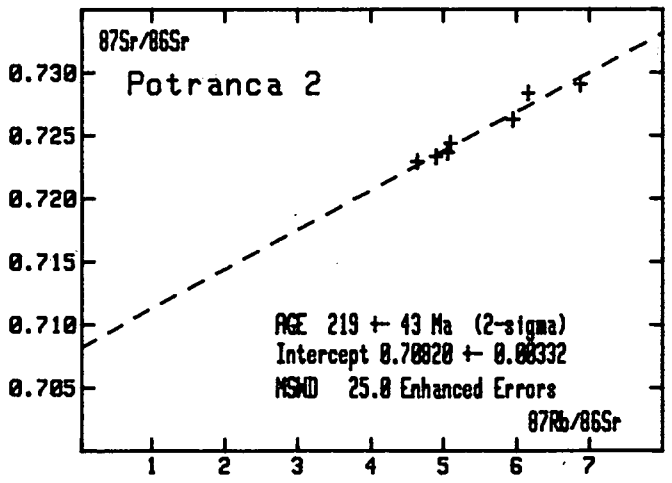

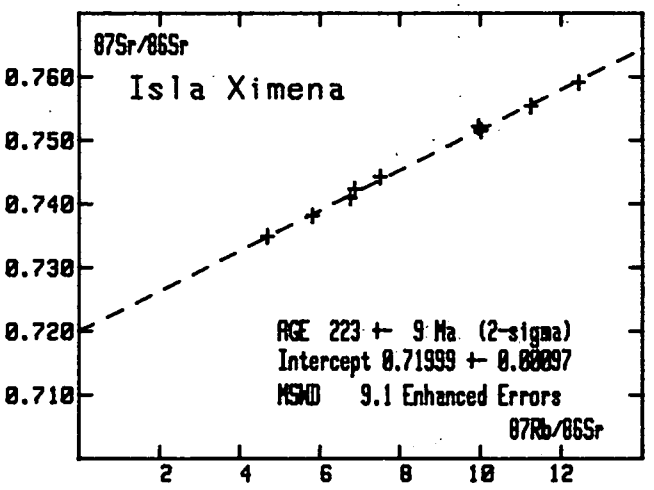

Fig. 5.3 Rb-Sr whole-rock isochron diagrams for island sites in the metasedimentary basement (1).

Isla Potranca.

Re-collection from the fossiliferous rocks here yielded no new palaeontological information as the samples were too badly deformed (H. Brunton, British Museum of Natural History, personal communication). Rb-Sr analysis of whole-rock shales from this crucial locality was also only partially successful (Figure 5.3.). The nine data points are again scattered about a possible Permian isochron (253 ± 44 Ma) with a sensible intercept of 0.7054 ± 0.0032 and fall well below any reasonable Devonian isochron. The scatter may indicate partial resetting - if the two lowest points are omitted, a somewhat improved fit to a younger line of 219 ± 43 Ma with an intercept of 0.7082 ± 0.0033 is obtained. Because of the high Rb/Sr ratios, closed system accumulation of ^{87}Sr is quite rapid in these samples and a pre-Permian age is impossible unless open system behaviour has occurred.

Isla Ximena.

Nine samples from two horizons at the same locality (red and black shales respectively) have given an errorchron (Fig. 5.3) with a reasonably small degree of scatter (MSWD=9.1). The age is rather younger than in the above examples - 223 ± 9 Ma with an intercept of 0.7200 ± 0.0010. This could represent later deposition, during Triassic times, although the high initial $^{87}Sr/^{86}Sr$ ratio may either indicate resetting or an ancient Rb-enriched source region. The *maximum* possible age of either sedimentation or provenance, assuming a mean $^{87}Rb/^{86}Sr$ ratio of 7.0, would be about 380 Ma (Middle Devonian).

'Isla Maureen'.

Seven samples of muscovite-bearing shales give an errorchron (MSWD=93) corresponding to an age of 215 ± 34 Ma (?Triassic-L.Jurassic) and an intercept of 0.7098 ± 0.0027 (Figure 5.4). The comparatively low age, the very high degree of scatter and the slightly high initial $^{87}Sr/^{86}Sr$ ratio are all suggestive of partial resetting and it is not necessary that the inferred age corresponding to a discrete event, i.e. it could be intermediate between the true ages of diagnesis and metamorphism. Assuming closed system behaviour and a mean $^{87}Rb/^{86}Sr$ ratio of 5.0, this interval is unlikely to exceed about 80 Ma, so that the depositional age of these rocks could not be older than Middle Carboniferous.

Isla Teresa.

Ten samples of pelitic shales showing a strong penetrative S_2 cleavage gave another reasonable fit to a line (MSWD=7.3), this time giving a Middle Jurassic age of 168 ± 5 Ma (the low error being due to the wide range in Rb/Sr ratios) with an intercept of 0.7144 ± 0.0002 (Fig. 5.4). This is most easily interpreted as almost complete resetting during the second phase of deformation. Calculations as above imply a maximum age of *ca.* 415 Ma.

Fjordo Puelma.

Eleven samples of highly cleaved pelitic schists (albeit from the eastern belt), gave a similar result to the above, i.e. 159 ± 11 Ma , intercept 0.7131 ± 0.0006, but with rather more scatter (MSWD=15.5). Eight of these, from a single 20 m outcrop, gave a perfect isochron (MSWD=2.2) suggestive of a single discrete event and corresponding to 134 ± 5 Ma and an intercept of 0.7141 ± 0.0002 (Fig. 5.4). This age is close to the Jurassic-Cretaceous boundary and is much younger than any other determined from the metasediments. Either deformation continued as late as this, or resetting has occurred in response to the thermal effects of the granite intrusion exposed some 5 km to the east (Figure 5.6 and below). Once again, the maximum closed sytem age of crustal development is Devonian (*ca.* 370 Ma).

Summary.

Six suites of metasedimentary basement rocks have been analysed, giving variably defined ages ranging from Permian to late Jurassic. The younger ages, which tend to be the better defined, mostly come from rocks in which the S_2 deformation phase is predominant and probably relate to resetting at this time or during Mesozoic orogenic activity. The older ages may reflect diagenesis, which would imply deposition of the turbiditic sediments throughout late Palaeozoic time. Such a diachronous development of the accretionary wedge is quite feasible, although there is little direct evidence for it. On the other hand, the individual data sets do not generally preclude an older and more uniform sedimentation age, with partial resetting during Permian times, perhaps due to thermal/deformational events associated with the late Palaeozoic magmatic arc to which they represent fore-arc accretion. This is emphasized by the isochron plot of Fig 5.4, in which the weighted mean of each data set is plotted as a single point. With the exception of the sets for Isla Potranca itself, and the nearby Isla 'Maureen', which may each have experienced an

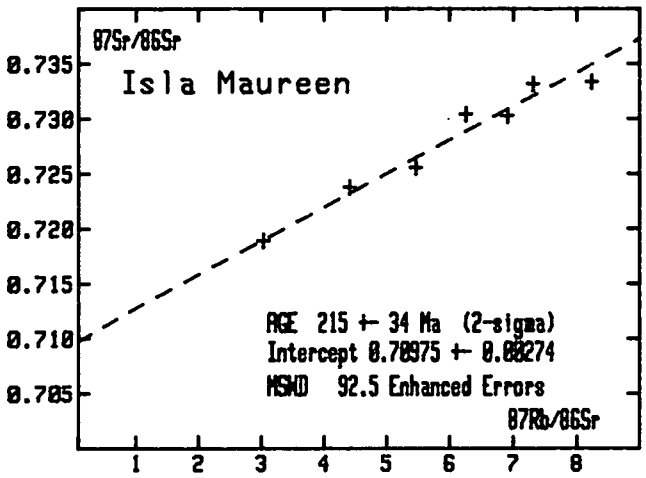

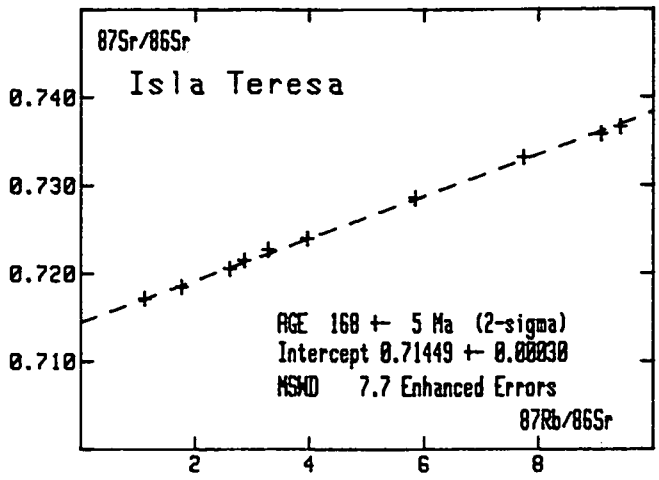

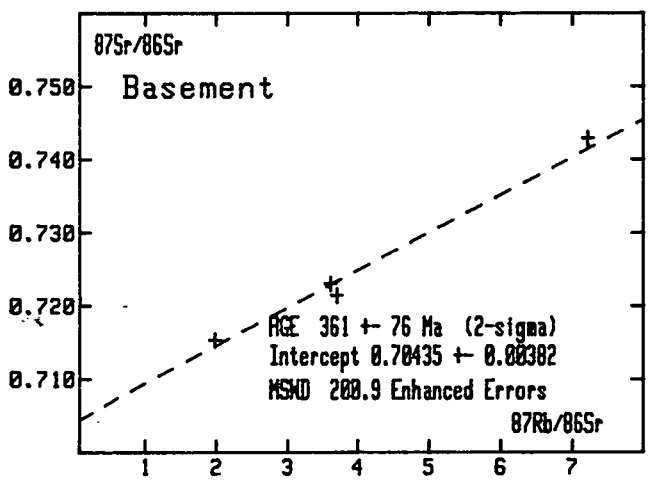

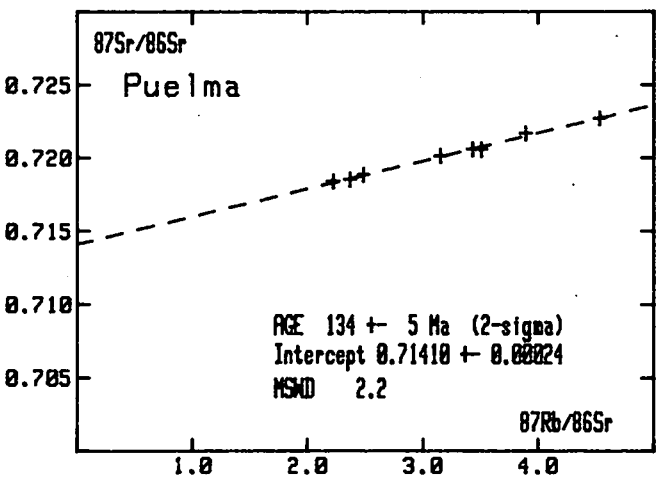

Fig. 5.4 Rb-Sr whole-rock isochron diagrams for island sites in the metasedimentary basement (2). The final diagram i s a plot of the weighted means of data suites for islas Lemu, Ximena, Teresa and Fiordo Puelma.

increase in Rb/Sr ratios during metamorphism, the array scatters about a line which is consistent with the oldest known palaeontological age for the rocks - Middle Devonian. The intercept on this line is 0.705 (albeit with a large error), which conforms with the idea that the provenance was chiefly oceanic sediments or juvenile calk-alkaline igneous rocks. Future application of the Sm-Nd system may resolve this further, but at this stage it is emphasized that there is no evidence for early Palaeozoic or older continental basement anywhere within the coastal domain of southern Chile - an important fact for any interpretation of the pattern of subsequent Andean igneous history.

5.1b Volcanic Rocks.

Ibañez Group.

Volcanic rocks which have been presumed to be equivalents of the Jurassic Tobifera formation were sampled from the Ibañez Group near Puerto Ibañez (Fig.5.2). These were red, purple and green pyroclastic rocks, mostly indurated tuffs and volcanic breccias. Such rocks are difficult to sample meaningfully for isochron dating and are generally thought to be prone to resetting. The data scatter, only slightly more than anticipated from analytical errors, about a line corresponding to 96 ± 12 Ma (Fig 5.5, Table 5.1). This would represent a Middle Cretaceous age for rocks well constrained by their stratigraphy as probably 170 Ma old. This implies resetting on a whole-rock scale during emplacement of the easternmost granite batholith (see below). This is also compatible with the moderately high initial $^{87}Sr/^{86}Sr$ ratio of 0.7076 ± 0.0003.

Laguna San Rafael.

Pyroclastic rocks very similar in appearance to those of the Ibañez Group crop out at Laguna San Rafael, on the western edge of the plutonic complex (see below). According to the 1:1,000,000 Geological Map of Chile (Inst. Invest. geol. 1980), these rocks are of Lower Cretaceous age, in common with other exposures along the Canal Moraleda. These have also given a much younger radiometric age, 36 ± 24 Ma (Fig. 5.5). Resetting is again the most likely explanation, the intercept of 0.7050 ± 0.0004 being compatible with a primary value of 0.7040 for these rocks 110 Ma ago. However, in this case the resetting event is clearly a very late one, associated with the Tertiary zone further characterized below.

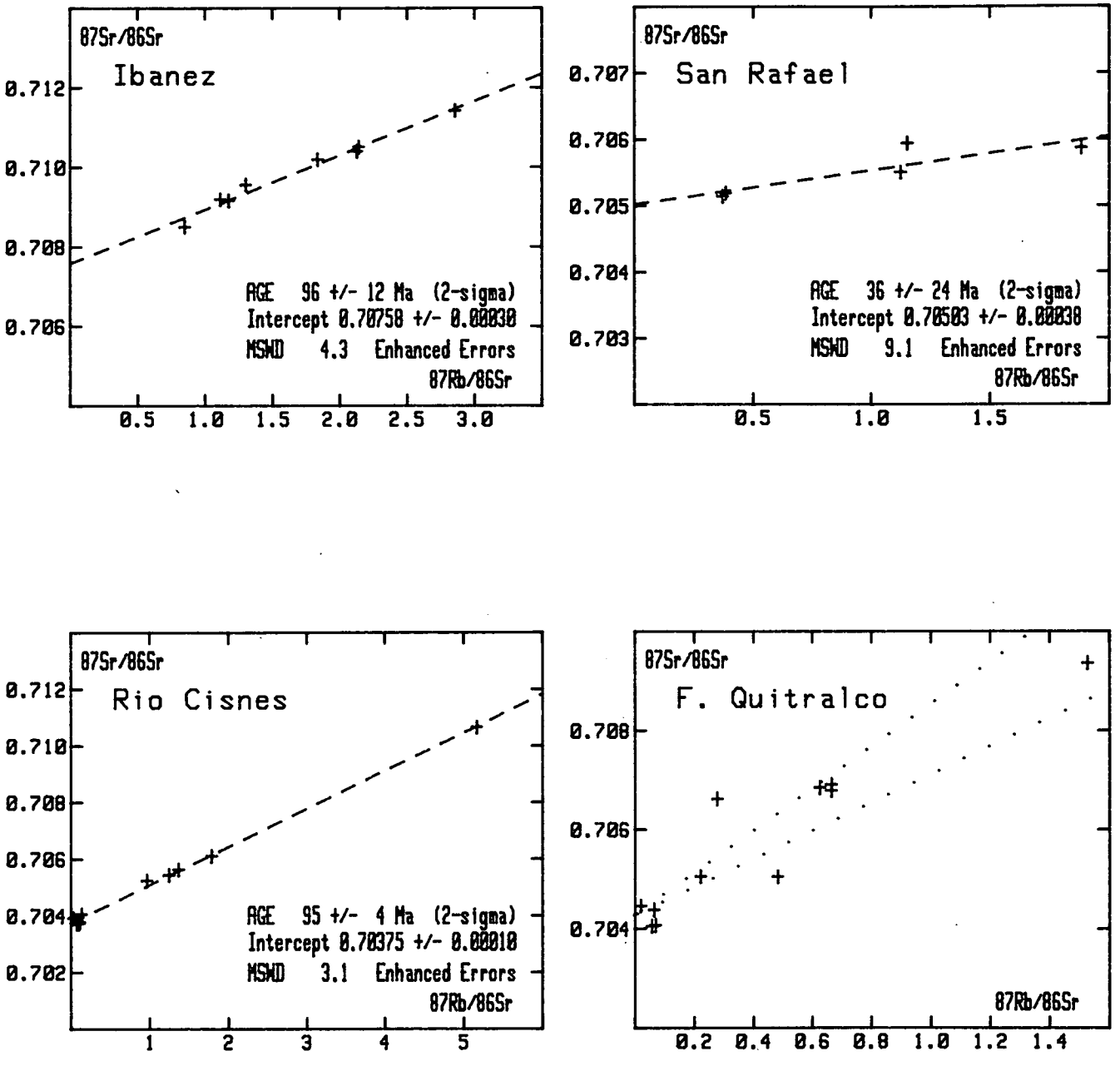

Fig. 5.5 Rb-Sr whole-rock isochron diagrams for back-arc volcanic rocks (top two diagrams), pink granite from the eastern belt of the Mesozoic arc (Rio Cisnes) and the plutonic complex at Fiordo Quitralco. The reference lines in the latter correspond to 200 and 300 Ma.

Thus neither attempt at dating volcanic rocks in this area was of stratigraphic use, but both served to identify the intensity and extent of thermal (or hydrothermal) events associated with later arc magmatism.

5.1c The Magmatic Arc.

Bartholomew & Tarney (1984) postulated five main components to the magmatic arc between 45°S and 46°S, which were, from E to W: (i) an eastern belt of rather uniform, high-level pink granites of Middle Cretaceous age, (ii) a plutonic complex of migmatites and tonalitic agmatites representing deep crustal emplacement of more primitive magmas, (iii) a zone of Jurassic and Cretaceous plutons emplaced into the metasedimentary basement complex discussed above, (iv) a zone of late Cretaceous volcanics and Tertiary trondhjemite and tonalite intrusions centred on the line of the Canal Moreleda and (v) small plutons of Late Cretaceous granite emplaced yet further west within the Palaeozoic accretionary prism. They correlated the formation of these N-S belts with episodic migration of the magmatic arc during alternating periods of compressional and extensional tectonics during active subduction. This analysis was based on only rather limited geochronological evidence but, working over a somewhat larger area, we have been able to substantiate and extend their main conclusions.

Rio Cisnes Granite.

Samples were taken from a new road-section through the eastern igneous belt in the upper Rio Cisnes (Fig. 5.2). A variety of rock-types was exposed, from coarse hornblende-plagioclase rocks to pink granite. All plot close to a straight line in the isochron diagram, but the age is best defined by the granites alone, which give 95 ± 4 Ma (MSWD = 3.1) with an intercept of 0.7038 ± 0.0001 (Fig. 5.5). This is in reasonably good agreement with two previous whole-rock isochrons for samples from the eastern batholith: 100 ± 6 Ma from Rio Simpson and 106 ± 9 Ma from Lago Paloma (Halpern & Fuenzalida (1978) as well as a number of comparable mineral ages (ibid; Bartholomew 1984). This suggests that this zone of the arc was formed during a short interval in mid-Cretaceous (Albian) times. The new data represent the best determination yet of the initial $^{87}Sr/^{86}Sr$ ratio of these rocks which are clearly derived from a low Rb/Sr source region, presumsably the upper mantle, with very little crustal contamination during emplacement.

Plutonic Complex.

Little data exists for this deeply eroded zone. Halpern and Fuenzalida (1978) report several Rb-Sr biotite ages from foliated diorites of *c.* 15 Ma, but Bartholomew (1984) obtained scattered whole-rock data suggesting ages of *c.* 100 Ma (with initial $^{87}Sr/^{86}Sr$ ratios of close to 0.7045). It has been generally assumed that the complex is an upthrust deep-level equivalent of the eastern batholith with Miocene reworking, supported by whole-rock isochron plots of 107 ± 18 and *c.* 92 Ma (Bartholomew 1984). Apparent older isochron trends of 400-520 Ma for garnetiferous migmatites from Fjordo Quitralco (Bartholomew 1984) were interpreted as mixing lines resulting from contamination with the metasedimentary basement exposed to the west. We have obtained a two-point intersection age of 222 ± 5 Ma (intercept 0.7089) for schists from Fiordo Sangra which seems to confirm that the accretionary metasediments are involved in this zone. Most of the remaining data is highly scattered, with the samples from Fiordo Quitralco plotting between reference lines corresponding to 200-300 Ma (Fig. 5.5), originating with a low $^{87}Sr/^{86}Sr$ ratio of *c.* 0.704, implying that some of the magmatism or migmatite formation is relatively old. On the other hand, samples of biotite-granites from Estuario Francisco trend with a much lower slope, probably confirming the involvement of Tertiary plutonism as suggested by the mica ages of Halpern & Fuenzalida (1978) and clearly established in the next zone to the west (see below). Results from the plutonic complex thus remain highly inconclusive, due in part to the logistic difficulties of sampling for isochron work but also showing evidence for a complex history of intrusion and reactivation.

Jurassic-Cretaceous granites.

Further west, the western belt of the Patagonian batholith consists of discrete granite-diorite plutons emplaced directly into the Palaeozoic metasediments. The Peninsula Gallegos pluton (furthest west) was dated by Bartholomew (1984) at 68 ± 2 Ma with an initial $^{87}Sr/^{86}Sr$ ratio of 0.7046 ± 0.0002, but the Taitao and Melchor plutons gave poorly defined ages of 181 ± 42 Ma and 132 ± 36 Ma respectively. Halpern & Fuenzalida (1978) also report a 176 Ma Rb-Sr biotite age from Isla Victoria. We have supplemented these data with a good whole-rock isochron age of 124 ± 2 Ma (MSWD=3.0) for a granite body in Fiordo Puelma (Fig 5.6.), confirming the importance of the very early Cretaceous magmatism. However, three samples from Peninsula Sisquelan lie on a much younger isochron of 23 ± 9 Ma (Fig 5.6). Most of the rocks have low initial $^{87}Sr/^{86}Sr$ ratios, that of the Puelma granite being the highest at 0.7051 ±

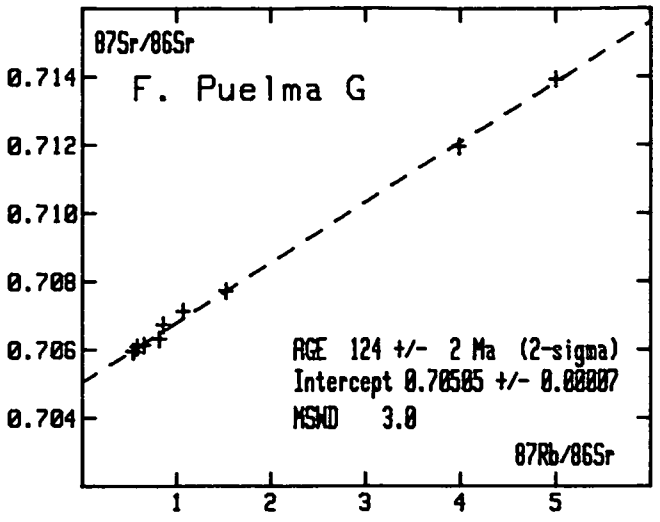

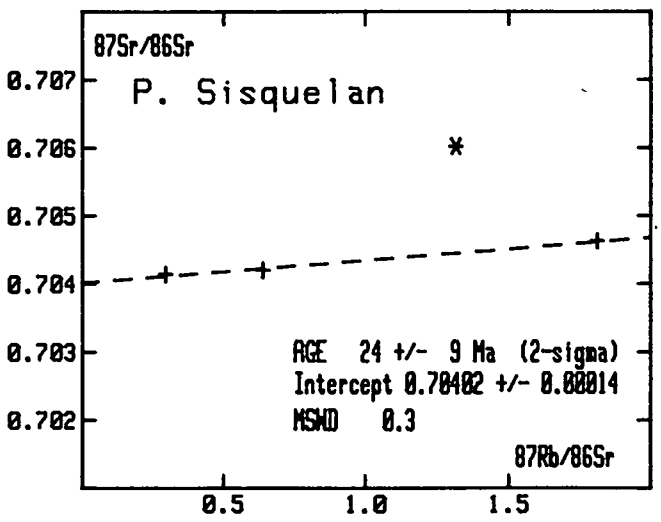

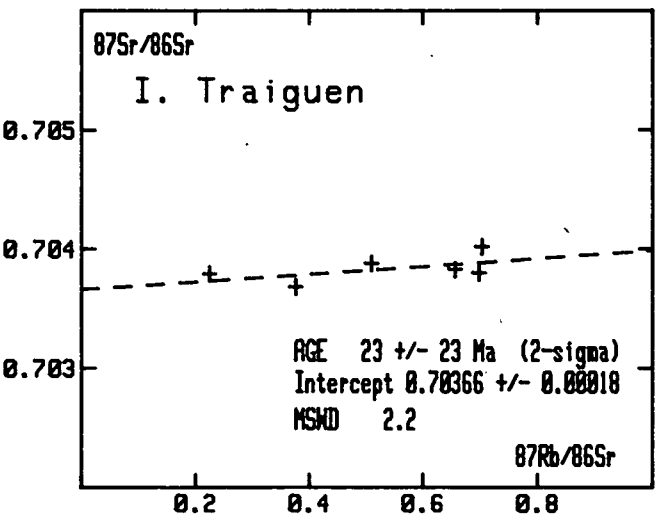

Fig. 5.6 Rb-Sr whole-rock isochron diagrams for granitic rocks from the western part of the Mesozoic-Cenozoic magmatic arc in the Canal Region.

0.0001. These clearly limit the degree of interaction between the mantle-derived primary magmas and the crustal metasediments to a minimum, and confirms the unlikelihood of any underlying older crust in southern Chile.

5.1d Tertiary Plutonism.

The junction between the archipelago and the mainland is the site of a down-faulted rift basin occupied by presumed late Cretaceous sediments and volcanic rock and intruded by biotite-granites similar to those further west. Bartholomew (1984) gave preliminary 2-point whole-rock Rb-Sr ages of 19 and 16 Ma for the Chaculay pluton, and we have obtained a good isochron (MSWD=2.2) for six samples from the granite exposed on south-east Isla Traiguen which yields an age of 23 ± 23 Ma and an intercept of 0.7037 ± 0.0002 (Fig. 5.6). The high error is due to the restricted range of Rb/Sr ratios, but the very low inferred initial $^{87}Sr/^{86}Sr$ ratio precludes any possibility of resetting of a pre-Tertiary age. This zone is probably the site of Neogene crustal extension and magmatism as envisaged by Bartholomew & Tarney (1984), but our evidence from E. Francisco and P. Sisquelan (above) suggests that it becomes a broader feature south of 46°S, with intrusion of mantle-derived granitic magmas into the older units on either side.

5.1e Conclusions.

The ANDCHRON programme in southern Chile has been reasonably sucessful in defining the age span and evolution of the Upper Palaeozoic accretionary wedge. Data for the igneous rocks is rather patchy due to sampling problems and heterogeneity and at this stage still incomplete due to the fact that the 1984/85 samples and mineral separates have not yet been received from Chile. The overall pattern is consistent with existing ideas of development at the continental plate margin by accretion of both terrigenous and oceanic sediments, welded onto the continental landmass during Mesozoic time by subduction-related magmatism. The igneous rocks, with the possible exception of some members of the 'plutonic complex', were derived from primitive (upper mantle) source regions and did not react significantly with older rocks, probably indicating that they were mostly emplaced during periods of aborted back-arc extension.

References:

Bartholomew, D.S. 1984. *Geology and geochemistry of the Patagonian batholith (45° - 46° S), Chile.* PhD thesis, University of Leicester.

Bartholomew, D.S. & Tarney, J. 1984. Crustal extension in the southern Andes (45°-46°S). In B.P. Kokelaar, M.F. Howells & R.A. Roach (eds).,Volcanic processes in marginal basins. *Spec. Publ. Geol. Soc., Lond.*, 195-205.

Godoy, E., Davidson, J., Hervé, F., Mpodozis, C. & Kawashita, K. 1984. Deformacion sobre impuesta y metamorfismo progresivo en un prisma de acrecion paleozoico: Archipielago de los Chonos, Aysen. In IX Congr. Geol. Argent. Actas, Bariloche.

Halpern, M. & Fuenzalida, R. 1978. Rubidium-Strontium geochronology of a transect of the Chilean Andes between latitudes 45° and 46° S. *Earth Planet. Sci. Lett.*, 41, 60-6.

Hervé, F., Davidson, J., Godoy, E., Mpodozis, C. & Covacevich, V. 1981. The late Palaeozoic in Chile, stratigraphy, structure and possible tectonic framework. *Rev. Ac. Bras. Cienc.*, 53, 362-73.

Miller, H. & Sprechmann, P. 1978. Ein Devonische faunula aus dem Chonos-Archipel Region Aisen, Chile und ihre stratigraphische Bedeutung.*Geol. Jahrb., Reiche.* B, 28, 37-45.

TABLE 5.1 Rb/Sr DATA FROM SOUTHERN CHILE

	Rb ppm	Sr ppm	$^{87}Rb/^{86}Sr$	$^{87}Sr/^{86}Sr$
I. BASEMENT				
ISLAS LEMU-KENT-DRING				
SLL 215	73	255	0.834	0.71040
SLL 220	53	242	0.629	0.71042
SLL 226	88	96	2.647	0.71633
SLL 229	65	109	1.734	0.71501
SLL 231	218	142	4.441	0.72364
SLL 232	195	143	3.791	0.72255
SLL 256	74	92	2.312	0.71825
ISLA POTRANCA				
SLL 335A	196	122	4.638	0.72292
SLL 335B	192	109	5.094	0.72436
SLL 335C	174	103	4.896	0.72330
SLL 335D	174	85	5.949	0.72626
SLL 335E	187	88	6.154	0.72835
SLL 338A	200	84	6.867	0.72907
SLL 338B	154	88	5.057	0.72361
SLL 338C	145	96	4.326	0.72062
SLL 338D	155	105	4.291	0.72028
ISLA XIMENA				
SLL 383	149	92	4.689	0.73490
SLL 385	178	89	5.806	0.73817
SLL 386	211	82	7.503	0.74425
SLL 387	222	94	6.870	0.74229
SLL 388	205	88	6.765	0.74093
SLL 389	202	59	10.013	0.75154
SLL 390	199	58	9.947	0.75216
SLL 391	233	55	12.430	0.75910
SLL 392	211	55	11.252	0.75537

	Rb ppm	Sr ppm	$^{87}Rb/^{86}Sr$	$^{87}Sr/^{86}Sr$
ISLA MAUREEN				
SLL 339A	76	72	3.030	0.71892
SLL 339B	198	70	8.238	0.73340
SLL 339C	162	75	6.253	0.73038
SLL 339D	160	105	4.407	0.72374
SLL 339E	179	71	7.300	0.73315
SLL 339F	147	62	6.903	0.73025
SLL 339G	179	95	5.467	0.72554
ISLA TERESA				
SLL 403	134	43	9.088	0.73581
SLL 404	153	47	9.422	0.73661
SLL 405	65	57	3.267	0.72270
SLL 406	62	63	2.863	0.72147
SLL 407	64	105	1.761	0.71846
SLL 408	84	61	3.962	0.72393
SLL 409	182	68	7.745	0.73318
SLL 410	71	78	2.605	0.72050
SLL 411	52	134	1.122	0.71714
SLL 412	127	63	5.843	0.72856
FIORDO PUELMA				
SLL 300A	59	72	2.367	0.71855
SLL 300B	188	120	4.531	0.72273
SLL 300C	65	76	2.485	0.71885
SLL 300D	114	105	3.151	0.72015
SLL 300E	160	119	3.895	0.72170
SLL 300F	72	59	3.506	0.72058
SLL 300G	46	60	2.219	0.71842
SLL 300H	102	86	3.432	0.72061
SLL 301A	132	67	5.700	0.72580
SLL 301B	123	66	5.351	0.72540
SLL 301C	182	82	6.438	0.72818

	Rb ppm	Sr ppm	$^{87}Rb/^{86}Sr$	$^{87}Sr/^{86}Sr$
II.VOLCANICS.				
IBAÑEZ				
84/29	146	198	2.131	0.71040
84/30	83	204	1.173	0.70916
84/31	172	233	2.146	0.71051
84/32	114	179	1.835	0.71019
84/33	48	165	0.848	0.70850
84/34	100	261	1.112	0.70919
84/35	106	237	1.299	0.70956
84/36	145	147	2.855	0.71142
SAN RAFAEL				
SLL 276B	77	193	1.153	0.70594
SLL 276D	126	193	1.885	0.70587
SLL 276E	100	257	1.126	0.70550
SLL 276F	46	360	0.372	0.70514
SLL 276G	113	846	0.385	0.70519
III. MAGMATIC ARC				
RIO CISNES				
84/10	156	270	1.678	0.70717
84/11	112	198	1.639	0.70731
84/12	24	508	0.137 (±1%)	0.70405
84/13	6	531	0.033 (±4%)	0.70392
84/14	27	693	0.113 (±1%)	0.70378
84/15	23	612	0.108 (±1%)	0.70374
84/16	104	168	1.787	0.70611
84/17	54	339	0.462	0.70482
84/18	88	261	0.981	0.70586
84/19	58	425	0.393	0.70461
84/20	70	208	0.967	0.70524
84/21	98	208	1.370	0.70563
84/22	88	205	1.249	0.70544
84/23	133	75	5.164	0.71066
84/24	14	540	0.076 (±2%)	0.70373
84/25	102	236	1.257	0.70558
84/26	113	81	4.029	0.70937
FIORDO SANGRA				
SLL 331A	150	100	4.330	0.72257
SLL 331B	57	276	0.597	0.71076

	Rb ppm	Sr ppm	$^{87}Rb/^{86}Sr$	$^{87}Sr/^{86}Sr$
QUITRALCO				
SLL 307A	17	769	0.066 (±1%)	0.70438
SLL 307B	15	745	0.059 (±1%)	0.70405
SLL 307C	18	788	0.071 (±1%)	0.70407
SLL 307D	6	850	0.020 (±4%)	0.70446
SLL 308	58	255	0.666	0.70697
SLL 310A	38	399	0.278	0.70662
SLL 310B	69	315	0.627	0.70685
SLL 311	96	180	1.529	0.70936
SLL 320	29	381	0.222	0.70505
SLL 321	61	365	0.483	0.70505
SLL 322	60	264	0.665	0.70679
ESTUARIO FRANCISCO				
SLL 280	7	373	0.057 (±3%)	0.70306
SLL 281	22	485	0.523 (±1%)	0.70420
SLL 282A	18	417	0.127 (±2%)	0.70494
SLL 282B	31	600	0.150 (±1%)	0.70481
SLL 282C	7	440	0.047 (±4%)	0.70510
SLL 283	20	682	0.086 (±1%)	0.70420
SLL 285B	23	979	0.067 (±1%)	0.70433
SLL 285C	53	435	0.350	0.70485
FIORDO PUELMA				
SLL 298A	53	287	0.535	0.70595
SLL 298B	56	279	0.582	0.70609
SLL 299	109	199	1.526	0.70773
SLL 306B	79	280	0.818	0.70632
SLL 306C	57	305	0.542	0.70595
SLL 306E	134	98	3.986	0.71196
SLL 306F	132	77	4.999	0.71393
SLL 294	71	242	0.857	0.70673
SLL 295	84	228	1.067	0.70713
SLL 297	60	269	0.652	0.70614

	Rb ppm	Sr ppm	$^{87}Rb/^{86}Sr$	$^{87}Sr/^{86}Sr$
PUERTO SISQUELAN				
SLL 287	73	161	1.318	0.70602
SLL 288	25	249	0.296 (±1%)	0.70414
SLL 289	69	110	1.814	0.70463
SLL 290	48	218	0.638	0.70420
IV. TERTIARY BASIN				
ISLA TRAIGEN.				
SLL 323	12	161	0.225 (±2%)	0.70397
SLL 324A	24	134	0.510 (±1%)	0.70388
SLL 324B	29	119	0.704 (±1%)	0.70402
SLL 327A	34	141	0.698 (±1%)	0.70380
SLL 327B	33	144	0.657 (±1%)	0.70383
SLL 328	21	164	0.376 (±1%)	0.70368

5.2.THE COASTAL BATHOLITH OF CENTRAL CHILE.

Central and northern Chile differ from the region just described, by the presence of a well defined Palaeozoic magmatic belt. A few isolated Lower Palaeozoic plutons are known from the extreme north of Chile, adjacent to known extensions of the Brazilian and Arequipa shields. Plutonism which is undoubtedly related to subduction processes began in the northeastern part of the Eastern Altiplano in Carboniferous-Permian times and spread westward as far as the coastal ranges by Triassic times. Throughout much of central Chile the Palaeozoic plutons are geographically split between the Altiplano in the east and the Coast Ranges in the west. However, unlike the Mesozoic-Cenozoic igneous belts, the Palaeozoic belt does not parallel the present day coastline, but swings away eastwards across the axis of the Andes south of about 38°S (Fig. 5.1), probably due to smaller size of the pre-existing continent. Moreover, the coastal part of the belt is not seen north of 25°S. During Mesozoic and Cenozoic times, plutonism developed in the west and progressed eastward paralleling the present day coastline and crosscutting the trend of the pre-existing Palaeozoic belt. These later magmatic belts are thought to be related to thinning and rupturing of the continental margin during aborted back-arc spreading. The evidence for this concept is discussed in more detail in Section 5.3.

A comprehensive reconnaissance of part of the coastal batholith has been undertaken in central Chile in liason with staff from the University of Chile in Santiago. The study extends fron latitude 30°30'S to 37°S. The area is readily divided into two sections by the east-west valley of the Aconcagua River, 32°30'S. South of this divide (Fig. 5.7), late Carboniferous to early Permian granitoids dominate the magmatic belt and were intruded into an accretionary prism which underwent contemporaneous metamorphism. Jurassic plutons increase in volume northwards and Cretaceous plutons occur further east. North of the Aconcagua river, a presumed east-west fault zone limits the northerly extent of the Palaeozoic plutons which do not reappear for some 500kms. However, the continuity of the Mesozoic and Cenozoic granitoids is unaffected by this boundary and they can be traced continuously across it. The Mesozoic and Cenozoic outcrops parallel the coast in discrete north-south trending belts which show distinct age ranges and a pronounced eastward migration of magmatism with time. The jumps in the sites of the magmatic belts correspond

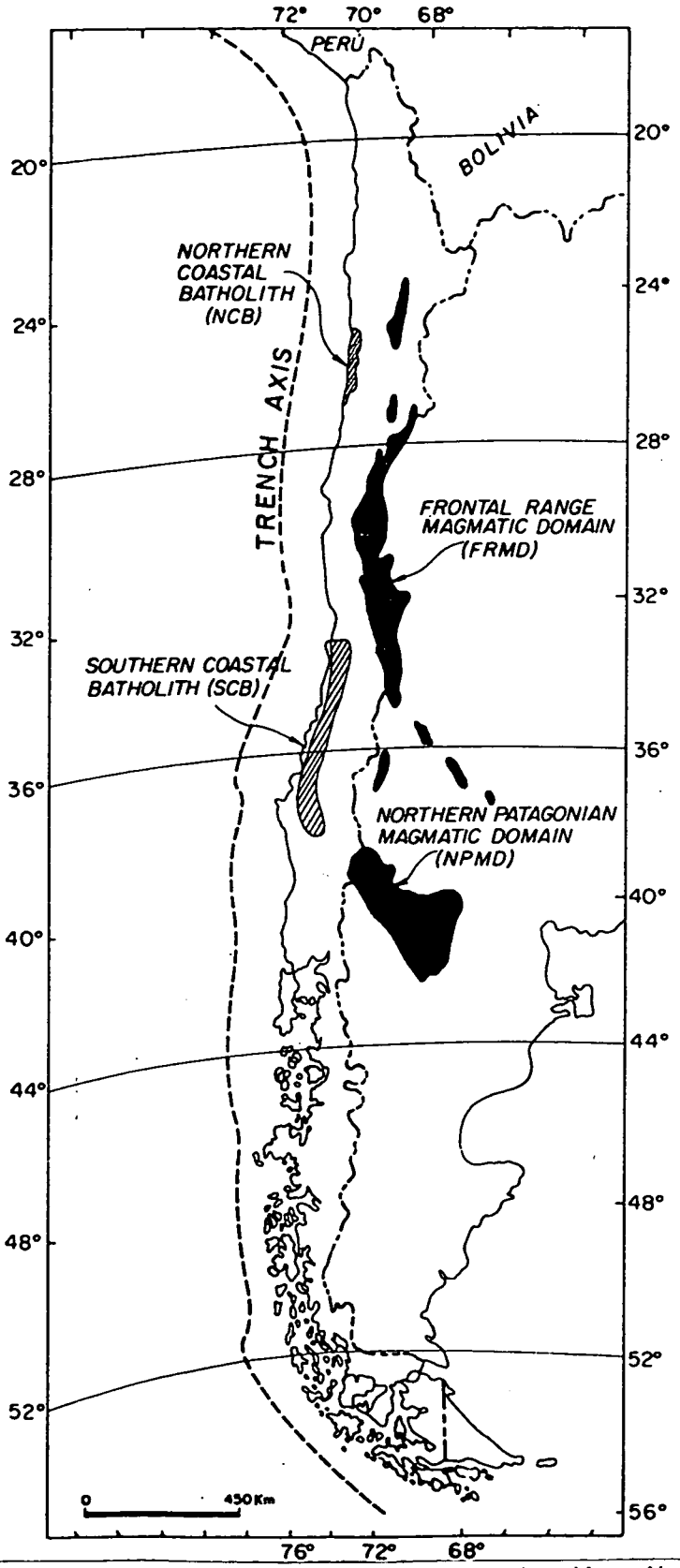

Fig. 5.7 Sketch map of South America showing the distribution of Palaeozoic magmatic belts. The Southern Coastal Batholith is the main subject of Section 5.2a, the Northern Coastal Batholith and Frontal Range are dealt with in Sections 5.3 and 5.4

to essentially non-magmatic intervals and may relate to hiati in subduction or changes in the dip angle of the subducted lithosphere. Periods of rapid migration may correspond to other significant changes in the Pacific Ocean spreading history.

5.2a Granitoids of the Coast Range of Central Chile 32°30'S - 38°S.

The coast range of Central Chile is of low relief and is separated from the main Andean range by the Central Valley, a late Cenozoic tectonic depression which parallels the continental margin. Rock exposures are usually spectacular at the coast itself, but are very limited inland, a fact which has precluded detailed mapping of the area. The only geological map available for the region as a whole is at a scale of 1:1.000.000 (a sketch map is shown in Fig. 5.8).

This southern part of the coastal batholith (SCB; Hervé et al in press). is mainly composed of tonalite, granodiorite, diorite with minor gabbro and granite. Andesitic and dacitic dykes and minor bodies intrude the granitoids. Near its northern end, cordierite-garnet-sillimanite gneisses are included in the magmatic rocks, apparently as rafts of the country rock. To the south, the batholith is flanked on its western side by a low P/T metasedimentary belt, in which biotite, andalusite and sillimanite zones develop on approaching the granitoids. In the Nahuelbuta mountains, undated metasediments also crop out east of the granitoids. The metamorphic rocks are part of a subduction complex which developed in the proto-Pacific margin of Gondwana during late Paleozoic times. As in southern Chile (Section 5.1), the eastern portions of this complex consist mainly of flyschoid detrital sequences, with preserved primary sedimentary features, and a weak crenulation foliation, whereas the western portions consist of grey schist, metabasic rocks of oceanic affinities, cherts serpentinite and minor marble, and has a very prominent S_2 flat-lying foliation. In contrast to southern Chile, however, it is the eastern portion into which the igneous rocks are mostly emplaced.

Stratigraphic evidence for the Palaeozoic age of SCB granitoids is scarce. Late Triassic sediments, sometimes with volcanic horizons, unconformably overlie the SCB granitoids in the lower course of the Bio-Bio river, near Santa Juana (Tavera, 1960), near Cauquenes (Lagno 1981) in the eastern flank of the Coast Range between Cauquenes and the Maule river (IIG 1982), and in the western coastal areas near Vichuguen and Hualane (Corvalan, 1976). These suggest a

Fig. 5.8 Geological sketch map of the area of the Coastal Batholith of central Chile south of the Rio Aconcagua.

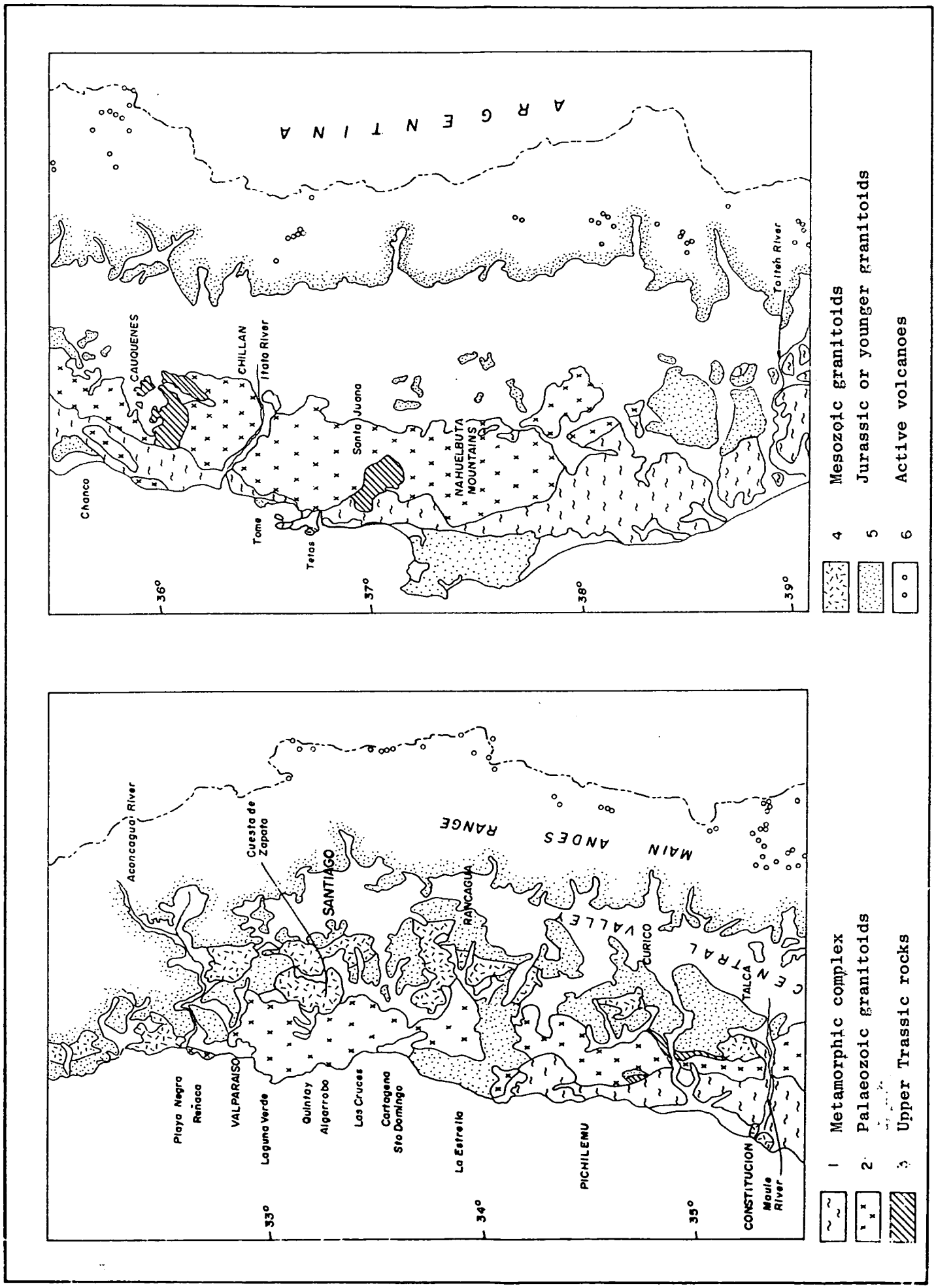

minimum age of *c.* 220-230 Ma for the batholith. Late Cretaceous sediments overlie the SCB granitoids in isolated patches along the shoreline from Algarrobo in the north, to Matanzas, Chanco, and Tome. The Triassic cover rocks are mildly folded, rarely develop a slaty cleavage and are essentially unmetamorphosed.

The Coast Range in the considered sector constituted a fore-arc region to the large-scale magmatic arcs developed along the margin of South America during Mesozoic and Cenozoic times. The metamorphic rocks appear to extend westwards as far as the inner slope of the Chile-Peru trench, as revealed by seismic records (Mordojovich, 1976).

Palaeozoic ages.

The oldest radiometric dates are Pb-U ages of *c.* 400 Ma for zircons from amphibolites and granitoids at Quintay (Corvalan and Munizaga, 1972). Unfortunately no indications were provided as to the crystallographic characteristics of the zircon populations analysed, and it is now known that such rocks often contain older 'inherited' zircons. A Silurian-Devonian tectonomagmatic phase (the "Quintay phase") was postulated on the basis of these data.

Shibata et al.(1984) have reported an Rb-Sr whole-rock isochron of 296 ± 5 at Valparaiso. New Rb-Sr isochrons (based on the data in Table 5.2) near the northern part of the batholith have yielded ages of 299 ± 31 Ma at Reñaca, 292 ± 2 Ma at Algarrobo and 308 ± 15 Ma at Santo Domingo (Fig. 5.9).. In the Nahuelbuta mountains, where the core of the batholith is mainly composed of tonalite and granodiorite, new Rb-Sr data define a 294 ± 24 Ma isochron (Fig. 5.9) which is consistent with a 312 ± 35 Ma age previously presented by Hervé et al. (1976). The similarity in age with the rocks of the northern end of the SCB is further stressed by a set of K-Ar biotite ages which range from 284 ± 5 Ma to 298 ± 4 Ma. At Rio Itata (36°30'S), a Rb-Sr whole-rock errorchron of 372 ± 5 Ma was obtained from granitoids which yielded a K-Ar biotite age of 296 ± 2 Ma.

Thus all these results are consistent with a single magmatic event *c.* 295 ± 5 Ma ago (very close to the Permian-Carboniferous boundary). The importance of this late Paleozoic igneous event is evident throughout the length of the SCB. Its intensity is recorded by almost complete resetting of Rb-Sr systems

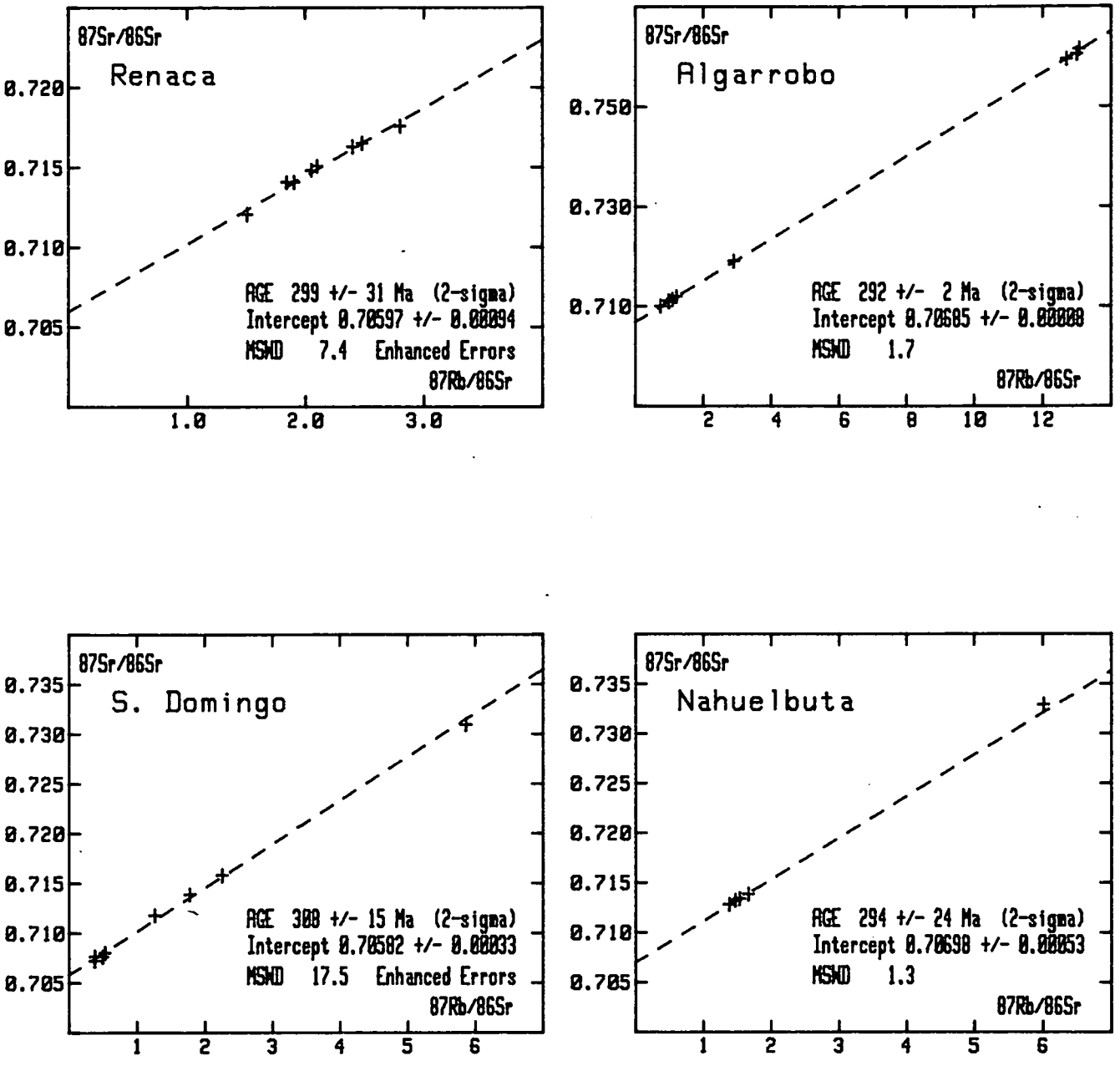

Fig. 5.9 Rb-Sr whole-rock isochron diagrams for Palaeozoic granitoid rocks from the Coastal Batholith south of the Rio Aconcagua.

in the metamorphic rock inclusions at Quintay (320 Ma; Cordani et al., 1976), as well as in the metamorphic ages of the western high P/T belt of the accretionary complex at Pichilemu (311 ± 10 Ma; Hervé et al., 1984). The eastern metaclastic low P/T belt where the SCB is emplaced has yielded possibly somewhat older isochrons (344 + 44 Ma) or errochrons (384 ± Ma) inland from Pichilemu (Hervé et al 1984), perhaps reflecting the influence of older provenance.

K-Ar ages on the Palaeozoic SCB rocks, mainly from hornblende and biotite, give results between 300 Ma and 245 Ma, but the majority are around 280-300 Ma. The essential concordance between these ages and the whole rock Rb-Sr isochron ages may be considered indicative of shallow emplacement and/or rapid uplift and regional cooling of the plutons without later reheating. The absence of metamorphism in the Triassic sediments overlying the SCB supports this interpretation. In the next section however some possible cases of Mesozoic resetting of Rb-Sr and K-Ar systems will be reported.

Initial $^{87}Sr/^{86}Sr$ ratios of the Palaeozoic plutons of the SCB consistently fall within the range 0.706 to 0.707 , which is significantly higher than in oceanic basalts (mostly <0.705) and andesites which are thought to be derived from the upper mantle. However, on mineralogical and geochemical criteria they are "I-type" granitoids and, at the northern end they have been assigned to the "Ilmenite Series" by Shibata et al. (1984). Thus a simple explanation would be that the Palaeozoic magmas were derived from an upper mantle source but were modified by extensive interaction with pre-existing continental crustal rocks. This is more likely to involve hybridisation with anatectic melts at the base of the crust than simple assimilation of cold country rocks. Alternatively, it is possible that the mantle source region itself was within a 'fossilised" region of the mantle with long-term Rb enrichment relative to Sr, resulting in moderately elevated $^{87}Sr/^{86}Sr$ ratios. Such an enriched lithospheric source has been postulated for Mesozoic basalt magmas in Antarctica (Kyle et al., 1984) and may have been a significantly widespread feature of the mantle underlying this part of Gondwana during late Palaeozoic times.

Triassic ages..

Small granitoid plutons with K-Ar ages between 220 Ma and 190 Ma crop out west of the SCB and occasionally intrude the Palaeozoic batholith. The western bodies e.g. Topocalma, Pichilemu (Godoy, 1970), Constitucion (Gana & Hervé, 1983)

and Tetas, are mainly composed of monzogranitic rocks. They are located in the relatively high P/T western belt of the Palaeozoic accretionary prism, which is not intruded by the Palaeozoic SCB rocks. This western belt, composed of accreted oceanic lithologies, underwent its main (D_2) metamorphic phase 311 ± 10 Ma ago (Hervé et al 1984). The Triassic plutons develop narrow contact metamorphic aureoles in the schists, post-dating the generation of the fabric and mesostructures of the rocks. These aureoles indicate a high "epizonal" level of emplacement, suggesting that the K-Ar ages are close to the age of emplacement. No Rb-Sr data is yet available for these plutons.

The La Estrella pluton at 34°15'S. (Davila et al., 1979) is a small stock of orthoclase-biotite leucogranite with a K-Ar biotite age of 218 ± 21 Ma. It intrudes rocks of the SCB which locally have K-Ar biotite ages of 254 ± 10 Ma, perhaps indicating a partial resetting of a Permo-Carboniferous age. Resetting to a K-Ar Triassic age has been detected in the metamorphic rocks surrounding the 158 ± 2 Ma Pichilemu intrusive (K-Ar, biotite). At this locality, whole rock K-Ar ages from quartz slate and crossite-bearing schist and metachert give *c.* 210 Ma, while minerals from metamorphic rocks away from the pluton yield Palaeozoic ages (Hervé et al, 1974). A similar resetting also occurs near the Constitucion granitoids, where white mica in schists near the contact aureole gives 210 Ma (Gana & Hervé, 1983).

Jurassic ages.

Mid-Jurassic plutons appear to be an important component of the batholith north of about 37°S (Fig. 5.8). The Jurassic plutons crop out in close spatial relationship with the Palaeozoic SCB rocks, and lack of detailed mapping has in many cases precluded the identification of the size and shape of the plutons. This has been the case for the outcrops occurring in the eastern flank of the Coast Range between 35° and 36°30'S., where the first Jurassic K-Ar ages obtained were interpreted as probable reset ages of the Palaeozoic intrusives. However, near Cauquenes, the Tomenelo stock (Lagno 1981) composed of gabbro, diorite and granodiorite, which intrudes Late Triassic rocks, has a K-Ar biotite age of 180 ± 10 Ma (Hervé & Munizaga 1978), which is probably close to the age of intrusion. Smaller bodies of similar lithology and contact characteristics occur in the eastern flank of the SCB Palaeozoic rocks, intruding the Late Triassic sequences or the SCB itself. North of 36°S., and particularly near the Maule river valley, larger plutons of Jurassic age are recognized. The Monticillos granodiorite (Gana & Hervé 1983) has given K-Ar ages of 175 ± 5 Ma

and 165 ± 5 Ma on hornblende and biotite respectively. South of the Maule river, similar ages were obtained by Hervé & Munizaga (1978) on granodiorites and a gabbro stock. No Rb-Sr dates are available for any part of this plutonic field.

Undisputed geochronological evidence for a Jurassic plutonic and tectonic event has been obtained from rocks of the Coast Range between the Maipo and Aconcagua rivers, where the SCB is exposed in the shoreline. The first indications of Jurassic plutons were given by U-Pb ages from zircons at Limache and some K-Ar and Rb-Sr mineral ages at Quintay and Laguna Verde (Corvalan & Munizaga, 1972). However, Cordani et al. (1976) suggested that an important thermal event had taken place in the region, based on a Rb-Sr whole rock isochron for metamorphic rocks occurring as inclusions in the granitoids. This has been confirmed by Rb-Sr and K-Ar dating in the course of Project ANDCHRON, supplemented by U-Pb dating by one of the Chilean collaborators. At Quintay, a reasonable errorchron (MSWD=7) of 167 + 14 Ma was obtained for a suite of gabrro, gneissic tonalite and granodiorite, microline- and aplitic granite which intrude the metasedimentary rocks. At Laguna Verde, an ill defined errorchron of 155 ± 92 Ma for two-pyroxene diorite coincides well with unpublished Jurassic U-Pb ages for zircon (Godoy, pers. comm.) and with Rb-Sr biotite ages. At Cuesta de Zapata, some 30 km SE of Quintay, a 173 ± 28 Ma isochron was obtained for diorites which lie to the east of the late Paleozoic Algarrobo tonalite, Fig. 5.10. The rocks at these three localities probably represent magmas intruded during Jurassic times, all with low initial $^{87}Sr/^{86}Sr$ ratios of *c.* 0.704.

Other localities with an indication of the Jurassic tectono-magmatic event are Las Cruces. Here, foliated granitoids with a very heterogeneous lithology (including coarse leucogranites, biotite- and garnet-gneiss and microcline augen gneiss which probably represent metasedimentary material) have given a 162 ± 40 Ma Rb-Sr whole-rock errorchron with higher initial $^{87}Sr/^{86}Sr$ ratio (0.7142), Fig. 5.10). These values are compatible with the resetting in Jurassic times of material with $^{87}Sr/^{86}Sr$, $^{87}Rb/^{86}Sr$ and initial $^{87}Sr/^{86}Sr$ values similar to the average 300 Ma Palaeozoic granitoids of the area. K-Ar ages of *c.* 160 Ma have been obtained from Panul. Palaeozoic granitoids south of the Aconcagua river at Playa Negra and Reñaca yield Jurassic (reset) K-Ar mineral ages, whereas huge masses of pyroxene diorite which crop out north of

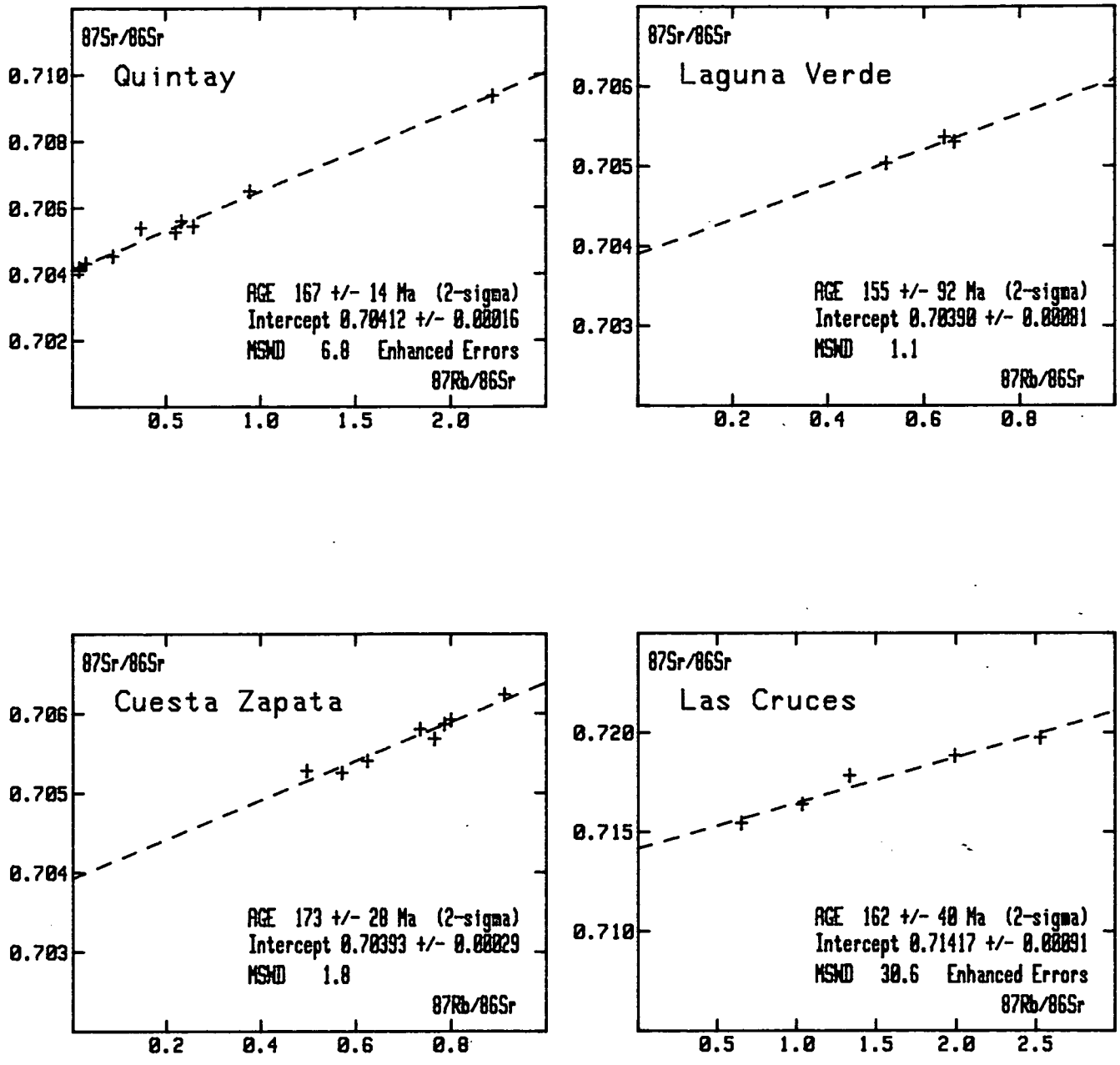

Fig. 5.10 Rb-Sr whole-rock isochron diagrams for Jurassic granitoid rocks from the Coastal Batholith south of the Rio Aconcagua.

the Aconcagua river have yielded many consistent Jurassic Rb-Sr and K-Ar ages (see below).

A discontinuous belt of Cretaceous intrusions crops out in the eastern part of the Coast Range. They intrude Neocomian marine fossiliferous rocks, and have K-Ar ages between 118 and 85 ma (Corvalan & Munizaga, 1972; Davila et al, 1979). Granodiorite, tonalite, diorite and gabbro are associated with hydrothermal alteration and/or skarn Cu deposits. South of about 36°S, Cretaceous granitoids no longer occur in the Coast Range but in the Main Range, east of the Central Valley.

Basic dyke swarms are very conspicuous in the coastal outcrops of the SCB between Santo Domingo and the Aconcagua River. They cut through both Palaeozoic and Jurassic granitoids, but appear to be more characteristic of the Palaeozoic. In the Cartagena area, mafic dykes range in age from 180 Ma to 115 Ma, and one has a ^{40}Ar-^{39}Ar age of 170 ± 5 Ma (Irwin J., written communication.)

5.2b Granitoids of the Coast Range of Central Chile, 30°30'S - 32°30'S.

The granitoids of this segment, which are of Mesozoic and Cenozoic age only, occur in three N-S trending belts: western (WB), central (CB) and eastern (EB) (Fig. 5.11). Several studies have discussed this spatial arrangement with reference to temporal relationships between the belts and their significance in the tectonic evolution of the Andes. In the northern Andes, Farrar et al (1970) provided radiometric data for a systematic eastward migration of magmatism. Likewise, chronological evidence and stratigraphic relationships led Aguirre et al.(1974) to recognise, from east to west, three main chronological groups of intrusion in central Chile: Jurassic, Cretaceous and Tertiary. More recently, Vergara and Drake (1979), Drake et al. (1982), Munizaga and Vicente (1982), Rivano (1984) and Rivano et al. (1985) have given further support for a magmatic zonation in the Andes south of 31 S.

All the plutons in this area are epizonal. The host rocks into which the Mesozoic and Cenozoic magmas were emplaced resulted from the preceding Middle-to-Late Palaeozoic tectonic and magmatic events of this part of the Andes. They consist of igneous rocks, highly deformed metasediments, and oceanic rocks

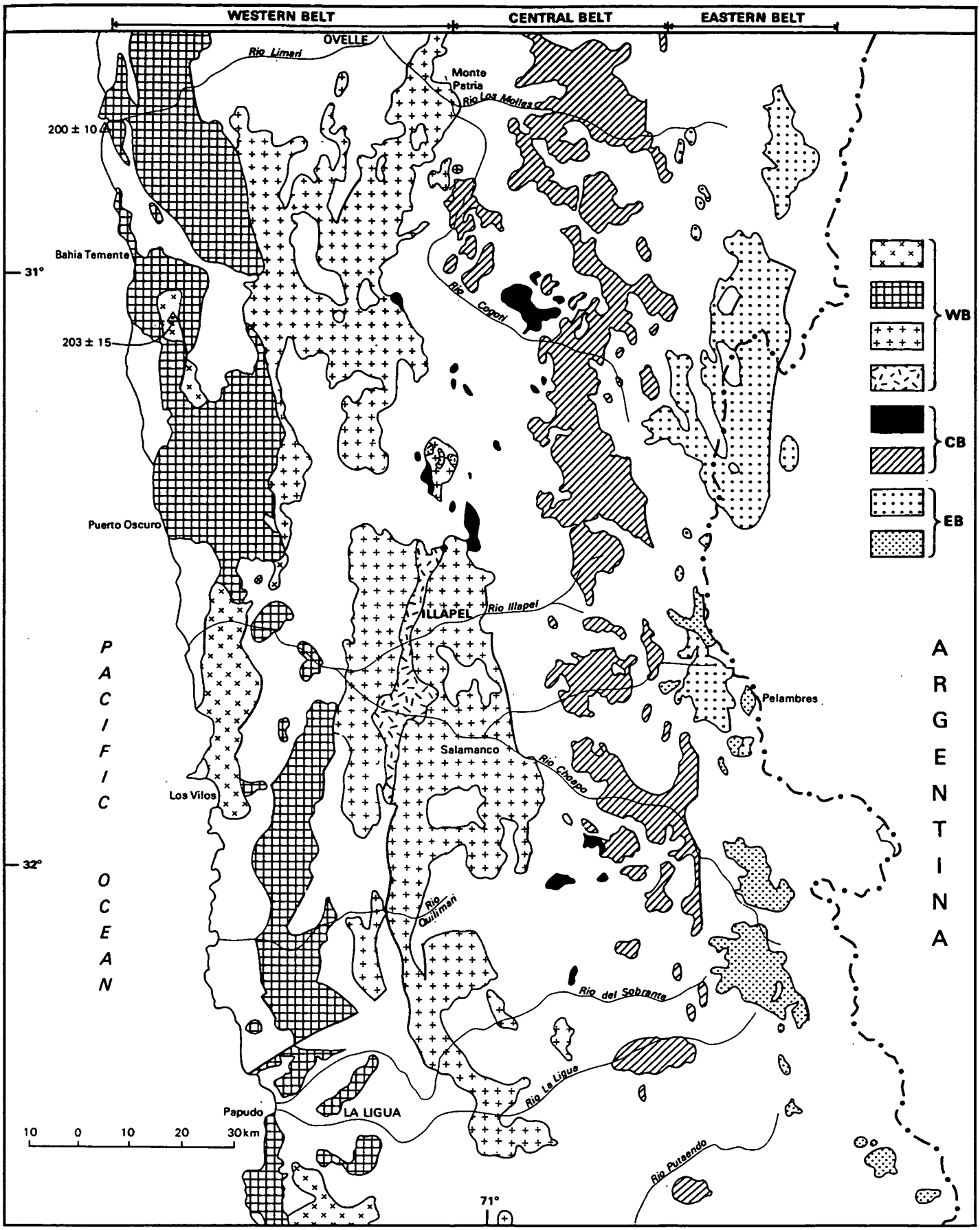

Fig. 5.11 Geological sketch map of the area of the Coastal Batholith of Central Chile north of the Rio Aconcagua. The shaded areas are units and superunits of the Mesozoic batholith described in Section 5.2b : WB = western belt, CB = central belt, EB = eastern belt.

accreted to the earlier continental margin (Herve et al 1981; Theile & Herve 1984; Ribba 1985). The country rocks adjacent to the western flank of the WB consist of Upper Palaeozoic low-grade metasediments and metavolcanic rocks, together with Lower Mesozoic sediments and siliceous volcanics. Various roof-pendants are recognized in the central and eastern parts of the WB. These consist of volcanogenic sequences and minor clastic sediments and limestones assigned to Lower Cretaceous formations. Plutons of the CB are roofed by gently folded Upper Cretaceous volcanoclastic sequences. The envelope of the EB comprises rather more deformed sedimentary and volcanic formations with ages decreasing eastwards from Late Jurassic to Palaeogene. There is no evidence of deposition of younger cover rocks over any of the plutonic belts.

The granitoids have been tentatively sub-divided into units and super-units according to the criteria of Cobbing and Pitcher (1972) such as their uniformly linear distribution, similarities in compositional and textural variation, the nature, abundance and shapes of inclusions, the distribution of dyke swarms and the consistency of geochemical and age relationships to other rocks. Unfortunately, the present state of knowledge of the plutonic belts is still variable, due to logistic difficulties in the field work and incomplete radiometric dating. Thus the classifications suggested here are likely to be subject to future modification as a result of more detailed work. The modal compositions of the various units are summarized in Fig. 5.12.

Western Belt

The Mincha Superunit occupies the eastern flank of the WB (Fig. 5.11) and comprises four units. The Millahue and Tranquilla units are lithologically homogeneous and consist of leucomonzogranite and leucosyenogranite as the commonest varieties. The Puerto Oscuro unit consists of equigranular two-pyroxene diorites and monzodiorites and some olivine leucogabbros and quartz-diorites. The Cavilolen unit includes medium-to fine grained granodiorites and tonalites which have microdioritic inclusions in variable proportions. The Illapel Superunit is the more abundant in outcrop (3000 km^2) in this part of the WB. The Chalinga unit is mainly tonalitic and quartz-dioritic. The Limahuida unit occurs as an elongated pluton within the central part of the Chalinga unit and consists of leucodiorites and trondjhemites.

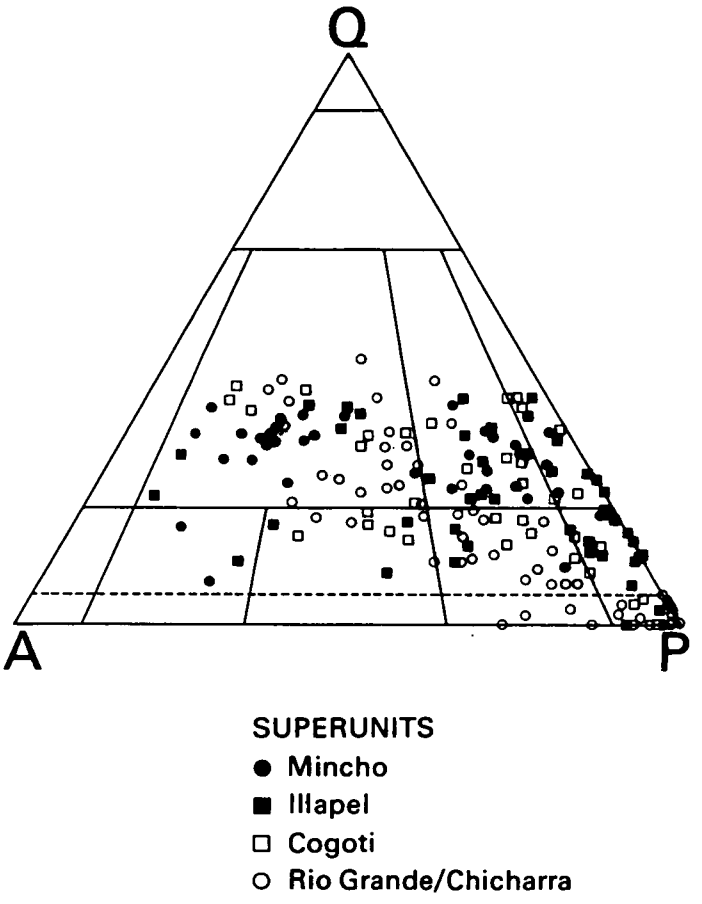

Fig. 5.12 Quartz - Alkali-Feldspar - Plagioclase plot for modal analyses of the Mesozoic granitoids of central Chile.

Central Belt

This belt is markedly less voluminous than the WB, and includes the Cogoti Superunit and San Lorenzo unit. The former comprises the Fredes and Nogalada units. The Fredes unit constitutes the most abundant outcrops of the superunit and represents a mafic event formed by hornblende pyroxene and biotite diorites and quartz diorites, whereas the Nogalada units are composed of fine-grained leucogranites. The San Lorenzo unit occurs as small plutons (1-5 km^2) of fine-grained to porphyritic diorites.

Eastern Belt

The rocks of this belt have medium grain size and variable composition between gabbro and granite. The rocks of Rio Grande Superunit form the most important member of the EB and can be divided into Rio Las Cuevas (leucomonzogranites and leucogranodiorites) and Rio Tascadero (monzonite and monzodiorite) units. The rocks of Rio Las Cuevas type are the most abundant in outcrop and seem to be a core facies whereas the Rio Tascadero rocks are often located in the zones of the plutons. The Rio Chicharra Superunit includes medium-grained monzodiorites with hornblende, clinopyroxenes and biotite (Rio Cerro Blanco unit) and dacite porphyry (Portezuelo del Azufre units).

Geochronology

The geochronological characterization of this plutonism is based on the radiometric data obtained by K-Ar and Rb-Sr methods, the latter data being largely new (Table 5.3). The results are consistent with the stratigraphic relationships and the well known eastward migration of magmatism with time.

Leucogranites from the Millahue unit near the mouth of the Rio Limari gave a Rb-Sr age of 200 ± 10 Ma, similar to the 203 ± 15 Ma Rb-Sr age (Fig. 5.13) of Tranquilla leucogranitoids collected 10 km to the southeast of Bahia El Teniente. Neither set of data plot on a perfect isochron but the errors quoted incorporate the uncertainty due to the amount of scatter about the best fit lines. A K-Ar age of 191 Ma was determined for a Millahue leucogranite and these data taken together establish the intrusive age of the Millahue unit as close to 200 Ma. Furthermore, two rather imprecise Rb-Sr isochrons of 204 ± 11 and 192 ± 11 (Fig. 5.13) have been obtained at 30°S. in leucogranitoids from a separate belt 100 km to the east. The significance of these presumed Late

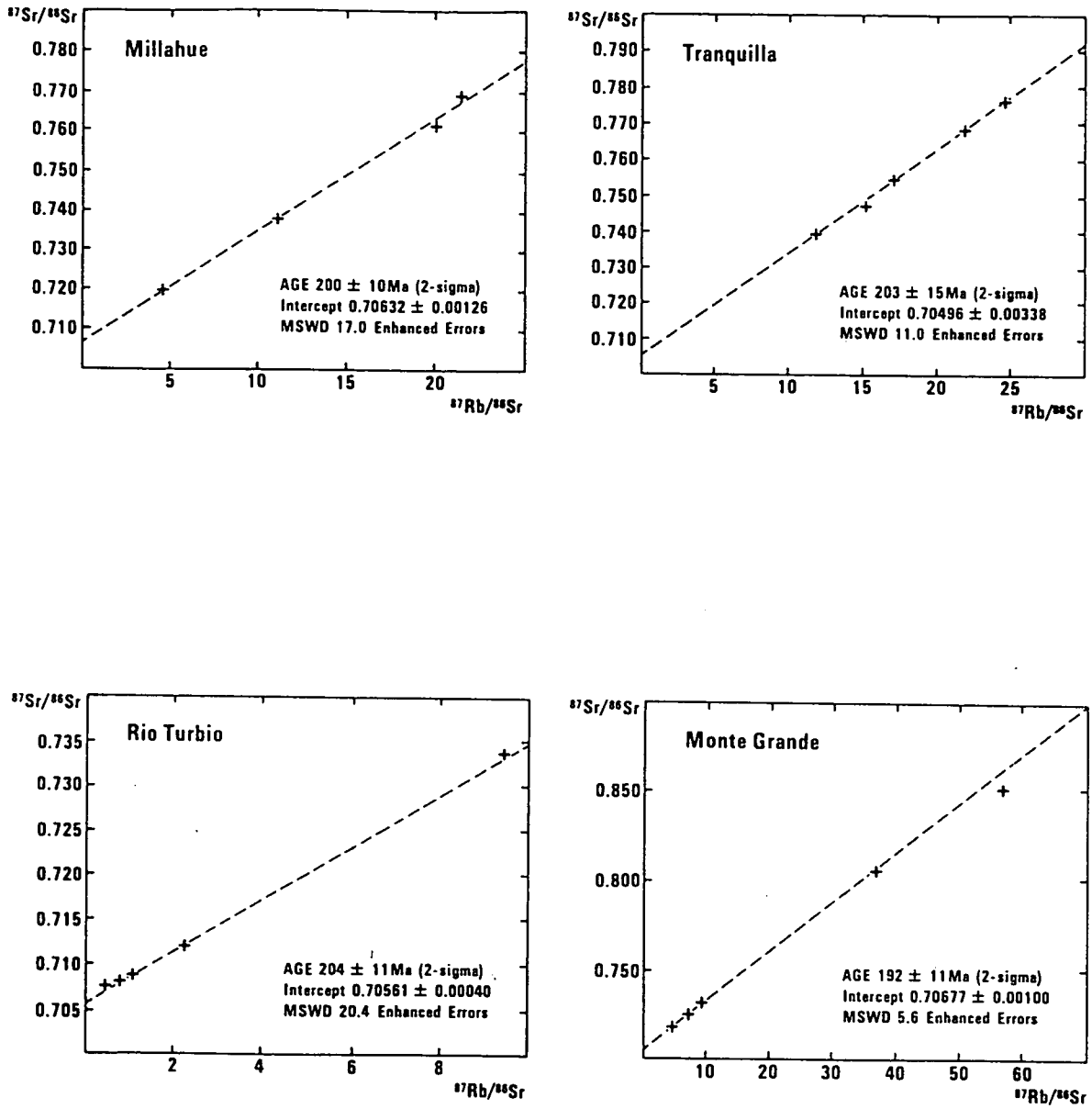

Fig. 5.13 Rb-Sr whole-rock isochron diagrams for granitoid rocks of the Tranquilla and Millahue units of the Coastal Batholith of central Chile.

Triassic ages is discussed below. The initial $^{87}Sr/^{86}Sr$ ratios of all these isochrons are relatively high, mostly demonstrably greater than 0.705, and comparable to the Palaeozoic SCB granitoids from south of the Rio Aconcagua.

About 20 km to the east of the mouth of the Rio Limari, samples from the Puerto Oscuro and Cavilolen units gave a 143 ± 13 Ma Rb-Sr isochron (Fig. 5.14). However granitoids from the same units sampled 200 km further south, between Papudo and Quintero gave a good Rb-Sr isochron age of 164 ± 2 Ma (Fig. 5.14). These isochrons all have lower initial $^{87}Sr/^{86}Sr$ ratios, significantly less than 0.704. K-Ar ages of Puerto Oscuro and Cavilolen rocks range between 187 and 140 Ma, the younger ages corresponding to samples north of Rio Illapel.

K-Ar dates on Chalinga unit are in the range of 134-80 Ma. The oldest (>130 Ma) were obtained at 31°S and the younger ones correspond to samples collected south of 31°30'S. At 32°S. the Limahuida unit appears to be younger than 96 Ma, as is suggested by a K-Ar age on pegmatite dyke within it. Rb-Sr data from Chalinga and Limahuida granitoids at Illapel 31°30'S suggest an age of 88 ± 19 Ma (Fig. 5.14).

There are no Rb-Sr controls on the rocks of the CB or EB. Eleven K-Ar ages have been determined from this part of the CB. The Fredes unit rocks have ages between 67 and 35 Ma: the older ones (67 - 54 Ma) from south of Rio Illapel and the younger ones (47-35) from north of 31°30'S. No age determination on the Nogalada granitoid is yet available and the only age from the San Lorenzo unit is 65 ± 3 Ma. In the EB, K-Ar ages of 24 ± 4 and 25 ± 1 Ma were obtained for the Rio Las Cuevas unit, similar to ages of 26 ± 2 Ma for basic and ultrabasic enclaves from the El Polvo gabbro and peridotite. The youngest plutonic episode of the area is represented by the Rio Chicharra superunit: fourteen K-Ar ages indicate a range between 17 and 8 Ma. Considering the high cooling rate of these epizonal plutons and the systematic age differences between the separate belts, the K-Ar ages are thought to be close to the emplacement age of the plutons.

The available radiometric data show discrete ranges for each of the belts with a pronounced eastward migration with time: WB (Jurassic-to Late Cretaceous), CB (Early Tertiary), EB (Late Tertiary). This eastward migration of the belts and the absence of younger rocks in the more western belts may

reflect a sequence of uplift-erosion soon after the intrusive events. The jumps in the sites of the magmatic belts correspond to intervals (85-70 Ma) and (38-36 Ma) which are essentially non-magmatic, both here and to the north and south of this area. Despite the still patchy distribution of geochronological evidence, it is possible to recognize a N-S diachronism within belts although all tend to be younger to the east (Fig. 5.11). The Illapel river appears to be the boundary between two geochronological zones of each belt (Fig. 5.11).

5.2c Conclusions.

The available geochronological data on the granitoids of the Coastal Batholith both north and south of the Aconcagua River suggest a complex constitution of the plutons.

A late Carboniferous or early Permian magmatic event is well established through Rb-Sr whole rock isochrons, and its products make up the bulk of the southern coastal batholith. No evidence has been found with the Rb-Sr method for plutons older than late Carboniferous, and the SCB probably represents a magmatic accretion to the margin of Gondwana during Permo-Carboniferous times. This plutonic belt crosscuts the metasediments of an accretionary prism which was probably located well outboard of the continent and which underwent metamorphism shortly before and contemporaneously with the plutonism. The rather high initial $^{87}Sr/^{86}Sr$ ratios of the late Palaeozoic granitoids, could indicate contamination with older continental rocks, either an unobserved deep crystalline basement or the continent-derived metasediments of the accretionary prism. Alternatively, the underlying mantle could have been isotopically anomolous, having developed such moderate $^{87}Sr/^{86}Sr$ ratios as a result of a long period of isolation prior to the Permo-Carboniferous event.

The Triassic plutons which pierce the high P/T belt of the accretionary prism, were intruded after metamorphism had ceased and the metamorphic complex had been uplifted and eroded.

The Jurassic plutons were intruded into the late Palaeozoic plutonic complex, probably after its incorporation into the continental land mass. They represent the first major magmatic event of the Andean cycle, related to eastward subduction of the present-day Pacific Ocean plate beneath South America, which generated plutonic belts migrating progressively eastwards as

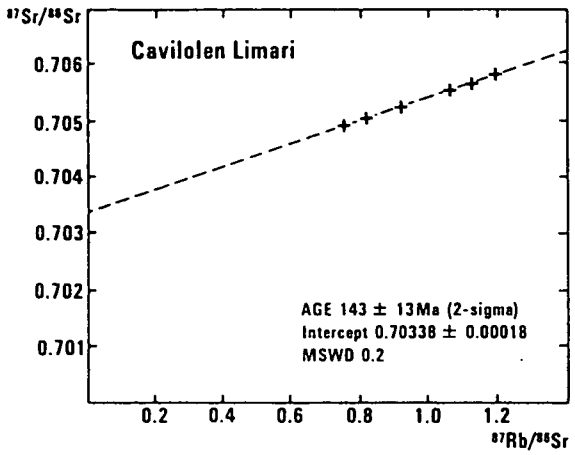

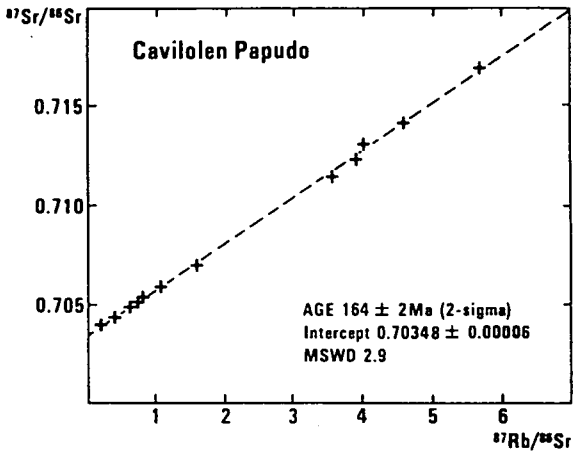

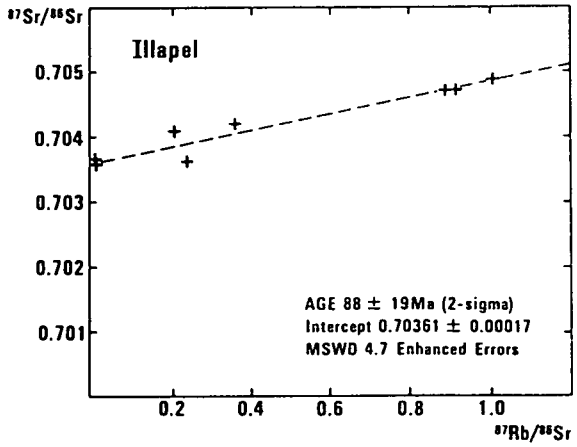

Fig. 5.14 Rb-Sr whole-rock isochron diagrams for granitoid rocks of the Puerto Oscuro and Cavilolen units (top) and the Chalinga and Limahuida units (bottom) of the Coastal Batholith of central Chile.

far as the present day volcanic belt of the main Andean Range. The $^{87}Sr/^{86}Sr$ initial ratios of the Mesozoic and Cenozoic granoitoids are low, similar to those of present day volcanics of the region. The Andean intrusive mechanism clearly did not allow significant contamination of magmas on their way through a crust of normal thickness.

The interpretation of the variations in the isotope compositions of the Palaeozoic and later magmas is considered further in Section 5.c.

References:

Aguirre, L., Charrier, R., Davidson, J., Mpodozis, C., Rivano, S., Thiele, R., Tidy, E., Vergara, M. & Vincente, J.-C. (1974). Andean magmatism: its paleogeographic and structural setting in the central part (30° to 35°S) of the southern Andes. *Pacific Geol.*, 8, 1-38.

Cobbing, E.J. & Pitcher, W.S. (1972). The Coastal Batholith of central Peru. *J. geol. Soc. Lond.*, 128, 421-60.

Cordani, U., Munizaga, F., Hervé, F., & Hervé, M. (1976) Edades radiometricas provenientes del Basamento Cristalino de la Cordillera de la Costa de las Provincias de Valparaiso y Santiago, Chile. *Actas, 1er Congreso Geologico Chileno, Santiago*, 2, F213-F222.

Corvalan, J. (1976). El Triasico-Jurasico de Vichuquen-Tilicura y de Hualane, Provincia de Curico: implicaciones paleogeograficas. *Actas 1er Congreso Geologico Chileno, Santiago*, 1, A137-A154.

Corvalan, J. & Munizaga, F. (1972). Edades radiometricas de Rocas Intrusivas y Metamorficas de la Hoja Valparaiso-San Antonio. *Boletin Instituto de Investigaciones Geologicas, Santiago*, 28, 40 p.

Davila, A., Herve, F. & Munizaga, F. (1979). Edad K-Ar en granitoides de la Cordillera de la Costa de la provincia de Colchagua, VII Region, Chile Central. *Actas 2° Congreso Geologico Chileno, Arica*, 1, F109-F120.

Drake, R., Vergara, M., Munizaga, F. & Vincente, J.C. (1982). Geochronology of Mesozoic-Cenozoic magmatism in Central Chile, lat. 31°-36°S. *Earth Sci. Rev.*, 18, 353-64.

Farrar, E., Clark, A., Haynes, S., Quirt, G., Conn, H. & Zentilli, M. (1970). K-Ar evidence for the post-Palaeozoic migration of granitic intrusion foci in the Andes of northern Chile. *Earth Planet. Sci. Lett.*, 10, 60-6.

Gana, P. & Hervé, F. (1983). Geologia del Basamento Cristalino en la Cordillera de la Costa entre los rios Mataquito y Maule, VIII Region, *Rev. Geol. Chile*, No.19-20, 37-56.

Godoy, E. (1970). *El granito de Constitucion y su aureola de metamorfismo de contacto.* Unpubl. thesis, Univ. de Chile, Santiago.

Hervé, F., Munizaga, F., Godoy, E. & Aguirre, L. (1974). Late Palaeozoic K/Ar ages of blueschists from Pichilemu, Central Chile. *Earth Planet. Sci. Lett.*, 23, 261-4.

Hervé, F., Munizaga, F., Mantovani, M. & Hervé, M. (1976). Edades Rb/Sr Neopaleozoicas del basamento cristalino de la Cordillera de Nahuelbuta. *Actas 1er Congr. Geol. Chileno, Santiago.*, II, F19-F26.

Hervé, F & Munizaga F. (1978). Evidencias geocronologicas de un magmatismo intrusivo triasico superior-jurasico en la cordillera de la costa de Chile entre los 35°30' y 36°30' L.S. *VII Congreso Geologico Argentino, Neuquen*, 11, 505-607.

Hervé, F., Davidson, J., Godoy, E. et al. (1981). The Late Palaeozoic in Chile: stratigraphy, structure and possible tectonic framework. *Acad. Brasil Cienc. An.*, 53, 361-73.

Hervé, F., Kawashita, K., Munizaga, F. & Bassei M. (1984). Rb-Sr isotopic ages from late Palaeozoic metamorphic rocks of Central Chile. *J. geol. Soc. Lond.*, 141, 877-884.

Hervé, F., Davidson, J., Mpodozis, C., Rapela, C., Ramos, V. & Godoy, E. (in press). A General View on the Chilean-Argentinian Andes. *AGU Geology Series.*

I.I.G. (1982). Mapa Geologico de Chile escala 1:1.000.000, Instituto de Investigaciones Geologicas,Santiago, Chile.

Kyle, P.R., Pankhurst, R.J. & Bowman, J.R. (1983). Isotopic and chemical variations in Kirkpatrick Basalt Group rocks from South Victoria Land. In R.L. Oliver, P.R. James & J.B. Jago (eds), *Antarctic Earth Science.* Australian Academy of Science, Canberra, 234-8.

Lagno, L. (1981). Geologia del Cuadrangulo Pocillas, Cauquenes, VII Region, Chile. *Memoria inedita, Depto. Geologia, Univ. de Chile, Santiago.* 154 p.

Mordojovic, C. (1976). La plataforma continental de Chile entre Constitucion y Guafo. Algunos antecedentes morfologicos y geologicos. *Actas 1er Congreso Geologico Chileno, Santiago*, v. 3, K3-K22.

Munizaga, F. & Vincente, J.-C. (1982). Acerca de la zonacion plutonica y del volcanismo miocenico en los Andes de Aconcagua (lat. 32°-33°S). *Rev. Geol. Chile.*, 16, 3-21.

Ribba, L. (1985). Geologia del cuadrangulo El Transito. *Memoria, Fac. Ciencs. Fisicas y Matematicas, Univ. de Chile, Santiago.*

Rivano, S. (1984). Geologia del Meso-Cenozoico entre los 31° y 33°Lat.Sur. In Seminario "Actualizacion de la Geologia de Chile". *Serv. Nac. Geol. Miner., Santiago* (unedited).

Rivano, S., Sepulveda, P., Hervé, M. & Puig, A. (1985). Geocronologia de las rocas intrusivas entre los 31°-32° L.S., Chile. *Rev. Geol. de Chile* No.25.

Shibata, K., Ishihara, Sh. & Ulriksen, C. (1984). Rb-Sr ages and initial $^{87}Sr/^{86}Sr$ ratios of Late Paleozoic Granitic Rocks from Northern Chile. *Bull. Geol. Surv. Japan*, 35, (II), 537-545.

Tavera, J. (1960). El Triasico del valle inferior del Rio Bio-Bio. *Inst. Geol. Univ. Chile, Santiago, Publ.*, 18, 321-48.

Thiele, R. & Hervé, F. (1984). Sedimentacion y tectonica de ante-arco en los terrenos preandinos del Norte Chico, Chile. *Rev. Geol. Chile*, 22, 61-75.

Veragara, M. & Drake, R. (1979). Edades K-Ar en secuencias volcanicas continentales post-neocomianas de Chile Central: su depositacion en cuencas intermontanas restringidas. *Rev. Assoc. Geol. Argentina*, 34, 42-52.

TABLE 5.2 Rb/Sr DATA SOUTH OF RIO ACONCAGUA

	Rb ppm	Sr ppm	$^{87}Rb/^{86}Sr$	$^{87}Sr/^{86}Sr$
REÑACA.				
CBV 47	103	121	2.479	0.71650
CBV 48	86	119	2.098	0.71508
CBV 49	81	127	1.840	0.71407
CBV 50	80	122	1.906	0.71408
CBV 51	86	121	2.050	0.71481
CBV 52	89	107	2.398	0.71630
CBV 53	138	142	2.800	0.71758
CBV 54	108	208	1.501	0.71206
ALGARROBO				
ALG 1	66	190	1.012	0.71093
ALG 2	65	188	0.996	0.71110
ALG 3	82	195	1.229	0.71197
ALG 4	216	48	13.060	0.76149
ALG 5	184	42	12.687	0.75945
ALG 6	198	44	12.988	0.76049
ALG 7	71	187	1.107	0.71135
ALG 8	167	166	2.909	0.71905
ALG 9	43	165	0.758	0.71003
SANTO DOMINGO				
CBV 1	135	174	2.252	0.71582
CBV 6	130	213	1.774	0.71388
SD 1	113	258	1.263	0.71180
SD 2	87	480	0.527	0.70802
SD 4	206	101	5.867	0.73095
SD 5	60	456	0.381	0.70724
SD 6	59	444	0.384	0.70766
SD 7	95	557	0.493	0.70764
NAHUELBUTA				
NAH 1	96	197	1.384	0.71283
NAH 5	10	219	1.538 (±3%)	0.71340
NAH 8	8	465	1.670 (±3%)	0.71386
NAH 9	123	240	1.476	0.71322
PM 516	-	-	6.010	0.73290

	Rb ppm	Sr ppm	$^{87}Rb/^{86}Sr$	$^{87}Sr/^{86}Sr$
QUINTAY				
CBV 11	155	202	2.221	0.70560
CBV 12	8	133	0.075	0.70432
CBV 13	64	320	0.583	0.70560
CBV 16	51	228	0.646	0.70545
CBV 17	27	355	0.217	0.70454
CBV 18	50	153	0.945	0.70650
CBV 19	38	297	0.367 (±1%)	0.70539
CBV 20	39	206	0.551 (±1%)	0.70526
CBV 21	4	310	0.038 (±6%)	0.70419
CBV 22	3	225	0.038 (±8%)	0.70411
LAGUNA VERDE				
CBV 62	77	349	0.643	0.70537
CBV 63	68	376	0.523	0.70504
CBV 64	83	365	0.664	0.70531
CUESTA DE ZAPATA				
ZAP 1	56	328	0.498	0.70528
ZAP 2	89	335	0.766	0.70568
ZAP 3	86	310	0.800	0.70592
CBV 55	79	366	0.625	0.70540
CBV 56	91	290	0.912	0.70624
CBV 57	70	357	0.573	0.70525
CBV 58	131	332	0.786	0.70587
CBV 59	82	324	0.736	0.70580
LAS CRUCES				
CBV 26	64	139	1.335	0.71783
CBV 27	79	115	1.994	0.71884
CBV 28	42	185	0.656	0.71544
CBV 30	62	173	1.037	0.71639
CBV 31	116	113	2.530	0.71974

TABLE 5.3. Rb-Sr WHOLE ROCK DATA NORTH OF RIO ACONCAGUA.

	Rb ppm	Sr ppm	$^{87}Rb/^{86}Sr$	$^{87}Sr/^{86}Sr$
MILLAHUE UNIT NEAR LIMARI				
TEN 21	110	69	4.609	0.71947
TEN 23	202	53	11.097	0.73765
TEN 24	232	32	21.369(0.8%)	0.76931
TEN 26	237	35	20.017(0.7%)	0.76185
TRANQUILLA LEUCOGRANITOID				
TEN 30	246	33	21.808	0.76794
TEN 32	286	34	24.628(0.7%)	0.77605
TEN 33	248	42	17.053(0.7%)	0.75499
TEN 34	249	47	15.170	0.74758
TEN 36	202	50	11.861	0.73950
PUERTO OSCURO AND CAVILOLEN UNITS.				
: At Limari				
TEN 43	86	330	0.752	0.70491
TEN 44	92	328	0.815	0.70504
TEN 46	148	360	1.194	0.70582
TEN 47	168	434	1.122	0.70564
TEN 48	92	292	0.918	0.70522
TEN 49	136	369	1.065	0.70553
: At Papudo				
CBV 70	146	105	4.009	0.71307
CBV 71	89	419	0.616	0.70488
CBV 72	111	308	1.047	0.70601
CBV 73	35	568	0.180(0.9%)	0.70391
CBV 74	115	85	3.901	0.71234
CBV 75	127	236	1.551	0.70700
CBV 76	118	97	3.533	0.71142
CBV 77	92	374	0.721	0.70517
CBV 78	192	121	4.586	0.71411
CBV 79	83	404	0.596	0.70488
CBV 80	207	105	5.692	0.71690
CBV 81	63	482	0.380(0.6%)	0.70436
CBV 82	102	386	0.770	0.70525
CBV 83	105	383	0.794	0.70537

	Rb ppm	Sr ppm	$^{87}Rb/^{86}Sr$	$^{87}Sr/^{86}Sr$
RIO TURBIO				
ELQ 3	56	350	0.465	0.70735
ELQ 5	86	111	2.245	0.71178
ELQ 6	79	211	1.084	0.70859
ELQ 7	122	37	9.505	0.73358
ELQ 8	87	320	0.785	0.70790
MONTEGRANDE				
ELQ 18	69	6	36.759 (3%)	0.80475
ELQ 19	87	58	4.361	0.71871
ELQ 20	73	4	56.861 (4%)	0.85030
ELQ 21	136	43	9.108 (0.6%)	0.73205
ELQ 22	134	54	7.148 (0.6%)	0.72594
ILLAPEL				
CHO 6	92	298	0.891	0.70471
CHO 7	98	283	1.005	0.70487
CHO 8	95	303	0.912	0.70472
CHO 9	2	585	0.006 (18%)	0.70364
CHO 10	2	647	0.007 (17%)	0.70356
CHO 11	65	523	0.128	0.70420
CHO 12	35	441	0.232	0.70363
CHO 22	34	492	0.203 (0.8%)	0.70407

Errors are 0.01% on $^{87}Sr/^{86}Sr$ and 0.5% on $^{87}Rb/^{86}Sr$ unless otherwise shown in parentheses (1 sigma). Rb and Sr determined by X-ray fluorescence and $^{87}Sr/^{86}Sr$ on a VG Micromass 354 mass spectrometer.

Ages calculated using $\lambda Rb = 1.42 \times 10^{-11} a^{-1}$.

5.c NORTHERN CHILE - CHAÑARAL TO EL SALVADOR (26°S - 26°30'S)

Work began in this transect in November 1984 in support of an SNGM effort to produce a metallogenic map, but developed rapidly when it became clear that it was of great tectonic significance. Although confined to a rather narrow segment (with some previous ANDCHRON data from the coast at 25°30'S), coverage was more complete than in the other transects. There was also a background of previous geochronological and geochemical work by West German researchers working in the Coast Range throughout this area (Damm & Pichowiak 1981, Berg & Baumann 1985).

The interest in this work arises from two factors. Firstly, it is one of the most extensively active mining regions in Chile, with porphyry-Cu well developed at Portrerillos (now closed) and El Salvador, Cu, Ag and Au in the Inca de Oro districts and Cu-Fe in the area of the Atacama fault zone. Reconnaissance work on ore genesis has been carried out throughout the region by geologists from Oxford Polytechnic in collaboration with SNGM and is supplemented in ANDCHRON by detailed examination of one of the potentially important new Au-prospects in the Andes at Silica del Hueso (see Section 6.1).

The second factor arises from the presence within the transect of two separate Palaeozoic igneous belts (Figs. 5.15 and 5.16). One of these is in the east, in the Altiplano region of the High Andes close to the border with Argentina. This is actually more extensively developed a little further south (27°30' - 30°30'S), where our work in the Rio Las Molles and Rio Turbio sections is referred to below but has not been completed in time for inclusion here, and continues through more broken outcrops to the north as far as 21°S. The other Palaeozoic belt is that of the Coast Ranges, where it can be traced intermittently from the Mejillones Peninsula (23°S) at least as far as 28°S, with its most abundant outcrops occurring within the present transect. The coastal plutons are intruded into deformed turbiditic sediments which have been interpreted as comparable with the accretionary complex of southern Chile, whereas the Altiplano belt is apparently emplaced into sparsely exposed continental volcanics and volcanigenic sediments. Prior to the initiation of this work it was not clear why there are two such belts, whether they represent precisely simultaneous magmatism, what their tectonic significance is or how they are related to the single Palaeozoic belt of the Southern Coastal Batholith (Section 5.1). Our geochronological and radiogenic isotope studies have

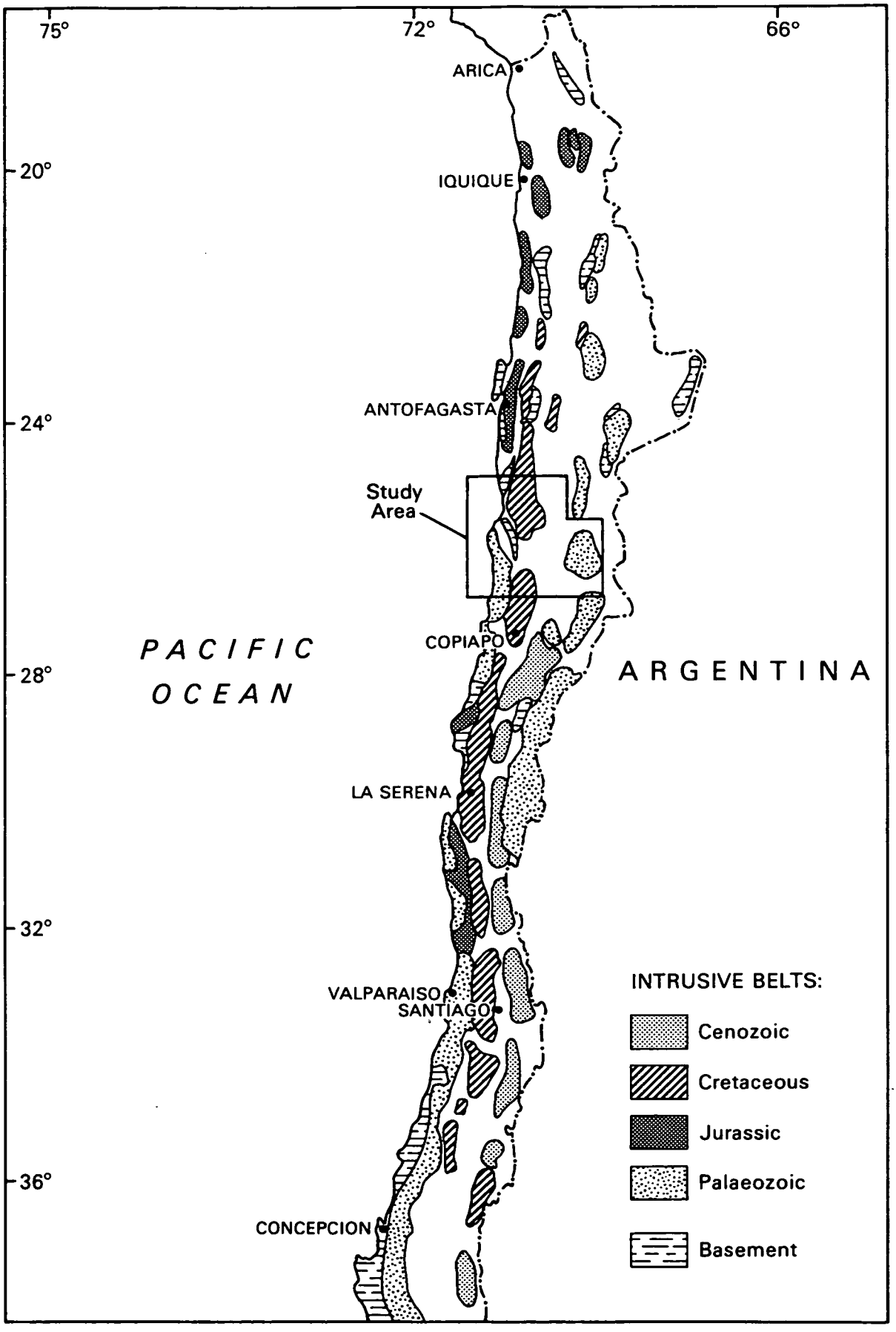

FIG. 5.15 SKETCH MAP OF CENTRAL AND NORTHERN CHILE SHOWING THE DISPOSITION OF MAGMATIC ARCS OF DIFFERENT AGES. SOUTH OF 32° S THERE IS A SIMPLE EASTWARD MIGRATION OF MAGMATISM WITH TIME, WHEREAS NORTH OF THIS THERE ARE TWO (DISCONTINUOUS) PALAEOZOIC BELTS (SEE ALSO FIG. 5.7).

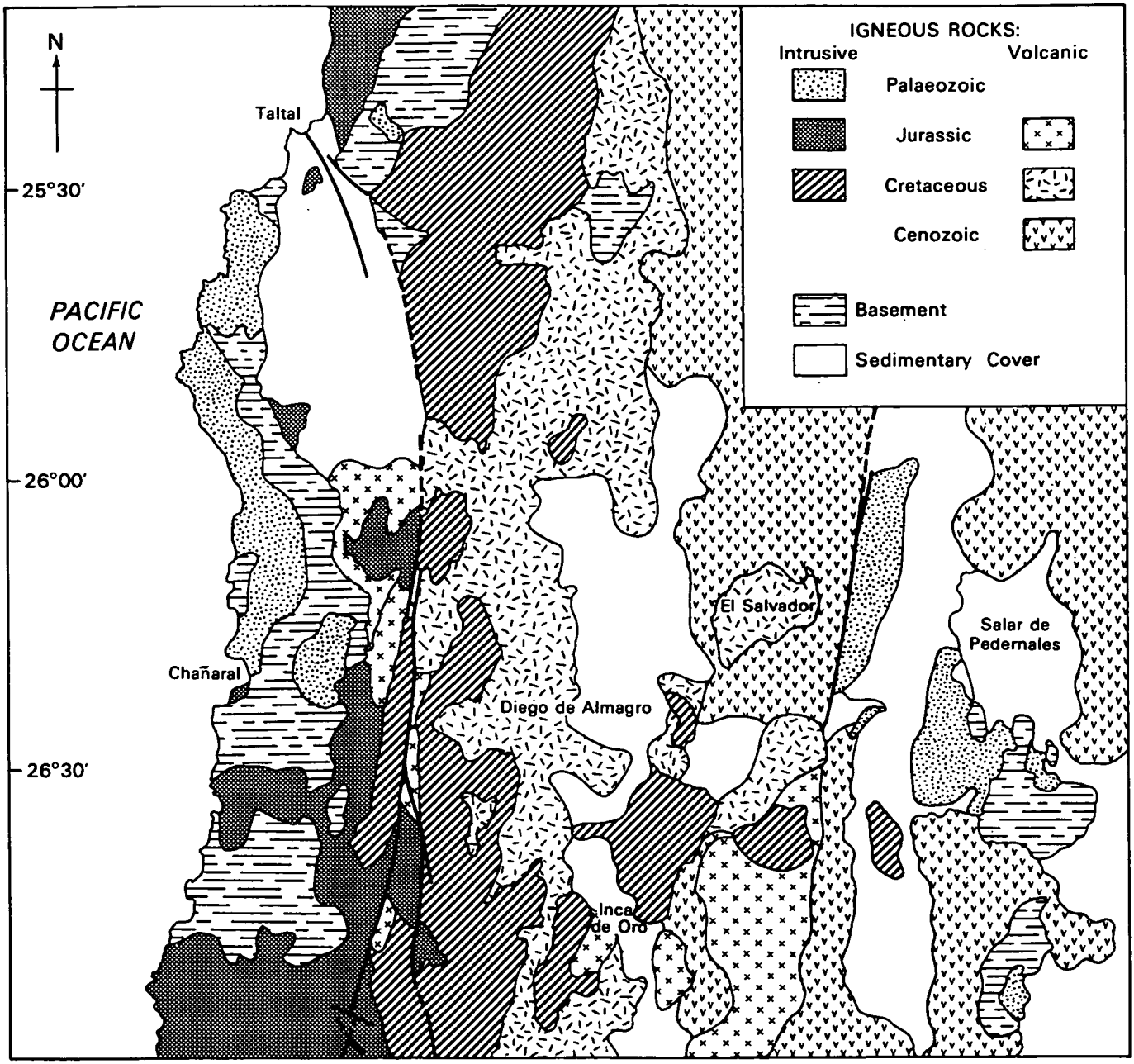

Fig. 5.16 Geological sketh map of the El Salvador - Chanaral transect of northern Chile.

provided at least partial answers to these questions and a new basis for understanding the metallogenesis of the region.

5.3a. Geochronology

The results are best considered according to the areal distribution of the three main intervals of activity which can be identified: Late Palaeozoic (but extending into Triassic), Early Mesozoic and Cretaceous. The data is presented in Tables 5.4 and 5.5.

The Palaeozoic plutons are those which occur in both belts. We have produced the first comprehensive set of ages for the Altiplano, consisting of six Rb-Sr whole-rock isochrons (Figs. 5.17 and 5.18). The oldest of these is 270 ± 10 Ma (Permian) for eight samples of granodiorite from large body cut by Quebrada Doña Ines Chica. Another Permian age (257 ± 3 Ma) was obtained from the small mass of granodiorite at Montandon. Suites of similar rocks from Corral del Alhambre in the Pedernales body to the southeast give a 19-point isochron (MSWD=2.7) of 248 ± 2 Ma (Permo-Triassic) and at La Ola, further east, 234 ± 2 Ma (mid-Triassic). Thus, within these most typical rock types, there is apparent evidence for a younging of emplacement ages towards the southeast, although this observation needs to be taken with some caution since biotite from one of the Montandon samples gave a significantly older K-Ar age of 275 ± 6 Ma. Since many of these rocks contain some evidence for secondary alteration (e.g. epidote veining), the possibility must be considered that the ages are partially reset. We do not favour this idea since collecting of large samples on this scale is generally known to give intrusive ages for such medium-to-coarse grained granitoids, but support from further K-Ar and U-Pb dating would be welcome. The Pedernales granite, observed as a late-stage intrusion, gave isochrons with indistinguishable slopes for the pink and grey phases, corresponding to still younger ages of 209 ± 19 and 212 ± 19 Ma, which perhaps should be compared with the early Mesozoic plutons in the Coast Range south of Chañaral. The initial $^{87}Sr/^{86}Sr$ ratios for all these suites fall in the range 0.7065-0.7086 (Fig. 5.19).

Results for the Coast Range Palaeozoic intrusives are also shown in Fig. 5.17. This incorporates relevant West German data (Damm & Pichowiak 1981, Berg & Baumann 1985), which consists of several Rb-Sr biotite-WR pairs, one Rb-Sr whole-rock isochron and three U-Pb zircon ages, as well as four

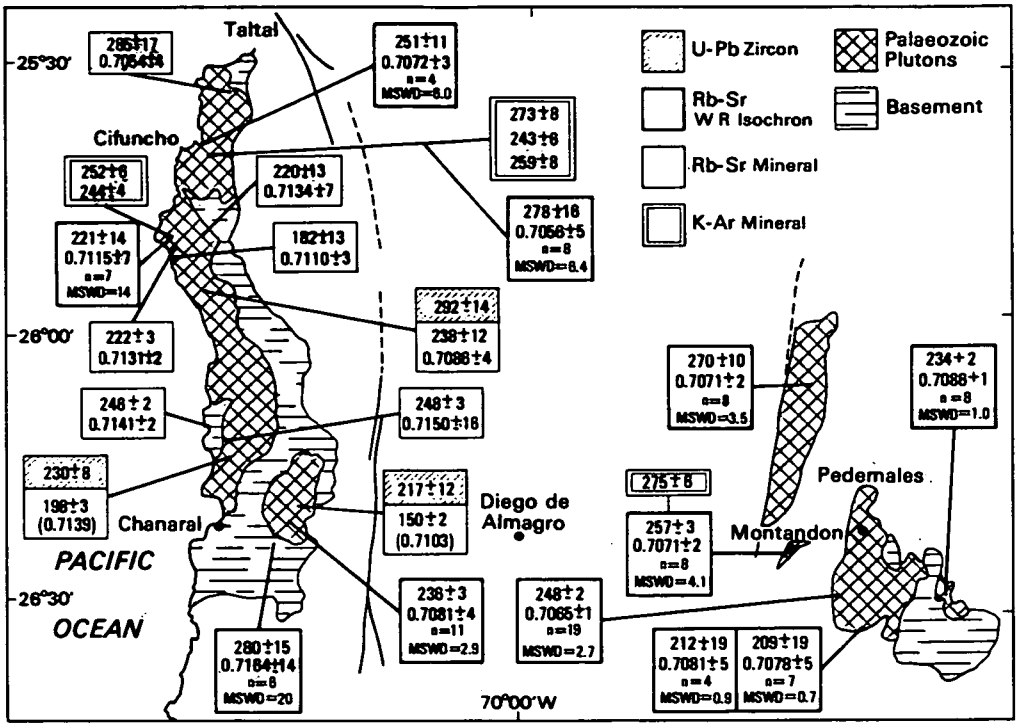

Fig. 5.17 Distribution of Palaeozoic ages in the El Salvador - Chanaral transect (this study and German data referred to in text).

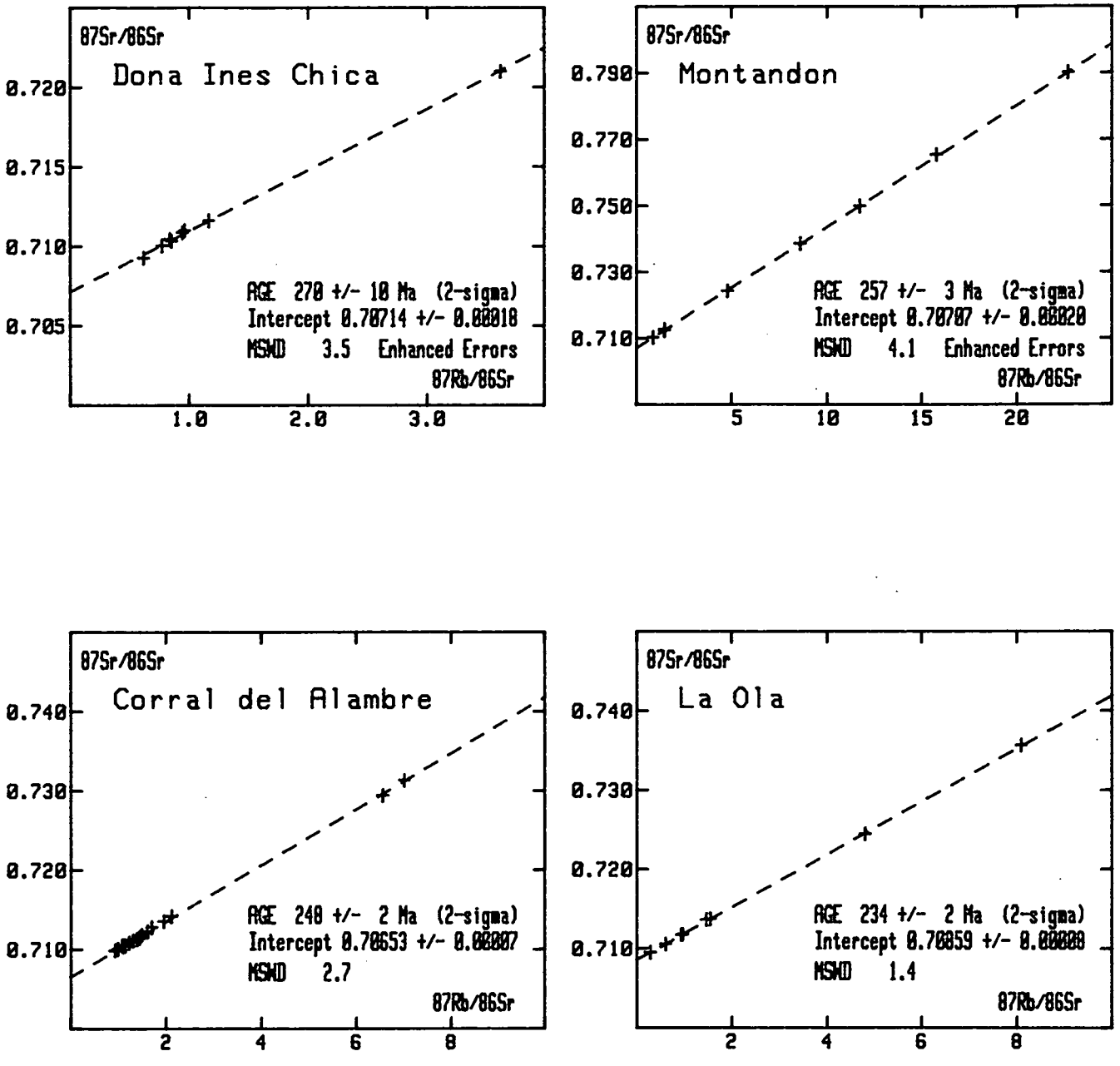

Fig. 5.18 Rb-Sr whole-rock isochron diagrams for new data from the Palaeozoic belt of the Altiplano near El Salvador.

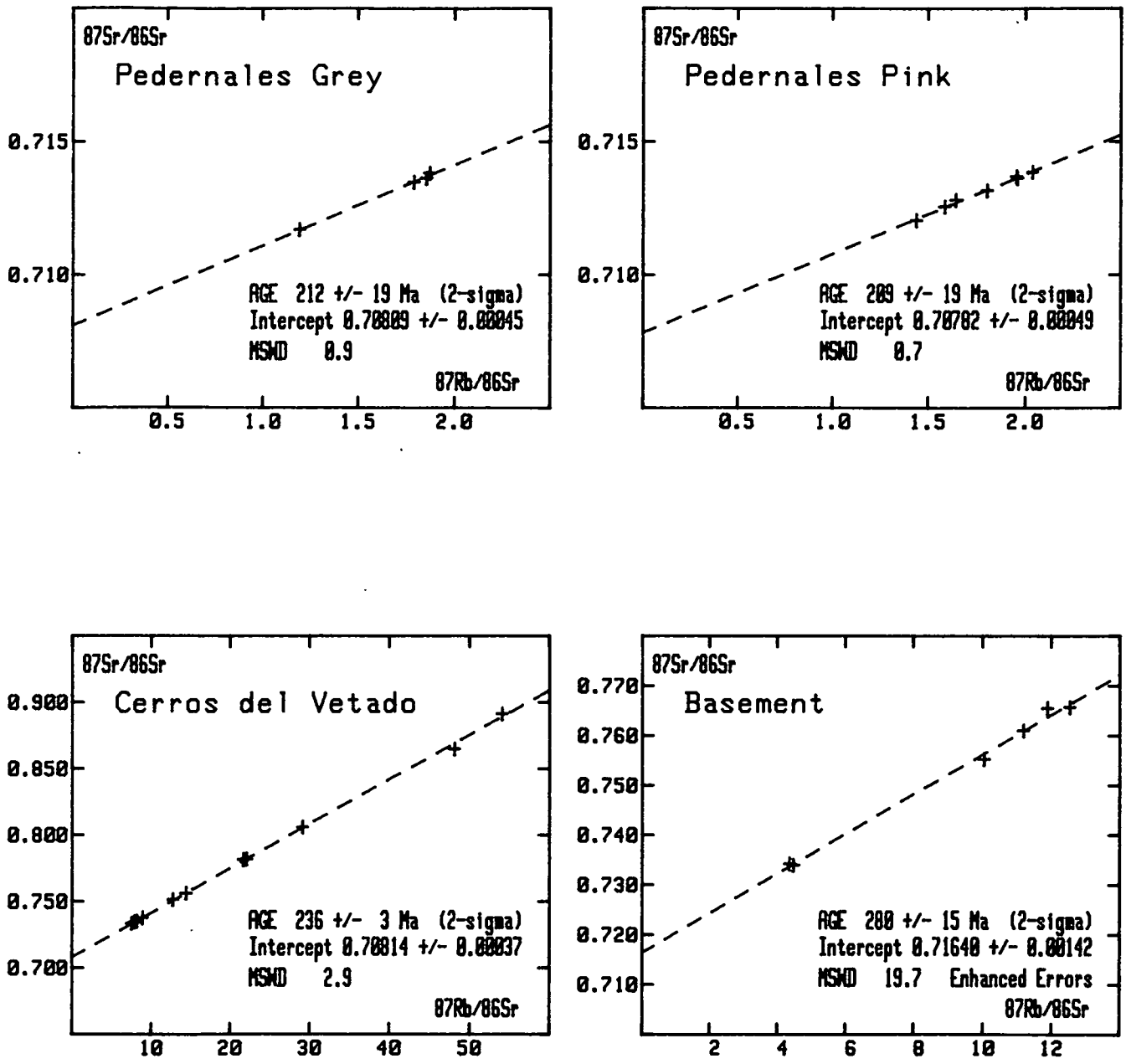

Fig. 5.19 Rb-Sr whole-rock isochron diagrams for the Pedernales grey and pink granites (top), the Cerros del Vetado intrusion (Coast Ranges), and the Palaeozoic metasedimentary basement of Quebrada Las Animas.

whole-rock isochrons and K-Ar ages determined during ANDCHRON. A few older K-Ar ages listed in Naranjo & Puig (1984) have not been included but are consistent with the new findings. The U-Pb zircon ages and whole-rock isochrons range from 292 ± 14 Ma down to 217 ± 12 Ma - a range comparable to that observed in the Altiplano. Since the youngest of these ages, for the Cerros del Vetado granite-adamellite pluton, has been more precisely determined by us as 236 ± 3 Ma (Fig. 5.19), the period of igneous activity is seen to correspond almost exactly with the Permian to early Triassic emplacement of the *granodiorites* of the Altiplano. Most of the mineral ages fall in the same range and there is general concordance for individual localities. However, in the south, near Chañaral, two of the localities have yielded Jurassic Rb-Sr biotite ages which are undoubtedly reset by younger thermal events. Apart from this, there are significant differences from the Altiplano belts in that the Coast Range Palaeozoic plutons are include more leucocratic monzogranites and monzogranodiorites and have initial $^{87}Sr/^{86}Sr$ ratios extending up to much higher values of >0.710. This was taken by Berg et al (1983) as signifying production of the granitoid melts by processes which included large-scale anatexis of crustal rocks. This possibility is re-emphasized by a new Rb-Sr whole-rock isochron for phyllites from the local basement outcrops in Quebrada Las Animas (Fig. 5.19) which probably reflects isotopic homogenization during metamorphism 280 ± 15 Ma ago with a mean $^{87}Sr/^{86}Sr$ ratio at that time of 0.7164. This high value probably reflects detrital input of terrigenous material derived by erosion of rocks with a much older crustal provenance, a point reinforced by the presence of an inherited zircon component with a U-Pb age of as old as 2700 Ma (Berg & Baumann 1985). Nevertheless, we would also point out that some of the plutons, including Cerros del Vetado, have rather lower initial $^{87}Sr/^{86}Sr$ ratios of <0.710, and these may reflect contamination by assimilation or even a long-term mantle enrichment in lithophile elements rather than direct anatexis. The importance of these results is re-considered in Section 5.3b.

The early Mesozoic plutons (Fig. 5.20), occur in the eastern part of the Coast Range, intruding the older rocks to the west and are abruptly cut off by the Atacama fault zone to the east. In these eastern outcrops, the mineral ages obtained are mostly Middle Jurassic (150-160 Ma) and are supported by a concordant U-Pb zircon age of 160 ± 2 Ma (Berg & Baumann 1986). These rocks, which include granodiorites, diorites and gabbros, are often badly altered and we have only managed to obtain a single whole-rock isochron, from west of

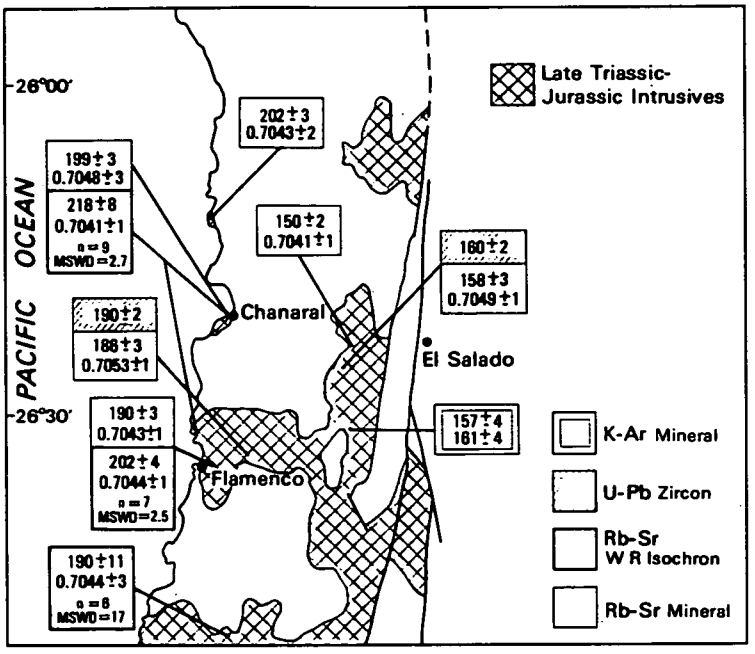

Fig. 5.20 Distribution of Late Triassic - Early Jurassic ages in the El Salvador - Chanaral transect (this study and German data referred to in the text).

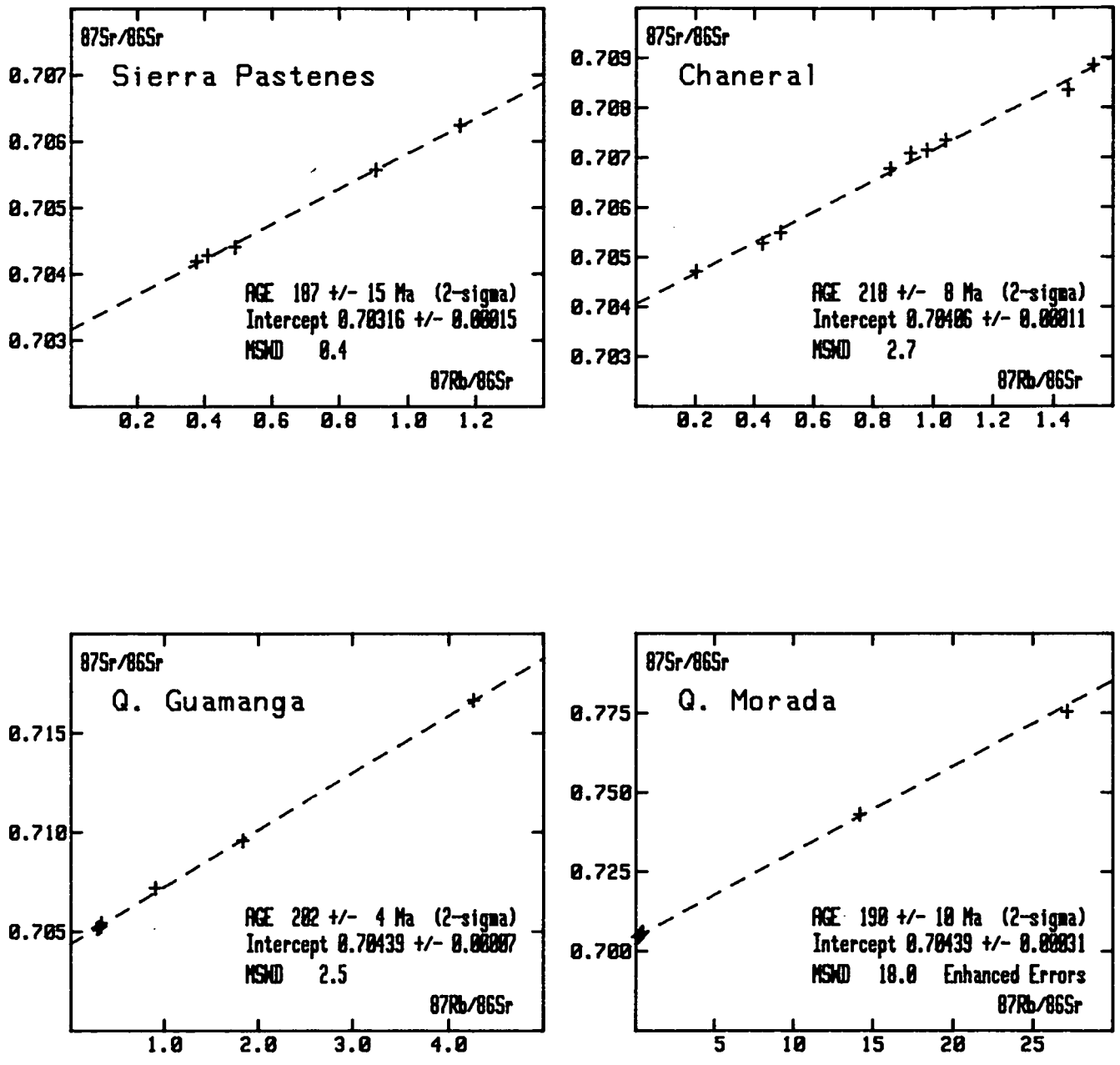

Fig. 5.21 Rb-Sr whole-rock isochron diagrams for Late Triassic - Early Jurassic granitoids of the Coast Range near Chañaral.

Sierra Pastenes, of 187 ± 15 Ma (Fig. 5.21). The very low intercept value associated with this age (0.7031 ± 0.0002) is rather improbable and suggests that the true age is close to the lower limit of error, i.e. comparable to the 150-160 Ma group.

In addition, there is now a well defined group of late Triassic or earliest Jurassic plutons, recognizable from the German Rb-Sr mineral dates and three new whole-rock isochrons (Fig. 5.21), along the western coastline and from Bahia Flamenco through into Quebrada Guamanga. Age determinations range from 190 ± 2 Ma (U-Pb) to 218 ± 8 Ma for the El Barquito intrusion on the southern side of Bahia Chañaral, and it is possible that these represent the true duration of igneous activity which could thus overlap with emplacement of the Pedernales granites in the Altiplano belt. In contrast with the Palaeozoic intrusives of the Coast Range, however, the present group are clearly distinguished by their low initial $^{87}Sr/^{86}Sr$ ratios of 0.704-0.705 (0.7040-0.7045 on the basis of the new whole-rock isochrons alone), which preclude anatexis of, or significant contamination by, an old crustal source region.

The Cretaceous group of intrusions (Fig. 5.22), which comprise rather more basic rock types (granodiorites, tonalites and diorites) can also be subdivided into sets of distinct age. The oldest set occurs within and immediately to the east of the Atacama fault zone itself, where U-Pb zircon ages, Rb-Sr biotite dates and a new nine-point Rb-Sr whole-rock isochron from Quebrada El Saladito (Fig. 5.23)are all concordant at (essentially) 130 Ma (basal Cretaceous). Further south in the same belt, west of Sierra de San Juan, a somewhat younger five-point isochron age of 103 ± 2 Ma (Fig 5.23) is supported by a K-Ar biotite age of 109 ± 3 Ma. The youngest ages in this group come from the finer-grained dioritic stocks of the central valley region of Inca de Oro, where they emerge from a flat-lying cover of Tertiary and Recent sediments. They have been dated by two K-Ar biotite ages of 82 (± 2, ± 5) Ma and a whole-rock isochron of 96 ± 10 Ma (Fig. 5.23). The error on the latter is rather high due to the small spread of Rb/Sr ratios, but the result is essentially concordant and confirms a Late Cretaceous age of intrusion. This is significant in that much of the Cu-Ag-Au mineralization in the Inca de Oro district occurs in the volcanic rocks intruded by these stocks.

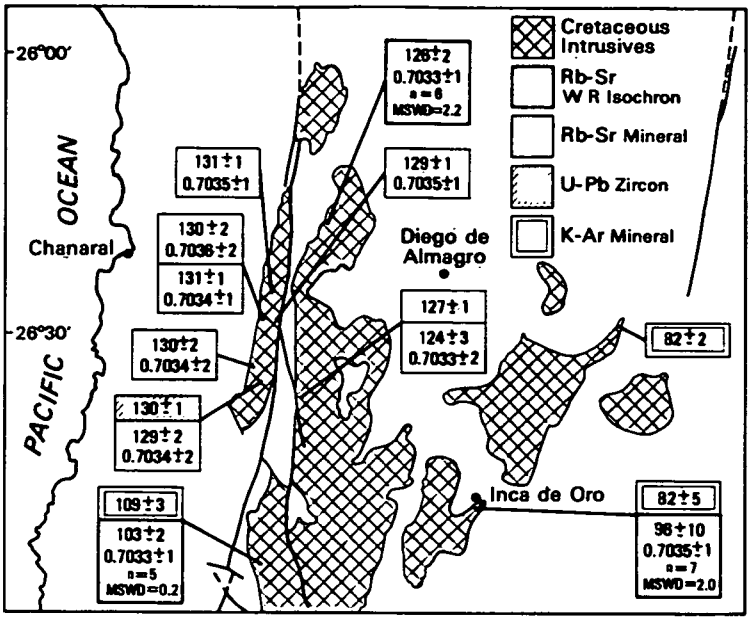

Fig. 5.22 Distribution of Cretaceous ages in the El Salvador - Chanaral transect (this study and German data referred to in the text).

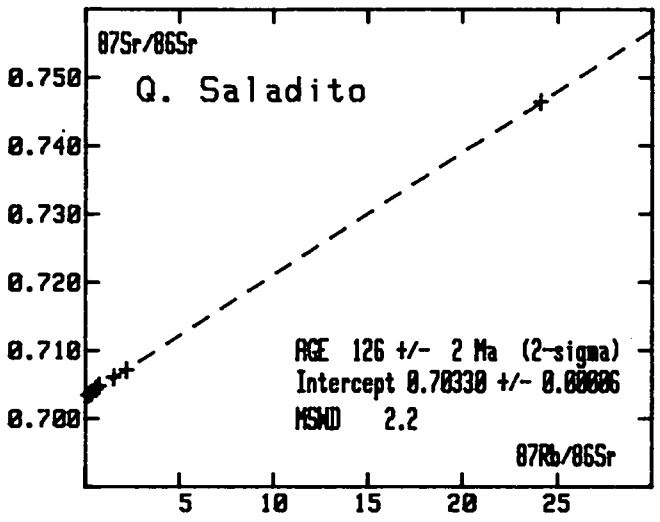

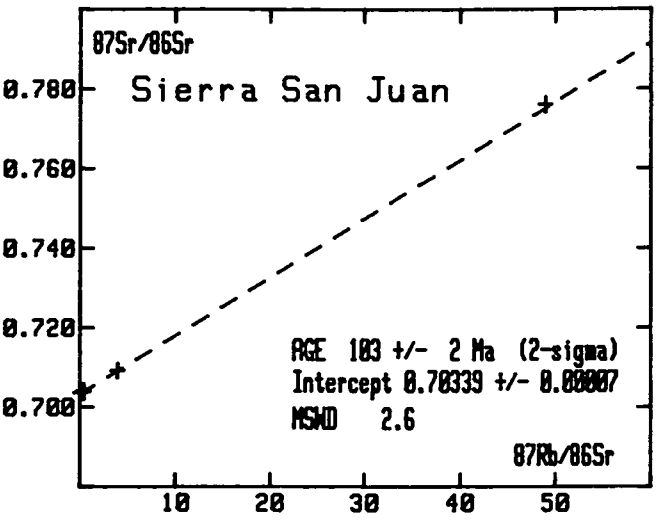

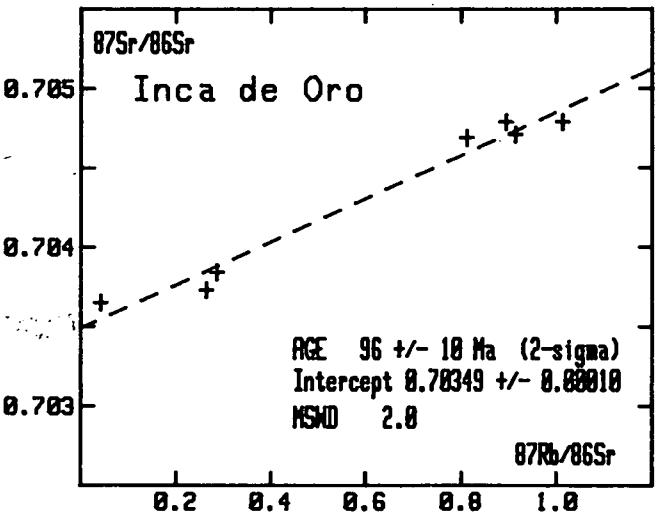

Fig. 5.23 Rb-Sr whole-rock isochron diagrams for Cretaceous granitoids of the El Salvador - Chañaral transect.

5.3b Radiogenic Isotope Geology.

The pattern of initial $^{87}Sr/^{86}Sr$ ratios exhibited by the intrusive rocks of this transect repeats individual features noted in the the other transects, notably in that the Mesozoic granitoids all have low values indicative of mantle origin (mostly 0.704 or less) whereas the Palaeozoic granitoids invariably have significantly higher values (mostly greater than 0.705). However, this pattern is more completely devloped here, where rocks of a wide age range are present throughout. The range of calculated initial $^{87}Sr/^{86}Sr$ ratios is also wider here than elsewhere, extending up to 0.715 for some of the biotite/whole-rock pairs of the Palaeozoic plutons in the Coast Range. However, despite our arguments that the Rb-Sr data generally record times of intrusion, there is inevitably some doubt that even slight post-consolidation alteration or reheating could result in partial resetting and rotation of isochrons to an erroneously younger age, with a concommittant artificial increase in intercept values. This is particularly a problem with the Rb-Sr mineral dates, although the intercepts on the whole-rock isochrons also extend up to 0.7115. The most effective way of removing this source of uncertainty is to involve another radiogenic isotope system: Sm-Nd (see Section 2.f). Initial $^{143}Nd/^{144}Nd$ ratios can be used in an equivalent manner to initial $^{87}Sr/^{86}Sr$ ratios with three important differences:

(i) Because Sm/Nd ratios are *lower* in crustal rocks than in the mantle, involvment of old crustal rocks in magma genesis results in *lower* $^{143}Nd/^{144}Nd$ ratios than in uncontaminated mantle-derived magmas, i.e. the opposite trend to Sr isotopes.
(ii) The low Sm/Nd ratios of already crystallized granitoids results in a very slow rate of growth of radiogenic ^{143}Nd, so that closed system resetting even significantly later than emplacement does not disturb the magmatic initial $^{143}Nd/^{144}Nd$ ratio significantly. In similar circumstances the build-up of ^{87}Sr is often extremely rapid.
(iii) Nd is more resistant than Sr to isotopic exchange during rock-fluid interaction and alteration.

These features all make Nd-isotopes a much more reliable indicator of crustal involvement in magma genesis than Sr-isotopes. Because of the much more difficult and time-consuming procedures for separating and analysing Nd-isotopes to the required standard of precision, only a small selection of

samples, almost entirely from this transect, has been so analysed. The results for both Rb-Sr and Sm-Nd analyses for 18 samples are given in Table 5.5. The initial radiogenic/non-radiogenic isotope ratio for the two systems are generally expressed as ϵ-values (per-mil deviations from an 'ideal' standardized growth curve for the mantle), which have the advantage of being comparable on a time-independent basis, i.e. data for rocks of different ages can be compared without further correction.

These ϵ-values are plotted in Fig 5.24, where there is a clear anti-correlation between the two parameters. The highest ϵNd values are shown by the Cretaceous rocks from the Inca de Oro region which, as already noted have the lowest ϵSr values. These, indeed, fall within the sector of the diagram which signifies long-term depletion of the source region in lithophile elements (e.g. Rb) compared to the bulk Earth. The trend defined by these values together with those for the Triassic-Jurassic group of plutons from the Coast Range closely matches the 'Mantle Array' which includes most data for Mid-Ocean Ridge and oceanic island basalts - a class of magmas known to be derived from depleted mantle sources with no crustal contamination. In contrast, the high ϵSr of the Palaeozoic granitoids (from both belts), but is indeed complemented by low ϵNd, confirming the involvement of old crustal Nd. This conclusion is now independent of the uncertainties over possible resetting of the Rb-Sr systems, although the observed parallel behaviour suggests that such uncertainties can indeed be discounted.

5.3c Tectonic Significance.

As suggested above, highest values of initial $^{87}Sr/^{86}Sr$ which are observed in the coastal Palaeozoic plutons could be taken as indicative of direct melting (anatexis) of old crystalline basement or of sedimentary material with an old provenance, such as the ?Lower Palaeozoic accretionary metasediments into which they are emplaced. This is supported by their general petrography (which shows a predominance of leucocratic granitoids with few more basic counterparts) and geochemistry (Berg & Breitkreuz 1983; see also Fig. 5.25). These are all characteristic of 'S-type' granites as defined by Chapell & White (1974), whereas most igneous rocks produced at present day subducting plate margins are 'I-type'. Other evidence of the age of possible crustal source regions comes from the recognition of mid-Proterozoic (1000-1500 Ma) components of inherited zircons, even at Cerros del Vetado where the initial $^{87}Sr/^{86}Sr$ ratio

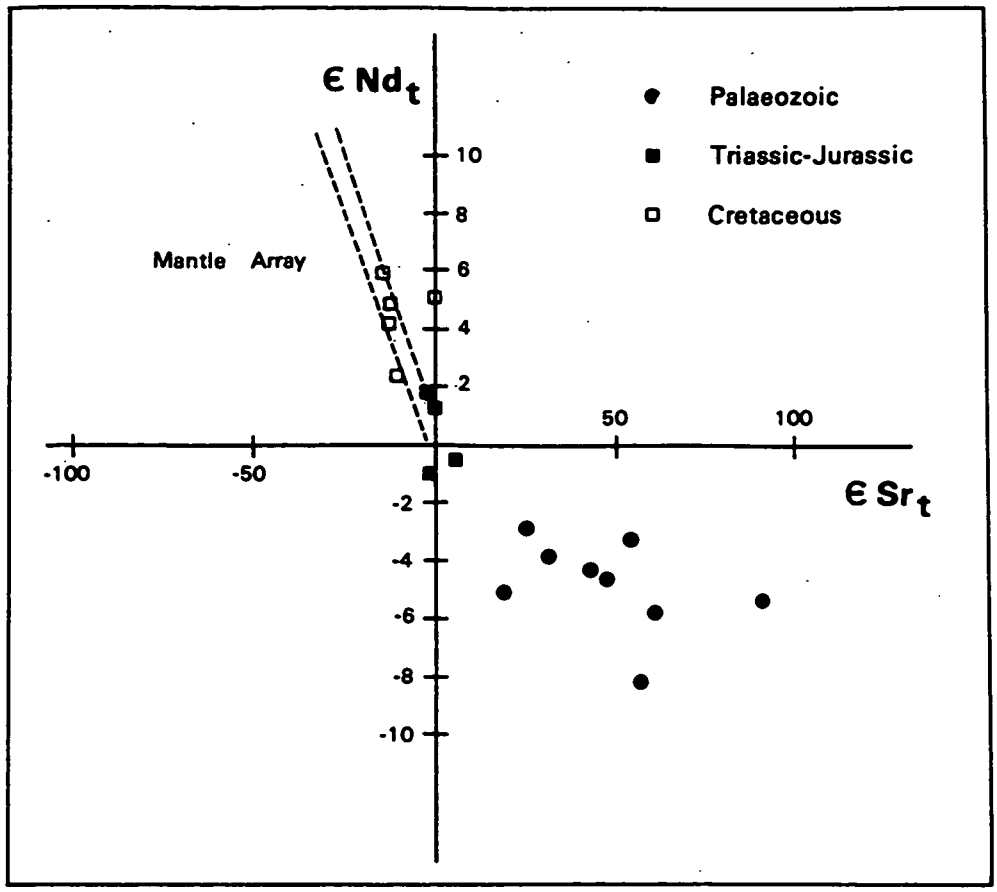

FIG. 5.24 PLOT OF INITIAL SR AND ND ISOTOPE COMPOSITIONS IN GRANITOIDS OF THE EL SALVADOR - CHAÑARAL TRANSECT AS EPSILON-VALUES. THE SQUARE IS FOR PERMIAN RHYOLITE FROM THE CORDILLERA DOMEYKO AND THE CIRCLES ARE FOR THE ORDOVICIAN ALTO DEL INCA INTRUSION.

is only 0.709 and from the Sm-Nd model ages of 1000-2000 Ma calculated for separation from the depleted mantle growth curve.

It has often been assumed that 'S-type' granitoids are symptomatic of compressional tectonics resulting from continent-continent collision and massive over-thickening of the crust. Some workers have interpreted the northern Chile situation in this way, invoking a landmass to the west which has subsequently been removed by strike-slip faulting or tectonic erosion. However, it is becoming apparent that crustal melting can also occur in an extensional environment, such as exists from time-to-time in active subduction tectonics. Moreover, it is important to realize that most of the features described above could equally well arise from extensive contamination of mantle-derived magmas by assimilation of such crustal material and that direct melting within the crust is not necessarily involved. Since there is considerable overlap of petrological and geochemical properties between the Palaeozoic and Mesozoic granitoids (e.g. Fig. 5.25), a *partially* common origin from the mantle (*sensu lato*) may seem a reasonable hypothesis, with the differences being mainly ascribed to degree of contamination. This is strengthened in the case of the Palaeozoic igneous rocks from the Altiplano area, and indeed those from the Southern Coastal Batholith (Section 5.2) and the Cordillera Domeyko (Section 5.4), where initial $^{87}Sr/^{86}Sr$ ratios are commonly rather lower (0.705-0.707). However, the observation that the effects are universal (none of the Palaeozoic rocks analysed in ANDCHRON have initial $^{87}Sr/^{86}Sr$ ratios less than 0.705) and fairly uniform, probably requires a mechanism for massive contamination other than assimilation during uprise of the magmas. We consider that melting at the crust-mantle boundary layer and the inevitable hybridization between crustal and mantle melts formed within such a localized zone is a suitable way of generating the observed geochemical and isotopic characteristics. Such high-level melting would imply a rapidly-subducting but shallow-dipping Benioff zone beneath an over-thickened continental crust.

The contrasting characteristics of the typically 'I-type' Mesozoic granitoids include a wider range of petrological compositions, a less lithophile-enriched geochemistry (Figs 5.24 & 5.25), except for those Cretaceous rocks which seem to represent extreme fractional crystallization), an absence of old inherited zircons, low initial $^{87}Sr/^{86}Sr$ and high initial $^{143}Nd/^{144}Nd$ ratios and young model Sm-Nd ages (mostly less than 500 Ma). These magmas are clearly derived within the mantle and have been emplaced with little or no

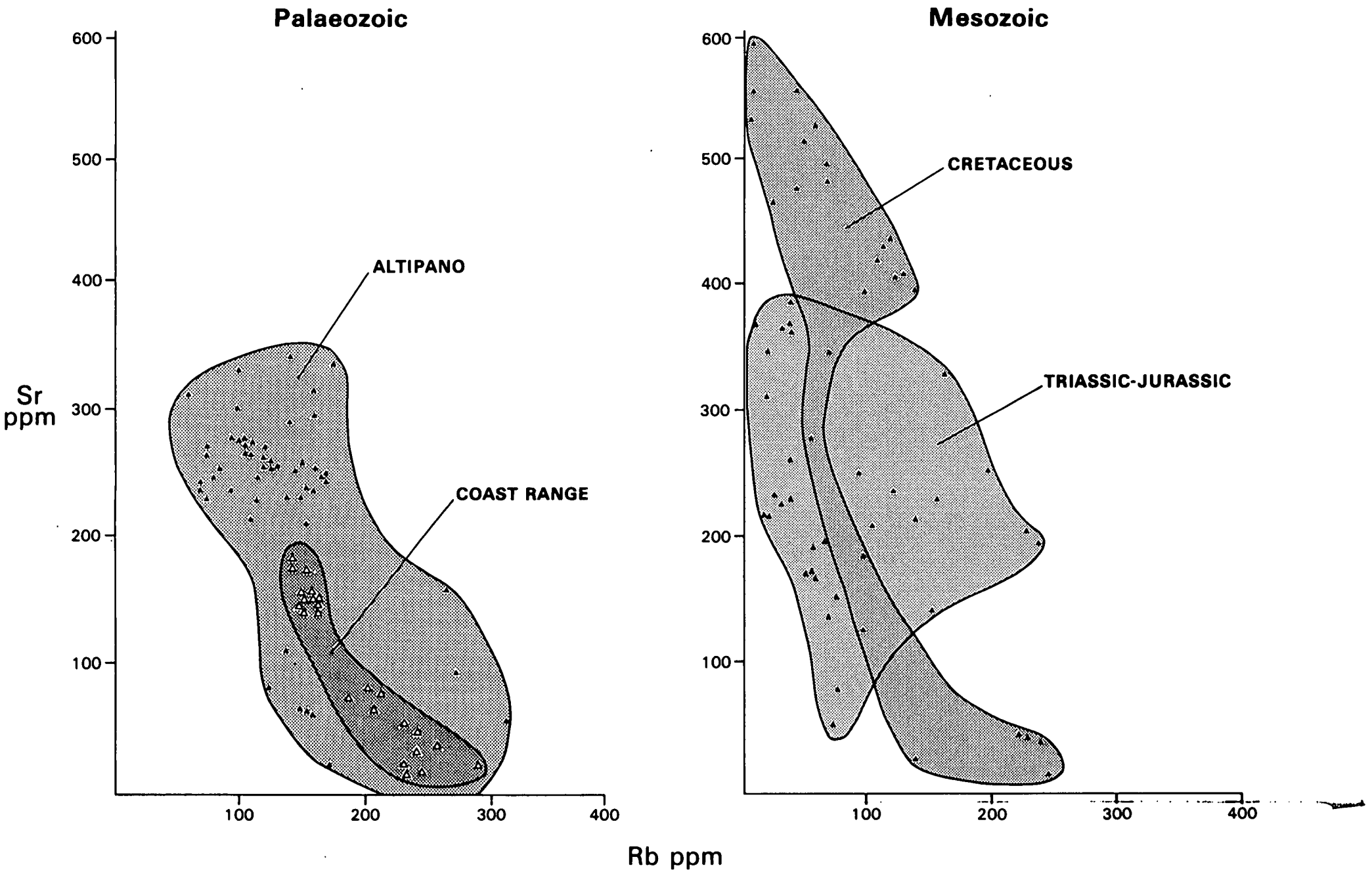

Fig. 5.25 Rb and Sr concentrations in granitoids of the El Salvador - Chanaral transect, grouped by age.

crustal contamination. Nevertheless, some differences are apparent even within this group. The Triassic-Jurassic granitoids have initial $^{87}Sr/^{86}Sr$ ratios of 0.7040-0.7045, essentially identical to those of Jurassic plutons from other regions of Chile (see previous sections) and the Jurassic-Cretaceous rocks of the Coastal Batholith of Peru (Beckinsale et al 1985). The homogeneity of these isotopic compositions is striking and probably reflects a uniform mantle source region of a relatively undepleted nature, possibly within the lithosphere immediately underlying the continental crust. The depleted-mantle isotopic characteristics of the mid-Cretaceous granitoids of this transect (Fig 5.24) are indicative of a deep mantle source region, perhaps even involving melting of parts of the subducting plate. The tapping of deep sources in a continental setting invariably necessitates an extensional tectonic regime. Back-arc extension during the Jurassic and early Cretaceous is well known from central and southern Chile, in the latter at least resulting in the emplacement of mantle-derived *basic* magmas.

The geochronological data above has established that magmatism in the two Palaeozoic belts was essentially synchronous, from Permian to mid-Triassic times and that the rock types are essentially indistinguishable. This allows the hypothesis that they once formed part of the same, perhaps rather broad magmatic arc, with magmatism extending from the fore-arc accretionary wedge to the back-arc continental platform. The overall trends in isotope geochemistry of the subsequent Mesozoic granitoids suggest a progressive change from shallow, mostly compressional, subduction, to much steeper subduction with the development of extensional tectonics and deeper magma sources. This scenario is illustrated in the cartoons of Fig. 5.26, where the tectonic models of Uyeda (1984) are employed, subduction changing from 'Chilean' type to 'Mariana' type between Triassic and late Cretaceous times. It is important to note that at the present day a reversion to Chilean type has taken place, the Recent volcanic products of the High Andes being more varied in their geochemical and isotopic characteristics than the Late Cretaceous granitoids analysed here.

This model also has implications for the origin, transport and concentration of metal ores. Those metals which are abundant in ancient metamorphic rocks or which are effectively concentrated by crustal processes are most likely to be found as ores in the Palaeozoic belts, whereas those which originate in the mantle or which are more easily redistributed by fluids of deep origin should occur in the Mesozoic belts.

Fig. 5.26 Cartoons showing a model for the changes in subduction regime with time in the southern Andes.

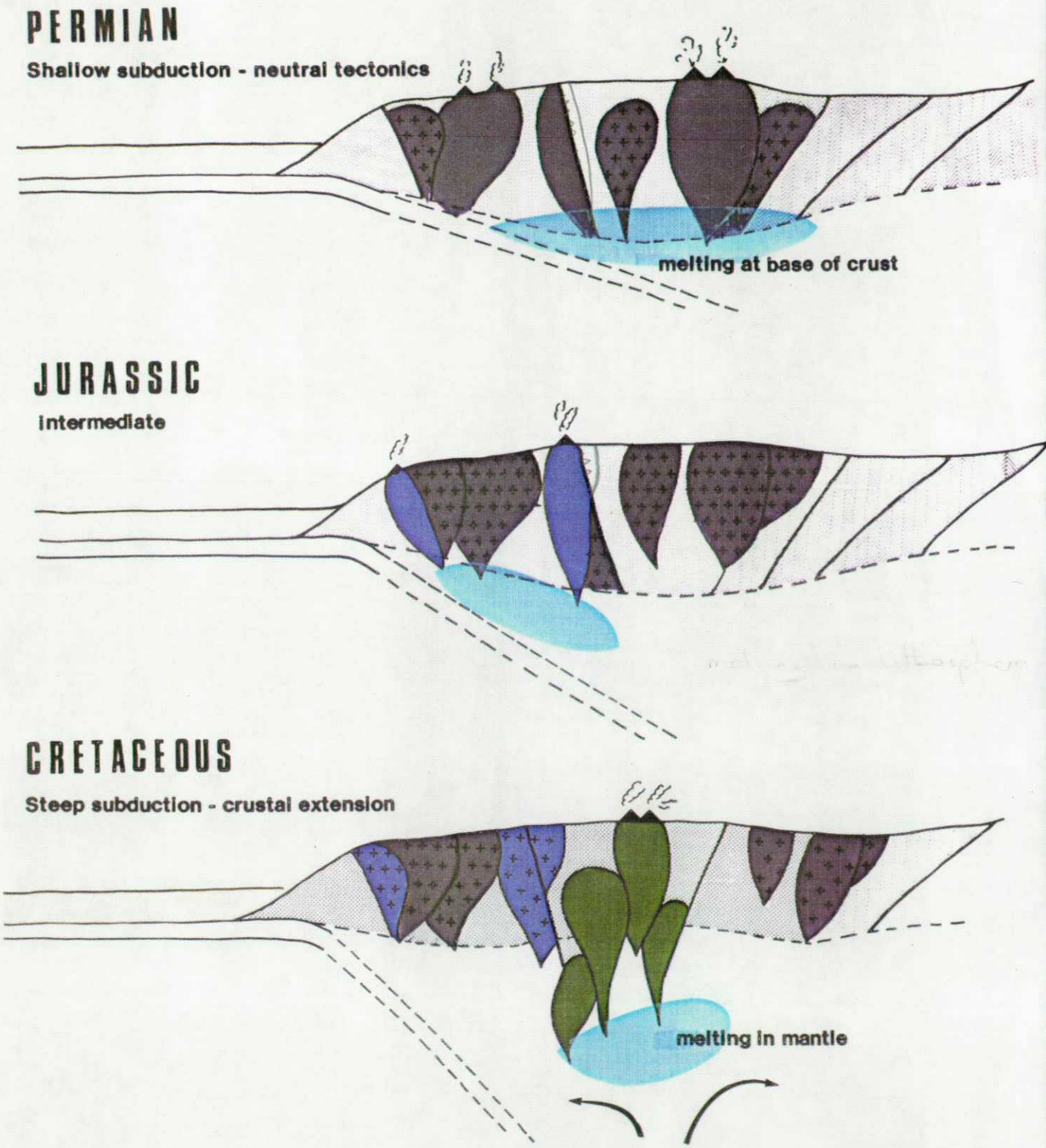

References:

Beckinsale, R.D., Sanchez-Fernandez,A.W., Brook,M., Cobbing,E.J., Taylor,W.P., and Moore,N.D. (1985). Rb-Sr whole-rock isochron and K-Ar age determinations for the coastal batholith of Peru. In W.S. Pitcher, M.P. Atherton, E.J. Cobbing and R.D. Beckinsale (eds), *Magmatism at a Plate Edge: The Peruvian Andes*. Blackie/Halstead Press, London, 177-202.

Berg, K. and Baumann, A. (1985). Plutonic and metasedimentary rocks from the Coastal Range of Northern Chile: Rb-Sr and U-Pb isotopic systematics. *Earth Planet. Sci. Lett.*, 75, 101-15.

Berg, K., Breitkreuz, C., Damm, K.-W., Pichowiak, S. & Zeil, W. (1983). The North-Chilean Coast Range - An Example for the Developement of an Active Contental Margin. *Geol. Rundschau*, 72, 2, 715-31.

Chappell, B.W. & White, A.J.R. (1974). Two contrasting granite types. *Pacific Geol.*, 8, 173-4.

Damm, K.-W., & Pichowiak, S. (1981). Geodynamik und Magmengenese in der Kustenkordillere Nordchiles zwisschen Taltal und Chanaral. *Geotekt. Forsch.*, 61, 166p.

Naranjo, J.A. & Puig, A. (1984). *Carta Geologica de Chile: Nos. 62-63, Hojas Taltal y Chañaral, Regiones de Antofagasta y Atacama*. Servicio Nacional de Geologia y Mineria, Santiago, Chile.

Uyeda, S. (1984). Subduction zones: their diversity, mechanism and human impacts. *Geojournal*, 8.4, 381-406.

TABLE 5.4 Rb-Sr WHOLE ROCK DATA: CHAÑERAL TO EL SALVADOR

	Rb ppm	Sr ppm	$^{87}Rb/^{86}Sr$	$^{87}Sr/^{86}Sr$
		1: PALAEOZOIC INTRUSIVES		
DOÑA IÑES CHICA				
MO 1045	94	235	1.168	0.71163
MO 1046	70	235	0.851	0.71034
MO 1047	60	312	0.618	0.70928
MO 1048	81	245	0.962	0.71100
MO 1049	141	113	3.628	0.72100
MO 1050	76	263	0.836	0.71045
MO 1052	74	270	0.771	0.71005
MO 1053	77	237	0.943	0.71087
CORRAL DEL ALHAMBRE				
MO 807	154	210	2.121	0.71416
MO 810	159	236	1.952	0.71355
MO 811	151	257	1.703	0.71278
MO 826	128	254	1.454	0.71157
MO 827	105	271	1.123	0.71047
MO 828	119	262	1.316	0.71111
MO 829	103	274	1.084	0.71050
MO 830	152	67	6.557	0.72940
MO 831	156	65	7.006	0.73133
MO 832	126	254	1.443	0.71140
MO 833	124	257	1.394	0.71129
MO 1012	97	300	0.932	0.70987
MO 1013	105	274	1.108	0.71039
MO 1014	106	267	1.146	0.71047
MO 1015	109	272	1.152	0.71048
MO 1016	95	278	0.993	0.71005
MO 1017	112	264	1.132	0.71083
MO 1018	132	232	1.616	0.71229
MO 1019	126	259	1.492	0.71185
MO 812	170	334	1.471	0.71269
MO 814	100	330	0.877	0.71024
MO 815	160	313	1.482	0.71243
MO 816	265	160	4.798	0.72429

	Rb ppm	Sr ppm	$^{87}Rb/^{86}Sr$	$^{87}Sr/^{86}Sr$
MONTANDON				
MO 812	170	334	1.471	0.71269
MO 814	100	330	0.877	0.71024
MO 815	160	313	1.482	0.71243
MO 816	265	160	4.798	0.72429
MO 1023	276	94	8.590	0.73862
MO 1024	314	58	15.776	0.76544
MO 1026	175	22 (±2%)	22.696	0.79013
MO 1027	326	80	11.736	0.74988
LA OLA				
MO 817	162	58	8.093	0.73566
MO 818	56	267	0.609	0.71058
MO 819	85	251	0.977	0.71180
MO 820	116	228	1.472	0.71363
MO 821	114	212	1.555	0.71375
MO 822	22	224	0.290 (±1%)	0.70953
MO 823	74	227	0.945	0.71175
MO 825	124	75	4.809	0.72448
PEDERNALES GREY GRANODIORITE				
MO 1028	141	282	1.194	0.71170
MO 1035	142	230	1.790	0.71348
MO 1036	149	231	1.872	0.71382
MO 1037	153	238	1.855	0.71363
PEDERNALES PINK GRANODIORITE				
MO 1038	141	282	1.441	0.71205
MO 1039	144	253	1.643	0.71281
MO 1040	172	244	2.038	0.71385
MO 1041	168	250	1.954	0.71369
MO 1042	167	248	1.958	0.71362
MO 1043	161	295	1.585	0.71255
MO 1044	159	256	1.804	0.71316

	Rb ppm	Sr ppm	$^{87}Rb/^{86}Sr$	$^{87}Sr/^{86}Sr$
CERROS DEL VETADO				
MO 1108	207	67	8.905	0.73770
MO 1109	236	15	48.104	0.86491
MO 1110	229	23	29.109	0.80581
MO 1113	209	77	7.881	0.73466
MO 1114	245	14	54.083	0.89129
MO 1115	185	72	7.544	0.73372
MO 1117	200	71	8.198	0.73532
MO 1123	238	48	14.449	0.75631
MO 1124	230	53	12.786	0.75152
MO 1125	238	32	21.688	0.78161
MO 1142	255	34	22.087	0.78190
CIFUNCHO: 1				
MO 747	292	23	37.385 (±1%)	0.82882
MO 749	149	156	2.757	0.72019
MO 750	152	141	3.127	0.72156
MO 751	151	151	2.899	0.72084
MO 752	160	150	3.120	0.72172
MO 753	162	143	3.287	0.72146
MO 754	156	155	2.917	0.72032
CIFUNCHO: 2				
MO 730	152	172	2.558	0.71560
MO 732	137	172	2.302	0.71486
MO 733	155	154	2.910	0.71742
MO 734	161	151	3.088	0.71755
MO 735	145	146	2.882	0.71686
MO 736	118	268	1.272	0.71075
MO 737	116	246	1.366	0.71078
MO 738	142	182	2.253	0.71460

	Rb ppm	Sr ppm	$^{87}Rb/^{86}Sr$	$^{87}Sr/^{86}Sr$
2: LATE TRIASSIC-JURASSIC INTRUSIVES				
CHAÑERAL				
MO 1143	57	192	0.857	0.70678
MO 1144	66	197	0.979	0.70715
MO 1145	54	170	0.924	0.70709
MO 1146	60	167	1.041	0.70735
MO 1147	38	229	0.489	0.70549
MO 1148	71	134	1.535	0.70885
MO 1149	76	151	1.451	0.70835
MO 1150	22	310	0.203 (±1%)	0.70471
MO 1151	38	258	0.429 (±1%)	0.70528
SIERRA PASTENES				
MO 839	90	287	0.908	0.70557
MO 840	102	256	1.152	0.70624
MO 843	59	418	0.409	0.70428
MO 844	56	429	0.376	0.70419
MO 845	67	394	0.491	0.70441
QUEBRADA MORADA				
MO 857	135	28	14.189 (±1%)	0.74312
MO 858	134	14	27.140 (±2%)	0.77547
MO 859	29	448	0.187 (±1%)	0.70461
MO 860	37	336	0.316 (±1%)	0.70533
MO 861	22	544	0.117 (±1%)	0.70449
MO 862	38	255	0.429 (±1%)	0.70596
GUAMANGA				
MO 1152	53	170	0.906	0.70719
MO 1160	137	215	1.835	0.70958
MO 1161	41	387	0.325	0.70526
MO 1162	75	51	4.263	0.71665
MO 1163	39	374	0.304 (±1%)	0.70520
MO 1165	37	365	0.292 (±1%)	0.70517
MO 1166	41	356	0.331 (±1%)	0.70543

	Rb ppm	Sr ppm	$^{87}Rb/^{86}Sr$	$^{87}Sr/^{86}Sr$
		3: CRETACEOUS INTRUSIVES		
INCA DE ORO				
MO 885	139	396	1.013	0.70479
MO 886	129	409	0.914	0.70471
MO 888	51	515	0.286	0.70384
MO 889	8	532	0.043 (±3%)	0.70365
MO 890	43	476	0.264 (±1%ø	0.70373
MO 891	122	437	0.812	0.70469
MO 892	125	407	0.894	0.70479
QUEBRADA SALADITO				
MO 1089	97	127	2.205	0.70714
MO 1090	102	397	0.747	0.70482
MO 1091	56	280	0.580	0.70440
MO 1092	98	183	1.540	0.70607
MO 1094	69	348	0.570	0.70442
MO 1095	46	391	0.341	0.70382
MO 1096	41	410	0.288	0.70372
MO 1098	23	467	0.145 (±1%)	0.70348
MO 1099	142	23	24.090 (±1%)	0.74646
SIERRA SAN JUAN				
MO 870	62	527	0.342	0.70385
MO 871	68	495	0.397	0.70393
MO 872	148	108	3.996	0.70920
MO 873	248	15	48.899 (±2%)	0.77610
MO 874	69	482	0.418	0.70393
MO 875	8	593	0.036 (±3%)	0.70363

TABLE 5.5 Sm-Nd DATA FROM NORTHERN CHILE.

$^{87}Sr/^{86}Sr_o$	ϵSr	Sm ppm	Nd ppm	$^{143}Nd/^{144}Nd$	$^{143}Nd/^{144}Nd_o$	ϵNd	Tdmur (Ma)
MO 1045 (Doña Iñes Chica)							
0.70714	+42.1	10.05	91.78	0.512193	0.512128	-4.2	871
MO 1013 (Corral del Alhambre)							
0.70650	+32.6	4.58	23.20	0.512321	0.512128	-3.8	1123
MO 1023 (Montandon)							
0.70722	+43.0	2.11	7.44	0.512378	0.512089	-4.3	2052
MO 819 (La Ola)							
0.70855	+61.5	8.01	41.53	0.512220	0.512041	-5.8	1236
MO 1110 (Cerros del Vetado)							
0.70810	+55.1	5.59	20.32	0.512430	0.512173	-3.2	1048
MO 752 (Cifuncho)							
0.71063	+91.2	8.73	43.97	0.512243	0.512047	-5.3	789
MO 730 (Cifuncho)							
0.70555	+19.7	5.17	24.44	0.512258	0.512025	-5.0	846
MO 974 (Alto del Inca)							
0.70799	+56.9	5.88	25.97	0.512056	0.512668	-8.1	1802
MO 979 (Alto del Inca)							
o.70732	+47.4	4.02	22.11	0.512165	0.512853	-4.5	1237
MO 941 (Formation Cas)							
0.70600	+25.9	5.52	27.40	0.512364	0.512145	-2.8	1086
MO 1146 (Chañeral)							
0.70412	-1.7	2.4	12.70	0.512613	0.512450	+1.8	671
MO 1120 (Cerros del Vetado Diorite)							
0.70478	+6.7	5.87	25.85	0.512558	0.512414	-0.4	945

$^{87}Sr/^{86}Sr_o$	ϵSr	Sm ppm	Nd ppm	$^{143}Nd/^{144}Nd$	$^{143}Nd/^{144}Nd_o$	ϵNd	Tdmur (Ma)
MO 1157 (Guamanga)							
0.70419	-1.0	4.89	23.48	0.512494	0.512327	-1.0	933
MO 1165 (Guamanga)							
0.70433	+1.0	3.07	16.27	0.512600	0.512449	+1.4	687
MO 883 (Inca de Oro)							
0.70435	+0.1	10.87	62.00	0.512827	0.512737	+5.2	350
MO 888 (Inca de Oro)							
0.70351	-12.7	2.59	12.94	0.512812	0.512747	+4.1	422
MO 1070 (Inca de Oro)							
0.70367	-10.3	8.26	40.00	0.512722	0.512656	+2.4	569
MO 1087 (Inca de Oro)							
0.70358	-11.7	2.93	11.60	0.512860	0.512778	+4.8	508
MO 871 (Sierra San Juan)							
0.70334	-14.7	4.50	27.48	0.512880	0.512813	+6.0	267

5.4 NORTHERN CHILE - CORDILLERA DOMEYKO AND AGUAS BLANCAS (23°30'S - 24°30'S.

This study, which was undertaken with the co-operation and full logistic support of the Chilean Geological Survey, is an initial reconnaissance transect through the Northern Chilean Andes at latitude approximately 24°S. Although incomplete, the transect intersects a wide variety of Palaeozoic and Mesozoic plutons, some of which are thought to represent the earliest igneous events in the central and southern Andes. Detailed mapping by SNGM in this area was only just starting in 1984 and work was concentrated at the eastern end of the transect in a suite of igneous rocks thought to be the Palaeozoic forerunners of the Miocene calderas in the high Puna.

The Cordillera Domeyko consists largely of extensive exposures of Late Palaeozoic-Early Triassic volcanic rocks and associated intrusions of batholithic size. They form part of the eastern magmatic belt which extends for more than 4000km from Argentina into Peru and Bolivia, and which includes the Altiplano area discussed in the preceeding section. Ignimbrite and intermediate lava flows are interbedded with lagoonal fossiliferous sediments of Carboniferous-Permian age (Osorio and Rivano 1985). The granitoids and the volcanic sedimentary suite respectively intrude and overly older rocks consisting of Ordovician granitoids and Devonian to Early Carboniferous marine sediments (Davidson et al 1981, Mpodozis et al 1983). Confirmation of the Ordovician age of basement granitoids was obtained from Rb-Sr analysis of samples collected from the Alto del Inca pluton on the Argentinian border (Fig.5.27 and Table 5.6), which gives an age of 433 ± 22 Ma with an initial $^{87}Sr/^{86}Sr$ ratio of 0.7072 but with considerable scatter of data points.

The igneous rocks of the Cordillera consist of silicic to intermediate volcanic rocks associated with granodioritic plutons exposed in the axes of the Imilac and Almeida ranges or as arcuate plutons in the more deeply eroded Mariposas range. These igneous rocks outcrop over a distance of some 100km in two elongate horsts which are separated by post-Cretaceous grabens now occupied by the Punta Negra, Imilac and Atacama salars (Fig. 5.28). The horsts are cross-cut by high angle reverse faults which are Tertiary in age and frequently associated with geothermal and volcanic activity. The batholithic core rocks are flanked by 2000m of massive rhyolites, breccias, andesitic flows, ignimbrites and volcanoclastic sediments. The occurrance and distribution of

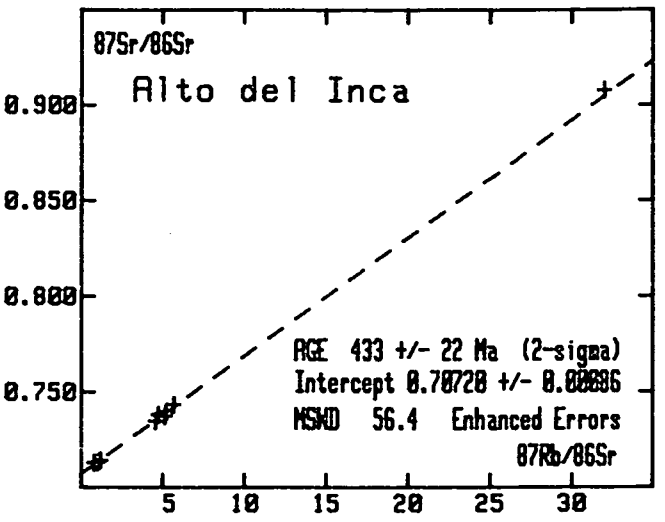

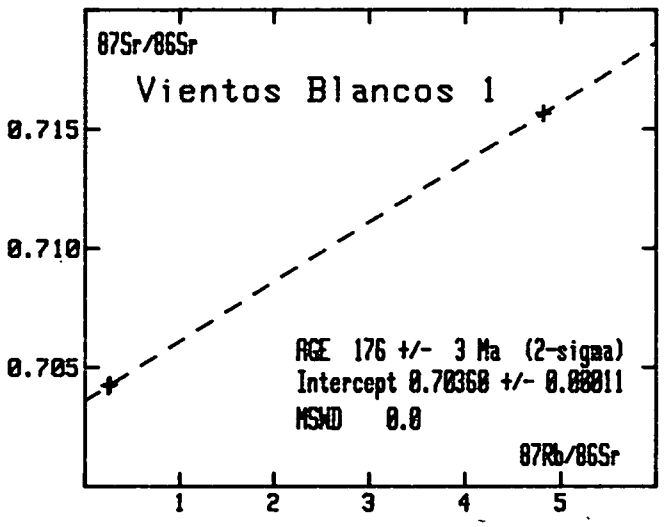

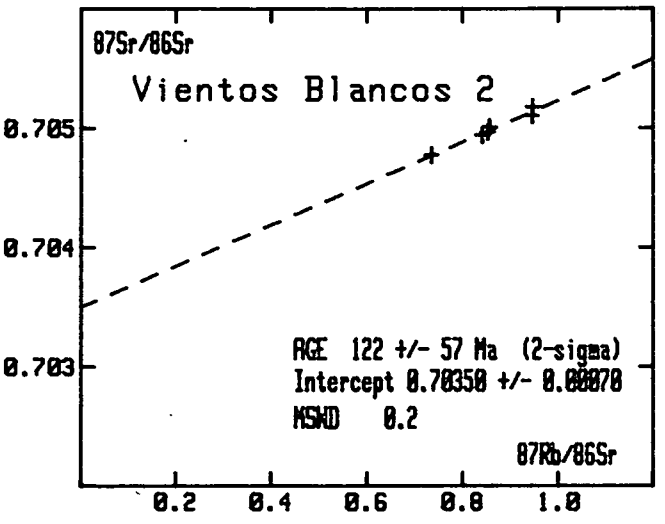

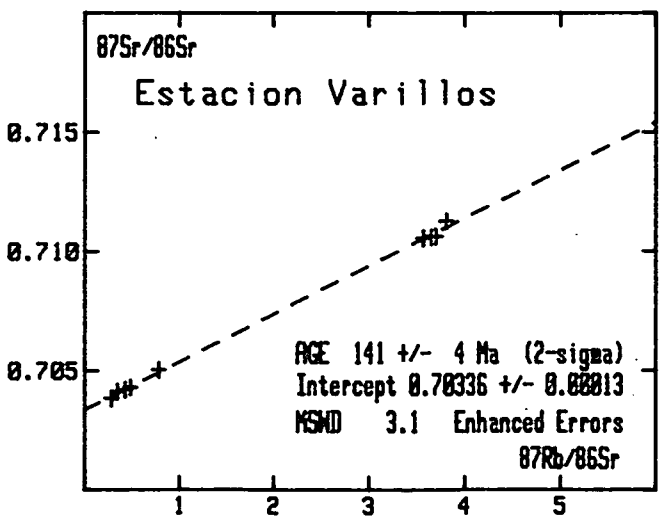

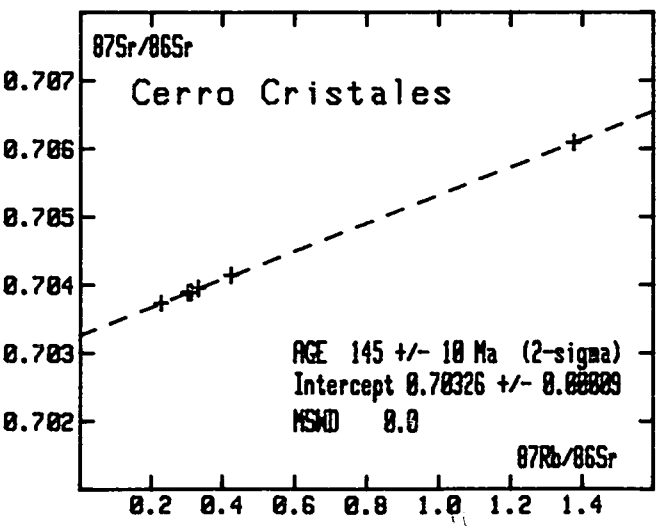

Fig. 5.27 Rb-Sr whole-rock isochron diagrams for the Alto del Inca intrusion (Cordillera Domeyko) and granitoids from the Aguas Blancas area, northern Chile.

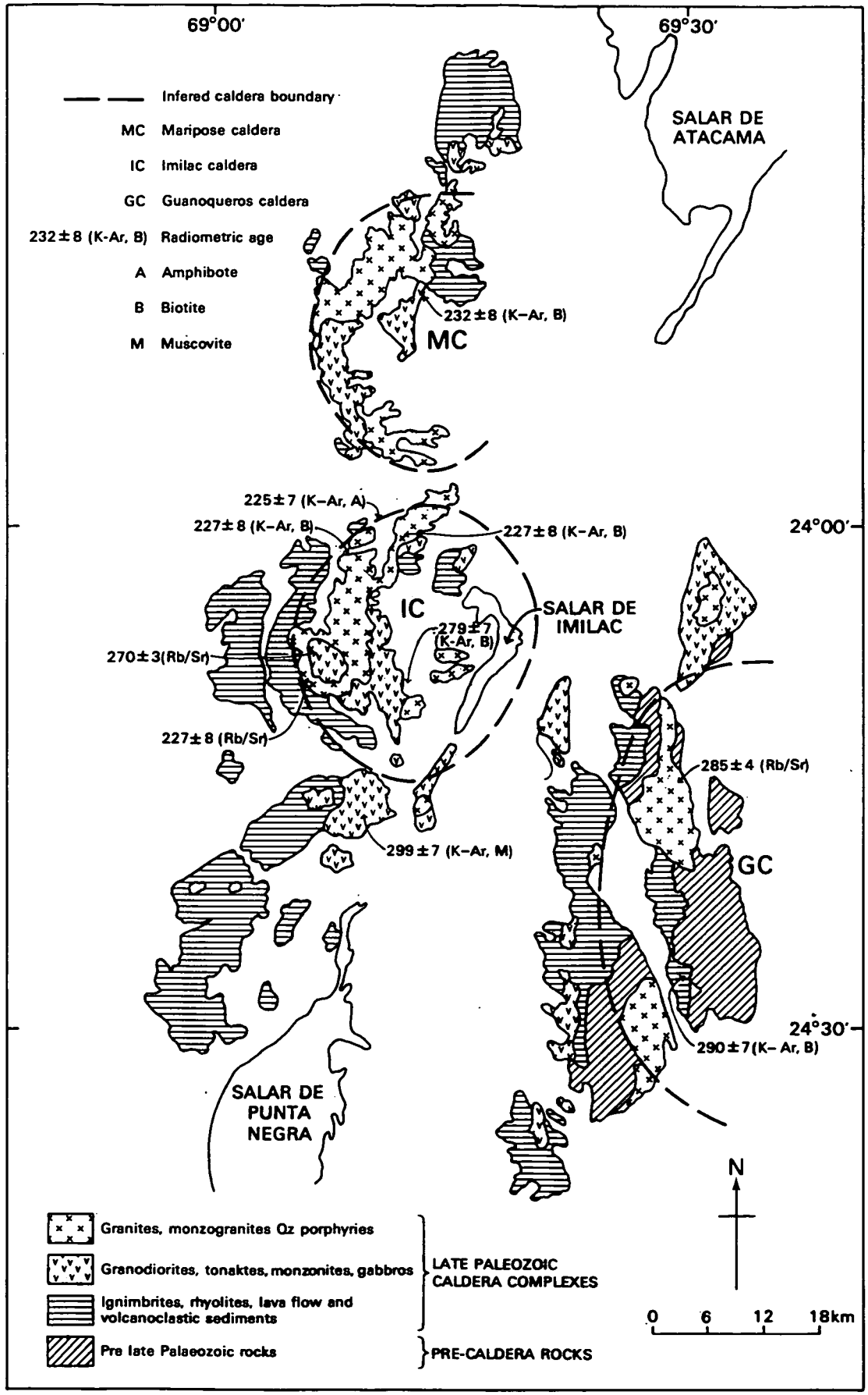

Fig. 5.28 Geological sketch map of the Palaeozoic caldera region of Imilac, northern Chile.

such a thick sequence of rhyolitic ash flow tuffs in close association with large granitic plutons suggests that they are the eruptive material of caldera-like structures and that the plutons are their eroded roots. The existance of three calderas has been inferred: Guanaqueros, Imilac and Mariposas. Additional calderas may have occurred in areas which are now occupied by younger batholithic rocks or covered by Mesozoic-Cenozoic strata.

The existance of the Guanaqueros caldera is inferred from the occurrence of a thick pile of outward-dipping rhyolitic ash-flow tuff, lava flows and volcaniclastic sediments which are spatially related to a core of pink and red granites and granodiorites.

The Imilac caldera lies to the west of the late Cretaceous graben and is almost circular in form, some 25km in diameter. A central fine-grained granitic or granodioritic core is rimmed by more intermediate to basic rock types including gabbros, tonalites and granodiorites. The whole complex is surrounded by a silicic volcanic pile, deeply eroded on the eastern side where it is open to the Salar de Imilac.

The Mariposas caldera to the north of Imilac provides a deeper erosional view into the plutonic suite of a caldera. A rim and core are preserved similar to those atImilac, but the volcanic representatives are scattered at the northern end of the Sierras Mariposas.

Isotopic data has been collected from each of the three calderas (Table 5.6). Broadly speaking, igneous activity falls into two age bands, one Permo-Carboniferous and the other Late Triassic in age. Material from the rims of the Guanaqueros and Imilac calderas have given ages of 285 ± 4 Ma and 271 ± 17 Ma respectively with initial $^{87}Sr/^{86}Sr$ ratios of 0.7057 and 0.7060 (Fig 5.29). The equivalent volcanic representatives of this age are found in the Cas formation - an extensive exposure of rhyolitic ash-flow tuff outcropping in the Atacama and Antafogasta regions. The data points for this formation south of Imilac scatter in excess of experimental error but also strongly suggest an age of 271 ± 17 Ma for extrusion, with a similar initial $^{87}Sr/^{86}Sr$ ratio of 0.7060 (Fig 5.29). These ages probably correspond to earliest Permian, although a K-Ar age of 290 ± 7 Ma from a biotite in an ignimbrite at the base of the volcanic pile could be an indication of a Permo-Carboniferous age for the initiation of the complex.

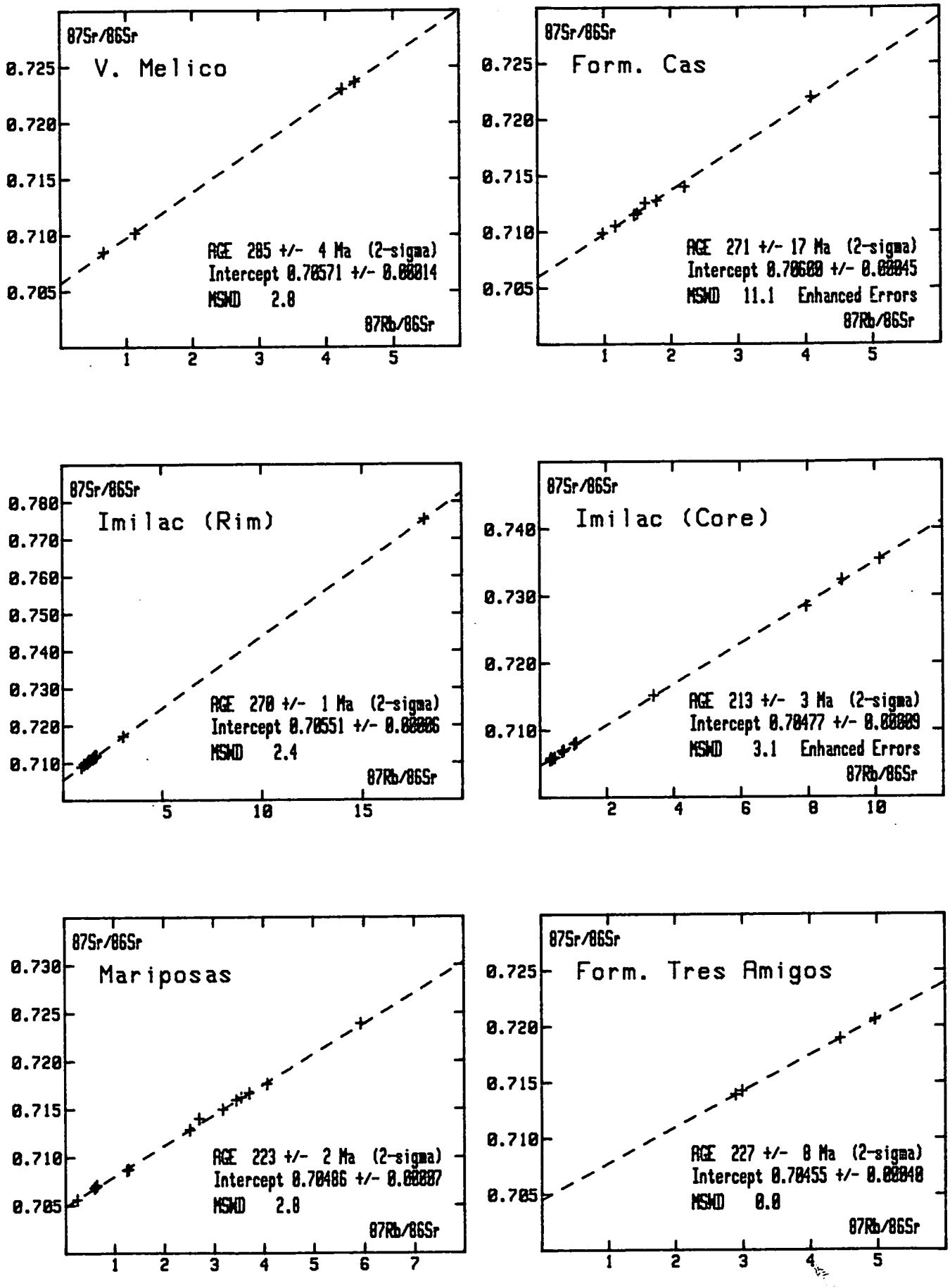

Fig. 5.29 Rb-Sr whole-rock isochron diagrams for plutonic and volcanic igneous rocks from the calderas of the Imilac region, northern Chile.

A later clearly identifiable period of activity is represented by the silicic monzogranitic cores best seen in Imilac and Mariposas, where results from two very good isochron suites yield ages of 213 ± 3 Ma and 223 ± 2 Ma with initial $^{87}Sr/^{86}Sr$ ratios of 0.7048 and 0.7049 respectively (Fig. 5.29). Volcanic activity associated with this plutonism is reflected in a Rb-Sr isochron of 227 ± 8 Ma obtained from the Tres Amigos rhyolite formation with an initial $^{87}Sr/^{86}Sr$ ratio of 0.7046 (Fig. 5.29). This data would support the theory that late Triassic calderas were founded on older calderas related to their own distinct volcanic piles.

A consistent trend is seen in the decrease of initial $^{87}Sr/^{86}Sr$ ratios with continued plutonism. In the Cordillera Domeyko this ranges from 0.7072 ± .0009 in the late Ordovician to 0.7048 ± .0001 by late Triassic times. Data for Jurassic and Cretaceous plutons from the Aguas Blancas district, further to the west in this transect show a continuation of this trend (Table 5.6, Figs 5.27), so that by early Cretaceous times, initial $^{87}Sr/^{86}Sr$ ratios had fallen to *c.* 0.7033. This relationship of decreasing initial 87Sr/86Sr ratios with time was discussed in relation to a second transect through northern Chile at latitude 26°S (see Section 5.3). Similar late Jurassic to early Cretaceous ages and low initial $^{87}Sr/^{86}Sr$ ratios were obtained for aplites and granodiorites from the latitude of Paposo, approximately half way between the two transects. This suggests a reduction in crustal involvement in magmatic activity with time, so that by Cretaceous times there would appear to be little or no crustal interaction with the granitic magmas.

The long magmatic history of the region and the likely presence of collapsed volcanic calderas are important antecedents for hydrothermal deposits. Most of the Au, Cu, Ag, Pb and Zn mineralization in the Imilac and Guanaqueros areas is located in veins hosted by the more basic outer rim components i.e. the earlier phase of caldera construction, isotopically characterized by the relatively higher initial $^{87}Sr/^{86}Sr$ ratios. Although no economic deposits were found, the caldera model for the Cordillera Domeyko could ultimatelyprovide a valuable key to exploration for similar precious metal deposits further north and south where there are further outcrops of the Late Palaeozoic belt.

References:

Davidson, J., and others. 1981. El Paleozoico de Sierra de Almeida, al oeste de Monturaqui, Alto Cordillera de Antofagasta, Chile. *Rev. Geol. Chile*, 12, 3-23.

Mpodozis, C., and others. 1983. Los granitoides de Cerros de Lila, manifestaciones de un episodo intrusivo y termal del Paleozoico inferior en los Andes del norte de Chile. *Rev. Geol. Chile*, 18, 3-14.

Osorio, & Rivano, S. 1985. Paraparchitidae (Ostracoda) del Paleozoico superior en la formacion Pular (Harrington 1961), Quebrada de Pajonales, vertiente occidental de la Sierra de Almeida, Antofagasta. *Actas 9° Congr. Geol. Chile*, 439-57.

TABLE 5.6: Rb-Sr WHOLE ROCK RESULTS FROM CORDILLERA DOMEYKO - AGUAS BLANCAS.

	Rb ppm	Sr ppm	$^{87}Rb/^{86}Sr$	$^{87}Sr/^{86}Sr$
ALTO DEL INCA				
MO972	71	200	1.0234	0.71310
MO973	76	187	1.1868	0.71406
MO974	68	246	0.7976	0.71291
MO976	204	19	32.0126	0.90765
MO977	119	67	5.1472	0.73732
MO978	128	81	4.5810	0.73467
MO979	130	72	5.2243	0.73943
MO980	127	65	5.6912	0.74321
MO981	120	74	4.7474	0.73804
VALLE MELICO				
MO982	92	407	0.6561	0.70848
MO984	194	127	4.4245	0.72362
MO986	198	136	4.2344	0.72297
MO987	151	386	1.1289	0.71017
FORMATION CAS				
MO934	135	178	2.2011	0.71402
MO935	131	214	1.7825	0.71279
MO937	119	213	1.6093	0.71257
MO938	117	234	1.4467	0.71151
MO939	119	234	1.4896	0.71163
MO940	114	338	0.9746	0.70989
MO941	123	306	1.1624	0.71053
MO942	153	109	4.0812	0.72200

	Rb ppm	Sr ppm	87Rb/86Sr	87Sr/86Sr
SIERRA MARIPOSAS				
MO995	112	86	3.7118	0.71666
MO996	116	82	4.0737	0.71762
MO997	113	103	3.1858	0.71495
MO998	118	99	3.4516	0.71592
MO1001	111	90	3.5534	0.71621
MO1002	133	64	5.9334	0.72390
MO1003	106	122	2.5244	0.71285
MO1004	91	205	1.2857	0.70874
MO1005	92	214	1.2560	0.70867
MO1006	40	476	0.2461	0.70560
MO1007	68	305	0.6443	0.70711
MO1008	65	311	0.6000	0.70684
MO1010	99	107	2.7083	0.71402
MO1011	68	311	0.6316	0.70699
TRES AMIGOS RHYOLITES				
MO950	195	126	4.4452	0.71890
MO951	205	119	4.9696	0.72059
MO952	191	190	2.8912	0.71390
MO953	197	191	2.9899	0.71420
IMILAC RIM				
MO964	141	246	1.6610	0.71173
MO965	517	83	18.1358	0.77526
MO966	152	274	1.6118	0.71174
MO967	148	330	1.2964	0.71065
MO968	132	281	1.3605	0.71088
MO969	117	358	0.9439	0.70895
MO970	226	214	3.0498	0.71722
MO989	114	306	1.0806	0.70976
MO990	143	274	1.5107	0.71129
MO991	41	306	1.2320	0.71010
MO992	161	287	1.6250	0.71200
MO993	159	297	1.5537	0.71154
MO994	170	291	1.6885	0.71207

	Rb ppm	Sr ppm	87Rb/86Sr	87Sr/86Sr
IMILAC MONZOGRANITE CORE				
MO943	53	428	0.3547	0.70574
MO944	53	511	0.3038	0.70561
MO945	129	109	3.4048	0.71518
MO946	66	423	0.4473	0.70595
MO947	56	510	0.3234	0.70589
MO948	57	458	0.3572	0.70576
MO949	56	465	0.3485	0.70577
MO954	139	45	9.0093	0.73236
MO955	140	40	10.1429	0.73544
MO957	77	310	0.7137	0.70701
MO958	85	240	1.0222	0.70799
MO959	122	44	7.9539	0.72846
MO960	86	232	1.0793	0.70817
MO961	73	312	0.6727	0.70689
CERRO CRISTALES				
MO918A	49	450	0.3123±.7%	0.70389
MO918B	38	482	0.2277±.8%	0.70373
MO920	63	427	0.4240±.6%	0.70414
MO921	53	461	0.3321±.6%	0.70395
MO922	48	455	0.3030±.7%	0.70389
MO923	100	209	1.3771	0.70609
ESTACION VARILLOS				
MO902	68	249	0.7833	0.70504
MO903	152	119	3.6549	0.71060
MO904	154	125	3.5688	0.71051
MO905	131	99	3.8094	0.71127
MO906	39	326	0.3459±.8%	0.70413
MO908	72	483	0.4295	0.70420
MO909	75	448	0.4841	0.70431
MO910	130	101	3.7015	0.71063
MO911	60	606	0.2832±.8	0.70383

	Rb ppm	Sr ppm	87Rb/86Sr	87Sr/86Sr
VIENTOS BLANCOS				
MO925	36	388	0.2666±.7%	0.70427
MO926	85	51	4.8127±.6%	0.71566
MO927	33	393	0.2449±.8%	0.70421
MO928	77	305	0.7344	0.70478
MO929	94	288	0.9461	0.70518
MO930	90	303	0.8527	0.70497
MO931	96	294	0.9453	0.70511
MO932	88	298	0.8557	0.70501
MO933	88	303	0.8407	0.70494

6. ANDEAN METALLOGENESIS: APPLICATION OF ISOTOPE GEOLOGY AND FLUID INCLUSIONS TO PROBLEMS OF ORE GENESIS AND EXPLORATION.

Several comprehensive regional appraisals of Andean metallogenesis have been published (Petersen 1970, Sillitoe 1976). These have drawn attention to the striking correlation between narrow longitudinal metallogenic zones and Mesozoic-Cenozoic calc-alkaline magmatic belts parallel to the continental edge. With some exceptions the overall pattern conforms to repeated mineralization above a subduction zone at a convergent plate margin.

Because of the paucity of reliable data for many areas, a degree of oversimplification is inevitable. However, by taking into account observed element associations, relative position with respect to the subducting plate and thickness of the overlying continental crust, major differences in the style and character of mineralization can be related to the spatial and temporal evolution of calc-alkaline magmatism. According to Sillitoe (1976), whose geotectonic model still provides the explanation for Andean metallogeny, there is a general transverse assymmetric metal zonation (Fig. 6.1). A discontinuous coastal Fe belt gives way successively to Cu-(Mo-Au), Cu-Pb-Zn-Ag and Sn-(W-Ag-Mo) belts further east. In northern Peru and southern Chile the mineralized cross section is approximately 150km in width, increasing to 500km over the Bolivian Altiplano. Zonation is by no means continuous throughout but is remarkably regular and is ascribed to the preferential release of different suites of metals from successively deeper parts of the subduction zone. Sufficient evidence exists to show that the locus of magmatic activity migrated progressively eastwards during the Jurassic and Cretaceous, and then retreated westwards during the Tertiary. By inference the spatially related mineralization is assumed to have followed a similar path. This appears to be true for the westernmost Fe and Cu belts, particularly with regard to the emplacement of porphyry coppers, although some doubt exists as to the position of the eastern Cu and Sn belts within this time-space framework.

The origin of the Bolivian Sn-W-Ag province is highly controversial and Sillitoe's views are not universally held. Many advocate a recycling of Sn from older metallogenic events and analysis of mid-Andean volcanics points to a primary Sn enrichment in the Precambrian-Palaeozoic metamorphic basement (Lehman and Pichler, 1980). There is no simple correlation between Sn

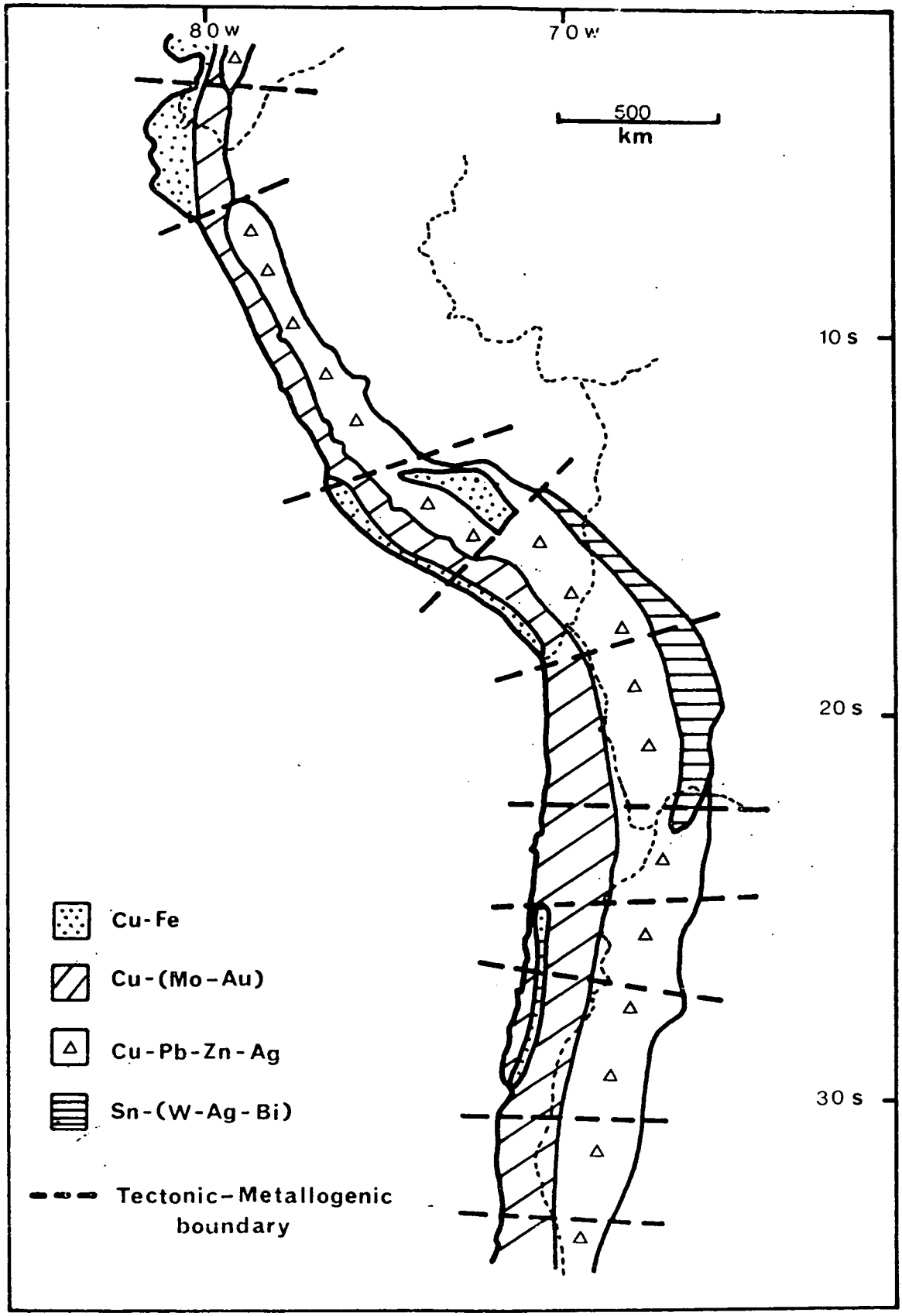

Fig. 6.1 Metallogenic map of the central Andes (after Sillitoe 1976).

concentration and crustal thickness, and no proof of a young Sn belt in accordance with classical plate tectonic concepts. Whatever explanation applies it is evident that extensive mineralization accompanied both intrusive and extrusive Andean magmatism from late Triassic to Recent times. Until 1980 little serious consideration had been given to precious metal epithermal Au-Ag deposits - the type which support extensive mining operations in the Cenozoic magmatic belts of the western USA. It is now realised they have a wide distribution in South America and are an integral facet of Andean metallogenesis. Because they are preferentially developed in the uppermost parts of volcanic systems they are only preserved in the youngest volcanic belts. The relevance of plate tectonics to the genesis of epithermal deposits has still to be determined since their present distribution is primarily a function of the depth of erosion.

Unfortunately, when assessed on the scale of districts or provinces , the grand model does not provide a satisfactory basis for exploration. Neither does it fully account for the marked tectonic segmentation of metallogenic belts and attendant changes in the intensity and character of mineralization (Sillitoe 1974). Whilst not invalidating the model, these shortfalls demonstrate the extent of research still to be undertaken. The voluminous literature on porphyry Cu deposits illustrates very clearly the intensity of scientific research and effort required to bridge the gap between metallogenic hypothesis and a working exploration concept. Other styles of mineralization now await the same detailed analysis. Future studies need to consider the more fundamental problems of Andean metallogenesis, namely the precise temporal relationship between mineralization and magmatism, the role of the basement as a source for metals and the influence of host rock lithology on metal associations. Nevertheless the sheer variety of ores and the diversity of ore environments necessitates a systematic "deposit by deposit" approach. For this reason ANDCHRON metallogenic studies initiated after 1983 were restricted to a limited number of deposits. Priority was given to those deposits or styles of mineralization identified as having high economic potential in areas delineated for geochronological study: in Chile the precious metal Au-Ag epithermal deposits of the El Salvador district; in Peru the Ag-rich polymetallic base metal deposits of the La Libertad province and Cu-Fe deposits of the coastal belt south of Lima.

In each case modern isotopic and/or fluid inclusion techniques were used either to solve outstanding aspects of ore genesis or test new methodologies for mineral exploration. Projects completed during the period 1983-86 include:

1. Isotopic and fluid inclusion study of the Silica del Hueso gold deposit, Chile.

2. Source of sulphur in Cretaceous ore deposits in the Chilean Andes

3. Metallogenic significance of lead isotope abundance studies on galena ores in the Chilean Andes.

4. Geochronology of copper-iron deposits in the Western Metallogenic Province, Peru.

5. Evaluation of strontium and sulphur isotopes as guide to silver-rich polymetallic vein deposits, Quiruvilca, Peru.

Chile.

For many years Chile's heavy dependance on copper exports and a State monopoly of mining and smelting have led to a mineral industry based on large tonnage, low grade, high investment Cu operations. With the advent of a less restrictive foreign investment policy, the granting of 2-year renewable exploration concessions and the relative stability of precious metal prices, several independant mines have recently come on-stream. The most successful is El Indio, a Cu-Au-Ag deposit with proven reserves of 5mil tons, averaging 0.3 ozs Au and 3.6 ozs Ag per ton. El Indio represents one of a group of precious metal deposits belonging to the epithermal type. Most are associated with young subaerial volcanic sequences; hence the current feverish mining activity in Chile and Peru. The extreme variability in ore grade, host rock association and mineralogy of epithermal deposits poses serious problems for exploration and, despite much progress, there is a general lack of basic information concerning the physico-chemical state of the ore fluids and controls of ore deposition. Within the Tertiary and Quaternary volcanic belts several new deposits have been discovered which are amenable to low cost, heap-leach techniques and offer Chile a chance to offset its economic tie to copper and

become a major South American precious metal producer. Through the support and co-operation of CODELCO access was granted to Silica del Hueso, an epithermal gold prospect in the El Salvador district soon to come on-stream. Given this opportunity and the significance of epithermal mineralization as a facet of Andean metallogenesis, a detailed investigation was commenced. Other projects undertaken include a Pb isotope abundance study of galena ores in the Chilean Andes and a related study of the source of sulphur in Cretaceous ore deposits from the same region. The Pb isotope project was initiated in 1984 and carried out in collaboration with A. Puig (SNGM, Chile) while he was registered for a CNNA M.Sc. degree at Oxford Polytechnic. The sulphur isotope study developed as a natural extension of the above work during his stay in the BGS laboratories, London.

Peru

Although Peru's annual metal output is second to Chile, the Peruvian segment of the Andes contains the greatest diversity of mineral deposits of the entire Andean chain as shown by its wide range of metal exports. For the most part the larger producing mines are highly mechanised, highly efficient and have attracted considerable geological interest for decades. At a local scale, studies have been concerned with the detailed mineralogy of the ores, the geometry of the oreshoots, the geology of the mine area and other aspects which directly and indirectly influence mining and metallurgical operations. Excellent examples of such investigations are given by Lewis (1955), Ward (1961) and Petersen et al.(1977). More recently modern isotopic and fluid inclusion techniques have been employed providing a better insight into the genesis of the ores (Rye and Sawkins 1974, Landis and Rye 1974, Norman & Landis 1983). In contrast, regional studies have sought to establish metallogenic provinces and their relationship to the tectonic evolution of the Andes, particularly the link with Mesozoic-Cenozoic magmatism. The work of Clark and Zentilli (1972) and Sillitoe (1974,1976) illustrates this approach very clearly.

With the exception of the porphyry copper deposits (e.g. Michiquillay, Cerro Verde, Toquepala), metallogenic studies designed to define the genetic coherence of various styles of mineralization or groups of deposits have been lacking. This is true for the silver-rich basemetal deposits of the Western

Cordillera polymetallic belt and the copper-iron deposits of the Coastal copper belt which account for more than 50% of Peru's non-fuel mineral exports. A situation now prevails where the geological databank for these deposits is inadequate to support exploration in areas with no recorded mining history. The lack of data is especially crucial with regard to the nature and origin of the ore fluids, the source of metal, the timing of mineralization and the influence of the host rock environment on mineral enrichment and deposition. As a result no conceptual model of ore genesis has yet been deduced which satisfactorily accounts for those magmatic processes which give rise to ore deposits and those that don't. The generalisation that most ore deposits associated with the Andean orogen are temporally, spatially and genetically related to intrusive and extrusive calc-alkaline magmatism is too broad, and does not constitute a reliable exploration discriminant.

The metallogenic investigations of Project ANDCHRON in Peru are a combination of work initiated prior to 1984 in direct support of Peruvian geologists based in British Universities, and projects initiated during field visits to Peru by BGS staff in 1984 and 1985. The former is represented by the geochronological study of Cu-Fe deposits in the Arequipa segment (Raul-Condestable, Marcona, Eliana) in collaboration with Dr. J.L. Injonque-Espinoza (INGEMET) for which he was awarded the degree of PhD by the University of Nottingham (1985). The latter comprise isotopic and fluid inclusion investigations of Cu-Pb-Zn-Ag mineralization at Julcani and Quiruvilca. Both types of research embody two main objectives:

1. To supplement and improve the geological data bank for base metal ore genesis related to Mesozoic-Cenozoic magmatic processes (excluding porphyry coppers).

2. To evaluate the contribution of isotopic and fluid inclusion techniques to mineral exploration.

Raul-Condestable, Marcona and Eliana belong to the group of magnetite-chalcopyrite-amphibole deposits which make up the Coastal Copper sub-province of the Western Metallogenic Province (see Fig.6.1). They define a linear belt between latitudes 14° and 18°S and are closely associated with a cycle of basic magmatism which proceeded intrusion of the Coastal Batholith. Most are developed at the contact with, or within units of, the batholith but some

display textural characteristics suggesting a stratiform volcanogenic origin. Magnetite-amphibole deposits with or without chalcopyrite are recognised throughout the Andean Cordillera, the greatest number being located in a belt south of latitude 25°S in northern Chile. Those in Peru display a complex history of burial metamorphism and hydrothermal reworking which has tended to obscure their origin. The geochronological investigation described below was carried out to establish the age of the ores and if possible resolve the "volcanogenic vs contact-metasomatic" controversy concerning their genesis.

Julcani and Quiruvilca belong to the Western Cordillera polymetallic sub-province of northern and central Peru which extends from Cajamarca in the north to Abancay in the south. Both are vein-type Cu-Pb-Zn-Ag deposits hosted by Tertiary volcanics.

Julcani was selected because recent deep underground workings at the mine have revealed veins passing into the underlying Lower Palaeozoic Excelsior Shales. This provided a unique opportunity to carry out several lines of investigation:

1. Use of strontium and lead isotopes to test the hypothesis that metals deposited in the volcanics were leached from the Palaeozoic shales by heated groundwaters during Tertiary volcanism.

2. Use of fluid inclusions and oxygen isotopes to determine the temperature and salinity of the ore fluids, the palaeogeothermal gradient below the volcanics, and the extent of water-rock interaction.

At Quiruvilca the mineralization consists of a dense network of fissure veins implying enclosure within a more extensive area of hydrothermal activity. Using Sr and S isotopes it was planned to:

1. study the extent of water-rock interaction around the central ore zone and assess the feasiblity of using isotopic anomalies as a guide to concealed mineralization.

2. obtain radiometric ages for the host volcanics and mineralization.

In theory, Julcani and Quiruvilca represent mineralization deep within a volcanic pile, in sharp contrast to the high level epithermal precious metal deposit at Silica del Hueso, Chile. Arrangements to sample Julcani were made with Minas Buenaventura S.A. for the period immediately following the 1985 Fluid Inclusion-Stable Isotope Course in Lima. Unfortunately unforeseen industrial disputes closed the mine and the research programme had to be abandonned with considerable loss of field time. Studies on polymetallic Cu-Pb-Zn-Ag deposits have therefore been confined to Quiruvilca. Samples collected in November 1985 were analysed in London the following year.

6.1 STABLE ISOTOPE, FLUID INCLUSION AND GEOCHRONOLOGICAL STUDY OF THE SILICA DEL HUESO GOLD DEPOSIT, CHILE.

6.1a Introduction.

As discussed above, known precious metal epithermal deposits are confined to relatively young volcanic belts. Silica del Hueso is no exception and occurs within the central Chilean Cretaceous magmatic arc. By comparison with the Jurassic magmatic arc to the west the depth of erosion is relatively little. Consequently the thickness of volcanics preserved is considerably greater and co-magmatic intrusions are only partially unroofed. The deposit is located 2.5km southeast of Portrerillos (see Fig. 5.16) and is still under evaluation by CODELCO. Like so many successful exploration ventures its discovery was almost accidental and will make interesting reading when published. Even so it has taken 4 years to prove the gold reserves and is not expected to come on-stream before 1987. Unlike epithermal deposits associated with Tertiary volcanics in the High Cordillera (e.g. El Indio, Esperanza, El Tambo), the genetic link with volcanic activity is not obvious and for some time the epithermal nature of Silica del Hueso was in question. However, during the most recent phase of exploration its geological and chemical characteristics have been revealed and it is now recognised as a jasperoidal, Carlin sub-type.

As early as 1928, Lindgren recognised the difficulty of formulating a rigid classification for epithermal deposits based on their ore assemblages. Later, Nolan (1933) simplified the scheme and proposed two general classes: gold-silver deposits and silver-gold deposits according to their Au to Ag weight ratios. He also noted that whereas silver-gold deposits were associated with well-defined fault fissures, the fluid channelways for gold-silver deposits were diffuse, irregular and spatially related to shallow intrusives. He considered that these features were probably due to the complex thermal patterns which prevail at shallow depth. The present classification draws heavily on close analogies with active terrestial geothermal systems and advocates two main groups: volcanic-hosted deposits and sedimentary-hosted deposits. The latter are typically formed in carbonaceous, silty dolomites and limestones. Au normally exceeds Ag, and is disseminated throughout the host rocks in micron-size grains. Associated trace elements include As, Ba,Hg, Sb and Tl. Deposits of this group are often referred to as the Carlin-type after

the large tonnage, low grade Au deposit in Nevada. However a variant of the Carlin-type sensu stricto displays intense silicification, quartz veining and jasper replacements, with the gold developed in the high silica zones (e.g. Preble deposit, Nevada).

6.1b Geological Setting and Mineralization.

At Silica del Hueso the mineralization is confined to two formations: the Asientos Formation comprising Jurassic limestone, calcareous siltstones and siltstones, and the Cerrillos Formation comprising possibly Cretaceous rhyolitic tuffs and flow breccias. Whereas the volcanics overlie the sediments with angular unconformity over most of the region, in the Silica del Hueso area the contact is faulted (Fig. 6.2). Various stocks of tonalitic, andesitic and monzonitic composition intrude the sequence and are host to porphyry Cu mineralization at Portrerillos. Their relationship to the gold mineralization is unknown though it is speculated that Silica del Hueso represents the displaced top section of the adjacent Portrerillos deposit. Considerable problems have been encountered in the evaluation of the ore bodies at Silica del Hueso due to discrepancies in gold assays from underground development, reverse circulation drill chips and diamond drill core. The gold zones are tabular, silicified structures which follow the stratification of the host rocks but are linked discontinuously to cross-cutting zones of intense silicification. The gold is typically fine grained (<10 microns) and disseminated throughout. Due to strong supergene leaching only oxidised relic pyrite disseminations remain, Enclosing the deposit is an extensive, irregular envelope of advanced argillic alteration; a feature more typical of volcanic-hosted deposits. Alteration excepted, Silica del Hueso belongs very clearly to the jasperoidal, sedimentary-hosted group. Confidentiality prohibits detailed description of the mineralization and the following report makes no reference to ore grades, tonnages or mine plans.

Objectives. Silica del Hueso was selected for study not only because of its intrinsic economic importance but also because it represents the first sediment-hosted type epithermal Au deposit discovered in Chile. Additional features which influenced our choice include access to underground exposures, availability of borehole core, good regional geologic control and a reliable

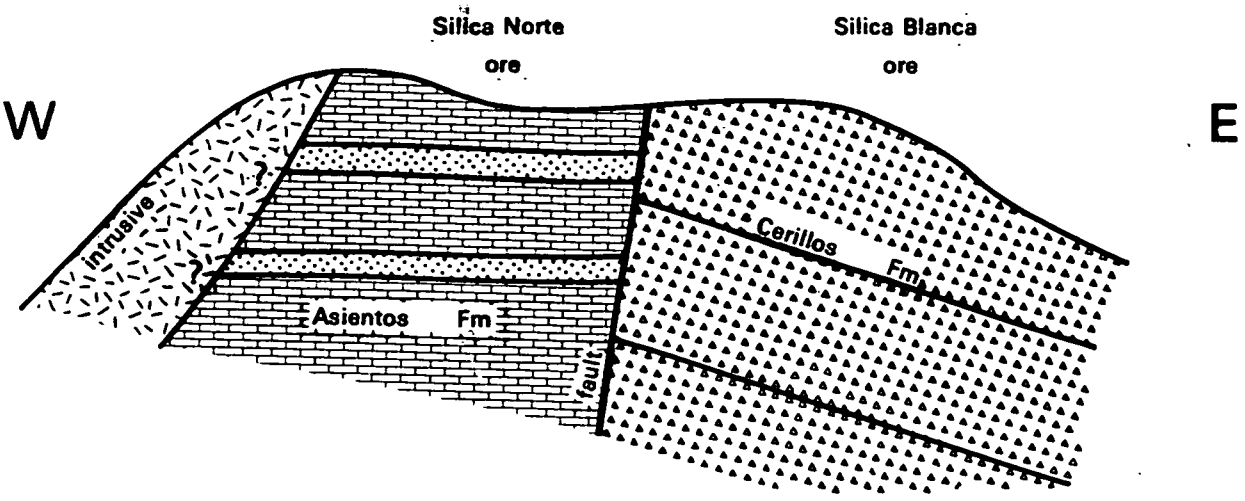

Fig. 6.2 Diagrammatic east - west geological cross section through Silica del Hueso, showing relative position of the ore zones.

geochronological framework provided by complementary ANDCHRON studies in the El Salvador district. Three important aspects of the mineralization were investigated.

1. An integrated fluid inclusion - oxygen isotope study of the auriferous quartz structures to establish thermal conditions during ore deposition, the salinity and source of the ore fluids, and the extent of fluid boiling. Boiling is common to most geothermal systems and induces a temperature decrease and a pH increase which together trigger mineral deposition. Comparable processes are calculated to have taken place during the formation of epithermal deposits: fluid inclusions provide the only direct means of verification. No such data exist for Silica del Hueso.

2. A systematic study of the variation in $^{87}Sr/^{86}Sr$ ratios of the volcanic host rocks, to constrain the range of rocks with which interaction may have occurred and to delimit if possible the area of fluid circulation. Continuous water-rock interaction such as occurs during mineralization is likely to cause a significant change in the initial $^{87}Sr/^{86}Sr$ ratio. By measuring the degree of disturbance it was hoped to estimate the overall dimension of the hydrothermal system and thereby assess the exploration value of such data for this type of deposit.

3. Age determination of the host rocks and associated mineralization.

6.1c Geochronology and Ore Genesis.

(i) Sampling.

To provide suitable material for the geochronological aspects of the investigation, representative samples were taken of major rock units in the area: the Asientos and Cerillos formations, the intrusive porphyry stocks peripheral to the ore zone, and the hydrothermally altered volcanics and minor porphyries within the ore zone. The Cerillos suite comprises vesicular and flow-banded, aphanitic and porphyritic andesites, whilst the Asientos suite includes limestones, calcareous siltstones and bituminous sandstones. Though every effort was made to collect fresh material, the intrusive porphyry stocks show weak but pervasive hydrothermal alteration (incipient kaolinization of

feldspars and chloritization of mafic minerals). The distribution and type of alteration does not correlate well with the alteration halo around Silica del Hueso and are thought to be a local features related to the emplacement of the intrusives. The intensity of alteration increases dramatically within the ore zone and samples from the altered suite show evidence of advanced argillic, propylitic and alunitic alteration. For the fluid inclusion and oxygen isotope studies sampling was largely confined to quartz/jasper structures and their immediate wallrocks exposed in underground and surface workings, and to borehole core material from the principle ore zones. Additional samples were taken from a stratabound barite-pyrolusite deposit in the Asientos Formation 1km to the east of Silica del Hueso. This material ultimately provided an important clue to the source and movement of ore fluids. A complete sample list is given in Table 6.1.

Table 6.1 Sample list for Silica del Hueso

A. Borehole core samples

Sample No	Rock Type	Borehole/Depth(m)
CH-85 96	altered volcanic	BH S-2,350
CH-85-97	altered porphyry	BH S-1,198.5
CH-85-98	latite	BH S-5,108.5
CH-85-99	altered volcanic	BH S-2,368
CH-85-100	silicified clastic	BH S-1,72.5
CH-85-101A	altered volcanic	BH S-2,390.5
CH-85-101B	altered latite	BH S-5,111.5
CH-85-102	altered sediment	BH S-1,92.8
CH-85-103	latite	BH S-5,114
CH-85-104	clastic	BH S-1,83
CH-85-105	altered clastic	BH S-1,122
CH-85-106	silicified sediment	BH S-1,85.5
CH-85-107	breccia	BH S-2,305.5
CH-85-108	breccia	BH S-2,305.1
CH-85-109	silicified tuff	BH S-2,55.2
CH-85-110	quartz breccia	BH S-2,180.6

B. Surface samples

Sample No	Rock Type
Sil-1	sandstone
Sil-2A	andesite
Sil-2B	andesite
Sil-3A	andesite
Sil-4	andesite
Sil-5A	andesite
Sil-5B	andesite
Sil-6	andesite
Sil-7A	limestone
Sil-7B	limestone
Sil-8A	calcareous siltstone
Sil-8B	calcareous siltstone
Sil-8C	calcareous siltstone
Sil-9A	fetid sandstone
Sil-9B	fetid sandstone
Sil-10	barite and pyrolusite
Sil-11	porphyry
Sil-12	porphyry
Sil-13	altered porphyry
Sil-14	altered porphyry
Sil-15	altered porphyry
Sil-16	sandstone
Sil-17	altered andesite
Sil-18	altered andesite
Sil-19	altered volcanic breccia
Sil-20	altered argillite
Sil-21	calcilutite
Sil-22	calcilutite
Sil-23	calcareous sandstone
Sil-24	acid volcanic
Sil 25	acid volcanic

(ii) Geochronology.

The results (Table 6.2 and Fig. 6.3) generally agree with the assumed age of the host rocks and confirm a somewhat younger age for mineralization. However they also reveal several new and important features which help to explain some of the more problematical aspects. An Rb-Sr isochron age for the Asientos Formation of 209 ± 37 Ma (MSWD = 0.5) is consistent with a Late Triassic - Early Jurassic age for the sediments, the high error being due to the small spread of Rb/Sr ratios. The initial $^{87}Sr/^{86}Sr$ ratio of 0.7067 ± 0.001 suggests derivation of material from an older provenance (or complete isotopic equilibrium with Lower Jurassic seawater). Data for the Cerillos Formation volcanics give an isochron age of 54 ± 11 Ma (MSWD = 0.5) and an initial $^{87}Sr/^{86}Sr$ ratio of 0.7047 ± 0.002 (Fig. 6.3). Including a sample of rhyolite from the adjacent Portrerillos area improves the regression and yields an age of 54 ± 1 Ma (MSWD = 0.4). Whereas the Cerillos volcanics were previously assumed to be Cretaceous the evidence given here suggests a Palaocene/Eocene age for extrusion and, by inference, a similar if not younger age for the mineralization. With regard to the unmineralized porphyry stocks, a 5-point regression gives an age of 46 ± 3 (MSWD = 1.3) and initial $^{87}Sr/^{86}Sr$ ratio of 0.7049 ± 0.0001 (Figure 6.3). Because of the weak alteration which affects all samples in this suite the age should be regarded as a minimum, and suggests that the intrusives are contemporaneous with or slightly younger than the Cerillos volcanics (the initial $^{87}Sr/^{86}Sr$ is indistinguishable from that of the volcanics). In the case of the highly mineralized samples (Figure 6.3), regression yields an errorchron (37 ± 4 Ma; MSWD = 29; initial $^{87}Sr/^{86}Sr$ = 0.7056 ± 0.0003). The data are therefore unsuitable for rigorous interpretation but indicate a possibility for mineralization at this time involving fluids with slightly elevated $^{87}Sr/^{86}Sr$. Those samples with low Rb/Sr ratios have initial Sr ratios consistent with closed-system Sr isotope rehomogenization of the volcanics and intrusive porphyries at c. 37 Ma ago. The validity of this argument and a possible explanation for those samples with $^{87}Sr/^{86}Sr$ ratios higher than 0.7055 is discussed later.

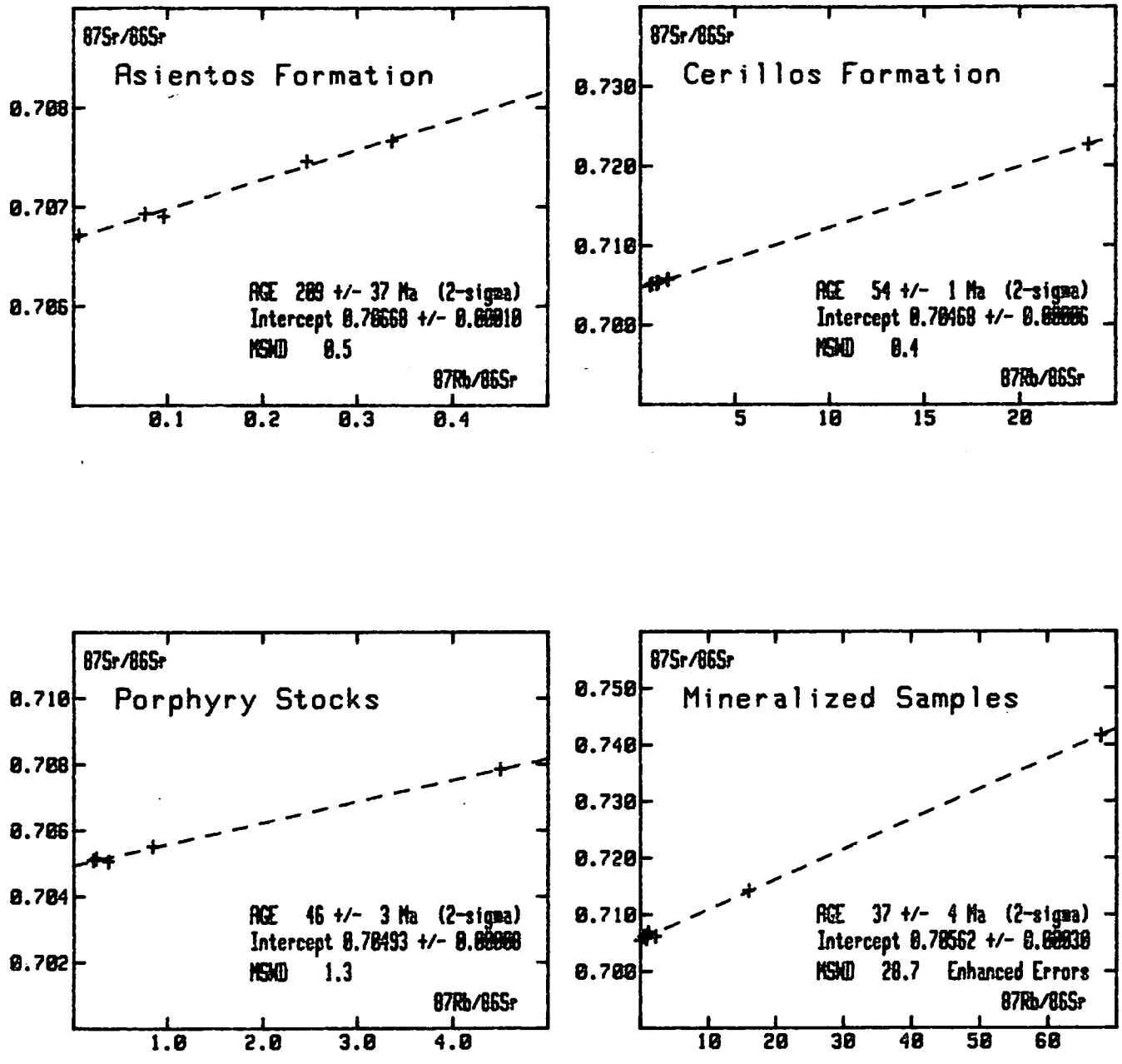

Fig. 6.3 Rb/Sr isochron diagrams for whole rock samples from Silica del Hueso.

TABLE 6.2 Rb-Sr WHOLE ROCK RESULTS FROM SILICA DEL HUESO .

	Rb ppm	Sr ppm	$^{87}Rb/^{86}Sr$	$^{87}Sr/^{86}Sr$
ASIENTOS FORMATION				
SIL 7A	27	322	0.2467	0.70747
SIL 7B	43	367	0.3370	0.70766
SIL 8B	0.3	146	0.0059	0.70672
SIL 9A	11	342	0.0962	0.70690
SIL 9B	10	366	0.0762	0.70693
CERILLOS FORMATION				
SIL 2A	84	466	0.5240	0.70506
SIL 2B	96	441	0.6326	0.70522
SIL 3B	133	403	0.9579	0.70540
SIL 4A	128	255	1.4586	0.70577
SIL 4B	112	228	1.4182	0.70580
SIL 5A	128	423	0.8739	0.70527
SIL 5B	129	425	0.8820	0.70539
SIL 24	151	18	23.5953	0.72270
INTRUSIVE PORPHRY STOCKS				
SIL 11	54	739	0.2133	0.70510
SIL 12	59	713	0.2421	0.70516
SIL 13	154	98	4.5022	0.70786
SIL 14	64	496	0.3761	0.70506
SIL 15	97	334	0.8459	0.70551
MINERALISED ZONE - HYDROTHERMALLY ALTERED VOLCANICS AND MINOR PORPHYRIES				
SIL 17	117	640	0.5308	0.70617
SIL 18	3	356	0.0254	0.70548
SIL 19	110	400	0.7924	0.70609
SIL 20	314	14	67.7861	0.74165
61B	4	9	1.1844	0.70690
97	186	34	15.9868	0.71424
101	153	196	2.2628	0.70617
69	72	230	0.9077	0.70582
61C	55	162	0.9804	0.70628

(iii) Sulphur and strontium isotopes

Near the top of the volcanic sedimentary sequence exposured at Silica del Hueso, barite occurs in a quartz vein which has sharp contacts with the host Cerillos volcanics. The sample (CH-85-73) and its paragenesis are described in section (iv). No sulphide minerals were observed near the barite-containing vein. Sparsely disseminated pyrite occurs in a latite sill several tens of meters below. A comformably stratabound barite bed occurs with pyrolusite in the Assientos Formation to the east of the mineralized area. This barite has a $^{87}Sr/^{86}Sr$ initial ratio of 0.70709±0.00007 (Table 6.3), which is highly radiogenic and may indicate a sea water source. The vein barite has a lower $^{87}Sr/^{86}Sr$ ratio of 0.70637±0.00007 (Table 6.3), which is still higher than those of the host volcanics (0.7048 - 0.7050 at 37 Ma ago) and the porphyries (0.7050 - 0.7055).

The $\delta^{34}S$ of the vein barite is 14.3‰. Fluid inclusions are of low salinity and give homogenization temperatures of around 244°C. However, variable vapour to liquid ratios observed in the inclusions indicate that these were affected by processes after their formation and therefore the calculated temperatures are questionable.

Two sources of sulphur are considered for the vein barite; a) magmatic and b) sea water. If the sulphur in the barite is considered to be derived from a magmatic source , its $\delta^{34}S$ of 14.3 ‰ indicates that the barite cannot be the only sulphur-containing product of the fluid. It must also have produced sulphides with lower values. Such sulphides are not reported to be abundant in this sector of the mine. This however, does not eliminate the possibility of a magmatic sulphur source. The $^{87}Sr/^{86}Sr$ of 0.70637±0.00007 of the vein barite is too radiogenic for the Sr to have been derived from the magmatic source of the Cerillos formation or the porphyries. The original composition could have been modified by passing through sedimentary rocks or by mixing of sea water in the hydrothermal system. The sea water at the time of alteration (c. 37 Ma) had a $^{87}Sr/^{86}Sr$ >0.7076 (Koepnick et al. 1985). The suggestion of sea water contribution to the hydrothermal system is discussed in section 6.1c (v).

The $\delta^{34}S$ of the vein barite of 14.3‰ falls in the range found for gypsum and anhydrite deposits of Triassic and Early Jurassic age (Claypool et al. 1980). It is tempting to relate the vein barite of the ore zone of Silica del

Hueso to the bedded barite of the Asientos Formation. The bedded barite has $^{87}Sr/^{86}Sr$ similar to that of the limestones in the sequence and is of seawater origin. The formation of the barite-pyrolusite association is probably by exhalation onto the sea floor. Subsequent hydrothermal activity caused the mobilization of the barite and its deposition at higher and cooler levels in the hydrothermal system. The difference between $^{87}Sr/^{86}Sr$ in the bedded barite and in the vein barite could be explained by isotopic exchange with the wall rocks. The obvious units are the volcanics of the volcano-sedimentary sequence which have initial $^{87}Sr/^{86}Sr$ <0.705. Hence, based on $^{87}Sr/^{86}Sr$ and $\delta^{34}S$ and in agreement with the geological setting, the vein barite can be considered to be of sedimentary origin subsequently remobilized by a hydrothermal system.

The nature of the hydrothermal fluid can be assessed from the fluid inclusions in the barite and quartz veins. The salinities of most samples are marked by uniformity and low values of 3.5-6.0 %NaCl equivalents. These salinities could be derived from meteoric ground water, sea water or mixtures of meteoric water with sea and/or magmatic fluids. The small variation in the fluid inclusion salinity, at low salinity levels, indicates that the water-rock ratio (W/R) could not have varied widely. Further, the small salinity variation is compatible (at high W/R) with different lithologies. The low variation in salinity further indicates that the fluid was not produced by simple mixing of a high salinity fluid with low salinity meteoric ground water.

The foregoing arguments strongly suggest that groundwater supplied the hydrothermal fluid. This suggestion supports the arguments based on strontium and sulphur isotope data. Had the mobilizing fluid been sea water it would have raised the $^{87}Sr/^{86}Sr$ to values higher than those measured.

Alunite occurs in an alteration zone adjacent to a vein in the volcano-sedimentary sequence. This complex consists of the silicified limestones of the country rock, a black jasper vein, an argillaceous alteration zone probably of an igneous rock and a wide alunite zone which is again bordered by the country rock. Alunite $KAl_3(OH)_6(SO_4)_2$ occurs in alteration mineral associations formed under acid conditions from volcanic rocks and in solfatares.

The $\delta^{34}S$ of the alunite is 17.5‰ (Table 6.3) and cannot be unequivocaly interpreted in terms of sulphur source. The association of alunite with highly altered igneous rocks suggests its origin to be sulphides of that source.

Oxidation of sulphides of magmatic source will not normally result in such a high value. Sulphates of magmatic origin could be the source but their formation should be related to that of sulphides. Sedimentary sulphate of sea water origin could be the source but then its occurrence would be expected to be more widespread, which is difficult to assess in this terrain.

The presence of alunite is an important indicator for the chemical conditions of alteration. Further isotopic studies ($^{87}Sr/^{86}Sr$, $\delta^{34}S$, $\delta^{18}O$) could contribute to its use as indicator for the origin of alteration hydrothermal fluids.

Table 6.3 $^{87}Sr/^{86}Sr$ initial ratios and $\delta^{34}S$ of barite and alunite.

Sample	$(^{87}Sr/^{86}Sr)_o$	$\delta^{34}S‰$
Barite, Asientos Formation		
SIL 10A	0.70709±0.00007	
Barite, Cerillos Formation		
CH-85-73	0.70637±0.00007	14.3
Alunite CH-85-61C		17.5
Limestones, Asientos Formation		
SIL 7A	0.70733±0.00007	
SIL 7B	0.70749±0.00007	
SIL 8A	0.70562±0.00007	
SIL 8B	0.70672±0.00007	
SIL 21	0.70731±0.00007	
SIL 23	0.70685±0.00007	

(iv) Fluid inclusions.

As noted for other sediment-hosted epithermal deposits, fluid inclusions are conspicuously few and, where developed, are close to the limit of optical resolution (1 μ). This is due to the generally fine-grained nature of the ore and gangue minerals. Consequently any information concerning the temperature and conditions during gold deposition, no matter how little, is of value.

Twenty six quartz-rich samples were prepared for examination, but only nine contained inclusions large enough for optical and thermometric analysis. The inclusions occur preferentially in discrete quartz veinlets, quartz breccias and minor quartz veins and are not developed in the more extensive zones of jasper/silicification. The most favoured site for inclusions is at the base (i.e. earliest growth) of interfering, elongate quartz crystallites which line the walls of millimetre-scale veinlets. Here the inclusions decorate well healed microfractures and are rare in the later euhedral terminations. Such veinlets show an ordered sequence of deposition indicative of systematic changes in the fluid regime during the final stages of hydrothermal activity. The wallrock to these veinlets is invariably highly silicified and in the area of altered volcanics contains occasional, rounded patches of clear quartz (100 - 500 μ). These may represent original quartz phenocrysts or partially digested fragments of earlier vein material. Unlike the veinlets, the quartz consists of coarse anhedral crystals. Irrespective of their origin they carry a few large inclusions (5 - 10 μ) and are interpreted as evidence of fluids which produced the main phase of silification/mineralization. The quartz breccia (CH-85-107) appears to be a brecciated variant of (CH-85-104). Both contain usable inclusions and texturally are similar to the anhedral quartz patches described above (i.e. they show no tendency for crystallite growth from the vein walls). Where the quartz structures are widest (0.5m), they show a complex history of multiple deposition, brecciation and dissolution indicative of feeder zones. In all instances the last quartz growths are crystal-lined vugs and irregular open spaces. One of the larger quartz structures carries minor barite and extends upwards into a deposit resembling quartz sinter, also with barite. The barite forms either single-bladed crystals or crystal rosettes and is frequently pseudomorphed by quartz, signifying early deposition. Where they remain they contain an abundance of inclusions especially along {210} cleavage fractures.

Thus one can envisage a tentative sequence of quartz deposition as follows:

1. Early quartz veining with barite, accompanied by silicification of the wallrocks
2. Brecciation and further silicification
3. Later stage quartz veinlets

The paragenetic sequence at Silica del Hueso has still to be established and until this is complete the samples examined can only be related to one another provisionally. Likewise the distribution of gold is imperfectly known. However, the samples include material which predates or is co-eval with the main phase of silicification. Hence the inclusions as a whole preserve a record, albeit fragmentary, of fluid events over a significant time interval which in all probability includes the period of gold deposition.

Inclusion types. The inclusions are predominantly two phase (liquid + vapour) types with vapour-to-liquid (V/L) ratios less than 0.17, consistent with fluid temperatures less than 300°C. In certain samples a second inclusion type is present in which V/L ratios exceed 50. The co-existance of vapour-rich inclusions and liquid-rich inclusions is normally taken to imply deposition from a boiling fluid. However, except in two samples (CH-85-75 and CH-85-107), the occurrence of vapour-rich inclusions merely indicates that a vapour phase was trapped along fractures in the quartz at some time after deposition. To verify that the crystal grew during fluid boiling requires a close agreement between the temperatures of homogenisation for both types of inclusion. Unfortunately, even though samples CH-85-75 and CH-85-107 show unequivocal evidence of boiling, the high V/L ratios preclude temperature measurement. It is therefore impossible to assign a specific temperature of boiling except to say that the vapour-rich inclusions occur in the earliest generations of quartz and are associated with inclusions having the highest homogenisation temperatures (i.e. >200°C). In the barites, post-trapping morphological readjustment of the inclusions has led to separation of vapour and liquid phases. The net effect gives rise to inclusions with highly variable and anomalous V/L ratios. As a result the inclusions are unreliable geothermometers but can still be used to derive estimates of fluid composition.

Results and interpretation. The thermometric results are listed in Table 6.4. Salinities are reported as NaCl wt% equivalents based on final ice melting temperatures in the system $NaCl-H_2O$. First ice melting temperatures (T_E) cluster around -21°C, consistent with NaCl dominant fluids. However, at low salinities final ice melting temperatures are very sensitive to dissolved CO_2: 0.5 mole% CO_2 produces a depression of freezing point equivalent to 0.7 wt% NaCl (Hedenquist and Henley 1985). Bulk gas analyses for CH-85-73 and CH-85-74 indicate up to 1 mole% CO_2 in solution, with minor traces of CH_4, N_2, and Ar. Ideally it would be desirable to have CO_2 concentrations for each inclusion but this is impractable. As a best estimate, true salinities may be lower by a maximum of 1.4% NaCl. Hence fluid compositions approximate to those encountered in typical geothermal systems: weakly bicarbonated NaCl solutions. Uncorrected for CO_2, salinities range from 1.4 to 6.2 wt% NaCl equivalents. Where the fluids are strongly boiling apparent salinities are low, in keeping with loss of CO_2. Temperature estimates show a much wider range of 140 -280°C. The lower values correspond to the waning phase of fluid circulation, the higher values to early quartz veins and the very first stages of crystal growth in thequartz veinlets. There is little appreciable change in salinity throughout quartz deposition, implying an open system with large recharge capacity. Near surface groundwaters which have acquired an enhanced salinity due to water-rock interaction best satisfy these characteristics. Temperatures for the quartz sinter deposit (150-220°C) are not compatible with deposition at the surface and suggest that the "sinter" is a vein/replacement manifestation. As stated above, the presence of vapour-rich inclusions demonstrates periodic boiling in response to change in hydrostatic pressure. From the distribution of inclusions in the quartz veinlets, it is predicted that boiling had ceased by the time the fluids had cooled to <200°C. Pressure corrections to the homogenization temperatures for epithermal deposits are small and thus measured temperatures approximate closely to trapping temperatures. Depth estimates based on the vapour pressure of a boiling 4 wt% NaCl solution at 200-240°C (Haas 1971) indicate deposition in excess of 250m. The presence of CO_2 however tends to trigger boiling at a greater depth for a given temperature and therefore fluids containing 1 mol% CO_2 may have started to boil at an even deeper level in the system (i.e. a greater hydrostatic head).

Table 6.4 Fluid inclusion thermometric results for Silica del Hueso

Sample No	Mineral	Th °C	Te °C	Tm ice °C	NaCl wt% equiv
CH-85-62	Q	196	-10	-2.8	4.8
				-3.2	5.2
		240		-2.2	3.7
		249		-3.3	5.3
		243		-0.2	
		229	-18	-2.7	4.7
		246	-18	-3.0	5.0
		178	-21	-2.3	3.9
		204		-1.9	3.2
		181		-3.3	5.3
		183		-2.2	3.7
		182		-2.8	4.8
		185			
CH-85-70	Q			-2.6	4.4
				-3.0	5.0
		170		-2.0	3.4
		164		-2.2	3.7
		175		-1.8	3.0
		197		-2.5	4.2
		204		-2.5	4.2
		203		-2.6	4.4
		207		-1.8	3.0
CH-85-73	Q	174		-1.9	3.2
		167	-30	-3.0	5.0
	B	245	-30	-2.8	4.8
		244	-28	-3.8	6.2
CH-85-74	Q			-2.4	4.0
CH-85-75		202	-28	-1.8	3.0
		170	-28	-0.01	
		280			
		300			

Table 6.4 (cont.)

Sample No	Mineral	Th °C	Te °C	Tm ice °C	NaCl wt% equiv
CH-85-75 (cont)	B	151	-28	-1.1	1.9
		152	-25	-2.0	3.4
		220	-21	-2.5	
CH-85-104	Q	161	-23	-2.8	4.8
				-2.7	4.7
		258		-0.04	
		260		0.02	
CH-85-107	Q	200		-1.2	2.0
		205		-1.1	1.9
		214			
				-2.1	3.5
		280	-30	-0.8	1.4
		140		-2.9	4.8
CH-85-107	Q	142		-2.8	4.7
		144		-2.5	4.2
		151		-2.3	3.9

Key:

Q	Quartz
B	Barite
Th	Temperature of homogenization
Te	Temperature of first melting (eutectic)
Tm ice	Temperature of final ice melting

(v) Oxygen isotopes.

Quartz veins from Silica del Hueso were analysed for their $\delta^{18}O$ composition in order to define the origin of the water in the fluids from which the veins were deposited and the type of water rock interaction prior to quartz deposition. The results are reported in Table 6.5 along with pertinent information derived from fluid inclusion studies.

The range of $\delta^{18}O$, from 11.9 to 23.5‰, is high compared to that common in epithermal deposits. The lowest values of 11.9 and 12.3‰ are from interbedded volcanic and sedimentary strata in borehole samples. Several quartz structures from this sequence have ratios between 15.8 and 19.9‰. It is noteworthy that two samples belonging to the same structure, 15m apart vertically and markedly different in ore grades, have virtually the same $\delta^{18}O$ within analytical precision - 15.8 and 15.9‰ (CH-85-73 and CH-85-74 respectively).

Veins having fluid inclusion features indicative of boiling have $\delta^{18}O$ of between 7.5 and 19.7‰, indistinguishable from those of quartz veins with no boiling features. (CH-85-107) has an oustandingly high value of 23.5‰.

Using the results of fluid inclusion thermometry, the $\delta^{18}O$ of the water was calculated according to Matsuhisa et al.(1979), giving a range of 2.5 to 12.5‰. The lower values are calculated for the late stage quartz. The brecciated quartz which shows features of boiling gives rise to a calculated water $\delta^{18}O$ of 15.9‰ . These values span a wide range, including compositions which could be attributed to seawater or magmatic water as well as highly modified meteoric water. However, the low salinities (0.8 to 6.0 wt% NaCl equiv.) exclude seawater as a major component. The criteria for postulating a magmatic origin are not very clear: low salinity may again suggest that magmatic fluids were not major contributors to the quartz-precipitating fluids. Information on the isotopic composition of precipitation at the time of activity of the hydrothermal system is not available. An approximation can be made, based on palaeogeographical considerations. Precipitation on the High Andes at El Tatio, at elevations higher than that of Silica del Hueso, currently has a $\delta^{18}O$ of $\simeq$ - 8.5‰ (Giggenbach 1978). The implied isotope shift from meteoric water with such a composition requires extensive exchange with mineral oxygen.

High $\delta^{18}O$ values in the range found in the samples from Silica del Hueso are not commonly reported for igneous terrains, and suggest exchange with sedimentary rocks. This shift is similar to those observed in Cortez and Humbolt, where the fluids are assumed to have interacted with high $\delta^{18}O$ sedimentary rocks (see Taylor 1979). Similar values are also encountered in the Carlin deposit, which is emplaced in a calcareous host rock, but there the high $\delta^{18}O$ values are mostly associated with high salinities (7.5 - 15% wt NaCl equiv.) (Radke et al. 1980). The composition of sedimentary rocks is so varied that low salinity levels in fluid inclusions cannot be regarded as a conclusive indication of the absence of such interaction. In addition the Sr isotopic composition of vein barite at Silica del Hueso is consistent with a contribution of Sr from sedimentary rocks. The large observed shift in $\delta^{18}O$ indicates a low water/rock ratio and/or interaction with high $\delta^{18}O$ carbonate rocks, whereas the low $\delta^{18}O$ values for the waters in equilibrium with late stage quartz indicates interaction with rocks already depleted in ^{18}O during earlier stages of the hydrothermal process.

In conclusion, the quartz veins were precipitated from fluids characterized by high δ^{18} and low salinity, suggesting derivation primarily from meteoric water but with extensive exchange with the country rock. The large shift in $\delta^{18}O$ could be due to recycling within a dominantly igneous environment, in a semi-enclosed type system, or else to exchange with high $\delta^{18}O$ sedimentary rocks, particularly carbonates. Interestingly, the salinity does not seem to change markedly. Several veins which show boiling features do not show anomalous $\delta^{18}O$ values. This indicates that boiling, in these cases, took place after the deposition of the bulk of the quartz vein, whereas quartz with outstandingly high $\delta^{18}O$ was deposited from a residual solution after boiling.

Table 6.5 $\delta^{18}O$ of vein quartz, homogenization temperature of fluid inclusions and calculated $\delta^{18}O$ of water.

Sample	$\delta^{18}O$ quartz (‰SMOW)	T_H °C	$\delta^{18}O$ water (‰SMOW)	remarks
CH 85 62	16.2	229	6.3	
CH 85 64	19.9			coarse crystalline
CH 85 64	19.3			fine crystalline
CH 85 70	19.7	197	7.9	boiling
CH 85 73	15.9	174	2.5	late stage
CH 85 74	15.8			
CH 85 75	19.4	220	9.0	boiling
CH 85 107	23.5	280	15.9	
BH 21 75	17.7	224	7.5	boiling
BH 22 13	12.3	233	2.6	late stage
BH 22 28	11.9			

(vi) Proposed model of ore genesis

The geochronological data confirm an age of late Triassic/early Jurassic for the Asientos Formation, but indicate a lower Tertiary age for the Cerillos volcanics which are in part hosts to the mineralization. The age of mineralization must be similar or younger, and is possibly dated by Rb-Sr at 37 Ma. Since data are not available for the adjacent Portrerillos porphyry, a presumed genetic link between porphyry copper mineralization and gold mineralization at Silica del Hueso cannot be proven. However intrusive activity of this age has been recorded in the El Salvador area.

The thermal regime and low salinity as indicated by the fluid inclusions is similar to that of other epithermal precious metal systems in Tertiary volcanics elsewhere. It is characterised by temperatures between 280° and 140°C, whilst the main phase of mineralization/silicification occupies a narrower range of 280°-200°C. Boiling occurred at several stages and is thought to have been significant in triggering ore deposition in the early, higher, temperature phase at Silica. Fluid inclusion porperties suggest that boiling took place under hydrostatic conditions equivalent to an overburden thickness of at least 250m. Therefore the siliciification at Silica cannot be wholly ascribed to surface geothermal phenomena.

Concerning the origin and evolution of the ore-bearing fluids several geochemical charateristics have been assessed. Sr-isotope data for minor barite associated with the ores indicate derivation by remobilisation of bedded barite of primary marine origin. Such deposits have been located in the Asientos Formation. The sulphur isotope composition of the barite supports this hypothesis. Calculated oxygen-isotope compositions of the fluids based on vein quartz show a wide range of values, which could be a result of groundwater interaction with high-$\delta^{18}O$ rocks, probably carbonates of sedimentary origin. Nevertheless, the Sr-isotope and salinity evidence argue against a large component of either sea water and/or magmatic water in the hydrothermal fluids. This emphasizes the important role of sedimentary rocks in determining the properties of the mineralizing solutions, and perhaps their metal content.

6.2 SOURCE OF SULPHUR IN POLYMETALLIC DEPOSITS IN THE CRETACEOUS ISLAND ARC, CHILEAN ANDES.

6.2a Introduction.

Base metal deposits in different morpho-tectonic settings within the Early Cretaceous magmatic arc in the Chilean Andes have similar Pb isotopic composition indicative of a common source (Puig, 1985). The Pb isotopic composition also indicates a larger influence of mantle than in the Pre-Jurassic and Jurassic hosted deposits. The Pb isotope ratios, correlate well with the stratigraphic ages of the host rocks. These phenomena were interpreted in terms of relationship between the metal deposits and their host rocks as contemporaneous formation or subsequent remobilization of Pb from the host rock to the metal deposit (Puig, 1985). The Pre-Jurassic and Jurassic hosted deposits have isotope composition indicative of old crustal Pb while the Tertiary rocks are isotopically more variable ,reflecting the influence of a more evolved crust (Puig, 1985). Polymetallic deposits occur in different parts of the Cretaceous island arc system i.e. the island arc proper, the back-arc basin and its margin. As the formation of these sulphide deposits is governed amongst other factors by the supply of sulphur, understanding the pathway of sulphur is an important part of the clarification of the process of formation of these deposits.

The stable sulphur isotope composition of minerals and dissolved sulphur containing compounds has been widely used as an indicator for their source and environment and temperature of formation. The polymetallic deposits provide the opportunity to assess the contribution of sulphur from the two main reservoirs i.e. magmatic and seawater and their variations in the different geological settings within the developed Early Cretaceous magmatic arc structure. The metals forming these deposits are probably derived from the host rock as is demonstrated by the Pb.

An extensive north-south trending magmatic arc which consists mainly of dacitic and andesitic lavas and hypabyssal bodies developed in Middle to Late Jurassic and moved eastwards with time till the end of Early Cretaceous. Between the magmatic arc and the Paleozoic foreland an elongated back arc basin developed during this period. The sedimentary sequence of this basin is

characterized by red beds interbedded on the margin with marine and evaporitic deposits. The marginal facies contains also shales which are locally bituminous. Towards the west the marine sequence is interfingered with andesitic flows from the arc (Coira et al. 1982). At the end of the Early Cretaceous this arc/back-arc pair was replaced by a single migrating magmatic arc (Vincente et al. 1973).

This study focuses mainly on Cretaceous deposits depicted in the map of Figure 6.4.. Several Jurassic deposits shown in Figure 6.5 have been studied as well.

6.2b Results and discussion.

Sulphur isotope ratios of galena from various locations between 24°11'S and 32°11'S emplaced in the Early Cretaceous magmatic arc and back-arc basin are given in Table 6.6. The sample numbers correspond to those shown on the map (Figure 6.4). The sulphur isotope composition of barite from massive barite deposits within the back-arc basin are also reported in Table 6.6. The distinction between margin and basin is based on sedimentological and structural considerations. Later tectonism has changed the relative position of the different morphotectonic units of the Early Cretaceous magmatic arc, resulting in the disturbance of the original belt system and leading to the present location depicted in figure 6.4 and 6.5. The position of the Talcuna district within the magmatic arc system is not conclusive. A prominent manganese horizon suggests the development of brackish or lacustrine environment in the area (Aguirre and Mehech,1964). The mine Maria Cristina in the district Sierra la Galena represents the margin (towards the foreland), the basin is represented by Sect. Chimborazo, Chanarcillo, Sierra la Galena, and the arc is represented by Arqueros, San Larenzo, Cogoti, Bellavista and El Bronce.

The massive barite deposits Manina, Gladys and La Jaula in the back arc basin may have obtained sulphur from contemporaneous sea water and its derivatives or by remobilization of older evaporitic sequences. A contribution from a magmatic source is probably marginal at the most. The sulphur isotope age curve, which depicts the variation in oceanic sulphate over time, shows high values of about 17‰ at the end of the Jurassic and reaches a minimum of 14‰ in the Early Cretaceous (Aptian-Albian), followed by a continuous increase till

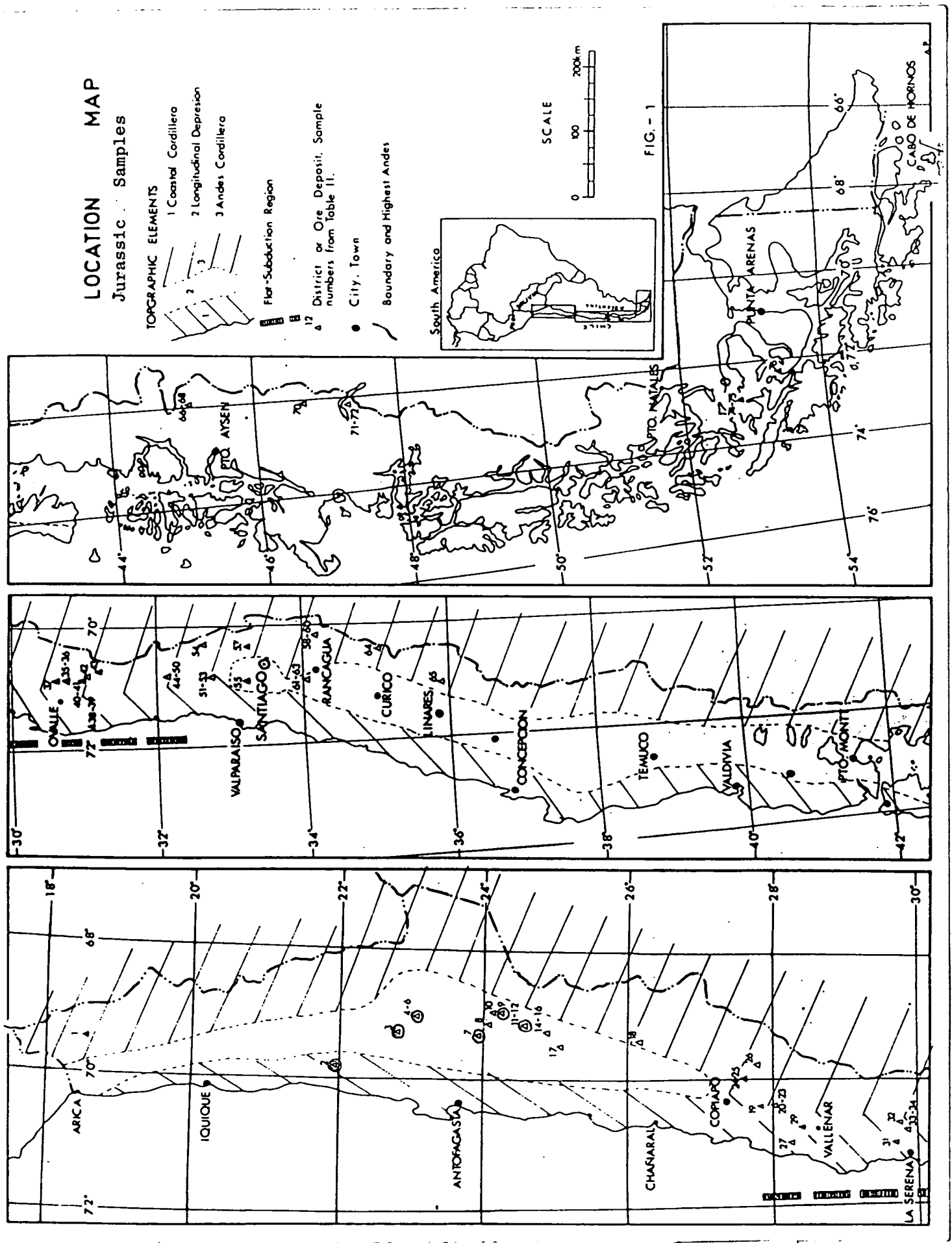

Figure 6.4 Location map for Cretaceous samples

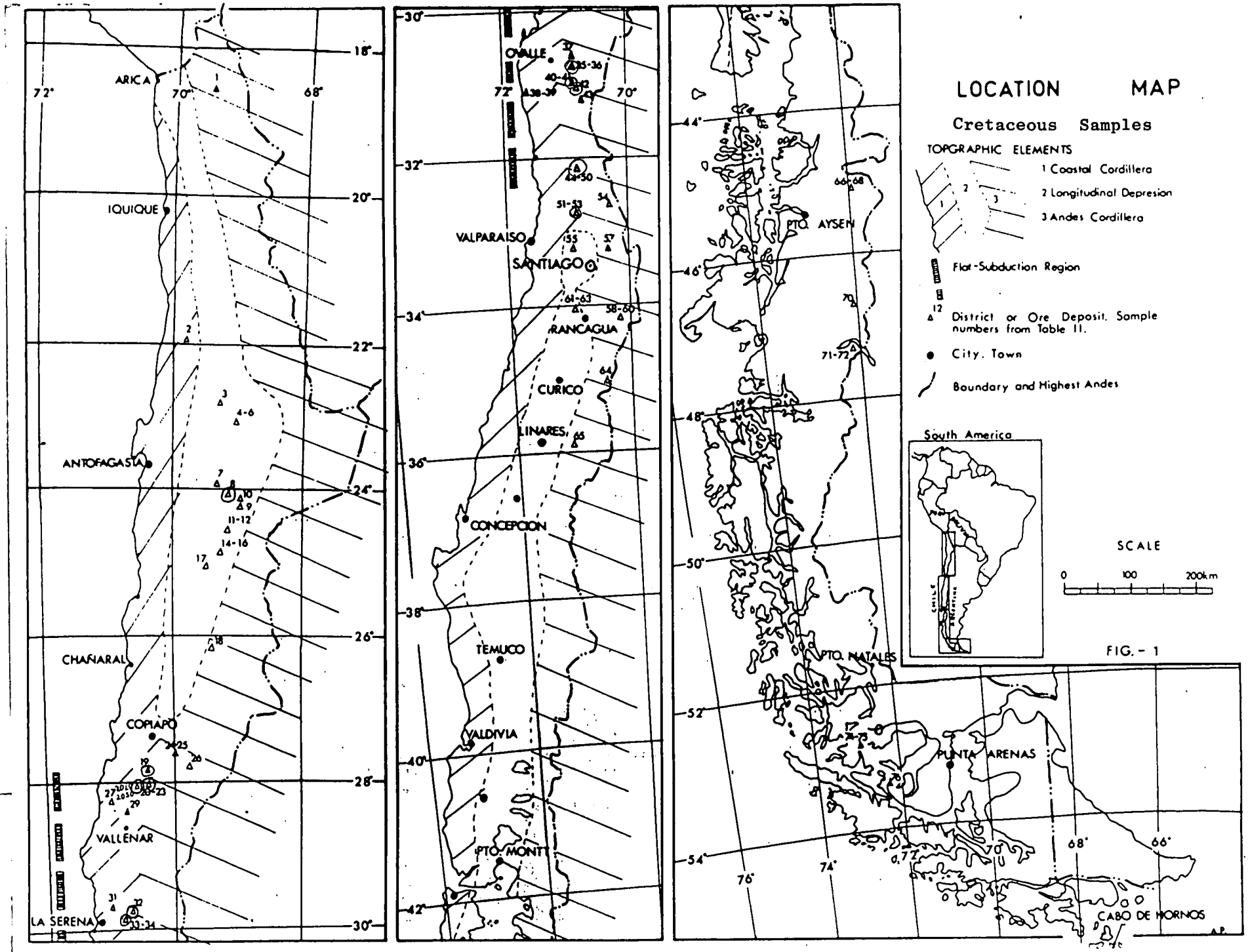

Figure 6.5 Location map for Jurassic samples

Table 6.6 Cretaceous samples: location, description and $\delta^{34}S$.

Morphotectonic Unit	Location Map No.	District	Mine	Sample No (AGP)	Type of Deposit	Country Rock	Sulphide minerals	Gangue mineral	$\delta^{34}S$ (Ga)
Margin	23	Sierra la Galena	Maria Christina	18	conduit?	Breccia like	Ga		-2,69
Margin?	33	Talcuna	Andacollo	35	vein	Tuff and andesite	Ga Sph Bo	Ba Cal Hem	-35.0
Margin?	34	Talcuna	Tambor 3	36	str. bound vein	Tuff and andesite	Ga Sph Bo	Ba Cal Hem	-27.4
Basin	8	Sect. Chimborazo	Alicia	02	vein	Shale + lavas intrunded by felsic dyke	Ga Cpy	Qz Cal Lim	-0.107
	19	Chanarcillo	El Plomo	19	stratabound	Calcareous breccia	Ga Sph Cpy Py	Qz Cal	1.15
	15	Sierra la Galena	Carolla	15	vein	limestone + volcanogenic sediments	Ga Sph	Ba	8.06
	16	Sierra la Galena	NN	16	vein	volcalogenic sediments	Ga Sph	Ba	3.84
	2020		Maniña	2020				Ba	18.82 *
	2030		Maniña	2030				Ba	21.15 *
	2040		Gladys	2040				Ba	21.40 *
	2050		La Jaula	2050				Ba	16.90 *
Arc	32	Argueros	Quitana	33	vein	andesite	Ga Bo		-3.83
	35	San Lorenzo	Variola 1	34	vein & breccia	andesitic lavas	Ga Sph Cpy Bo	Chl. Cal Qz	-6.37
	40	San Lorenzo	Republicana	27	vein	andersite	Ga Sph Cpy	Chl Cal Qz	-2.34
	41	San Lorenzo	Luz del Pilar	28	vein	andersite	Ga Sph Cpy	Ba Cal Qz	-2.94
	42	Cogoti	Ranchitos	29	vein	andersite	Ga Sph Cpy Bo	Cal	-2.13
	51	Bellavista	Veta Grande	50	vein	brecciated lavas intruded by dykes	Ga Sph Cpy	Qz Cal	-8.55
	52	Bollavista	San Luis	51	vein	laminated tuff	Ga		-18.89
	53	Bellavista	San Luis	51A	vein	volcanic Breccia	Ga		-2.86
	45	El Bronce	El Capote	39	vein	volcanic Breccia + lava	Ga Sph	Ba Qz Cal	-10.42
	49	El Bronce	El Chivato	43	vein	Epithermal related with caldera	Ga Sph	Ba Qz Cal	-2.67

* $\delta^{34}S$ Ba

Middle Miocene (Claypool et al. 1980). The barite deposits of the back-arc basin have isotopic ratios of 16.9 to 21.4‰. The shift to heavier compositions from the oceanic value of Claypool et al. (1980) may be due to deposition of sulphates in basins with restricted circulation in which intensive sulphate reduction processes takes place. This agrees with paleogeographical and sedimentological setting of these deposits in the shallow evaporitic back-arc basin. The sulphur isotopic composition of the galena samples of the Cretaceous arc system (Table 6.6) spans a wide range. Differences in ranges of isotopic composition show a relation to the morphotectonic setting and the type of host rock of the deposit. Comparisons can be made among the numerous vein deposits but too few sample of stratabound deposits are available to evaluate the significance of the difference between these and the vein deposits.

The Talcuna district, which is probably located in a marginal marine, brackish or even lacustrine environment, shows the lowest sulphur isotope ratios. The host rocks are tuffs and andesite and the associated galenas have $\delta^{34}S$ of -27.4 and -35.0‰ respectively. These low ratios are indicative of sulphide formed by sulphate reduction at low temperatures, probably through a bacterially mediated process in which the availability of lead (or other sulphide forming metals) was not a limiting factor.

The composition of the galena in the basin deposits, where the host rocks consists of calcareous and shaly sediments and lavas, is heavier ($\delta^{34}S$ = -0.11 to + 8.06‰). This range can be attributed to a magmatic origin or reduction of sea water sulphate at high temperature. Following the approach of Ohmoto and Rye (1979) and taking the isotopic composition of the massive barite from the back-arc basin as respresenting the sulphur source, temperatures in excess of 580°C are calculated. A bacterially mediated sulphate reduction process at low temperatures with low availability of metals can also yield this range of isotopic composition. It is however questionable whether these limiting conditions will allow the development of large veins. This range of higher isotope ratios may be due to an increase in pH associated with calcareous and shaly host rocks (Ohmoto and Rye, 1979), without direct contribution of sea water derived sulphur.

The galena samples from the arc region have a wide spread of composition (-2.11 to -18.89‰), which is lighter than the range found for the basin samples but heavier than the Talcuna district samples. Also in this morphotectonic unit

Table 6.7 Jurassic samples: location, description and $\delta^{34}S$.

Location Map No.	District	Mine	Sample No. (AGP)	Type of Deposit	Country Rock	Sulphide minerals	Gangue minerals	^{34}S
2	Puntillas	La Galenosa	06	vein	sandstone + quartzite + shale	Ga	Qz Lim, Hem	0.27
12	Sierra Agomedo	NN	03	vein	Palaezoic intrusives	Ga	Qz Cal Lim	4.40
11	Sierra Agomedo	Escondida	05	vein	Calcareous sandstone intruded by porphyritic tonalite	Ga	Ba Qz Lim	5.05
9	La Escondida	La Escondida	70	stockwork	Upp. Paleozic andesite intruded by lower Tertiary porphyry bodies	Ga	Ba Qz	-5.19
7	Cerro Boquete	Jardin	07	vein	Paleozoic Rhyolite intruded by Tertiary porphyritic bodies	Ga		-4.98
4	Caracoles	Sudamenicana	09A	vein	Limestone intruded by lower Tertiary porphyritic tonalite	Ga Sph Py	Ba Qz	-16.8
6	Caracoles	Atac Elen	11	vein		Ga		-12.8
3	SW Calama	Cerritos Bagosi	08	vein	Marine sediments intruded by lower Tertiary bodies			-1.26

a relation can be observed between host rock, type of deposit and the isotopic composition. The lowest value is recorded in laminated tuffs (#52: -18.89‰). Higher ratios are found in breccias (-10.42, -8.55 and -6.37‰ for #45, #51 and #35 respectively). The lava-hosted galenas have the highest ratios and a restricted range (-3.83 to -2.13‰).

Sulphur isotope ratios of galena samples from some deposits hosted by Jurassic strata are given in Table 6.7. The position of these deposits within the magmatic arc is not ascertained. The ratios cover a wide range ($\delta^{34}S$ of -16.8 to 5.05‰) and do not show a clear relationship with type of host rock. These deposits are more complex than the Cretaceous ones and more detailed geological information is required for the interpretation of their sulphur isotope composition.

Mineral pairs and triplets consisting of galena, sphalerite and chalcopyrite from the Jurassic and Early Cretaceous arc deposits were analysed in order to clarify the equilibrium relationship among the sulphide phases and to determine the emplacement temperature. Results shown in Table 6.8a and 6.8b indicate that the assemblage of sample 45 does not represent equilibrium conditions. The range of isotope composition of the triplet may suggest formation from a sulphur pool of the same isotopic composition as the other assemblages. Samples 51 and 49 show different ranges of isotope composition but the ranges for the individual samples are narrow (-7.60 to -8.55 and -1.43 to -2.67‰ respectively). These relationships can be expressed in terms of temperatures as shown in Table 6.8b. The calculation of temperatures from this narrow range of isotopic compositions results in an estimated error of 50°C. These temperatures are calculated from a few samples only, so that their regional significance is restricted. It is however significant that the spread within the individual assemblage is narrow. The two assemblages from the magmatic arc occur in slightly different host rock types (#51 - vein in volcanic breccias with lavas, #49 - epithermal related with caldera). The features suggest that the nature of the sulphur reservoir which produced these assemblages differ while the paragenesis of the minerals and possibly the thermal control are similar.

Table 6.8a $\delta^{34}S$ of Galena, Sphalerite and Chalcopyrite Assemblages.

Location map No	District	Mine	galena $\delta^{34}S$(‰)	sphalerite $\delta^{34}S$(‰)	chalcopyrite $\delta^{34}S$(‰)
7	Cerro Boquette	Jardin	-4.98	-2.69	n.d
51	Bellavista	Veta Grande	-8.55	-7.60	-7.95
49	El Bronce	El Chivato	-2.67	-1.87	-1.43
45	El Bronce	El Capote	-10.42	-2.62	0.18

Table 6.8b Relationship between $\delta^{34}S$ of sulphide pairs and the calculated temperatures

Location map No	$\Delta^{34}S$ sph-ga (‰)	Temp °C (1)	Temp °C (2)	$\Delta^{34}S$ cha-ga (‰)	Temp °C (1)	Temp °C (2)	$\Delta^{34}S$ sph-cha (‰)	Temp °C (1)	Temp °C (2)
7	2.29	318	289	n.d.			n.d.		
51	0.95	644	603	0.60	767	700	0.35	381	420
49	0.80	727	682	1.24	451	380	0.44	310	300
45	7.82	46	30	10.60	disequilib.		2.80	disequilib.	

(1) Kajiwara and Krouse (1971)

(2) Nielsen (1979)

6.2c Summary and conclusions

Galena from the Early Cretaceous magmatic arc deposit have a narrow $\delta^{34}S$ range (-2.13 to -3.83‰), which suggests a narrow isotopic composition range for the reservoir of reduced sulphur and restricted variation in fractionation during emplacement of the veins. This deposit was formed either by reduction of sea water sulphate at high temperatures (> 250°C, Nielsen 1979) or from a predominantly magmatic source. The later could be truly primary magmatic or secondary by leaching of magmatic rocks. As this narrow range of ratios is recorded from a large area and the fractionation factor between sulphate and sulphide is temperature-dependent, a larger variation could be anticipated from a sulphate reduction process. The sulphur isotope ratios of the vein galena in the magmatic arc are therefore interpreted as being predominantly of magmatic origin. The trend towards lower ratios in breccias and tuffs of the magmatic arc is the result of mixing of sulphur of magmatic origin with sulphur derived from sea water sulphate by high temperature chemical reduction or by low temperature bacterial reduction occurring in near surface environments. The Talcuna samples represent an end member dominated by the latter source.

The basin deposits which are hosted in calcareous rocks have heavier δS isotope values of -0.11 to 8.06‰. This heavier range may be due to the effect of increase in the pH, when passing into the calcareous environment, on fluids derived from the same source as for the magmatic arc deposits. However mixing with sea water derived sulphide could also yield this range.

Sulphide minerals, pairs and triplets (sphalerite, galena, chalcopyrite) show in part complex relationships of isotope composition. These relationships are indicative of formation under non-equilibrium conditions. Several pairs give rise to temperatures in the range 290-450°C. The back-arc basin barite deposits have isotopic compositions slightly higher than Cretaceous oceanic composition, reflecting deposition in a restricted basin in association with sulphate reduction activity.

6.3 LEAD ISOTOPE PATTERN OF ORES FROM THE CHILEAN ANDES.

Alvaro Puig has recently completed a comprehensive survey of the Pb isotopic composition of 81 galenas from 48 mining districts distributed along the Chilean Andes from 18° to 46°S (Puig 1985). The study is a reasonable representative sampling from all ages of mineralisation, from Upper Cretaceous to Tertiary, and from the host rocks ranging in age from Palaeozoic to Miocene.

Several authors have noted a longitudinal zonation of ore metals from iron in the west to tin in the east, which parallels the central Andean chain. The zonation has been explained (Sillitoe 1972) by variations in temperature and pressure conditions in the zone of magma generation associated with the tectonic setting. This simple pattern does not occur in Chile and south of 30°S the history of metallogenesis is very poorly known.

It is remarkable that the Pb isotope ratios from the ores of the mining districts along the length of the Andes from 18° to 46°S have a restricted range of values (206/204 from 18.68 to 18.28, 207/204 from 15.68 to 15.56 and 208/204 from 38.7 to 38.1). This relative uniformity of the Pb isotopic ratios testifies to the efficiency of the homogenisation that occurs during tectonism at a destructive plate margin. The isotope ratios are plotted in Fig. 6.6 in relationship to the Pb development model of Doe and Zartmann (1979). The Chilean Pb isotope data show a noticeable linear trend but the data cloud is centred on the average orogene curve. The steep slope of this trend (0.211 ± 0.017) can be interpreted on the basis of the older Pb models as arising from a two stage process beginning at 2.8 Ga and ending at the time of mineralisation (Upper Cretaceous to Tertiary). However there is no evidence for a basement of this age in this part of the Andes and even in southern Peru the age of the Arequipa Massif has been shown to be no older than 2.0 Ga (Shackleton et al. 1979). The general conformity of published data from the whole rocks (Tilton 1979, McNutt et al. 1979, Harmon et al 1984, Barriero and Stern 1982) suggests that the petrogenetic models for these rocks is largely applicable to the ores (Fig 6.6). Therefore the linear trend is best explained by a mixing model where the average composition conforms to mixing ratios of upper crust, lower crust and mantle used in the Doe and Zartman plumbotectonic model but where the radiogenic ratios are produced by an excess of upper crustal component and the less radiogenic ratios by an increasing mantle contribution. The conformity of these Pb isotope measurements to this model is also emphasised when it is

noted that the linear trend cuts the upper crustal curve around 350-300Ma ago, the time when these reservoirs would be expected to be an important source of Pb. To avoid confusion it is also important to note that these ages are considerably older than the actual times of ore formation and can be understood (as amplified in the next paragraph) if the time of ore emplacement is determined by the associated magmatic events but the source of the metals was in the pre-existing sediments.

As can be demonstrated in Fig. 6.7 there is an interesting diagnostic correlation of the Pb isotopic ratios with the age of the host rock. The data can be divided into three fields;

(i) a field hosted by pre-Jurassic and Jurassic rocks lying above the Doe and Zartman orogenic development curve in the uranogenic diagram and even more radiogenic in the Th/Pb diagram. This field is quite distinct and only slightly overlaps the other two fields.

(ii) The Lower Cretaceous field is narrow, less radiogenic and follows very closely the mantle, upper crustal mixing trend previously described.

(iii) The field for ores hosted by Tertiary rocks covers the previous field but is larger and may also indicate a less steep trend.

Within each field there are examples where the age of the thermal event associated with the mineralisation is known and these range from Upper Cretaceous to Miocene. Thus a most remarkable feature of the Pb isotope data is the correlation with the source of Pb rather than its formation age. This is clear since the field of the pre-Jurassic analyses compared to the lower Cretaceous field is in inverse position with respect to the usual evolution of the isotopes with time (i.e. the older sources are more radiogenic). The Tertiary field is broadly comparable to the Cretaceous, overlapping the pre-Jurassic field slightly. Consequently, the time of mineralisation is not represented by the Pb model ages. The Pb isotope development parallels the geological evolution of the Andean Cordillera as do Sr isotopes (McNutt et al 1979). The evolution began with an open marine basin in Cambro-Ordovician times and after phases of uplift and erosion during the late Ordovician, Silurian-Devonian marine sedimentation terminated by an episode of folding in Permian-Early Triassic times. The second cycle (Andean Orogenic cycle) was superimposed on the older one, beginning in the late Triassic. The early period of this phase was characterised by a well defined magmatic arc, back-arc basin pair. At the end of the Early Cretaceous the palaeogeography was fundamentally

changed when the arc, back-arc pair was replaced by a single eastward migrating magmatic arc. Prior to this time, upper crustal material chacterised by radiogenic Pb was available in sediments eroded from the continent. After closure of the back arc basin, a major source of radiogenic Pb was cut off and the Pb isotopic composition was more strongly influenced by mantle Pb from volcanic and plutonic activity. In early Tertiary times a magmatic arc producing a calc-alkaline volcanic pile interfingered with continental deposits was developed to the east. This phase, also associated with crustal thickening, has produced a more varible isotopic signature. In the uranogenic system these fields are in reasonable agreement with the average upper crustal and average orogenic development curves of the Doe and Zartman model, however the 208/204 ratios are systematically high (upper part of diagram in Fig. 6.7) suggesting that the Th/U ratio in the radiogenic source was much higher than assumed for the upper crust in this model.

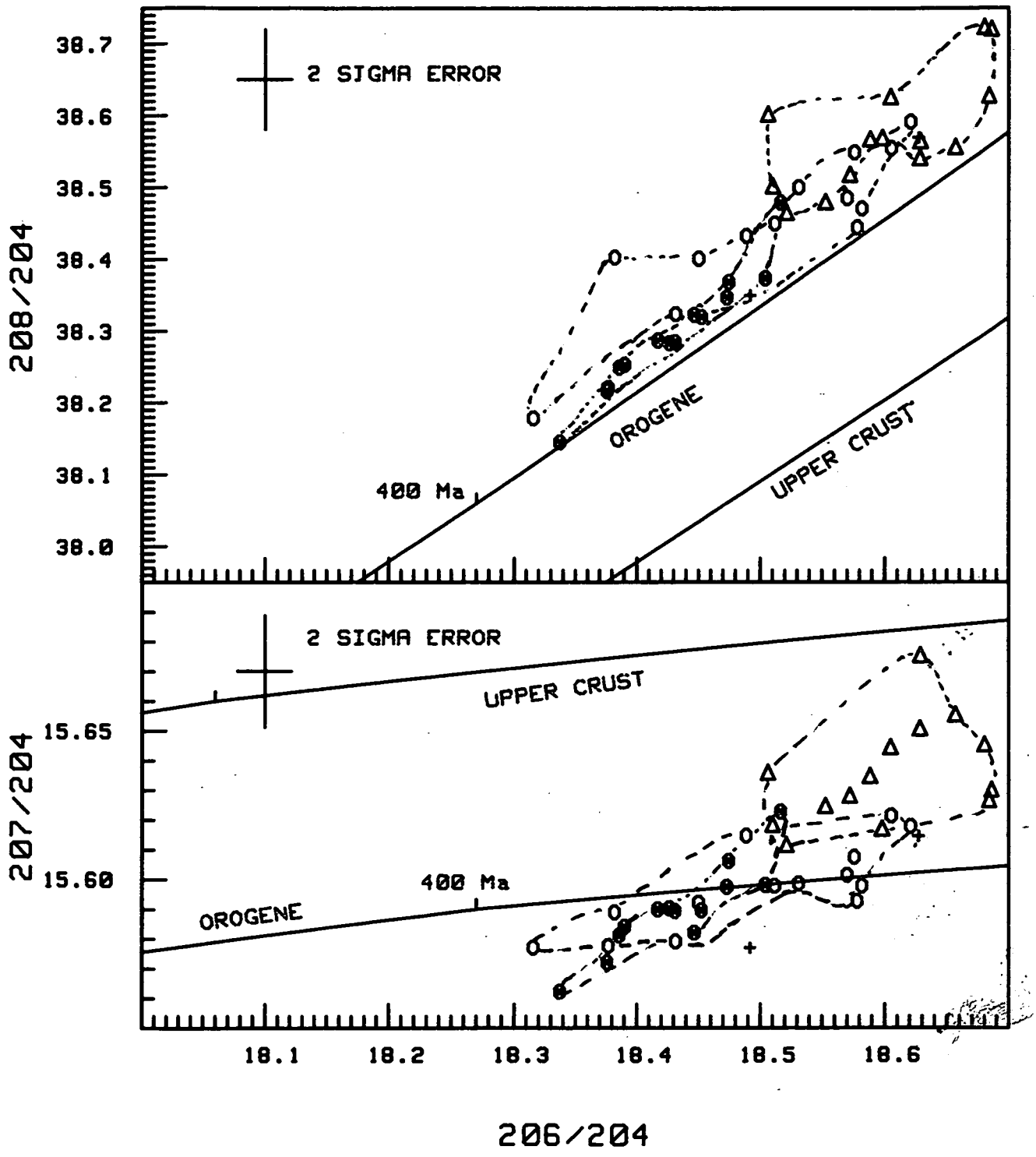

Fig. 6.7 Correlation of isotopic composition with geological age of host rock.

Open Triangles - pre-Jurassic and Jurassic.

Filled circles - Cretaceous.

Open circles - Tertiary and Miocene.

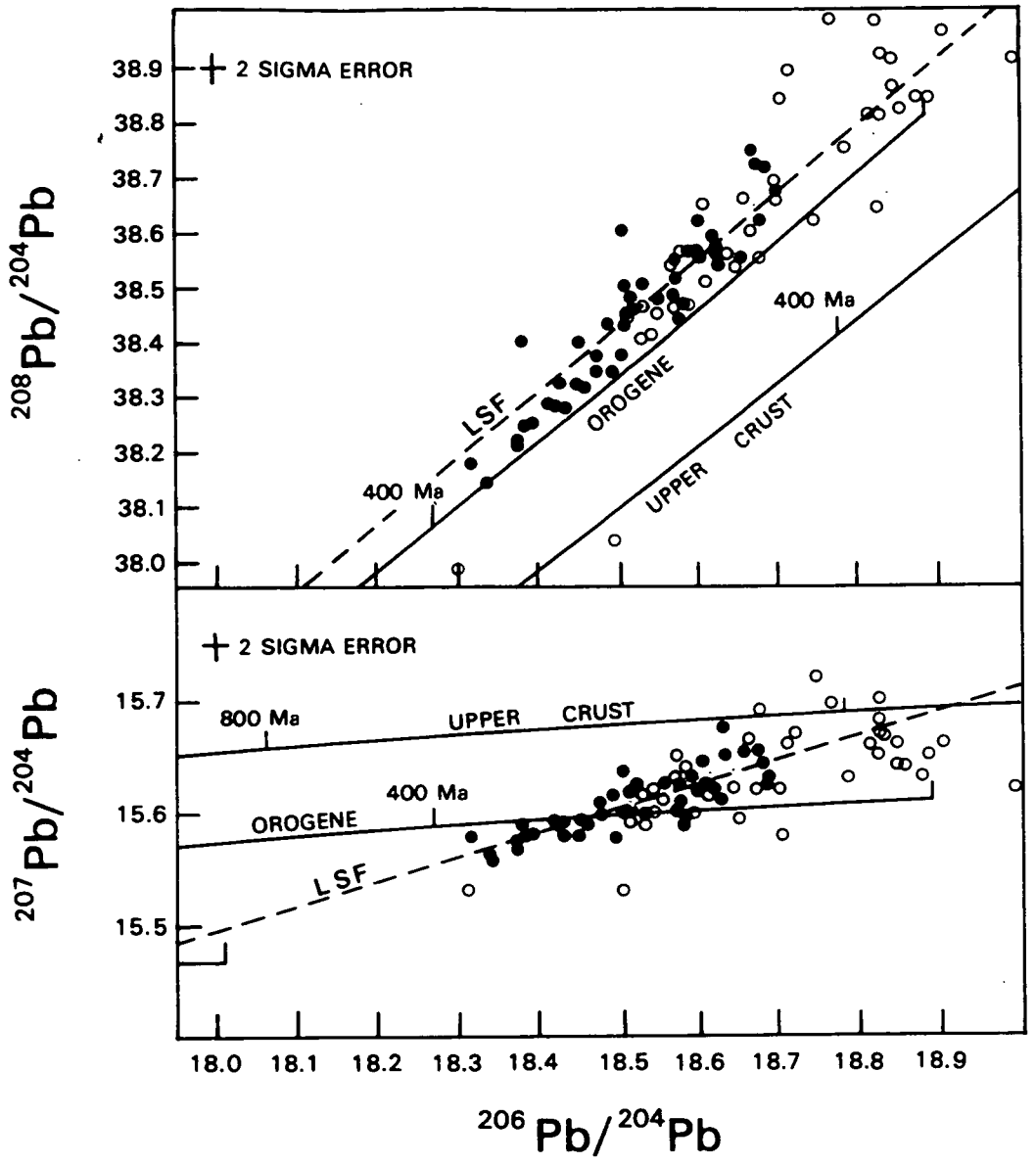

● Chilean ore data.

o Literature data mainly whole rock (references in text).

LSF Least squares fit to Chilean ore data.

Fig. 6.6 Comparison of lead isotopic data from Chile with published data.

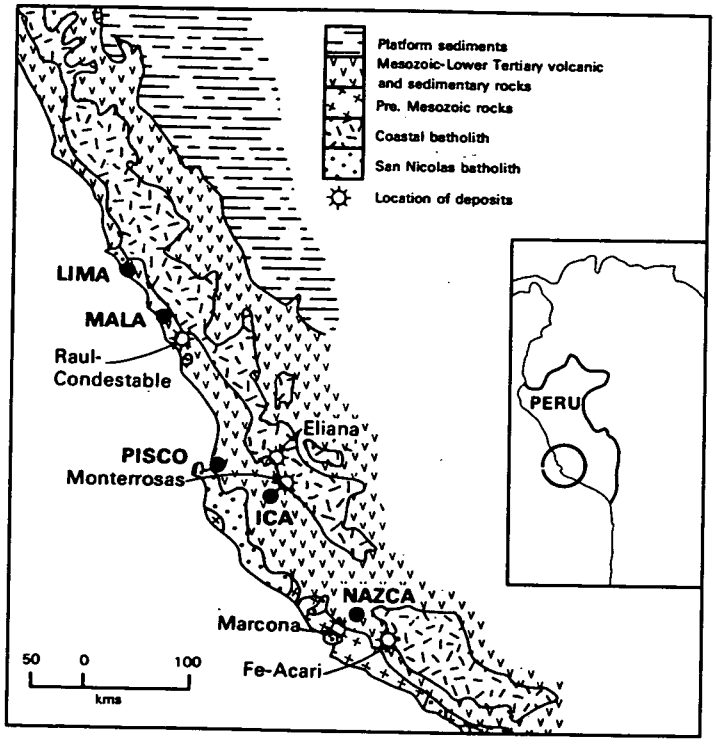

Figure 6.8 Regional geology and location of the Cu-Fe amphibole deposits.

6.4 GEOCHRONOLOGY OF COPPER-IRON DEPOSITS IN THE WESTERN METALLOGENIC PROVINCE, PERU.

6.4a Introduction.

The deposits which are the subject of this investigation constitute a distinctive 'subprovince' and form veins and *mantos* (tabular bodies more or less conformable with the enclosing sedimentary or volcanic rocks) of magnetite, with or without pyrite, andchalcopyrite with Co, Ag, and Au, associated with amphibole (tremolite-actinolite), clinopyroxene, apatite, scapolite and albite in varying proportions. They are hosted in Lower Palaeozoic pelites and Mesozoic sedimentary - volcanic sequences and intrusives. Though variable in mineralogy, they form a single family with gradations from Fe-rich to Cu-rich end members. Most are developed close to the margins of Mesozoic intrusives and have been described accordingly as contact-metasomatic deposits (Sillitoe 1976). However, for the mantos, their conformable nature and the preservation of relic sedimentary-volcanic structures has led other workers (e.g. Ripley and Ohmoto 1979) to propose a sea floor volcano-exhalative origin. Atkin et al. (1985) advocate a hydrothermal-replacement origin of a wide range of host rock compositions during burial metamorphism.

The deposits occur in an area to the west of the main Andean mountain chain, bounded by Lima in the north and Arequipa in the south. The regional geology comprises a local Precambrian basement (metamorphites and granitoids over 2000 Ma old), Lower Palaeozoic sediments of the San Juan, Chiquero and Marcona formations which were intruded by the San Nicolas batholith at c.390 Ma, and Jurassic and Cretaceous volcanics and sediments of the Canete basin in which clastic sediments of Neocomian to Aptian age are overlain by volcanics and volcanoclastics of Albian age (Casma Group). Both basement and cover rocks are intruded by the Coastal Batholith. The geology and mineralogy of these deposits and their geological setting have recently been summarised by Atkin et al. (1985). Four deposits have been dated, viz, Raul-Condestable, Eliana, Marcona and Hierro-Acari; their locations are shown in Fig. 6.8. The Monterrosas deposit was not dated but it is similar in all respects to the Eliana deposit.

The Raul-Condestable deposit occurs in volcanic and sedimentary rocks of the Chilca formation (part of the Casma Group) and was formerly considered to be of Aptian-Albian age. The Marcona deposit occurs in the Lower Palaeozoic Marcona formation and in the Rio Grande formation of Middle-to-Upper Jurassic age (Upper Callovian to Upper Oxfordian according to fossils: Caldas 1978). Both deposits consist of mantos, disseminated bodies, veins and stockworks; at Marcona low sulphur magnetite mantos predominate. The early formed silicates show a regular distribution with actinolite and epidote in the upper parts of the deposits and hornblende and/or hastingsite with diopsidic pyroxene towards the base. It has been suggested that this distribution reflects temperature and permeability gradients (Atkin et al. 1985).

The Eliana, Monterrosas and Hierro-Acari deposits occur in gabbros and diorites belonging to the (?)early Patap Superunit of the Coastal Batholith. The ore minerals occur as cross-cutting and replacement veins and as near horizontal replacement bodies in their igneous host, and in the case of the Eliana deposit, in the country rock to the gabbro.

6.4b Geochronology.

Potassium-argon age determinations were made on silicate minerals exhibiting clear relationships with the ore minerals (oxides and sulphides) and on later cross-cutting dykes (Table 6.9).

In the Raul-Condestable deposit two samples of hastingsite, formed during the premetallic phase (see Fig. 6.9), gave identical ages (within analytical error) of 128 ± 3 and 127 ± 3 Ma and cross-cutting dykes gave ages of 95 ± 2.6 Ma and 124 ± 3 Ma. Mineralization is thus tightly confined between 127 and 124 Ma (Valanginian) and this clearly indicates that the host volcanics and sediments are significantly older than the Aptian-Albian age (114-95 Ma) suggested by Salazar (1975).

Phlogopite and sericite from the Marcona deposit, both of which are late premetallic-to-metallic (Fig. 6.9), give indistinguishable ages of 154 ± 4 Ma and 160 ± 4 Ma respectively. Post-mineralisation dykes set a younger limit to mineralisation here of 137 ± 3 Ma. This late Jurassic age range accords well with the palaeontological dating of the host Rio Grande formation.

Table 6.9 K-Ar Results for Copper-Iron Deposits, Peru.

Sample details		%K	Rad. ^{40}Ar nl/g	Age (Ma)
Raul-Condestable				
Hastingsite,	24527	0.86	4.434	128 ± 3
Hastingsite,	24572	0.76	3.887	127 ± 3
Post mineralisation				
dykes:	24644	3.60	18.03	124 ± 3
	24549	1.59	6.009	95 ± 3
Marcona				
Phlogopite,	24748	7.39	46.20	154 ± 4
Sericite,	24804	8.09	52.81	160 ± 4
Post mineralisation				
dykes:	24721	3.74	20.73	137 ± 3
	24740	1.39	7.656	136 ± 3
	24687	6.69	31.66	118 ± 3
Eliana				
Hastingsite,	25178	1.59	7.186	113 ± 3
Actinolite,	25195	0.12	0.551	115 ± 5
Hierro-Acari				
Pre-mineralisation				
dyke:	21306	0.25	1.092	109 ± 4

It is notable that the mineralization in the Raul-Condestable and Marcona deposits was probably pene-contemporaneous with, or occurred soon after, the deposition of the host rocks and their subsequent burial metamorphism. This narrow time span cannot be resolved by radiometric methods.

Hastingsites from the Eliana deposit, which formed during the pre-metallic and metallic phases (Fig. 6.9), give identical ages of 113 ± 5 Ma and 115 ± 5 Ma. The Eliana deposit occurs in gabbro-diorites assigned to the Patap Superunit of the Coastal Batholith and in the adjacent volcanics assigned to the Casma group. Despite uncertainties in the Cretaceous time scale, the ages strongly suggest that the adjacent volcanic rocks are older that Albian-Aptian. Furthermore it is clear that the host diorites and gabbros, here assigned to the Patap Superunit, are significantly older than their supposed counterparts in the Lima Segment of the Coastal Batholith: Beckinsale et al. (1985) determined ages in the range 100-107 Ma for the Patap Superunit.

The Hierro-Acari deposit is hosted entirely within diorites of the Acari pluton and consists of veins of magnetite and pyroxene with minor amounts of apatite, actinolite and Cu-Fe sulphides. Atkin et al. (1985) considered that the mineralization was not magmatic but involved hydrothermal fluids. The age determination on a pre-mineralization dacitic porphyry can only set an upper limit to the age of mineralisation if it assumed that the dacite did not experience argon loss. It is possible however that the high temperature hydrothermal fluids reset the age of the dacite and that it corresponds closely to the time of mineralization.

6.4c Discussion.

Atkin et al. (1985) noted the similarities in mineral paragenesis, paragenetic sequence of deposition and mineral chemistry, together with the associated and extensive country rock alteration and burial metamorphism, and argued for a common origin of these deposits, notwithstanding the wide range of geological settings in which they occur. Despite the considerable time range over which these deposits formed (c. 45 Ma), these arguments are still valid. The similarities possibly reflect prolonged development of the extensional marginal basin of central Peru during Jurassic and Cretaceous times,which involved the formation of new crust composed of basaltic rocks - lavas dykes,

Figure 6.9 Summary of the paragenetic sequence and dated minerals, Raul - Condestable, Eliana and Marcona.

Raul - Condestable

Pyroxene
Garnet
Scapolite
Amphibole - dated phase
Apatite
Magnetite

Eliana

Scapolite
Amphibole - dated phase
Apatite
Magnetite
Chalcopyrite

Marcona

Pyroxene
Scapolite
Amphibole - dated phase
Magnetite
Pyrite
Chalcopyrite

sills and gabbros with volcaniclastics (Atherton et al., 1983). As stated by Atkin in discussing the Fe-Mg rich nature of the ore fluids and occurrence of other Cu-Fe-amphibole deposits in Chile, "It is probably not a coincidence that these deposits have developed along a subducting plate margin in association with calc-alkaline volcanism and plutonism which characteristically becomes depleted in iron and magnesium during differentiation."

6.5 EVALUATION OF STRONTIUM AND SULPHUR ISOTOPES AS A GUIDE TO SILVER-RICH POLYMETALLIC VEIN DEPOSITS, QUIRUVILCA, PERU.

6.5a Introduction.

The Quiruvilca Cu-Pb-Zn-Ag deposit is located in the La Libertad province of northern Peru, 80 Km east of Trujillo, at an altitude of 4000m. The deposit has a long history of exploitation and is currently worked by Corporacion Minera Nor Peru, SA. Quiruvilca Mine has over 20 Km of underground levels linked to the surface by shafts and haulage tunnels. Workings extend over a vertical distance of 400m though much of the older, eastern sector is now abandoned and access impossible. Concentrates from the flotation plant are transported 40Km by aerial ropeway to a distribution point in the Otuzco valley and thence by truck to the coast. Copper is also recovered from the acid mine waters using scrap iron but the availability of local ironwork is limited and the water is generally channelled to waste. Production was highest during the period 1940-68, since when ore grades and output have fallen.

6.5b Geological setting.

The Quiruvilca deposit comprises a dense network of fissure veins cutting volcanic rocks of the Lower to Middle Tertiary Calipuy Group. Throughout the region the Calipuy Group rest with marked unconformity on Lower Cretaceous sediments and dip gently to the west and east in response to slight flexuring . Within the immediate mine district the volcanics consist of interbedded andesites, andestic flow breccias and basalts, and are intruded by minor andesitic plugs and dykes. The instrusives are considered an integral part of the eruptive cycle and show a close temporal relationship to the mineralization. Immediately west of the mine district the volcanics are cut by several dacite plugs which, unlike the andesite plugs, show no evidence of associated mineralization. The veins occupy an area of 24 sq.km. and form an oblique grid pattern; one set trending ENE-WSW, the other E-W. Most of the economic oreshoots (>0.5m wide) occur on the former set and display sharp contacts with the wallrocks. Structural analysis of the fracture pattern suggests that the minerlized veins are the result of horizontal shear movement along E-W trending pre-mineralization faults. Post-mineralization movement on both vein

sets is apparent everywhere, as shown by the development of clay gouge and broken ore and the displacement of the ENE-WSW veins by E-W veins.

6.5c Mineralization.

Vein material is generally massive but in places it is vuggy or strongly banded. The principal ore and gangue minerals are listed in Table 6.10. It can be seen that the mineralogy is essentially a quartz-sulphide-sulphosalt-carbonate assemblage characterised by Cu, As, Pb, Zn, Ag and Sb. However no single vein shows the complete assemblage and detailed studies by the mine geologists over several decades have revealed a spatial zonation of ore minerals which may be divided into 4 zones (see Fig. 6.10). From the centre outwards these are: 1) an enargite zone, 2) a transition zone, 3) a lead-zinc zone, and 4) a stibnite zone. The enargite zone encloses most of the Quiruvilca workings and is the richest part of the deposit. Enargite (Cu_3AsS_4) is the principal copper mineral and is associated with pyrite, tetrahedrite-tennantite, sphalerite, chalcopyrite + minor quartz and calcite. The transition zone, as its name implies, lies between zones 1 and 3 and is delineated by the dissappearance of enargite and the appearance of significant galena. Pyrite and sphalerite are the main minerals accompanied by arsenopyrite, quartz, calcite and minor rhodocrosite. Veins in the lead-zinc zone carry galena, sphalerite, pyrite with subordinate chalcopyrite, arsenopyrite, tetrahedrite-tennantite in a quartz-dolomite-rhodocrosite-calcite gangue. On the periphery of the district is the stibnite (Sb_2S_3) zone, which is ill defined and speculative.

Mineral zonation is not exactly concentric and on the eastern side of the mine zones 2 and 3 are absent. Furthermore realgar (AsS) and orpiment (As_2S_3) stringers invade veins in the central zone, suggesting a reactivation of structures during the final, cooler, stages of mineral deposition. This raises the important question "Are the complex vein assemblages partly due to the superposition of hydrothermal pulses ?" Other anomalous patterns are seen at depth but for the moment these zones provide a broad overall description of the vein mineralogy.

As expected, the hydrothermal fluids responsible for the mineral deposition have altered to varying degrees most of the volcanic rocks in the mine district. Chloritization is the weakest type of alteration (pyroxene →

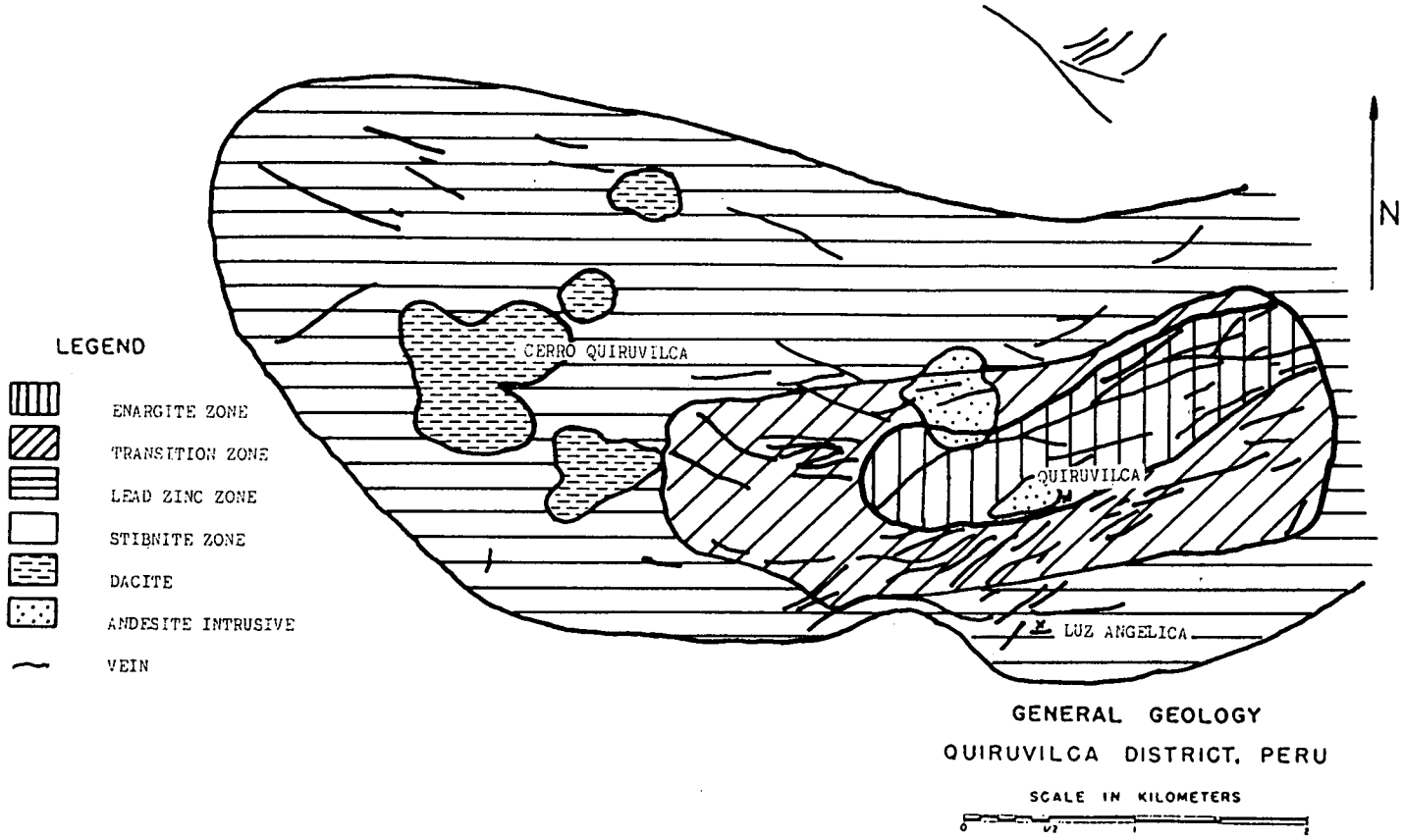

Figure 6.10 Schematic geological map of the Quiruvilca mine area (after Lewis, 1956)

Table 6.10 Principal ore and gangue minerals at Quiruvilca, Peru
(after Lewis 1956)

Pyrite
Galena
Enargite
Tetrahedrite-tennantite
Wurtzite
Sphalerite
Quartz
Marcasite
Arsenopyrite
Stibnite
(Realgar)
Rhodochrosite
Dolomite
Calcite

chlorite; hornblende to iron oxides + calcite; feldspar → albite + sericite) and grades into propylitization closer to the vein area (as above but with the addition of epidote). Argillitization is the strongest type of alteration and affects rocks adjacent to the veins and faults (feldspars, mafic minerals and groundmass → kaolin + quartz + sericite). Like the mineral zonation, this is an oversimplification and further work is needed to explain the detailed distribution of alteration mineral assemblages with respect to ore assemblages.

6.5d Strontium Isotopes.

Strontium isotopes are widely used as tracers for geological processes and in the study of hydrothermal ore deposits provide a means of identifying the source of the mineralizing fluids. The rationale is based on the knowledge that different rock types, by virtue of their age and chemistry, have characteristic $^{87}Sr/^{86}Sr$ ratios. Hence, during interaction with hot aqueous fluids, isotopic exchange takes place which results in the fluids acquiring an $^{87}Sr/^{86}Sr$ similar to the rock. For high integrated water/rock ratios, such as occurs during hydrothermal mineralization, the Sr-isotope composition of the rock is also changed. Thus by measuring the variation in Sr composition of the host rocks within and around a mineralized centre it is possible in theory to estimate the extent and intensity of hydrothermal circulation and to identify the main Sr isotopic components in the ore fluids. This assumes of course that wallrock alteration and ore deposition are related to fluids of the same source.

At Quiruvilca the extensive Calipuy Volcanics were anticipated to provide a perfect isotopically uniform background for this type of study. Accordingly surface samples of the unaltered volcanics were collected within a 3km radius of the central enargite zone, supplemented by underground samples of hydrothermally altered volcanics. From the Rb-Sr systematics and spatial variation in $^{87}Sr/^{86}Sr$ ratios it was hoped to place age constraints on the volcanism and mineralization, to set an outer limit for hydrothermal activity, and to establish whether the fluids had undergone significant exchange with rocks other than the Calipuy Volcanics during convective circulation. The latter point is especially important since it is related to the source of the metals. Mineralization of the type developed at Quiruvilca is the product of several interdependant factors: a heat source, a source of metal, a hydrological system capable of transporting sufficient metal from source to repository, an

environment favourable for metal sulphide deposition. The analytical data summarised in Table 6.11 are discussed with reference to these factors.

TABLE 6.11 Rb/Sr DATA FROM QUIRUVILCA MINE, PERU.

	Rb ppm	Sr ppm	$^{87}Rb/^{86}Sr$	$^{87}Sr/^{86}Sr$
UNALTERED VOLCANICS OF THE CALIPUY GROUP				
MO 1170	12	450	0.0773	0.70445
MO 1171	33	413	0.2271	0.70446
MO 1172	13	418	0.0882	0.70447
MO 1173	61	724	0.2430	0.70469
MO 1174	50	786	0.1835	0.70471
MO 1175	57	747	0.2204	0.70468
MO 1176	56	754	0.2120	0.70468
MO 1177	4	410	0.0289	0.70444
MO 1178	15	360	0.1191	0.70477
MO 1179	21	441	0.1356	0.70458
MO 1180	25	517	0.1385	0.70458
MO 1181	9	426	0.0596	0.70446
MO 1182	34	628	0.1574	0.70423
MO 1183	35	450	0.2263	0.70450
MO 1184	58	965	0.1723	0.70478
VOLCANICS WITH ADVANCED ARGILLIC ALTERATION				
QUI 21	151	55	7.9157	0.70705
QUI 22	68	176	1.1145	0.70511
QUI 24	240	51	13.6251	0.70787
QUI 26	98	277	1.0223	0.70543
QUI 27	181	30	17.3079	0.70913
QUI 29A	273	27	29.6102	0.71142
QUI 32	112	167	2.4380	0.70553
SLIGHTLY ALTERED VOLCANICS				
QUI 6	98	214	1.3188	0.70532
QUI 16	170	96	5.1272	0.70644
QUI 28	112	167	2.4064	0.70570
QUI 22	68	176	1.1145	0.70511
QUI 30	21	458	0.1307	0.70484

(i)Interpretation and discussion.

Firstly, surface samples of the Calipuy Volcanics collected outside the enargite zone but still within the area of veining show no visible alteration and no significant change in their initial $^{87}Sr/^{86}Sr$ ratios (0.7045 ± 0.0001). They are extremely homogeneous with respect to Sr content (>300 ppm) and Rb/Sr ratio (<0.25; equivalent to <100 ppm Rb). This implies that circulation of the mineralizing fluids was very localised and that fracture permeability of the volcanics was dominated by major through-going fissures. As a result, water-rock interaction is confined to the immediate wallrocks, with no detectable Sr-isotope expression in the host volcanics between veins over the greater part of the outer lead-zinc zone. This contrasts markedly with the hydrological patterns and wallrock alteration associated with porphyry copper deposits and high level epithermal deposits. Alternatively the lack of apparent disturbance could be due to a combination of low water/rock ratios and/or closed system circulation in the volcanics. Whichever explanation is true, the use of Sr isotopes for unaltered volcanics in the vicinity of the veins is inappropriate for the detection of concealed ore zones. A best estimated age for the Calipuy Volcanics in the Quiruvilca area, though poorly defined because of the low spread in Rb/Sr ratios, is 60 ± 49 Ma (Fig. 6.11). The initial $^{87}Sr/^{86}Sr$ ratio suggests a mantle source similar to that of the Coastal Batholith.

Underground samples collected in the enargite and transition zones, where wallrock alteration is well developed, Sr values are more variable. In the case of the most altered samples (i.e. those showing advanced argillic alteration) decreases in Sr (<300pm) are accompanied by increases in Rb (>100pm). These samples define an errorchron of 15 ± 1 Ma (MSWD = 9.3) which can be interpreted as a minimum age for the mineralization and is certainly significantly younger than the extrusive event (see Fig.6.12). Assuming this age, the calculated initial ($^{87}Sr/^{86}Sr$) ratio of the highly altered samples is 0.7051 ± 0.0003 which is demonstrably higher than for the fresh volcanics at this time (i.e. <0.7047). This implies involvement of a radiogenic component from a source not within the Calipuy Volcanics. Reference to Fig. 6.13 shows that with increasing alteration there is an antipathetic relationship between Sr content and Sr initial ratio. The corresponding Rb metasomatic effect is seen more clearly in Fig. 6.14. Therse effects can be described as the result of mixing between a low-Sr, high-Rb, radiogenic-Sr fluid component and a high-Sr,

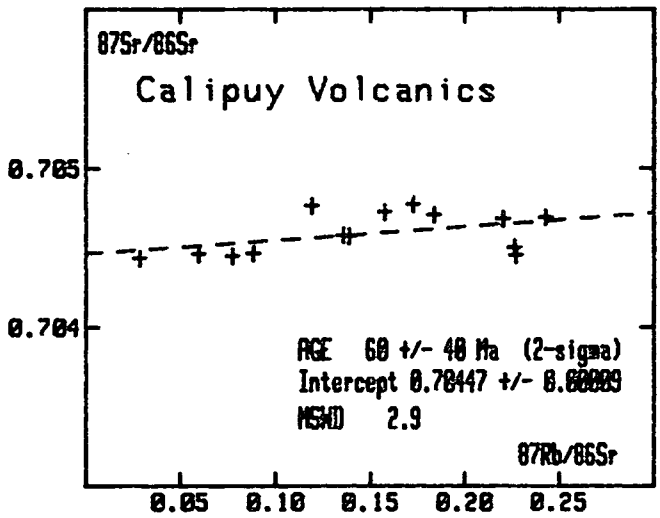

Fig. 6.11 Rb-Sr isochron for the Calipuy volcanis, Quiruvilca.

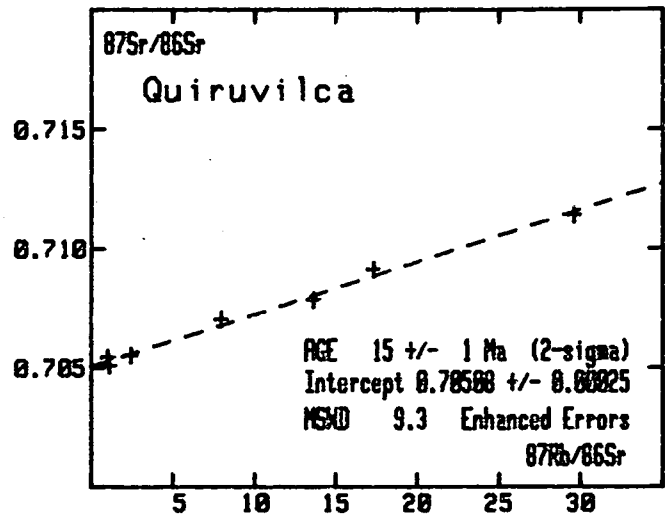

Fig. 6.12 Rb-Sr errorchron for hydrothermally altered volcanics.

Fig. 6.13 Plot of initial $^{87}Sr/^{86}Sr$ ratios vs. Sr ppm for whole rocks from Quiruvilca.

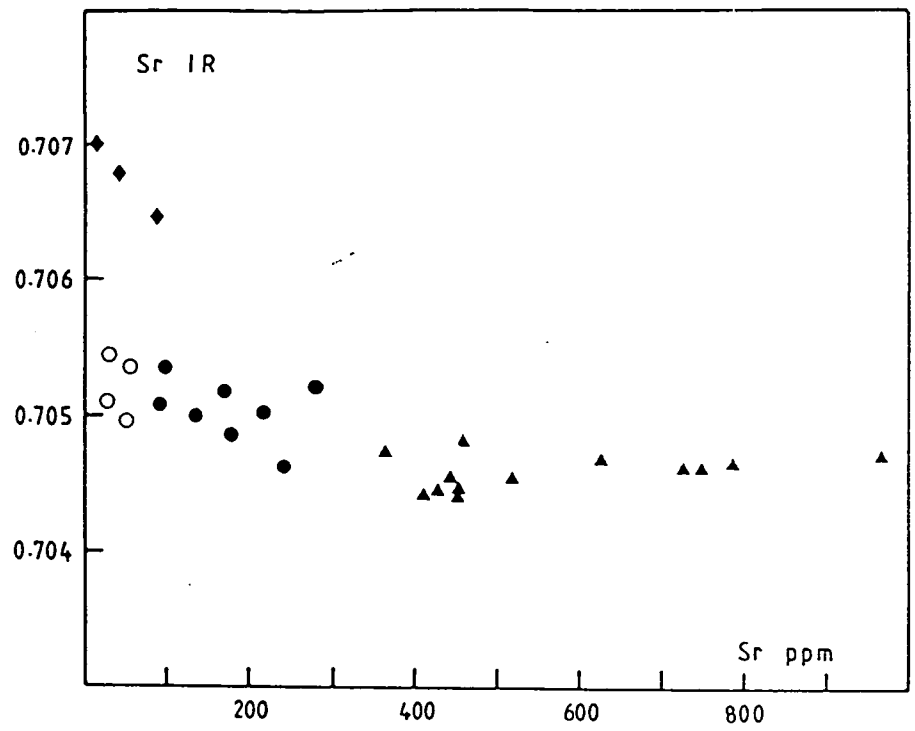

triangles - fresh volcanics
filled circles - slightly altered volcanics
open circles - extensively altered volcanics
diamonds - silicified samples

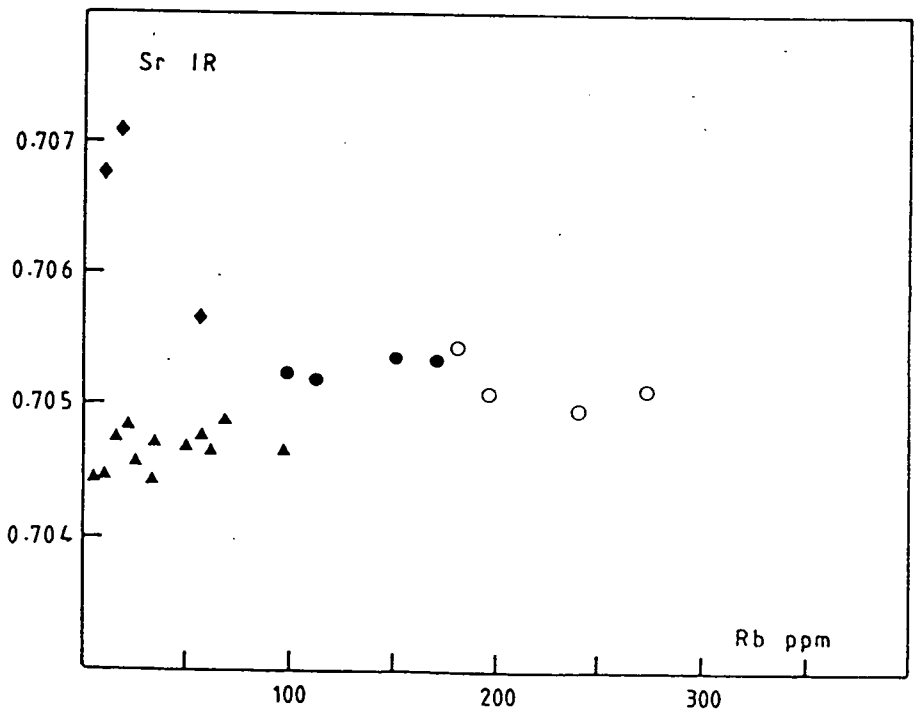

Fig. 6.14 Plot of initial $^{87}Sr/^{86}Sr$ ratios vs. Rb ppm for whole rocks from Quiruvilca.

low-Rb, volcanic unradiogenic-Sr component. In both figures the highly silicified samples (Qui 1,3 and 5) are anomalous and define a separate field which probably represents a superimposed alteration process (i.e. silicification of rocks already enriched in radiogenic Sr). The source of the radiogenic component remains enigmatic but two possible sources exist; Cretaceous sediments beneath the volcanics or a satellitic body of the Cordillera Blanca batholith at depth. The hypothesis of a link with the batholith, 45km to the southeast of Quiruvilca, has much merit. Both the mineralization and emplacement of older elements of the batholith are close in age (c. 12 Ma), (Pitcher et al 1985). Secondly the initial $^{87}Sr/^{86}Sr$ ratio for the batholith (0.70492 ± 0.00005) is indistinguishable from that calculated for the mineralized samples. Though the evidence is circumstantial it does support a model of ore genesis involving an input of metalliferous magmatic fluids from a granite stock at depth into a convecting hydrothermal system in the volcanics and possibly underlying sediments. However, without data for the Cretaceous sediments, it is impossible to eliminate their contribution to the total Sr budget.

6.5e Sulphur Isotopes.

Samples were collected from the main vein systems, from wallrocks adjacent to the ore veins and at a distance of a few meters from the veins, so as to record a range in the degree of alteration. This was performed, where possible, at both the 100 and 220 m levels, so as to provide indications not only for lateral but also for vertical variation trends. The sulphides in the altered wallrocks consist predominantly of pyrite in the form of idiomorphic pyritohedra or cubes 1-2 mm in size. The abundance of pyrite in the altered wallrock seems to increase with the degree of alteration. Small pyrite veinlets occur in rocks rich in sericite and/or kaolinite. These veinlets seem to preceed the emplacement of the ore-bearing veins. The veins are in part multiple and develop a zoned mineralogical composition summarized in Table 6.12. It is noteworthy that sulphate minerals were not detected either in the wallrocks or in the veins.

Table 6.12 Zonation of ore veins at Quiruvilca.

Zone	Vein	Description
Energite	Vein 3	enargite and tetrahedrite in pyrite margins.
"	Elisa	enargite, chalcopyrite, sphalerite and tetrahedrite in pyrite margin.
Transition	Satelite	pyrite, tetrahedrite, sphalerite.
"	Papelillo	pyrite, tetrahedrite, chalcopyrite.
Lead-zinc	Sopresa	sphalerite, galena, carbonate vug filling.
"	Luz Angelica	sphalerite, galena, carbonate and quartz.

(i) Results and discussions.

The sulphur isotope compositions (Table 6.13) show the following features. Despite the variability in sample origin, pyrite from wallrocks of different degrees of alteration and veins of varied mineralogical composition (pyrite, sphalerite, chalcopyrite, galena and tetrahedrite) exhibit a narrow range in isotope composition: $\delta^{34}S$ - 0.25 to + 3.07‰ (28 samples out of which 26 samples lie within a narrower range of + 0.55 to + 2.13‰). The two samples which fall outside this range do not have any particular mineralogical composition; the low value being for a galena sample from the Luz Angelica vein to the south of the main Quiruvilca vein systems. There is no apparent relationship between the type and degree of the wallrock alteration and the pyrite sulphur isotope composition. A single pyrite crystal from No. 3 vein was chosen for a detailed study in order to assess the trend and magnitude of change in isotopic composition during the formation of an individual crystal in an ore bearing vein. The crystal, 25mm from base to tip, was sampled in 5 growth zones. The isotopic composition (Table 6.13) is 0.60‰ in the inner zone, passing through a maximum of 2.10‰ in zone II to 1.03‰ in the outer zone. Hence a single pyrite crystal shows nearly as much variation during its growth as all the vein and wallrock pyrites analysed and virtually almost all the sulphides analysed.

This range of isotopic composition together with the feature of a narrow spread in the absence of sulphurs variation are strong indicators for a magmatic sulphur source (Ohmoto and Rye 1979, Nielsen 1979). The sulphides now concentrated in altered wallrocks and veins could be truly magmatic. On the other hand, they could be products of leaching (mobilization and concentration) of sulphur from disseminated sulphides in magmatic rocks which underwent this process without appreciable fractionation. The mineralogical features of the alteration zones and the Rb/Sr and $^{87}Sr/^{86}Sr$ characteristics of the alteration zones as compared with equivalent fresh andesitic country rocks suggest an intense hydrothermal activity. The difference in isotopic composition between coexisting sphalerite and galena is a proven reliable geothermometer (Ohmoto and Rye 1979). The present results are equivalent to temperatures between 430° and 500°C, using the calibration of Czamanska and Rye (1974). Even allowing for pressure corrections in fluid inclusion thermometry (Shepherd et al 1985), these temperatures are significantly higher than those estimated from fluid

Table 6.13 $\delta^{34}S$ in wall rock and vein sulphides.

Sample	Wall Rock mineral	$\delta^{34}S$(‰)	Vein sample	Vein mineral	$\delta^{34}S$(‰)
		Vein 3 (level 100)			
3 andesite, silicified	py	0.79	4i	py	0.60
5 pyrite veinlet preceeding	py	1.78	4ii	py	2.10
enargite vein			4iii	py	1.84
6 andesite, chloritized	py	0.83	4iv	py	1.98
			4v	py	1.03
			4vi	tet	0.85
		Elisa vein (level 200)			
24 andesite,altered	py	0.62	25A	cha	1.00
27 andesite	py	1.30	27-4	py	1.41
		Satellite vein (level 100)			
16 andesite "fresh"	py	3.07	15	sph	2.05
			15	ga	0.55
			15A	py	2.27
		Papelillo vein (level 100)			
			14A	sph	1.32
		Sopresa vein (100 level)			
			17	sph	2.13
			17	cha	1.37
			17	ga	0.23
		Sopresa vein (220 level)			
28 andesite, chloritized	py	0.48	29C	sph	0.83
29 pyrite veinlet	py	1.59			
30 andesite, highly	py	1.78			
chloritized					
		Luz Angelica vein			
21 andesite, silicified	py	1.95	20	sph	1.00
			20	ga	-0.25

py - pyrite, sph - sphalerite, cha - chalcopyrite, ga - galena,
tet - tetrahedrite,

inclusion vapour-to-liquid ratio (200-350°C). However the inclusion data refers to the later stages of hydrothermal quartz deposition, which could have taken place at temperatures lower than those of sulphide deposition.

The characteristics of the S-isotope composition at Quiruvilca are similar to those of the Ag, Pb, Sn, Cu, vein deposit at Casapalca, central Peru, which are hosted similarly in Tertiary andesites (Rye an Samkins, 1979). Here the sphalerite-galena pairs have a slightly greater difference, indicative of somewhat lower temperatures for formation.

The narrow range of sulphur isotope composition for wallrock and vein sulphides in the absence of sulphate-bearing phases suggest a sulphide-dominated, low fO_2, system. The H_2S in equilibrium with sphalerite and galena in this temperature range should have $\delta^{34}S$ of 1-1.5‰, which represents the bulk of the sulphur reservoir and corresponds to magmatic sulphur. Although the source of sulphur seems to be identical for the wallrock pyrite and vein sulphides, they may have been deposited at different episodes during the hydrothermal activity.

6.5f Summary.

The Cu, Ag, Pb, Zn Quiruvilca deposit is hosted in Lower Tertiary andesitic Calipuy volcanics, in veins trending NE-SW and E-W. The andesitic flows are intruded by andesitic and dacitic plugs and overlie unconformably the Lower Cretaceous sandy-siltstone Chimu formation and the Jurassic shaly Chicama formation. The ore veins form a zoned concentric arrangment - enargite, transition, lead-zinc, stibnite (from centre outwards).

The degree of alteration of the host rock varies and does not show a clear relationship with the size and mineralogical composition of the ore veins. The alteration assemblage is predominantly argillic, represented by sericite and/or kaolinite, with disseminated or veinlet-forming pyrite.

The sulphur isotope composition of the ore sulphides (sphalerite, galena, chalcopyrite, tetrahedrite and pyrite) and the wallrock pyrite is -0.25 to +3.07‰. In the absence of sulphate-bearing phases this represents a sulphide-dominated, low fO_2, largely low pH system, probably of magmatic origin.

The age of the host rock andesites as determined by Rb-Sr whole-rock techniques is 60 ± 40 Ma. The time of mineralization cannot be determined precisely but is estimated as 15±1 Ma, corresponding to the age of older units in the Cordillera Blanca. Sr-isotope systematics are very constrained in the country rock but highly modified in the alteration zones. An increase in the Rb/Sr ratio from 0.021-0.086 to 10.48 is associated with an increase of the measured $^{87}Sr/^{86}Sr$ ratio from 0.70443-0.70477 to 0.711416±16.

Fluid inclusions from late stage quartz indicate temperatures of about 300°C and fluids of low salinity, primarily of meteoric origin.When considering the formation of the deposit different controls are observed. The orientation of the veins is possibly related to major structures reported further to the south, or to fold structures in the underlying sedimentary sequence.

The hydrothermal alteration zones are not strictly related to the ore zones and are a complex function of the local fracture permeability of the host rocks and to features of the hydrological system which are controlled in part by the underlying sedimentary rocks. Wallrock alteration appears to preceed the emplacement of the ore minerals.

The zonation of ore minerals does not seem to be related to vein orientation hence is not structurally controlled nor is it related to the adjacent alteration features. The concentric zonation suggests a geochemical/thermal control reflecting lateral variation in the source of metal or mode of transport and conditions of emplacement. Locally, intense hydrothermal alteration caused the Rb/Sr ratio to increase by two orders of magnitude. Part of the increase can be accounted for by removal of Sr after the breakdown of plagioclase, but there is also a net addition of radiogenic Sr related to the addition of Rb. This can be derived either from the underlying sedimentary sequence or from an unknown magmatic source. It is noteworthy that the $^{87}Sr/^{86}Sr$ initial ratio of the added component (for 15 Ma) is 0.705 which is very similar to that of the Carhuish Super-unit of the Cordillera Blanca batholith (0.7053 ± 0.0001) (Pitcher et al 1985).

The source of sulphur, as evidenced by its isotopic composition, is magmatic. As disseminated pyrite is abundant in the country rock it could have provided the sulphur for the ore minerals. However, a truly magmatic source

should not be discounted as the bulk of the country rock does not seem to be affected by the hydrothermal activity.

The source of metal is obscure. The underlying sediments could be the source, but then the associated sulphur should have at least a noticeable sedimentary component. The host andesite could be the source. To prove this suggestion further geochemical and lead isotope investigations are required.

In combining the evidence for the source of the sulphur, modification of Sr-isotope systematics and the ore mineral zonation, a setting seems to emerge which could be explained by a magmatic intrusion at depth. This would provide the thermal and hydrological regime as well as the metals and sulphur. Under this scenario the similarity in $^{87}Sr/^{86}Sr$ initial ratio with the Cordillera Blanca would represent more than a coincidence.

6.6 REFERENCES FOR SECTION 6.

Arnold, M. and Sheppard, S.M.F. 1981. East Pacific Rise at latitude 21°N: isotopic composition and origin of the hydrothermal sulphur. Earth Planet. Sci. Lett., 56, 148-156.

Atherton, M.P., Pitcher, W.S. and Warden, V. 1983. The Mesozoic marginal basin of central Peru. Nature, 305, 303-306.

Atkin, B., Injoque, J and Harvey, K. 1985. Cu-Fe-amphibole mineralization in the Arequipa segment. In: Magmatism at a Plate Edge. The Peruvian Andes. Ed. Pitcher, W.S., Atherton, M.P., Cobbing, E.J. and Beckinsale, R.D., 261-270. Blackie Halstead Press, Lond.

Barreiro, B.A. and Stern, C.R. 1982. Lead isotopic composition of calc-alkaline volcanic rocks from the southernmost Andes. Trans Am. Geophys. Union. vol. 63, 1148.

Beckinsale, R.D., Sanchez, A., Brook, M., Cobbing, E.J., Taylor, W.P., and Moore, N.D, 1985. Rb-Sr whole rock isochron and K-Ar age determinations for the Coastal Batholith of Peru. In: Magmatism at a Plate Edge. The Peruvian Andes. Ed. Pitcher, W.S., Atherton, M.P., Cobbing, E.J. and Beckinsale, R.D. 177-202. Blackie Halstead Press, Lond.

Caldas, J. 1978. Geologia de los Cuadrangulos de Juan, Acari y Yauca. Bo. No.30, INGEMMET, Peru.

Clarke, A.H. and Zentilli, M. 1972. The evolution of a metallogeny at a consumable plate margin: The Andes between latitudes 26° and 29° South (abstract). C.I.M. Bull, 65, 37.

Claypool, G.E., Holser, W.T., Kaplan, I.R., Sakai, H., and Zak, I. 1980. The age curves of sulpher and oxygen isotopes in marine sulphate and their mutual interpretation. Chem. Geol. 28, 199-260.

Coira, B., Davidson, J., Mpodosis, C. and Ramos, V. 1982. Tectonism and magmatic evolution of the Andes of northern Argentina and Chile. Earth. Sci. Rev. 18, 303-332.

Coleman, M. L. and Moore, 1978. Direct reduction of sulphate to sulphur dioxide for isotopic analysis. Anal. Chem. 50, 1594.

Czamanska, G. K. and Rye, R.O. 1974. Experimentally determined sulphur isotope fractionations between sphalerite and galena in the temperature range 600°C to 275°C. Econ. Geol. 69, 17-25

Doe, B.R. and Zartman, R.E. 1979. Plumbotectonics: the Phanerozoic. In:Geochemistry of Hydrothermal ore deposits. John Wiley Interscience,Eds. H.L. Barnes pp. 22-70.

Giggenbach, W. F. 1978. The isotopic composition of waters from the El Tatio geothermal field, Northern Chile. Geochim. Cosmochim. Acta, 42, 979-988.

Haas, J.L. 1971. The effect of salinity on the maximum thermal gradient of a hydrothermal system. Econ. Geol, 66, 940-946.

Harmon, R.S., Barreiro, B.A., Moorbath, S., Hoefs, J., Francis, P.W., Thorpe, R.S., Deruelle, B., McHugh, J. and Viglino, J.A. 1984. Regional O, S and Pb isotope relationships in the late Cenozoic calc-alkaline lavas of the Andean Cordillera. Jour. Geol. Soc. Lond. 141, p. 803-822.

Hedenquist, J.W. and Henley, R.W. 1985. The importance of CO_2 on freezing point measurements of fluid inclusions: evidence from active geothermal systems and implications for epithermal ore deposition. Econ. Geol, 80, 1379-1406.

Injorque, J. 1985. Geochemistry of Cu-Fe-amphibole skarn deposits of the Peruvian Central Coast. PhD Thesis. University of Nottingham.

Kajiwara, Y. and Krouse, H.R. Sulphur isotope partitioning in metallic sulfide systems. Can. J. Earth Sci, 8, 1397-1408.

Koepnick, R.B., Burke W.H., Denison R.E., Hetherington, E.A., Nelson, H.F., Otto, J.B. and Waite, L.E. 1985. Construction of the seawater $^{87}Sr/^{86}Sr$ curve for the Cenozoic and Cretaceous: supporting data. Chem. Geol, 58, 55-81.

Landis, G.P. and Rye, R.O. 1974. Geologic, fluid inclusion and stable isotope studies of the Pasto Bueno tungsten- base metal ore deposit, northern Peru. Econ. Geol, 69, 1025-1059.

Lehman, B. and Pichler, H. 1980. Tin distribution in mid- Andean volcanic rocks. Mineral. Deposita, 15, 35-39.

Lewis, R.W. 1956. Geology and ore deposits of Quiruvilca, Peru. Econ. Geol. 51, 41-63.

Lindgren, W. 1928. Mineral Deposits (3rd editn.), McGraw Hill, New York. 1049p.

Matsuhisa, Y., Goldsmith, J.R. and Clayton, R.N. 1979. Oxygen isotope fractionation in the system quartz -albite-anorthite-water. Geochim. et Cosmochim.Acta, 43, 1131-1140.

McNutt, R.H., Clarke, A.H., and Zentilli, M. 1979. Lead isotopic composition of Andean igneous rocks latitudes 26° and 29°S. Earth Planet. Sci. Lett. 27, p 305-313.

Neilsen, H. 1979. Sulphur isotopes. In: Lectures in isotope geology (E. Jager and J.C. Hunziker eds.)., 283-312. Springer 320p.

Nolan, T.B. 1933. Epithermal precious-metal deposits in Ore deposits of the Western States. Amer.Inst.Min.Metall.Eng., New York, Pt.VI, 623-640.

Norman, D.I. and Landis, G.P.1983. Source of mineralizing components in

hydrothermal ore fluids as evidenced by strontium and stable isotope data from the Pasto Bueno deposit, Peru. Econ. Geol, 78, 451-465.

Ohmoto H. and Rye R.O. 1979. Isotopes of sulphur and carbon. In: Geochemistry of hydrothermal deposits (H.L. Barnes, ed)., 509-567. John Wiley 797p.

Petersen, U. 1970. Metallogenic provinces in South America. Geol. Rundsch., 59, 834-897.

Petersen,U., Noble, D.C., Arenas, M.J. and Goodell, P.C. 1977. Geology of the Julcani mining district, Peru. Econ. Geol, 72, 931-949.

Pitcher, W,S., Atherton, M.P., Cobbing, E,J. and Beckinsale, R.D. 1985. Magmatism at a plate edge. Blackie Halsted Press. 177-202.

Puig, A. 1985. The geological and metallogenic significance of lead isotope abundance studies on galena occurrences in the Chilean Andes. M. Phil. Thesis, Oxford Polytechnic 73p.

Radke, A.S., Rye, R.O. and Dickson, F,W. 1980. Geology and stable isotope studies of the Carlin gold deposit, Nevada. Econ. Geol, 75, 641-672.

Ripley, E. and Ohmoto, H. 1979. Oxygen and hydrogen isotopic studies of ore deposition and metamorphism at the Raul mine, Peru. Geochim. et Cosmochim. Acta, 43, 1633-1643.

Robinson, B.W. and Kusukabe, M. 1975. Quantitative preparation of SO_2 for $^{34}S/^{32}S$ analysis from sulphides by combustion with cuprous oxide. Anal. Chem, 47, 1179-1181.

Rye R.O. and Sawkins F.J. 1974. Fluid inclusions and stable isotope studies in the Casapalca Ag-Pb-Zn-Cu deposit Central Andes, Peru. Econ. Geol, 69, 181-205.

Salazar, H. 1975. Geologia de los Cuadrangulos de Mala, Lunahuana, Tupe, Conaica, Chincha, Tantar y Castrovirreyna. Informe Interno, INGEMMET, Peru.

Shackleton, R.M., Ries, A.C., Coward, M.P. and Cobbold, P.R. 1977. Structure, metamorphism and geochronology of the Arequipa Massif of coastal Peru. Jour. Geol. Soc. Lond., 136, pp 195-214.

Shepherd, T.J., Rankin, A,H. and Alderton, D.H.M. 1985. A practical guide to fluid inclusion studies. Blackie 155-162.

Sillitoe, R.H. 1972. A plate tectonic model for the origin of porphry copper deposits. Econ. Geol. 67, 184-97.

Sillitoe, R.H. 1974. Tectonic segmentation of the Andes:implications for magmatism and metallogeny. Nature, 250, 542-545.

Sillitoe, R.H. 1976. Andean mineralization: a model for the metallogeny of convergent plate margins. Geol. Assoc. Can. Spec. Paper, 14, 59-100.

Taylor, H.P. 1979. Oxygen and hydrogen isotope relationships in hydrothermal mineral deposits. In: Geochemistry of hydrothermal ore deposits (H.L. Barnes editor), 236-277, Wiley 798p.

Tilton, G.R. 1979. Isotope studies of Cenozoic Andean Calc-Alkaline rocks. Carnegie Inst. Washington Yearb. 78, p 298-304.

Vicente, J.C., Charrier, R., Davidson, J., Mpodosis, A.C. and Rivano, S. 1973. La arogensis subhercinica: fase mayor de la evolution paleogeographica y extractural de los Andes Argentino-Chilenos Centrales. Acta 5th Cong. Geol. Argent, 81-98.